

Republic of Iraq/ Ministry of Higher Education and Scientific Research
University of Babylon/ College of Medicine



**Molecular Characterization of Some Virulence Factors among
Klebsiella pneumoniae ST 258 Isolated from Hospitalized Patients in
Babylon Province**

A Thesis

Submitted to the Council of the College of Medicine, University of
Babylon, in Partial Fulfillment for the Requirements of the Degree of
Doctor of Philosophy in Medical Microbiology

By

Zainab Mahdi Kadhom Al-Sendi

B.V.M and S. / College of Veterinary Medicine / University of Karbala -2014

MSc. Microbiology / College of Medicine / University of Babylon -2017

Supervised by

**Professor
Dr. Ilham Abbas Bunyan**

2023 A.D

1444 A.H

بِسْمِ اللَّهِ الرَّحْمَنِ الرَّحِيمِ

وَيَسْأَلُونَكَ عَنِ الرُّوحِ قُلِ الرُّوحُ مِنْ أَمْرِ رَبِّي

وَمَا أُوتِيتُمْ مِنَ الْعِلْمِ إِلَّا قَلِيلًا

صَدَقَ اللَّهُ الْعَبِيَّ الْعَظِيمَ

سُورَةُ الْاِنشَاءِ

الآيَةُ (٨٥)

Certification

I certify that this thesis entitled "**Molecular Characterization of Some Virulence Factors among *Klebsiella pneumoniae* ST 258 Isolated from Hospitalized Patients in Babylon Province**" was prepared by "**Zainab Mahdi Kadhom Al-Sendi**" under our supervision at the college of Medicine, University of Babylon, as a partial requirement for the **Degree of Doctor of Philosophy in Medical Microbiology**.

Supervisor

Professor

Dr. Ilham A. Bunyan

College of Medicine

University of Babylon

/ / **2023**

In view of the available recommendation, I forward this thesis for debate by the examining committee.

Professor

Dr. Hayam K. Al-Mosudi

Head of Department of Microbiology

College of Medicine

University of Babylon

/ / **2023**

Examination Committee Certification

We, the member of examining committee, certify that this thesis entitled "**Molecular Characterization of Some Virulence Factors among *Klebsiella pneumoniae* ST 258 Isolated from Hospitalized Patients in Babylon Province**" presented by "**Zainab Mahdi Kadhom Al-Sendi**", is sufficient in fulfilling the scope and quality for the purpose of awarding for the Degree of **Doctor of Philosophy in Medical Microbiology**.

Professor

Dr. Azhar Omran Althahab

College of Science
University of Babylon
(Chairman)

Professor

Dr. Haider Sabah Kadhim

College of Medicine
Al-Nahrain University
(Member)

Professor

Dr. Oruba Kattof Hussein

College of Science for Women
University of Babylon
(Member)

Professor

Dr. Bushra Jabbar Al-Tamimi

College of Medicine
University of Babylon
(Member)

Assistant Prof.

Dr. Sura Ihsan Abed

College of Science
University of Babylon
(Member)

Professor

Dr. Ilham A. Bunyan

College of Medicine
University of Babylon
(Member and Supervisor)

Approved by the college committee on post-graduate studies

Professor

Dr. MOHEND ABBASS NORI ALSHALAH

Dean of College of Medicine
University of Babylon

Dedication

To the symbol of Kindness, Mercy and Love.....

My Parents

To those who supported and encouraged me.....

My Sisters and Brothers

To my lovely friends

For them, I Dedicate My simple and Modest Effort

Zainab 2023

Acknowledgments

There's always a blessing to thank god for; the ones you are aware of, and the ones that you are not. My great thanks to **“Allah”** the Most Gracious and Most Merciful, and to His prophet **“Mohammad”**

I am deeply indebted to the bright candle **“My Supervisor” Professor Dr. Ilham Abbas Bunyan** for her valuable guidance, assistance, cooperation and motivation throughout the course of preparing my thesis.

I would like to thank the staff of bacteriologist, Al-Hillah General Teaching Hospital and Imam Al-Sadiq Hospital for providing facilities during the research and also my thanks to all the patients for their great cooperation in collecting samples.

Finally, my special thanks to all friends and colleagues.

Zainab 2023

Summary

This cross-sectional study collected 100 clinical specimens from Al-Hilla General Teaching Hospital and Imam Al-Sadiq Hospital during the period Oct 2021- Apr 2022; patients with age ranged between 3 to 55 years old from both sexes, 65% of which were male and 35% female. Forty strains of *Klebsiella pneumoniae* were isolated from 100 specimens of various infection locations by different diagnostic methods. 11(27.5%) of the forty isolates were from sputum, 8(20%) from urine, 7(17.5%) from wound swabs, 6(15%) from burn swabs, 5(12.5%) from burn tissue, and 3(7.5%) from ear swabs. *K. pneumoniae* was isolated from 26 men (65%) and 14 women (35%).

Phenotypic detection showed that 18(45%) *K. pneumoniae* isolates were hemolysin, 22(55%) could make siderophores, 37(92.5%) could agglutinate erythrocytes, 25(62.5%) could produce serum resistance, 5(12.5%) could produce lipase, 4(10%) could produce gelatinase, and 39(97.5%) had hyper-mucoviscosity.

Biofilm-forming were studied, it was found these isolates formed 37(92.5%) of these isolates formed a strong biofilm, 2(5%) formed a moderate biofilm, and only one (2.5%) isolate formed a weak biofilm. Antibiotic resistance against *K. pneumoniae* was shown to have a high resistance rate to Imipenem 33(82.5%), Meropenem 31(77.5%), Fosfomycin 27(67.5%) and Ertapenem 26(65%).

All of the possible *K. pneumoniae* isolates had their DNA extraction and ran through a standard PCR for *pilv-l* gene primer amplification using the sequences, the results revealed that only 16(40%) of the 40 *K. pneumoniae*

Summary

isolates were related to *K. pneumoniae* ST 258 by sharing the same 320 bp DNA fragment with the allelic ladder.

Some virulence genes were detected in 16 *K. pneumoniae* ST 258 isolates and compared with 16 *K. pneumoniae* isolates. The results showed that *fimH* all 16(100%) were positive to *fimH* gene of *K. pneumoniae* ST 258 isolates while 12/16(75%) ordinary *K. pneumoniae* isolates were found at (688bp).

mrkD gene were detected 13/16(81.2%) were positive to *mrkD* gene of *K. pneumoniae* ST 258 isolates while 11/16(68.7%) *K. pneumoniae* isolates were found at (240bp). *magA* gene were detected in 15/16(93.7%) were positive to *magA* gene of *K. pneumoniae* ST 258 isolates while 10/16(62.5%) *K. pneumoniae* isolates were found at (1282bp). In addition, *wzy* gene were detected in 15/16(93.7%) were positive to *wzy* gene of *K. pneumoniae* ST 258 isolates while 11/16(68.7%) *K. pneumoniae* isolates were found at (641bp), *rmpA* gene were detected in 16/16(100%) were positive to *rmpA* gene of *K. pneumoniae* ST 258 isolates while 12/16(75%) *K. pneumoniae* isolates were found at (535bp), *luxS* gene were detected in 14/16(87.5%) were positive to *luxS* gene of *K. pneumoniae* ST 258 isolates while 9/16(56.2%) *K. pneumoniae* isolates were found at (447bp), *bla_{OXA-48}* gene were detected in 13/16(81.2%) were positive to *bla_{OXA-48}* gene of *K. pneumoniae* ST 258 isolates while 8/16(50%) *K. pneumoniae* isolates were found at (428bp). However, *bla_{TEM}* gene were detected in 13/16(81.2%) were positive to *bla_{TEM}* gene of *K. pneumoniae* ST 258 isolates while 9/16(56.2%) *K. pneumoniae* isolates were found at (1080bp). *bla_{SHV}* gene were detected in 12/16(75%) were positive to *bla_{SHV}* gene of *K. pneumoniae* ST 258 isolates while 10/16(62.5%) *K. pneumoniae* isolates were found at (930bp), *bla_{CTX-M}* gene were detected in 15/16(93.7%) were positive to *bla_{CTX-M}* gene of *K. pneumoniae* ST 258 isolates while 8/16(50%) *K. pneumoniae* isolates were

Summary

found at (585bp). Furthermore, neighbor phylogenetic distances in this tree indicated a wide biological diversity of *K. pneumoniae* and *K. pneumoniae sub spp. pneumoniae* ST258 sequences.

Macrogen Korea sequenced PCR-amplified genes. The Gene Bank found 99% compatibility between *Klebsiella pneumoniae sub spp. pneumoniae* ST258 gene and *pneumonia* ST 258 gene in NCBI under sequencing (ID: HG785581.1). Another part of sequencing for *Klebsiella pneumoniae sub spp. pneumoniae* ST 258 gene shows compatibility of 99% in Gene Bank under sequence ID: HG785581.1, thus recording one Transversion G/C in location (278 nucleotide) and Transversion A/T in (316 nucleotide) from this isolate.

The sequencing result of the first *K. pneumoniae* gene shows one Transversion T/A in location (1830475 nucleotide) from the Gene Bank found part of the gene having 99% compatibility with the subject in NCBI under sequence (ID: CP052490.1), so recorded one Transition G/A in location (1830608 nucleotide) noticed from the gene in this isolate. The sequencing result of the second *K. pneumoniae* gene shows one Transversion T/A in location (1830566 nucleotide) from the Gene Bank found part of the gene having 99% compatibility with the subject in NCBI under sequence (ID: CP052490.1), so recorded one Transition C/T in location (1830630 nucleotide) from this isolate. *mrkD* gene for *K. pneumoniae* has one Transition G/A at location (502 nucleotide) from the Gene Bank discovered section of the gene having 99% compatibility with the topic in NCBI under sequencing (ID: KF777765.1). Another section of sequencing for *mrkD* gene to *K. pneumoniae* in same isolate suggests compatibility of 99% in Gene Bank of *mrkD* under sequence ID: KF777765.1, was recorded Transition T/C in place (714 nucleotide) from Gene Bank detected part. The results show 99% compatibility in Gene Bank of *mrkD* under sequence (ID:

Summary

KF777765.1) was recorded Transversion A\C in location (751 nucleotide) from the Gene Bank identified part of *mrkD* gene at same isolate. However, *K. pneumoniae* second *mrkD* gene has one Transition G\A (502 nucleotide) from the Gene Bank and 99% compatibility with NCBI's sequence subject (ID: KF777765.1).

Another part of sequencing for *mrkD* gene to *K. pneumoniae* in same isolate shows 99% compatibility in Gene Bank under sequence ID: KF777765.1, was recorded Transition T\C in place (714 nucleotide) from the Gene Bank detected region. This isolate Gene Bank of *mrkD* sequence ID: KF777765.1 showed Transition A\G in situ (804 nucleotide).

The third *K. pneumoniae mrkD* gene sequencing result shows one Transition A\G (502 nucleotide) from the Gene Bank designated part of the gene with 99% consistency with the topic in NCBI under sequence (ID: KF777765.1). Another part of sequencing for *mrkD* gene to *K. pneumoniae* in same isolate suggests compatibility of 99% in Gene Bank of *mrkD* under sequence ID: KF777765.1, was recorded Transversion T\G in place (603 nucleotide) from Gene Bank detected part. The Gene Bank discovered part of the *mrkD* gene at the same isolate with 99% compatibility under sequence ID: KF777765.1.

K. pneumoniae ST258 *mrkD* MacroGen Korea sequenced three PCR-amplified genes. The initial gene's sequencing showed 100% compatibility with the Gene Bank's *mrkD* gene under sequence ID: CP046967.1, hence no modification was recorded. The second gene shows *K. pneumoniae* ST 258 has one Transition T\C (4039924 nucleotide) in the *mrkD* gene, which is 99% consistent with the topic in NCBI under sequencing (ID: CP046967.1). The *luxS* gene sequencing for *K. pneumoniae* and *K. pneumoniae* subsp. *pneumoniae* ST258 showed 99% compatibility in Gene Bank under sequence ID: CP114753.1, hence no Gene Bank change was reported. Local

Summary

K. pneumoniae ST 258 gene phylogeny included single-region strains. The samples were clustered in tight phylogenetic distances. The two samples were only near Venezuela (GenBank acc. No. HG685581.1).

List of Contents

No.	Subjects	Page
	Summary	I
	List of Contents	VI
	List of Tables	IX
	List of Figures	X
	List of Appendix	XIV
	List of Abbreviations	XV
Chapter One: Introduction and Literatures Review		
No.	Subjects	Page
1.1	Introduction	1
	Aim of study	4
1.2	Literatures review	5
1.2.1	<i>Klebsiella</i> spp.	5
1.2.2	Taxonomy of genus <i>Klebsiella</i>	5
1.2.3	Epidemiology	7
1.2.4	Pathogenesis	10
1.2.5	Virulence factors	13
1.2.5.1	Hemolysin production	13
1.2.5.2	Sidrophores production	14
1.2.5.3	Lipopolysaccharide and serum resistance	16
1.2.5.4	Capsular polysaccharide (CPS) (K-antigen)	19
1.2.5.5	Pili (Fimbriae)	21
1.2.5.6	Other virulence factors	25
1.2.6	Outer membrane proteins (OMPs)	25
1.2.7	Extended spectrum β -lactemase	27
1.2.7.1	Definition and Classification of ESBL	29
1.2.7.2	General structure and function of ESBLs	31
1.2.7.3	Mode of action of ESBLs	32
1.2.8	Mechanism of resistance to β -lactam antibiotics	33
1.2.9	Biofilm formation	35
1.2.10	Antibiotic susceptibility test	38
1.2.11	<i>K. pneumoniae sub spp. ST 258</i>	40
1.2.12	Virulence genes of <i>Klebsiella pneumonia</i>	41

Chapter two: Materials and Methods		
No.	Subjects	
2.1	Materials	44
2.1.1	Laboratory instruments and equipment	44
2.1.2	Chemical and Biological Materials	45
2.1.2.1	Chemical Materials	45
2.1.2.2	Biological Materials	46
2.1.2.3	Phenotypic diagnostic Kits	47
2.1.2.4	Antibiotics used in this study	47
2.1.3	Commercial kits	48
2.2	Methods	49
2.2.1	Preparation of Reagents and Solutions	49
2.3	Subjects of the Study	51
2.3.1	Study Design	51
2.3.2	Ethical approval	51
2.3.3	Experimental Scheme	52
2.3.4	Collection of samples	53
2.4	Laboratory diagnosis	54
2.4.1	Morphological tests	54
2.4.2	Biochemical tests	55
2.5	Identification of <i>Klebsiellae</i> by GN-ID with VITEK-2 Compact	58
2.5.1	Inoculum Preparation	58
2.6	Detection of some virulence factors of <i>K. pneumoniae</i> isolates	59
2.7	Biofilm production: Tissue culture plate method (TCP)	61
2.8	Colanic acid extraction and measurement of concentration	62
2.9	Genotyping Assays	63
2.9.1	DNA Extraction	63
2.9.2	Measurement of DNA concentration and purity	65
2.9.3	Agarose gel preparation	65
2.10	Polymerase chain reaction (PCR) diagnosis	66
2.10.1	Preparation of primers solution	66
2.10.2	Monoplex PCR mixture and PCR program conditions	66
2.10.3	Molecular detection of <i>K. pneumoniae</i> ST 258 by specific primer gene	66
2.10.4	Detection of some of <i>K. pneumoniae</i> virulence genes	67
2.11	Gene Sequencing of <i>K. pneumoniae</i> and <i>K. pneumoniae</i> ST	70

Contents

	258, <i>mrkD</i> and <i>luxS</i>	
2.12	Statistical Analysis	71
Chapter Three: Results and Discussion		
No.	Subjects	Page
3.1	Data Description of Study Population	72
3.2	Isolation of <i>Klebsiellae pneumoniae</i> from different site of infection	74
3.3	Identification of <i>K. pneumoniae</i> by biochemical tests and vitek II system	76
3.3.1	Phenotypic Characterization and Microscopic Identification	76
3.3.2	Biochemical Identification	77
3.3.3	Vitek II Identification	80
3.4	Phenotypic detection of virulence <i>K. pneumoniae</i>	81
3.5	Biofilm formation	85
3.6	Antibiotic susceptibility test	91
3.7	Molecular identification of <i>K. pneumoniae</i> ST 258 by specific primer gene	96
3.8	Colanic acid production by <i>K. pneumoniae</i> and <i>K. pneumoniae sub spp. pneumoniae</i> ST 258	99
3.9	Detection of virulence factors genes	101
3.9.1	Detection of Fimbrial Adhesin type 1 gene (<i>fimH</i> gene) and Fimbrial Adhesin type 3 gene (<i>mrkD</i> gene)	101
3.9.2	Detection of <i>magA</i> (<i>K1</i>) gene and Capsule gene (<i>K2</i>) (<i>wzy</i> gene)	106
3.9.3	Mucoid phenotype A gene (<i>rmpA</i> gene)	110
3.9.4	Detection of quorum sensing <i>luxS</i> gene	112
3.9.5	Detection of <i>bla_{OXA-48}</i> , <i>bla_{TEM}</i> , <i>bla_{SHV}</i> and <i>bla_{CTX-M}</i> genes	114
3.10	DNA sequencing	121
3.10.1	DNA sequencing for <i>Klebsiella pneumoniae</i> and <i>Klebsiella pneumoniae subspp. pneumoniae</i> ST258	121
3.10.2	DNA sequencing for some important virulence genes	127
3.11	Phylogenic tree of <i>K. pneumoniae</i>	154
3.12	Phylogenic tree of <i>K. pneumoniae</i> ST 258	155
Conclusions and Recommendations		
Conclusions		157
Recommendations		158
References		159
Summary in Arabic		i

List of Tables

Table No.	Subjects	Page
2-1	Laboratory Instruments and Equipment	44
2-2	Instruments and Disposable Materials	45
2-3	Chemical Materials	45
2-4	Culture Media Used	46
2-5	Phenotypic Diagnostic Kits	47
2-6	Antibiotics Used in this Study	47
2-7	Commercial Kits Used in the Present Study	48
2-8	DNA extraction kit (Korea / UK)	48
2-9	Master Mix Used in PCR (promega/USA)	48
2-10	Classification of bacterial adherence by TCP method	62
2-11	The sequence of primers that used in this study	67
2-12	The Components of the Maxime PCR PreMix kit	67
2-13	Reaction components of PCR	67
2-14	The optimum condition of detection	67
2-15	Characteristics of the primers used in RCR	68
2-16	Reaction components of all PCR	68
2-17	The optimum condition of detection of virulence genes	69
3-1	Types of Bacterial isolates recovered from sample	74
3-2	Distribution of <i>K. pneumoniae</i> according to samples types & patients sex	75
3-3	Distribution of <i>K. pneumoniae</i> according to patients age	75
3-4	Biochemical tests for characterization of <i>K. pneumoniae</i>	78
3-5	Biofilm formation of <i>K. pneumoniae</i> isolates	86
3-6	Pattern phenotypic virulence factors and biofilm formation among <i>K. pneumoniae</i>	89
3-7	Antibiotic resistance of <i>K. pneumoniae</i> isolates	91
3-8	Colanic acid producing by <i>K. pneumoniae</i> and <i>K. pneumoniae</i> sub spp. <i>pneumoniae</i> ST 258	99
3-9	Pattern of antibiotic resistance and occurrence of virulence factors genes among two types of strains (<i>K. pneumoniae</i> ST 258 and ordinary strain <i>K. pneumoniae</i>) isolates (Total No. =32)	119
3-10	Determinate of DNA sequencing for <i>Klebsiella pneumoniae</i> subsp. <i>pneumoniae</i> ST258 gene	122
3-11	Determinate of DNA sequencing for <i>K. pneumoniae</i> and <i>K. pneumoniae</i> subsp. <i>pneumoniae</i> ST258 <i>mrkD</i> gene	129

Contents

3-12	Determinate of DNA sequencing for <i>K. pneumoniae</i> and <i>K. pneumoniae</i> subsp. <i>pneumoniae</i> ST258 <i>luxS</i> gene	153
3-13	The NCBI-BLAST Homology Sequence identity (%) between local <i>K. pneumoniae</i> isolates and NCBI-BLAST submitted <i>K. pneumoniae</i> isolates in other countries	154
3-14	The NCBI-BLAST Homology Sequence identity (%) between local <i>K. pneumoniae</i> sub-spp <i>pneumoniae</i> ST 258 isolates and NCBI-BLAST submitted <i>K. pneumoniae</i> sub-spp <i>pneumoniae</i> ST 258 isolates in Venezuela	156

List of Figures

Figure No.	Subjects	Page
2-1	Experimental Scheme	52
2-2	Standard curve of colanic acid when used galacturionic acid	63
3-1	Distribution of samples according to site of infections	72
3-2	Distribution of the patients according to the age	73
3-3	Frequency of patients according to sex	73
3-4	phenotypic detection of virulence among <i>K. pneumoniae</i>	82
3-5	Agarose gel electrophoresis (1.5%) of RCR amplified of <i>pilv-l</i> gene (320bp) of <i>K. pneumoniae</i> ST 258	97
3-6	Concentration of colanic acid $\mu\text{g/ml}$ producing by <i>K. pneumoniae</i> and <i>K. pneumoniae</i> sub spp. <i>pneumoniae</i> ST 258	100
3-7	Agarose gel electrophoresis (1.5%) of RCR amplified of <i>fimH</i> gene (866bp) of <i>K. pneumoniae</i> ST 258	102
3-8	Agarose gel electrophoresis (1.5%) of RCR amplified of <i>mrkD</i> gene (240bp) of <i>K. pneumoniae</i> ST 258	103
3-9	Agarose gel electrophoresis (1.5%) of RCR amplified of <i>magA</i> gene (1282bp) of <i>K. pneumoniae</i> ST 258.	107
3-10	Agarose gel electrophoresis (1.5%) of RCR amplified of <i>wzy</i> gene (641bp) of <i>K. pneumoniae</i> ST 258	107
3-11	Agarose gel electrophoresis (1.5%) of RCR amplified of <i>rmpA</i> gene (535bp) of <i>K. pneumoniae</i> 258	110
3-12	Agarose gel electrophoresis (1.5%) of RCR amplified of <i>luxS</i> gene (447bp) of <i>K. pneumoniae</i> ST 258	113

Contents

3-13	Agarose gel electrophoresis (1.5%) of RCR amplified of <i>bla</i> _{OXA-48} gene (428bp) of <i>K. pneumoniae</i> ST 258	116
3-14	Agarose gel electrophoresis (1.5%) of RCR amplified of <i>bla</i> _{TEM} gene (1080bp) of <i>K. pneumoniae</i> ST 258	116
3-15	Agarose gel electrophoresis (1.5%) of RCR amplified of <i>bla</i> _{SHV} gene (930bp) of <i>K. pneumoniae</i> 258	117
3-16	Agarose gel electrophoresis (1.5%) of RCR amplified of <i>bla</i> _{CTX-M} gene (930bp) of <i>K. pneumoniae</i> 258.	117
3-17A	Alignment analysis of <i>Klebsiella pneumoniae</i> with Gene Bank at NCBI. Query represents of sample; subject represents a database of National Center Biotechnology Information (NCBI).	123
3-17B	Alignment analysis of <i>Klebsiella pneumoniae</i> with Gene Bank at NCBI. Query represents of sample; subject represents a database of National Center Biotechnology Information (NCBI).	124
3-17C	Alignment analysis of <i>Klebsiella pneumoniae</i> subsp. <i>pneumoniae</i> ST258 with Gene Bank at NCBI. Query represents of sample; subject represents a database of National Center Biotechnology Information (NCBI).	125
3-17D	Alignment analysis of <i>Klebsiella pneumoniae</i> subsp. <i>pneumoniae</i> ST258 with Gene Bank at NCBI. Query represents of sample; subject represents a database of National Center Biotechnology Information (NCBI).	126
3-18A1	Alignment analysis of <i>mrkD</i> gene of <i>Klebsiella pneumoniae</i> with Gene Bank at NCBI. Query represents of sample; subject represents a database of National Center Biotechnology Information (NCBI).	130
3-18A2	Alignment analysis of <i>mrkD</i> gene of <i>Klebsiella pneumoniae</i> with Gene Bank at NCBI. Query represents of sample; subject represents a database of National Center Biotechnology Information (NCBI).	131
3-18B1	Alignment analysis of <i>mrkD</i> gene of <i>Klebsiella pneumoniae</i> with Gene Bank at NCBI. Query represents of sample; subject represents a database of National Center Biotechnology Information (NCBI).	132
3-18B2	Alignment analysis of <i>mrkD</i> gene of <i>Klebsiella pneumoniae</i> with Gene Bank at NCBI. Query represents of sample; subject represents a database of National Center Biotechnology Information (NCBI).	133
3-18C1	Alignment analysis of <i>mrkD</i> gene of <i>Klebsiella</i>	134

Contents

	<i>pneumoniae</i> with Gene Bank at NCBI. Query represents of sample; subject represents a database of National Center Biotechnology Information (NCBI).	
3-18C2	Alignment analysis of <i>mrkD</i> gene of <i>Klebsiella pneumoniae</i> with Gene Bank at NCBI. Query represents of sample; subject represents a database of National Center Biotechnology Information (NCBI).	135
3-18D1	Alignment analysis of <i>mrkD</i> gene of <i>Klebsiella pneumoniae</i> subsp. <i>pneumoniae</i> ST 258 with Gene Bank at NCBI. Query represents of sample; subject represents a database of National Center Biotechnology Information (NCBI).	136
3-18D2	Alignment analysis of <i>mrkD</i> gene of <i>Klebsiella pneumoniae</i> subsp. <i>pneumoniae</i> ST258 with Gene Bank at NCBI. Query represents of sample; subject represents a database of National Center Biotechnology Information (NCBI).	137
3-18E1	Alignment analysis of <i>mrkD</i> gene of <i>Klebsiella pneumoniae</i> subsp. <i>pneumoniae</i> ST 258 with Gene Bank at NCBI. Query represents of sample; subject represents a database of National Center Biotechnology Information (NCBI).	138
3-18E2	Alignment analysis of <i>mrkD</i> gene of <i>Klebsiella pneumoniae</i> subsp. <i>pneumoniae</i> ST258 with Gene Bank at NCBI. Query represents of sample; subject represents a database of National Center Biotechnology Information (NCBI).	139
3-18F1	Alignment analysis of <i>mrkD</i> gene of <i>Klebsiella pneumoniae</i> subsp. <i>pneumoniae</i> ST258 with Gene Bank at NCBI. Query represents of sample; subject represents a database of National Center Biotechnology Information (NCBI).	140
3-18F2	Alignment analysis of <i>mrkD</i> gene of <i>Klebsiella pneumoniae</i> subsp. <i>pneumoniae</i> ST 258 with Gene Bank at NCBI. Query represents of sample; subject represents a database of National Center Biotechnology Information (NCBI).	141
3-19A1	Alignment analysis of <i>luxS</i> gene of <i>Klebsiella pneumoniae</i> with Gene Bank at NCBI. Query represents of sample; subject represents a database of National Center Biotechnology Information (NCBI).	142

Contents

3-19A2	Alignment analysis of <i>luxS</i> gene of <i>Klebsiella pneumoniae</i> with Gene Bank at NCBI. Query represents of sample; subject represents a database of National Center Biotechnology Information (NCBI).	143
3-19B1	Alignment analysis of <i>luxS</i> gene of <i>Klebsiella pneumoniae</i> with Gene Bank at NCBI. Query represents of sample; subject represents a database of National Center Biotechnology Information (NCBI).	144
3-19B2	Alignment analysis of <i>luxS</i> gene of <i>Klebsiella pneumoniae</i> with Gene Bank at NCBI. Query represents of sample; subject represents a database of National Center Biotechnology Information (NCBI).	145
3-19C1	Alignment analysis of <i>luxS</i> gene of <i>Klebsiella pneumoniae</i> with Gene Bank at NCBI. Query represents of sample; subject represents a database of National Center Biotechnology Information (NCBI).	146
3-19C2	Alignment analysis of <i>luxS</i> gene of <i>Klebsiella pneumoniae</i> with Gene Bank at NCBI. Query represents of sample; subject represents a database of National Center Biotechnology Information (NCBI).	147
3-19D1	Alignment analysis of <i>luxS</i> gene of <i>Klebsiella pneumoniae</i> subsp. <i>pneumoniae</i> ST258 with Gene Bank at NCBI. Query represents of sample; subject represents a database of National Center Biotechnology Information (NCBI).	148
3-19D2	Alignment analysis of <i>luxS</i> gene of <i>Klebsiella pneumoniae</i> subsp. <i>pneumoniae</i> ST 258 with Gene Bank at NCBI. Query represents of sample; subject represents a database of National Center Biotechnology Information (NCBI).	149
3-19E1	Alignment analysis of <i>luxS</i> gene of <i>Klebsiella pneumoniae</i> subsp. <i>pneumoniae</i> ST258 with Gene Bank at NCBI. Query represents of sample; subject represents a database of National Center Biotechnology Information (NCBI).	150
3-19E2	Alignment analysis of <i>luxS</i> gene of <i>Klebsiella pneumoniae</i> subsp. <i>pneumoniae</i> ST 258 with Gene Bank at NCBI. Query represents of sample; subject represents a database of National Center Biotechnology Information (NCBI).	151
3-19F1	Alignment analysis of <i>luxS</i> gene of <i>Klebsiella pneumoniae</i> subsp. <i>pneumoniae</i> ST 258 with Gene Bank at NCBI. Query represents of sample; subject represents a database of National Center Biotechnology Information (NCBI).	152
3-19F2	Alignment analysis of <i>luxS</i> gene of <i>Klebsiella pneumoniae</i> subsp. <i>pneumoniae</i> ST 258 with Gene Bank at NCBI.	153

Contents

	Query represents of sample; subject represents a database of National Center Biotechnology Information (NCBI).	
3-20	Phylogenic tree of <i>K. pneumoniae</i>	155
3-21	Phylogenic tree of <i>K. pneumoniae</i> sub-spp <i>pneumoniae</i> ST 258	156

List of Appendix

Subjects
Appendix (1): Questionnaire sheet
Appendix (2): Antibiotics by Vitek Report of <i>K. pneumoniae</i>

List of Abbreviations

<i>Abbreviation</i>	<i>Meaning</i>
CFU	Cell forming unit
CPS	Capsule polysaccharide
DAMB	Dimethyl amine benzaldehyde
EDTA	Ethylene diamine tetra-acetic acid
ESBL	Extended-spectrum beta-lactamase
gm	Gram
IMP	Imipenase
K2A	Capsule-associated gene A
LPS	Lipopolysaccharide
MBLs	Metallo—lactamases
MDE-MATE	Multidrug and hazardous compound extrusion family
MDR	Multi-drug resistant
MFS	Main facilitator superfamily
MR/K-HA	Mannose-resistant, Klebsiella-like hemagglutination
°C	Degrees Celsius
OM	Outer membrane
PBPs	Penicillin-binding proteins
PCR	Polymerase chain reaction
RND	Nodulation-cell-division family
SMR	Small multidrug-resistance family
TSI	Sugar Iron Agar
UTIs	Urinary tract infections
UV	Ultraviolet
VIM	Verona integron-boring metallo beta-lactamase

Chapter One

Introduction and Literatures Review

1.1 Introduction

Klebsiella pneumoniae is a type of Gram-negative bacteria that can cause infections in humans, particularly in individuals with weakened immune systems. *K. pneumoniae* infections can range from mild, such as urinary tract infections, to severe, such as pneumonia or bloodstream infections (Cillóniz *et al.*, 2019).

Klebsiella pneumoniae is commonly found in the environment, including soil and water, and can also be present in the digestive tract of healthy individuals without causing harm (Choby *et al.*, 2020). However, when the bacteria enter the bloodstream or other parts of the body where they should not be, they can cause infections. It is known for its ability to develop resistance to antibiotics, which can make it difficult to treat. This has led to an increase in the number of infections caused by multi-drug resistant strains of *K. pneumoniae*, particularly in healthcare settings (Paczosa and Mecsas, 2016).

Extended-spectrum beta-lactamase (ESBL) enzymes and multi-drug resistant (MDR) *K. pneumoniae* have increased drug resistance. *K. pneumoniae* also has virulence factors include lipid A (endotoxin), capsular polysaccharide, adhesins, and siderophores (Riwu *et al.*, 2020).

K. pneumoniae is divided into 77 serological types (K) based on its capsule polysaccharide (CPS) pathogenicity. Bacterial capsule hinder phagocytosis. *K. pneumoniae* capsular antigens K1 and K2 are particularly significant. Capsular polysaccharides, type 1 and type 3 pili, and biofilm formation are *K. pneumoniae* main virulence factors. These bacteria generate a thick extracellular biofilm as a virulence factor to cling to living or abiotic surfaces and resist antimicrobial treatments. Infections require biofilm-producing bacteria (Dai and Hu, 2022).

The genome of *K. pneumoniae* is approximately 5.5 million base pairs in size and contains around 5,000 to 6,000 genes. The genome of *K. pneumoniae* is composed of a single circular chromosome that contains the bacterium's genetic information. This chromosome is divided into several different regions, including a core genome that is conserved across different strains of *K. pneumoniae*, as well as variable regions that are unique to specific strains (Morgenroth-Rebin, 2023).

K. pneumoniae is known for its ability to acquire and transfer genes through horizontal gene transfer, which allows it to rapidly adapt to different environments and acquire resistance to antibiotics. As a result, the genome of *K. pneumoniae* can be quite diverse and can vary widely between different strains (Michaelis and Grohmann, 2023).

The *K. pneumoniae* genome has been extensively studied in recent years, and a number of virulence factors, antibiotic resistance genes, and other important features have been identified. This knowledge has helped researchers to better understand the biology of *K. pneumoniae* and to develop new strategies for diagnosing and treating infections caused by this bacterium. The *K. pneumoniae* capsule genome has gene clusters *cps*, *magA*, and *rmpA*. K1-specific capsular polymerase gene *magA* (35-Kbp) trans-acts to biosynthesize *cps*. *MagA* is identical to LPS glycosylation, transfer, and biosynthesis genes (Wang *et al.*, 2020).

rmpA can increase colony mucoidy of different *K. pneumoniae* serotypes and regulate additional capsular polysaccharide synthesis via plasmid. Pilli, protein, and bacterial adhesin are adhesives. *mrkD* encodes type 3 fimbria adhesion and extracellular matrix binding. *K. pneumoniae* uses enterobactin, yersiniabactin, and hydroxamate siderophores to get iron from host transport proteins transferrin and lactoferrin. *entB*, *ybtS*, *kfu*, and *iutA*

genes produce enterobactin, yersiniabactin, iron-uptake system, and hydroxamate siderophore) (Walker & Miller, 2020).

The strain *pneumoniae* ST 258 is a multi-drug resistant strain that has become a cause for concern in healthcare settings, as it is often associated with infections that are difficult to treat. This strain is resistant to multiple antibiotics, including carbapenems, which are often used as a last resort for treating bacterial infections. Infections caused by *pneumoniae* ST 258 can be severe and potentially life-threatening, especially in people with weakened immune systems or underlying health conditions. Preventive measures such as good hand hygiene, infection control practices, and appropriate use of antibiotics are crucial to prevent the spread of this strain and reduce the risk of infection (Ahn *et al.*, 2021).

Aim of Study

The study was aimed to evaluate some of *K. pneumoniae* virulence factors associated with pathogenicity by phenotypic and genotypic methods.

The objectives

1. Isolation and identification *K. pneumoniae* by different methods.
2. Phenotypic detection of some virulence factors (Hemolysin, Sidrophores, Haemagglutinin, Serum resistance, Lipase, Hyper viscosity, Gelatinase) and biofilm formation.
3. Study of antimicrobial susceptibility among the isolates.
4. Genotypic detection of *K. pneumoniae* sub spp. *pneumoniae* ST 258 by specific primer gene (*pilv-l* gene).
5. Colanic acid extraction and measurement of concentration.
6. Genotypic detection of some virulence genes (*fimH*, *mrkD*, *luxS* *magA* (*K1*), *wzy* (*K2*), *rmpA*, *bla* (*TEM*, *SHV*, *CTX-M*, *OXA-48*).
7. Determination of DNA sequencing for some important virulence genes (*luxS*, *mrkD*), ST258 (*pilv-l*).
8. Phylogenic tree of *mrkD*, *luxS* genes and new strain of *Klebsiella sub spp. pneumoniae* ST 258.

1.2 Literatures Review

1.2.1 *Klebsiella spp.*

It was named for the German microbiologist who made the initial discovery of it in 1834. *Klebsiella* is also known as Fried Landers Bacilli, after the person who first gave the bacteria that name, Fried Landers (Christodoulides, 2013). Except from *Klebsiella mobilis*, members of the genus *Klebsiella* are non-motile, non-sporulating, lactose-fermenting, oxidase-negative, urease-positive (aside from *K. terrigena*), catalase-positive, Triple Sugar Iron Agar (TSI) or liquefy gelatin-free (De Jesus *et al.*, 2015).

Gram-negative with a conspicuous polysaccharide capsule, containing a broad capsule rich in glucouronic acid and pyruvic acid, this significant thickness gives the colonies their glow and mucoid look on agar plates; growth temperature range: 12-43°C; optimum: 37°C. Isolates are non-haemolytic (gamma-haemolysis) when cultured on blood agar (Priyanka *et al.*, 2020).

Klebsiella can be found in single, double, or triple rows of rods with a diameter of 0.3-1.0 µm and a length of 0.6-6.0 µm. Large, mucoid (the degree of mucoidness depends on the amount of carbohydrate in the culture medium and varies from strain to strain), pink colonies are typical for *Klebsiella*, an facultative anaerobic bacterium, on MacConkey agar, indicating lactose fermentation and acid production (Ali & Sana'a, 2019).

1.2.2 Taxonomy of genus *Klebsiella*

Klebsiella is distinguished by a nomenclature in its taxonomy that reflects its interesting taxonomic history. *Klebsiella* (family Enterobacteriaceae) is a genus of bacteria that has historically been classified

into three species based on the diseases they were known to cause: *K. pneumoniae*, *K. ozaenae*, and *K. rhinoscleromatis* (Munk *et al.*, 2022).

New methodologies in taxonomy, such as numerical taxonomy, led to frequent reorganization of the species within this genus. Over time, three major categories—Cowan's, Bascomb's, and rskov's—emerged. From the early 1980s, environmental *Klebsiella* isolates that had been previously classified as "*Klebsiella*-like organisms" (groups J, K, L, and M) have progressively been classified into provisional taxa (Ali, 2021).

Four new species, *K. terrigena*, *K. ornithinolytica*, *K. planticola*, and *K. trevisanii*, emerged from these clusters. As a result of their shared DNA sequences, the final two species were lumped together in 1986 to form *K. planticola* (Navon-Venezia *et al.*, 2017). While *K. terrigena* and *K. planticola* were formerly thought to be of no clinical consequence and confined to aquatic, botanical, and soil settings, they have lately been discovered to appear in human clinical specimens (Rahman, 2017).

These results show that *K. planticola*, in particular, is often isolated from human illnesses (3.5%-18.5% of all *Klebsiella* species isolated in clinical settings). Almost half of these isolates were found in body fluids that come from the respiratory system, while the rest were found in wounds and urine (Lengerova, 2023).

It is challenging to determine the relevance of these strains as disease-causing agents because majority of the isolates were isolated from poly microbial specimens. 6 of the 94 isolates, however, were found in mono microbial specimens and so could be linked to specific infections. There may therefore be a third *Klebsiella* species that can infect humans, in addition to *K. pneumoniae* and *K. oxytoca* (Tsuka *et al.*, 2021).

Having Great Britain and the former Commonwealth countries stick to Cowan's classification while the United States uses rskov's classification has just added further complexity to the process of adopting a common nomenclature (Rufai and Singh, 2015). *K. pneumoniae* and *K. aerogenes* are both names for the same bacterium, although they have different meanings in different countries. The United States has led the way in convincing most European nations to adopt the rskov categorization system, which is currently the most widely used system worldwide (David *et al.*, 2919).

1.2.3 Epidemiology

Klebsiella species can be found almost wherever on Earth. *Klebsiella* can be found in the environment, including in sewage, soil, and on plants, and on the mucosal surfaces of mammals like humans, horses, and pigs. Similar to *Enterobacter* and *Citrobacter*, but unlike *Shigella* spp. and *E. coli*, which are found in people but not in nature, *Klebsiella* belongs to the genus of bacteria known as gram-negative rods (Martin *et al.*, 2016).

Saprophytically, *K. pneumoniae* lives in the human nasopharynx and intestines. From one study to the next, carrier costs can vary widely. The rate of detection in the nasopharynx is between 1 and 6%, while it is between 5 and 38% in stool samples. *Klebsiella* spp. are considered fleeting members of the flora since they are rarely discovered on human skin and cannot thrive there (Di Domenico *et al.*, 2017).

In a hospital setting, colonization rates rise precipitously with patient duration of stay, dramatically altering the prevalence of carriers. Carriage rates of *Klebsiella* are high even among hospital staff (Nekkab, 2018). Patients in hospitals have been shown to harbor organisms at a rate of 77% in their feces, 19% in their throats, and 42% on their hands. Antibiotic use,

rather than care delivery practices, may explain why *Klebsiella* colonization rates are so high in hospitals (Shaikh *et al.*, 2015).

The patient's history of antibiotic use is substantially related with the development of *Klebsiella*. A two- to fourfold rise in *Klebsiella* colonization rates was seen in one study 2 weeks after hospital admission; this increase occurred largely in individuals receiving antibiotics, especially in persons getting broad-spectrum or multiple medicines (Ohalete, 2016).

A significant factor in determining the colonization pattern in a healthcare facility is the local antibiotic policy. The discovery that individuals with hospital-acquired intestinal *Klebsiella* were four times as likely to contract a *Klebsiella* nosocomial infection as those without carriers highlights the significance of increased colonization (D'Angelo *et al.*, 2016).

Additionally, widespread antimicrobial therapy has frequently been blamed for the emergence of *Klebsiella* strains that are resistant to many classes of antimicrobials. Demands for techniques to avoid the overuse of antibiotics in prophylaxis and empirical therapy are growing as people realize that they can mitigate these unintended consequences through responsible antibiotic usage (Sathiya, 2018). The gastrointestinal tracts of patients and the hands of hospital staff are the most common reservoirs for the spread of *Klebsiella* in a hospital setting, second only to contaminated medical equipment and blood products (Padmini *et al.*, 2017).

Infectious diseases in hospitals, especially those caused by multi-resistant strains, are a major reason for concern. These bacteria were mostly *Klebsiella* strains that had developed resistance to aminoglycosides by the 1970s. Strains that can develop ESBLs, making them resistant to extended-spectrum cephalosporins, have evolved since 1982. (Ohalete, 2016).

Both *K. pneumoniae* and *K. oxytoca* isolates share the characteristic of resistance to ceftazidime. The β -lactamases of ceftazidime-resistant *Klebsiella* bacteria are most often of the SHV-5 type in Europe, although the TEM-10 and TEM-12 types are more common in the United States (Torres *et al.*, 2017). An estimated 5% of *K. pneumoniae* strains examined in the United States were found to produce extended-spectrum beta-lactamase, according to data from the National Nosocomial Infection Study. These strains appear to be significantly more common in Europe. Clinical *Klebsiella* isolates in France and England have been reported to have an ESBL producer frequency of 14–16%. (Sheu *et al.*, 2019).

The prevalence may be as high as 25% - 40% in certain areas or hospitals. As a result of the underestimation of the occurrence of ceftazidime-resistant isolates by the typical disc diffusion criteria used in the normal laboratory, the true percentage of such strains may be significantly greater (FarajzadehSheikh *et al.*, 2019).

Usually, plasmids are what mediate ESBLs. Multiresistant plasmids are common in strains because of the easy way which these plasmids can be passed between various Enterobacteriaceae family members. Hence, ESBL-producing isolates have evolved resistance to many different types of antibiotics (Mathers *et al.*, 2015). It is unfortunate that the emergence of these multidrug-resistant *Klebsiella* strains is accompanied by a relatively high stability of the plasmids encoding ESBLs. Patients have been found to still be colonized by ESBL-producing *Klebsiella* bacteria years after ceftazidime and other extended-spectrum cephalosporins have been stopped. Invasive operations and prolonged hospital stays appear to be the most common causes of infection with these strains (Sheu *et al.*, 2019).

Concerns have been raised over the necessity of testing every *Klebsiella* strain for ESBL production in recent years. Whether or whether a high percentage of ceftazidime-resistant strains are expected depends on the local epidemiological environment, although the answer is almost always yes (FarajzadehSheikh *et al.*, 2019).

In order to detect such isolates, two diagnostic techniques have been utilized most frequently up to this point. The double-disc synergy test, involves inoculating an agar surface with the test organism and then placing discs of clavulanic acid and an extended-spectrum cephalosporin, like ceftazidime, in close proximity to one another (Zaha *et al.*, 2019).

A number of measures have been recommended to prevent the nosocomial spread of *Klebsiella*, including strict adherence to basic epidemiological standards for the management of urinary catheters, intravenous tracheostomies, and wounds, as well as maintenance and care of equipment and good hand-washing practices. Montgomerie has provided a comprehensive study of the topic (Knight *et al.*, 2018). The regulation of antibiotic use in the hospital to prevent the misuse and overuse of antibiotics is another strategy to control *Klebsiella* infections. Nosocomial infection surveillance is also important for accumulating data that can be utilized to lower the prevalence of *Klebsiella* infections in hospitals (Torres *et al.*, 2017).

1.2.4 Pathogenesis

Klebsiella pneumoniae is a bacterium that can cause a variety of infections in humans, including pneumonia, urinary tract infections, wound infections, and bloodstream infections (Choby *et al.*, 2020). The pathogenesis of *K. pneumoniae* infections involves several factors, including:

1. Capsule: *K. pneumoniae* produces a thick polysaccharide capsule that protects the bacteria from host immune defenses. The capsule also helps the bacteria adhere to host cells and tissues.
2. Lipopolysaccharide: The lipopolysaccharide (LPS) on the surface of *K. pneumoniae* can cause inflammation and tissue damage in the host. LPS also helps the bacteria evade host immune defenses.
3. Fimbriae: *K. pneumoniae* produces fimbriae, which are thin, hair-like structures that help the bacteria attach to host cells and tissues.
4. Iron acquisition: *K. pneumoniae* requires iron for growth and survival, and it has several mechanisms for acquiring iron from the host, including siderophores and hemolysins.
5. Toxins: *K. pneumoniae* produces several toxins, including lipases, proteases, and endotoxins, which can cause tissue damage and contribute to the severity of infections.
6. Antibiotic resistance: *K. pneumoniae* is known for its ability to develop antibiotic resistance, which can make infections difficult to treat.

Overall, the pathogenesis of *K. pneumoniae* infections is complex and involves several virulence factors that allow the bacteria adhere to host cells, evade host immune defenses, and cause tissue damage (Hou *et al.*, 2022).

Nosocomial infections in people are commonly caused by bacteria of the genus *Klebsiella*. Among the *Klebsiella* species, *K. pneumoniae* is the most concerning because it is responsible for a sizable number of cases of urinary tract infections, pneumonia, septicemias, and soft tissue infections acquired in hospitals (Hasan *et al.*, 2021a). *Klebsiella* is primarily spread through the digestive system and the hands of healthcare workers. Nosocomial outbreaks are typically caused by these bacteria because of their rapid dissemination in

healthcare facilities (Piruozi *et al.*, 2019). Certain types of bacteria, the so-called extended-spectrum—lactamase (ESBL) producers, are commonly the source of *Klebsiella* spp. outbreaks in hospitals, especially in newborn wards, that are resistant to multiple antimicrobials (Pruss *et al.*, 2022).

Increases in the prevalence of ESBL-producing *Klebsiella* bacteria among clinical isolates have been seen during the past several years. As a result, there are fewer therapeutic alternatives available, which necessitate the development of novel approaches to the treatment of *Klebsiella* infections in healthcare facilities (Karlowsky *et al.*, 2022).

Recent discoveries concerning *Klebsiella* virulence factors have brought fresh insights into the pathogenic tactics of these bacteria, while the various typing methods remain valuable epidemiological tools for infection control (Hu *et al.*, 2021). Pathogenicity factors in *Klebsiella*, such as capsules or lipopolysaccharides, are currently being investigated as prospective candidates for vaccination efforts that may serve as immunological infection control methods (Ali *et al.*, 2022).

Yet, *Klebsiella* infections are almost always connected with a hospital stay. Opportunistic infections like *Klebsiella* spp. primarily infect immunocompromised patients with serious underlying illnesses like diabetes mellitus or persistent lung obstruction (Sendra *et al.*, 2022). *K. pneumoniae*, the most important species of *Klebsiella* from a medical standpoint, is the most common cause of nosocomial *Klebsiella* infections. *K. oxytoca* has been isolated from humans in quite small numbers. *Klebsiella* spp. are responsible for around 8% of hospital-acquired illnesses in the United States and Europe (Nibogora, 2020).

1.2.5 Virulence factors

Because host defense systems vary from site to site, *Klebsiella* virulence factors also vary based on the site of infection. Strains of *K. pneumoniae* that cause urinary tract infections (UTIs) are likely to have a different pattern of virulence factors than those isolated from the lungs of patients with pneumonia (Catalán-Nájera *et al.*, 2017).

1.2.5.1 Hemolysin production

Hemolysin is a cytolytic toxin produced by microorganisms with the virulence trait of erythrocyte lysis, which is linked to the microorganisms' pathogenesis (Van Cleemput, 2018). They are thought to play a significant role in the spread of germs, extraintestinal illnesses, and host nutrition release, and they may also modify host pathways by impacting host cell survival, inflammatory response, and cytoskeletal dynamics (Villa *et al.*, 2017).

K. pneumoniae hemolysin has a cytopathic effect on both vascular and non-vascular cells in culture. Morphological alterations proved that the cell had undergone lysis and was in the process of disintegrating its membrane and cytoplasmic architecture. Albumin and normal sera both reduce hemolysin's hemolytic action (Kontturi, 2020).

To account for their hemolytic and cytopathic effects, it is postulated that these agents modify the membranes' atomic structure. Differences in reactive site availability on cells or separate enzymes may be at the root of the observed variation (Palacios *et al.*, 2018). The cytolytic toxin regarded a significant virulence factor in a vast variety of Gram positive and Gram negative bacterial infections. The hemolysin is a major factor in the pathogenicity of *Klebsiella pneumonia* in a variety of animal models of extraintestinal illness (Sarowska *et al.*, 2019).

Alpha-hemolysin is a ubiquitous exotoxin produced by *K. pneumonia* that increases pathogenicity in a variety of clinical illnesses. Transmembrane holes are formed when the toxin attaches to its intended cell or protein-free liposomal target. Certain strains of *K. pneumoniae* are considered particularly dangerous because they produce a very infectious protein called alpha hemolysin. Microbes with hemolysin plasmids may be better able to utilize iron released from lysed erythrocytes, as proposed by (O'brien *et al.*, 2017).

Hemolytic *K. pneumonia* is commonly seen in extraintestinal infections, the production of hemolysin may be a virulence factor and responsible for pathogenicity. Research with genetically characterized strains in animal models has established hemolysin's significance as a virulence factor (Hauser *et al.*, 2016).

1.2.5.2 Sidrophores production

In environments with little iron stress, bacteria and fungi produce compounds called sidrophores (Latin for "iron carriers"), which are chelating agents specific to ferric ions despite their low molecular weight. The iron that these compounds scavenge from the environment is then made available to the microbial cell, as iron is a mineral that is virtually always necessary for cell growth and survival (Albelda-Berenguer *et al.*, 2019).

This has been linked to virulence processes in microbes that cause disease in both animals and plants. Also, they may be useful in agriculture and have potential clinical applications. Iron is required for nearly every biological action, including respiration and DNA synthesis, making it a vital element for all forms of life. In order to remove iron from these insoluble mineral phases, microbes secrete Sidrophores, which combine with ferric ions to create soluble Fe^{+3} complexes (Venkataramani, 2021).

Aerobic bacteria, like all other forms of life, need iron to carry out a wide range of metabolic activities within the cell. Heme proteins and ferritin, an iron-storage molecule, make up the bulk of the iron contained inside of cells (Fuhrmann, 2021). As iron outside of cells is strongly bonded to proteins, pathogenic bacteria that cause infections in humans and other animals must have a way to scavenge the iron they need from these proteins (Pal *et al.*, 2022).

In addition to competing with mammalian proteins like transferrin and lactoferrin for iron, siderophores have a very high affinity for iron and can solubilize and transport ferric iron (F^{+3}) in the environment. The vast majority of bacteria and fungi rely on siderophores, which are specialized iron transport molecules, to solubilize and transfer iron (Kreuder, 2016).

The use of chelating chemicals has been studied for their potential to combat a variety of human diseases and infections. There are some siderophores that are used therapeutically to treat chronic and acute iron overload disorders, and these are used to prevent iron toxicity in people. To counteract the risk of infection during treatment for iron excess, however, siderophores that are inactive against bacteria must be employed (Wilson *et al.*, 2016).

The transfer of antibiotics to microbes is a second clinical application of siderophores. Since they are too large to diffuse through the outer membrane porins, some Gram-negative bacteria are resistant to antibiotics. Nonetheless, the siderophores receptor allows the produced siderophores-antibiotic combination to enter the cell (Santos *et al.*, 2018).

As evidence of siderophores' biological significance, it has been shown that pathogenic bacterial mutants lacking siderophores are consistently less virulent in disease models. Hence, siderophores are substances released under

low iron stress that act as a particular ferric iron chelate agent, and it is used in the biological control of phytopathogenic fungus and bacteria because of these properties (Pokorzynski *et al.*, 2017).

While, all *K. pneumoniae* strains were shown to generate enterochelin, yersiniabactin production is up during pulmonary infection and up during *in vitro* iron-limiting growth circumstances, while aerobactin production is down during pulmonary infection and up during iron-rich conditions (Liu *et al.*, 2018).

The complexity of these siderophores systems *in vivo*, as well as the absence of definite research addressing the importance of these iron acquisition mechanisms, are likely to blame for the contradictory findings (Albelda-Berenguer *et al.*, 2019). It is produced by *Klebsiella* spp. and encoded by the *Yersinia* high-pathogenicity island, but its role in prevalence and pathogenesis is unknown. Most aerobactin is synthesized by genes carried on the plasmid ferric uptake regulator gene (*Fur*) (180 kilodaltons) that was isolated from *Klebsiella* (Arezes, 2015).

1.2.5.3 Lipopolysaccharide and serum resistance

The bactericidal impact of serum and phagocytosis by polymorphonuclear granulocytes make up the host's initial line of defense against invading pathogens. Specifically, complement proteins are responsible for mediating the bactericidal activity of the serum. These proteins form a membrane assault complex on the surface of the microbe following a cascade-like activation (Larsen *et al.*, 2019).

The terminal complement proteins C5b-C9 form a complex that causes a transmembranous opening in the outer membrane of gram-negative bacteria, which allows Na⁺ to enter the cell and causes osmotic lysis of the bacteria (Cubero *et al.*, 2019).

To activate the complement cascade, two distinct mechanisms can be used: the classic complement pathway, which normally requires specific antibodies, and the alternative complement pathway, which can be triggered even in the absence of antibodies. As a sort of innate immunity, the alternative pathway allows the host to respond to invading pathogens before particular antibodies have been generated (Wang *et al.*, 2016). A critical component of this defense system is the opsonin C3b, which is produced via activation of C3 in both complement pathways and then contributes to the development of the terminal C5b-C9 complex (Le Fournis *et al.*, 2020).

Pathogenic germs are adapting to this host defense by learning how to avoid the bactericidal impact of serum. Human serum has a bactericidal effect on most gram-negative bacteria, especially those that are harmless to humans, but pathogenic strains commonly show resistance to the serum. Serum resistance is a common trait among enterobacterial clinical isolates and has been linked to both the onset and severity of infections (Hancock *et al.*, 2021).

Since the serum bactericidal system's primary function is hypothesized to be to prevent microorganisms from invading and persisting in the blood, slight variations in the susceptibility of individual bacterial strains to this system may have a significant impact on both the likelihood that an infection will take hold and the length of time it will take to fully establish (Harder *et al.*, 2017). The precise process that makes some bacteria immune to serum. In addition to outer membrane proteins as TraT lipoprotein and porins, lipopolysaccharides (LPS) have also been linked to the development of invasive bacteria (Martin & Bachman, 2018).

There are two possible explanations for *Klebsiella*. It's possible that capsule polysaccharides have a surface structure that does not activate

complement, effectively covering and masking the underlying LPS. Yet, in some *Klebsiella* capsule types, the O side chains of the LPS can penetrate the capsule layer and enter the external milieu (Short *et al.*, 2020).

Because LPS can often activate complement, C3b is then deposited onto the LPS molecules. C3b is located far from the bacterial cell membrane because it is preferentially attached to the longest O-polysaccharide side chains. This stops membrane damage and apoptosis by inhibiting the production of the lytic membrane assault complex (C5b-C9) (Krzyżewska-Dudek *et al.*, 2022).

Serum resistance is determined not only by LPS's steric obstruction of the lytic complement action, but also by the amount of C3b deposited. Serum-resistant cultures have smooth LPS, which activates only the alternative complement pathway, in contrast to serum-sensitive strains, which activate both the classical and alternative complement pathways. Serum-sensitive strains activate both complement pathways, which increases the amount of deposited C3b, leading to more extensive damage and bacterial death (Whitfield *et al.*, 2020).

It is important to keep in mind that all prior research in this area has been conducted using organisms that express the O1 serotype. Despite O1 being the most common O antigen among clinical *Klebsiella* isolates, a variety of other O serotypes are identified; several of these are neutral polysaccharides. There were formerly 12 chemically distinct O kinds of *Klebsiella*, but structural studies have since reduced that number to 8. (Doorduyn *et al.*, 2016). It is not known if the O1 antigen alone or *Klebsiella* LPS in general confers serum resistance. Nevertheless, environmental factors influence the make-up and action of LPS, so serum resistance does not appear to be a fixed trait, even within a specific O serotype (Bhunja, 2018).

1.2.5.4 Capsular polysaccharide (CPS) (K-antigen)

Commonly, *Klebsiella* will produce a large capsule made of acidic polysaccharides. The capsular repeating subunits are divided into 77 serological kinds; these subunits are made up of four to six sugars and, very commonly, uronic acids (as negatively charged components) (Villa *et al.*, 2019).

Klebsiella virulence depends on the presence of capsules. Massive layers of the capsular material, which is fibrillated, cover the surface of the bacterium (Ghigo *et al.*, 2017). By doing so, the bacterium is shielded from both phagocytosis by polymorphonuclear granulocytes and death by bactericidal serum factors (Majkowska-Skrobek *et al.*, 2018).

Inhibiting the activation or uptake of complement components, particularly C3b, is likely the chemical mechanism at work here. *Klebsiella* capsule polysaccharides have been shown to decrease the development and functional capacity of macrophages *in vitro*, in addition to their antiphagocytic role (Alves, 2016).

In addition, mice displayed a dose-dependent decrease in the generation of antibodies to the particular capsular antigen after being injected with high doses of *Klebsiella* capsular polysaccharide (CPS), suggesting that such injections may cause immunological paralysis (Forsythe 2018). Despite widespread belief that *Klebsiella* CPS mediated virulence features, this view has lately been discarded due to substantial variation in virulence between capsular forms. In a mouse peritonitis model, bacteria expressing the capsule antigens K1 and K2 were found to be very virulent, while isolates of other serotypes showed low or absent virulence (Wyres *et al.*, 2019). *Klebsiella* serotypes K1, K2, K4, and K5 were more virulent than *Klebsiella* strains

expressing other capsule types in experimentally generated cutaneous sores (Alves, 2016).

Although only a small subset of the 77 distinct K antigens have been extensively examined for virulence, A strains expressing capsule types K1 and K2 are thought to be highly likely to be pathogenic (Abed *et al.*, 2016). In some cases, the mannose concentration in the CPS may be related to the virulence conferred by a given K antigen. Mannose—2/3-mannose or L-rhamnose—2/3-L-rhamnose are found in tandem in low-virulence capsular types such the K7 or K21a antigen (Mandour, 2018). Macrophages have a surface lectin that recognizes these sequences and facilitates opsonin-independent (complement- and antibody-independent) phagocytosis (Ghigo *et al.*, 2017).

The term "lectinophagocytosis" refers to a type of nonopsonic phagocytosis in which one cell recognizes another based on the surface carbohydrates of the target cell (Alves, 2016). Bacterial surface lectins, like fimbriae, or phagocyte lectins, which function as receptors, can mediate lectinophagocytosis. There should be a stronger correlation between infectious diseases and *Klebsiella* strains harboring capsule types lacking of these mannose or rhamnose sequences (Teng *et al.*, 2017).

In the past, researchers have found a wide variety of conflicting outcomes when trying to link specific *Klebsiella* serotypes to infection sites or symptoms. The most common capsular types reported in the various studies vary (Opoku-Temeng *et al.*, 2019). This could have been a result of serotype variations among different regions. Nonetheless, most studies concur that the K2 serotype is one of the most often found capsule types in individuals with a urinary tract infection (UTI), pneumonia, or bacteremia. Although K2 strains are extremely rare in the natural environment, they are

likely to be the most common serotype of human clinical isolates worldwide (Paczosa & Meccas, 2016).

Hence, the hypothesis of lectinophagocytosis is highly congruent with the reported preponderance of the K2 serotype in *Klebsiella* infections. Some *Klebsiella* serotypes, such the K2 type, are selected for because they lack features frequently present on bacteria that are recognized by the host's innate defense responses (Ghigo *et al.*, 2017).

1.2.5.5 Pili (Fimbriae)

Getting near to host mucosal surfaces and staying close by adhering to host cells are crucial first steps in any infectious process (adherence). In the *Enterobacteriaceae*, many forms of pili are responsible for the bacteria's sticky capabilities (Conover *et al.*, 2016). The pili, also called fimbriae, are filamentous outgrowths on the surface of bacteria that are not flagellar in nature. With a diameter of 1–11 nm and a length of up to 10 µm, these structures are made up of polymeric globular protein subunits (pilin) that have a molecular mass of 15–26 kDa (Wyres *et al.*, 2020).

The ability of pili to agglutinate erythrocytes from a variety of animal species is the primary method by which their existence is established. These adhesins are classified as either mannose-sensitive or mannose-resistant hemagglutinins (MSHA and MRHA, respectively) based on whether or not D-mannose inhibits the response. *Klebsiella spp.* has two of the most common pili forms found among enterobacteria (Martens *et al.*, 2018).

Common or Type 1 Pili: The type 1 pili are the most thoroughly studied bacterial adhesin. Guinea pig erythrocytes are agglutinated by MSHA. Located on the fimbrial shaft, the adhesion protein in this pilus type can bind to the mannose-containing trisaccharides on the host glycoproteins (Conover *et al.*, 2016).

Short oligomannose chains linked to the glycoproteins via N-glycosidic bonds likely make up the sugar structures. It is believed that the binding of bacteria to mucus or to epithelial cells in the urogenital, respiratory, and intestinal tracts is where these pili really shine in terms of their importance to bacterial pathogenicity (Ageorges *et al.*, 2020).

Studies on *E. coli* were the primary focus of elucidating their function in the etiology of UTI, but similar descriptions for *K. pneumoniae* have been made using animal models. While type 1 pili are typically linked to the development of lower UTIs, they may also play a role in the pathogenesis of pyelonephritis (Rana *et al.*, 2020). These structures have been demonstrated to bind to proximal tubulus cells very well in this environment. Binding to soluble, mannosyl-containing glycoproteins in urine, like the Tamm-Horsfall protein, or in saliva is also possible for type 1 fimbriae (Zalewska-Piątek *et al.*, 2020).

That type 1 pili mediate bacterial colonization of the urogenital and respiratory tracts can now be understood thanks to these results. When bacteria attach to respiratory tract cells, they weaken the body's natural defenses against colonization in the upper airways, allowing a growth of facultative pathogenic bacteria. Patients requiring prolonged mechanical breathing may be at increased risk for developing pneumonia due to this disability (Boopathi *et al.*, 2020).

Therefore, "phase variation" must be taken into account in evaluating the pathogenic role of type 1 pili. As was previously established, this form of adhesion facilitates bacterial colonization of the host mucosal surfaces through a very nonspecific binding. During infectious pathogenesis, pathogenic bacteria first colonize the mucous membrane, and then invade the underlying tissue (AL-Taai, 2016). Bacteria rely on type 1 pili to invade host

tissues, but once inside, they become useless because they stimulate an opsonin-independent leukocyte action called lectinophagocytosis (Follador *et al.*, 2016).

The hydrophilic nature of these pili weakens the repulsive forces between the bacterium and the leukocyte, allowing the adhesions to attach to specific mannose-containing receptors on the leukocyte surface (Laventie *et al.*, 2019).

The binding of adhesion molecules stimulates the leukocyte, which then ingests the bacterium and kills it inside the cell (Iliyasu *et al.*, 2020). To avoid being eliminated by this host defensive mechanism, bacteria suppress the expression of type 1 pili. This means that type 1 pili are crucial for host colonization, but their role in future stages of disease is less certain (Giannini *et al.*, 2019). It's pili of the Type 3 variety. Type 3 pili are the only fimbriae that agglutinate erythrocytes after they have been pretreated with tannin. Recent research has shown that type 3 pili are present in numerous enteric taxa, despite the label mannose-resistant, *Klebsiella*-like hemagglutination (MR/K-HA) suggesting otherwise (Kudinha, 2017).

In addition, serological tests demonstrated high antigenic variability among type 3 pili, indicating that type 3 pili are likely not universal among all enterobacterial taxa (Bonazzi *et al.*, 2018). Pili were first reported as the adhesion organelles of *Klebsiella* found in plant roots, but it was later discovered that they could also adhere to different types of human cells. Type 3 pili-expressing *Klebsiella pneumoniae* strains are able to colonize a variety of different epithelia, including those lining the lungs, the urinary system, and the blood vessels (Martens *et al.*, 2018).

To what extent this fimbrial type plays in the pathogenetic process is mostly unknown. The expression of type 3 pili in *Providencia stuartii* in

catheter-associated bacteriuria is the only piece of evidence connecting the type 3 MrkD hemagglutinin to disease to date (Uhlenbruck & Beuth, 2017).

Although this species is not typically found in the urine of non-catheterized or temporarily catheterized individuals, it is significantly more abundant in the urine of those who require long-term indwelling catheters (Jahan, 2018). *P. stuartii* ability to attach and persist to the catheter in the catheterized urinary tract by expression of the MR/K hemagglutinin was responsible for the greater prevalence of *P. stuartii* in catheter-associated bacteriuria (Ageorges *et al.*, 2020).

The relevance of these pili in infection, however, has not been studied using an experimental animal model. Unfortunately, the structure of the matching host receptors is unknown (Yero *et al.*, 2020). The adhesions of three previously unknown *Klebsiella* species have been discovered and described. CF29K, which is encoded on the R plasmid of *K. pneumoniae*, has been shown to mediate adherence to Intestine-407 and CaCo-2 human intestinal cell lines (Costa, 2019).

This type of adhesion appears to be identical to the CS31-A adhesive protein found in *E. coli* strains that cause diarrhea in humans and is a member of the K88 adhesion family. Evidence suggests that CF29K arises from horizontal gene transfer between *E. coli* and *K. pneumoniae* in the human gut, namely the transfer of the *cs31a* gene (Rana *et al.*, 2020). One more recently discovered *Klebsiella* adhesin appears to be formed of capsule-like extracellular material, and it mediates an adherence pattern defined by aggregative adhesion to intestinal cell types (Boopathi *et al.*, 2020).

The first two adhesions discussed above are not fimbrial, but a new fimbria called KPF-28 has been proposed as a third colonization component

of the human gut. Intriguingly, the vast majority of *Klebsiella pneumoniae* strains that generate ESBLs of the CAZ-5/SHV-4 type have this fimbrial type (Paczosa & Meccas, 2016). It is unclear, however, where these adhesions are most commonly seen, if they are expressed by various *Klebsiella* species, how they are isolated from their hosts, or what role they play in pathogenesis (Costa, 2019).

1.2.5.6 Other virulence factors

Klebsiella spp. cytotoxins (Endotoxins) and bacteriocins are just two of the many factors that contribute to their pathogenicity (Huszczynski *et al.*, 2020). Besides from producing both heat-labile and heat-stable endotoxins, *K. pneumoniae* may also create other virulence factors (Singha *et al.*, 2017).

Protein poisons called bacteriocins can be taken up by bacteria through specific surface receptors. Ghequire & Öztürk, (2018) are describe the mechanisms by which bacteriocins, produced by some bacterial species, inhibit or kill the growth of other, similar, or closely related bacterial strains, including inducing metabolic block, restricting DNA, inhibiting protein synthesis by effecting in *16S rRNA*, inhibiting peptidoglycan synthesis in the cell wall, and forming channels that allow ions to pass through the membrane (Haider, 2016). Klebocin, a bacteriocin made from *K. pneumoniae*, is divided into four classes (A, B, C, and D) based on whether or not the strain used a virulence factor in its production (Seo *et al.*, 2018).

1.2.6 Outer membrane proteins (OMPs)

Phospholipids, lipopolysaccharide (LPS), and outer membrane proteins make up Gram-negative bacteria's outer membrane (OM). Transport of molecules through membranes and their integrity rely on these proteins (Sperandeo *et al.*, 2017).

One of the most thoroughly studied OM proteins is OmpA, or outer membrane protein A. An eight-stranded all-next-neighbor antiparallel -barrel with small turns at the periplasmic barrel has been determined by crystallization (at a resolution of 1.65) (Patel *et al.*, 2017).

Several reports have pointed to OmpA's part in disease development. In order for *K. pneumoniae* to attach to and/or invade epithelial cells and macrophages, OmpA acts as a mediator (Paczosa & Mecsas, 2016). As a mediator of serum resistance, it may shield bacteria from the bactericidal effects of SP-D and SP-A, two lung collectins (Casals *et al.*, 2018).

On the other hand, OmpA is also a target of the innate immune system. In the innate immune system, neutrophil elastase is among the oxygen-independent weapons that degrades OmpA and causes cell death (Nady *et al.*, 2019). Serum amyloid protein A, an acute-phase protein, binds to OmpA, leading to enhanced bacterial absorption by neutrophils and macrophages (Gursky, 2020). By sensing pathogens, airway epithelial cells trigger signaling pathways that ultimately lead to the production of antimicrobial molecules, the expression of co-stimulatory molecules, and the release of cytokines and chemokines, all of which play an important role in the lung's defense against infections (Kuss & Kestra, 2020). CPS, the best-studied virulence factor of *Klebsiella pneumoniae*, is responsible for resistance to complement and antimicrobial peptide-mediated death. Also, isogenic CPS mutant strains are not as pathogenic as wild-type bacteria (Cole & Nizet, 2016).

There is substantial evidence that inflammatory responses are necessary for *Klebsiella infections* to be cured. By dampening the immune response of the host, CPS makes it easier for germs to thrive in a previously inhospitable environment (Alves, 2016).

It is unclear if *K. pneumoniae* uses any other parameters to regulate the inflammatory reactions of its hosts. Recombinant pure OmpA from *K. pneumoniae* has been shown in multiple investigations to trigger the production of inflammatory molecules in a TLR2-dependent manner in different cell types (Chang & Nizet, 2020).

Identifying *K. pneumoniae* OmpA could help activate host responses that ultimately result in the clearance of *K. pneumoniae* (Bengoechea & Sa Pessoa, 2019). Nonetheless, it's possible that the cellular responses to OmpA expressed in the complex lipid milieu of the bacterial OM differ from those to recombinant pure OmpA. (Viale & Evans, 2020).

1.2.7 Extended spectrum β -lactemase

Antibiotics like penicillin, cephalosporins, and even the monobactam aztreonam can be rendered ineffective by bacteria that produce extended-spectrum beta-lactamases (ESBLs). Researchers have found a correlation between infections caused by ESBL-producing organisms and negative outcomes (Andrews *et al.*, 2018).

Plasmid-mediated enzymes called extended-spectrum β -lactamases (ESBLs) impart resistance to all penicillins and cephalosporins, including sulbactam and clavulanic acid combinations and monobactams like Aztreonam (Singleton *et al.*, 2019).

Klebsiella pneumoniae, an opportunistic pathogen linked to severe infections in hospitalized patients, especially those who are immune-compromised due to other, more serious conditions, is the most prevalent bacteria found to produce ESBLs (Costa, 2019). Community- and ventilator-acquired pneumonia, urinary tract infections, abdominal diseases, and infections acquired through central venous catheters are all potential entry points for *Klebsiella pneumoniae* into the bloodstream (Roy, 2018).

ESBL-producing *Enterobacteriaceae* are common in both the community and in healthcare settings. The true prevalence of ESBL-producing microbes is likely underestimated because of the difficulty of accurately identifying them in clinical laboratory. Infections caused by these species are best treated with carbapenems (Al-Kaaby, 2016).

The epidemiology and therapy of bacteria that produce extended-spectrum beta-lactamases, as well as the many types of and methods for detecting these enzymes. There are other articles that go into greater detail about the clinical manifestations and diagnosis of infections caused by ESBL-producing organisms (Rakotovao-Ravahatra *et al.*, 2020).

Antibiotics are rendered useless when the beta-lactam ring is broken by enzymes known as beta-lactamases. In the 1960s, scientists in Greece found the first plasmid-mediated beta-lactamase in gram-negative bacteria. The patient (Temoniera) from whom it was first isolated inspired its name, TEM (Tanko *et al.*, 2020).

Later, a similar enzyme, designated TEM-2, was identified and characterized. It has the same biochemical features as TEM-1, but its isoelectric point was slightly different because of a single amino acid difference (Batabyal, 2018)

Among gram-negative bacteria, such as *Enterobacteriaceae*, *Pseudomonas aeruginosa*, *Haemophilus influenzae*, and *Neisseria gonorrhoeae*, these two enzymes are the most prevalent plasmid-mediated beta-lactamases. Penicillin and some other narrow-spectrum cephalosporins (such cephalothin and cefazolin) are hydrolyzed by TEM-1 and TEM-2. However, they are ineffective against oxyimino side chain cephalosporins of the next generation (cefotaxime, ceftazidime, ceftriaxone, and cefepime) (Tanko *et al.*, 2020).

This meant that a wide variety of bacteria that normally would have developed resistance to these antibiotics were initially susceptible to them. Due to the fact that sulfhydryl reagents have varying effects on substrate selectivity, a related but less prevalent enzyme was given the name SHV (Yanat *et al.*, 2017).

In Europe, *K. pneumoniae* and *Serratia marcescens* isolates with extended spectrum β -lactamase enzymes were initially discovered in 1983; in the United States, *K. pneumoniae* and *Escherichia coli* isolates were first described in 1989 (Tagliaferri *et al.*, 2019). Since then, the prevalence of bacteria that are able to manufacture ESBL enzymes has skyrocketed. The percentage of *K. pneumoniae* strains resistant to ceftazidime in the United States rose from 1.5% in 1987 to 3.6% in 1991; by 1993, as much as 20% of strains were resistant to ceftazidime in some teaching institutions (Widodo *et al.*, 2020).

1.2.7.1 Definition and Classification of ESBL

Beta-Lactam antibiotics are rendered useless by enzymes called beta-lactamases. To break down the structure and chemistry of these antibiotics, hydrolytic enzymes specifically target and cleave their chemical bonds. When it comes to antibiotic resistance, beta-lactamases with the ability to hydrolyze first-, second-, and third-generation cephalosporins, penicillins, and monobactams like aztreonam are considered to be ESBLs. Nevertheless, ESBLs are blocked by clavulanic acid and do not promote resistance to cephamycins (such as cefoxitin and cefotetan) or carbapenems (such as ertapenem, imipenem, and meropenem) (Agarwal *et al.*, 2023).

Beta-lactamases can be organized into two different categories. The Bush-Jacoby-Medeiros classification divides proteins into four functional categories (Groups 1–4), while the Ambler classification divides proteins

into four groups (A–D) based on their amino acid sequence similarity (Amraei *et al.*, 2022). They would be classified as serine beta-lactamases if they had a serine radical, or as metallo-beta-lactamases if they contained a zinc ion in their active site (Messasma *et al.*, 2021).

Metallic enzymes belonging to the class B beta-lactamase family require zinc ions to catalyze the breakdown of beta-lactam antibiotics. Zinc ions are used to break down the beta-lactam ring of the antibiotics (Lima *et al.*, 2020). Classes A, C, and D include enzymes that hydrolyze substrates via a serine at the active site after an intermediate has been formed, such as an acyl enzyme. By utilizing the free hydroxyl group on the serine residue side chain at the active site of the enzyme, serine beta-lactamases are able to hydrolyze the antibiotic's beta-lactam ring and render it inactive by forming a covalent acyl ester (Tooke *et al.*, 2019).

Group 1 cephalosporinases are C-class molecular enzymes. Most Enterobacteriaceae chromosomes have genes for these enzymes. These compounds are more effective than benzylpenicillin in inhibiting the growth of cephalosporins (Alfei & Schito, 2022).

They are effective against cephamycins, and there are even a few that are ineffective against ceftazidime. Both clavulanic acid and carbapenems are ineffective against these enzymes. Low expression of AmpC (cephalosporinase) can be increased in some species by exposure to specific beta-lactams, such as ampicillin, in the cases of *Pseudomonas aeruginosa*, *Serratia marcescens*, and *Enterobacter cloacae*. Triple antibiotic therapy with amoxicillin, imipenem, and clavulanic acid (Srivastava *et al.*, 2023).

In addition to the 2br subgroup of plasmid-mediated ESBLs, Group 1 also includes plasmid-mediated enzymes of the Amp type (ACT), ceftazidime (FOX), cephamycin (CMY), MIR (named after the Miriam Hospital in

Providence), and DHA (named after the Dhahran Hospital in Saudi Arabia) (Akpaka *et al.*, 2021).

Group 2 serine beta-lactamases, which include the A and D molecular classes, make up the biggest subgroup of beta-lactamases. Except for the 2nd subgroup, which is part of the D group, all of the molecules in question are part of the A group. Subgroup 2a penicillinases are a small group of beta-lactamases found primarily in Gram-positive bacteria. Because of their low affinity for penicillin, these enzymes are unable to hydrolyze carbapenems or cephalosporins (Abdul-Mutakabbir *et al.*, 2020).

Group 3 and molecular class B are the correct classifications for the metallo—lactamases (MBLs). To function properly, these enzymes need zinc ions in their active sites. For the purpose of classification, their ability to hydrolyze carbapenems in a manner analogous to that of serine beta-lactamases was used as a criterion. Its hydrolyzing activity for monobactams is limited, and they are not inhibited by clavulanate like serine beta-lactamases but by ethylene diamine tetra-acetic acid (EDTA) (Sawa *et al.*, 2020).

These enzymes are typically found in combination with a second or third beta-lactamase in clinical isolates. The three categories are B1, B2, and B3 for structural classifications and 3a and 3b for functional classifications. Imipenase (IMP) and Verona integron-boring metallo beta-lactamase (VIM) are examples of the B1 subclass and are members of the 3a subgroup (Akpaka *et al.*, 2021).

1.2.7.2 General structure and function of ESBLs

Antibiotic resistance among infectious pathogens is a global crisis that threatens human ability to effectively treat infectious diseases. This trend is

largely attributable to the increased use/misuse of antibiotics in human health, agriculture, and veterinary settings (Subramaniam & Girish, 2020).

Antibiotic resistance among germs that cause either common diseases or those acquired in hospitals is rising at a worrying rate. Multidrug-resistant bacteria such *E. coli*, *Klebsiella pneumoniae*, *Acinetobacter baumannii*, methicillin-resistant *Staphylococcus aureus*, penicillin-resistant *Streptococcus pneumoniae*, vancomycin-resistant *Enterococcus*, and extensively drug-resistant *Streptococcus pyogenes* are of special concern. TB (caused by the *mycobacterium* species) (Moussa *et al.*, 2021).

Globally, Gram-negative bacteria are the most common cause of resistance to β -lactam antibiotics due to their widespread usage in the treatment of bacterial illnesses. Overexposure of bacteria to several -lactams has led to the constant and dynamic creation and mutation of -lactamases in these bacteria, allowing them to become resistant to even the most cutting-edge β -lactam antibiotics (Jeffs & Lohans, 2022).

Extended-spectrum β -lactamases (ESBLs) are the name given to these enzymes. The scientific community is very concerned about finding a solution to the problem of treating organisms that are resistant to several drugs. It is challenging to resolve the occurrence of ESBL-producing organisms on a global basis for a number of reasons, including the difficulties in identifying ESBL production and variations in reporting. Infections caused by extended-spectrum beta-lactamases (ESBLs) have been on the rise recently (Brooks, 2021).

1.2.7.3 Mode of action of ESBLs

The mode of action of ESBLs is to break down the beta-lactam ring, which is a key component of many beta-lactam antibiotics. This ring is essential for the antibiotics to be effective in inhibiting bacterial cell wall

synthesis. ESBLs can break down this ring by cleaving the amide bond in the beta-lactam ring, resulting in the inactivation of the antibiotic (da Costa de Souza *et al.*, 2022). ESBLs are able to confer resistance to a broad range of beta-lactam antibiotics, including third- and fourth-generation cephalosporins, which are commonly used in the treatment of bacterial infections. This makes infections caused by bacteria producing ESBLs difficult to treat, as these bacteria are often resistant to multiple antibiotics (Lin & Kück, 2022).

1.2.8 Mechanism of resistance to β -lactam antibiotics

There is a class of antibiotics known as beta-lactams that targets the bacterial cell wall. These antibiotics consist of things like penicillin, cephalosporins, carbapenems, and monobactams. They interfere with the activity of carboxypeptidases and transpeptidases by binding to them. These enzymes, known as penicillin-binding proteins (PBPs), are responsible for generating the peptidoglycan cell wall that surrounds the bacteria by catalyzing the D-ala D-ala cross links. The integrity of the cell wall is compromised, which ultimately results in cell death (Nicoletti, 2020).

Bacterial resistance to β -lactams likely developed early in the evolution of bacteria, but has only recently become a beneficial and consequently chosen feature due to the widespread use of β -lactam antibiotics. Using a Darwinian approach, these medications selected for resistance by killing vulnerable bacteria while leaving resistant strains alive (Pereira *et al.*, 2022). Resistance to these antibiotics may be innate to certain species. It's also possible to pick up the trait through natural mutation or a genetic exchange. Resistance to β -lactams can arise for a number of different functional reasons, including the generation of lactamases, impermeability, efflux, and

target alteration. It is possible for these modalities to occur alone or in many permutations (Darby *et al.*, 2022).

Resistance in gram-positive cocci, such as pneumococci and methicillin-resistant *Staphylococcus aureus* (MRSA), is typically caused by alterations to the normal PBPs or the acquisition of new β -lactam-insensitive PBPs. When it comes to gram-negative bacteria, however, resistance is typically the result of a combination of naturally up-regulated impermeability and efflux, as well as endogenously acquired beta-lactamases (Jubeh *et al.*, 2020).

Despite the fact that PBPs are the primary targets of β -lactam antibiotics, these medicines also covalently target other enzymes. 1,d-transpeptidases (Ldts) are a family of enzymes responsible for forming alternative peptide cross-links in bacterial peptidoglycan, and they are inhibited by certain β -lactam subclasses (Atze, 2021).

Covalent complexes formed from β -lactams and Ldts are often stable, like those formed from PBPs, and they prevent peptidoglycan transpeptidation from occurring. Certain β -lactams have been shown to inhibit the activity of serine and cysteine proteases, in addition to other protein families (Mora-Ochomogo & Lohans, 2021).

All bacterial genomes contain single- and multidrug efflux pumps, proving their pervasiveness in microorganisms. Many bacterial strains' innate resistance phenotypes involve these mechanisms. Additionally, mutational alteration of the structural gene, overexpression owing to mutation in regulatory genes, or horizontal transfer of genetic elements can all result in clinically significant acquired resistance (Grézal *et al.*, 2023).

In bacteria, secondary transporters called efflux pumps facilitate the elimination of poisons by a coupled exchange of protons. There are a

number of different superfamilies of multidrug pumps. These include the main facilitator superfamily (MFS), the small multidrug-resistance family (SMR), the resistance nodulation-cell-division family (RND), and the multidrug and hazardous compound extrusion family (MDE) (MATE) (Henderson *et al.*, 2021).

MFS pumps are tightly associated to specific efflux pumps and appear to function as significant Na⁺/ H⁺ transporters, while the RND and MATE systems appear to function as detoxifying systems and transport heavy metals, solvents, detergents, and bile salts. In Gram-negative bacteria, the RND pump is part of a tripartite transport system that also includes outer membrane channel proteins and periplasmic membrane fusion proteins; in Gram-positive bacteria, MFS and SMR pumps are more common (Jagessar, 2020). Because of this, the pumps can release their substrates into the extracellular space without first passing them via the inner membrane or the cytoplasm. Some pumps, like MexY can transport aminoglycosides despite conferring resistance primarily to a wide variety of lipophilic and amphiphilic medicines (such as β -lactams, fluoroquinolones, tetracyclines, macrolides, and chloramphenicol) (Scoffone *et al.*, 2021).

1.2.9 Biofilm formation

Microorganisms and their extracellular products accumulate to establish a population on a surface in the form of a biofilm. Placing a foreign object, like a medical device, into a human body is fraught with risk due to biofilm formation (Khatoon *et al.*, 2018).

One of the many forms bacteria take on as they multiply is a biofilm. The biofilm growth phenotype describes a bacterial community in which the bacteria are arranged in a sessile aggregation (Del Pozo, 2018). When bacteria establish a biofilm inside a human host, the illness becomes

persistent and is difficult to treat. Extreme resistance to antibiotics and many other conventional antimicrobial agents and an excessive capacity to evade the human defenses are major features of persistent biofilm-based illnesses (Mahamuni-Badiger *et al.*, 2020).

Matrixes of exopolysaccharides, proteins, and extracellular DNA encapsulate colonies of bacteria that have adhered to a surface. Up to 80% of microbial infections in humans and many hospital-acquired diseases are thought to be aided in their persistence and aggressiveness by biofilm formation, especially in situations where implanted medical devices are necessary (Khelissa *et al.*, 2017).

As biofilm-associated bacteria have been shown to be 10-1,000 times more resistant to antibiotic treatment than planktonic cells, it is notoriously difficult to eradicate already-established biofilm infections. Human diseases rely on biofilms to survive in the environment, spread to new hosts, and become more infectious due to the boost in their own infectiousness (Kırmusaoğlu, 2016).

Biofilms are a type of microbial community comprised of cells that are attached to an interface, embedded in a matrix of exopolysaccharides, and demonstrate an altered phenotype. With the steadily increasing number of biomaterial devices used in urology, biofilm formation and device infection is becoming an increasingly pressing issue. Researchers have found that biofilm formation starts as soon as a catheter is inserted, when microbes adhere to a conditioning coating of host proteins on the catheter's surface (Poomathi *et al.*, 2020).

Biofilms are populations of bacteria that dwell in close proximity to surfaces. Biofilm bacteria differ greatly from their planktonic relatives. Biofilm bacteria are distinguished by the fact that their cells aggregate into

larger structures and are enclosed in an extracellular matrix that the bacteria themselves manufacture (Greene *et al.*, 2016).

Some of the cells in a colony of bacteria are metabolically dormant because their extracellular matrices shield them from outside aggression and act as a diffusion barrier for tiny molecules (Bunyan *et al.*, 2019).

Even in communities of sessile biofilms, no sessile individuals can arise and quickly proliferate and disperse. Therefore, biofilms not only shield bacteria from human defense processes like phagocytosis, but also provide a supply of resistant bacteria during antimicrobial therapy (Sharahi *et al.*, 2019).

Biofilm development is suspected in about 60% of bacterial illnesses being treated by doctors in the developed world. The methods that bacteria use to build biofilms are extremely diverse, varying even within strains of the same species, despite the fact that several aspects are recognized as general qualities of biofilm development. Not yet identified are genes that are expected to play essential roles in biofilm formation (Khatoon *et al.*, 2018).

At first, physical forces or bacterial appendages like flagella bring planktonic microbial cells to the conditioned surfaces. Bacterial biofilms have been associated to a variety of diseases and health problems, including CF, periodontitis, and nosocomial infections caused by medical devices including catheters and artificial heart valves (Schilcher & Horswill, 2020). Yet, there is evidence of biofilm generation in these facilities as well; bacterial populations of pathogenic and spoilage microorganisms have been isolated from biofilms (Alav *et al.*, 2018). Because the microbes in biofilms are so resistant to antimicrobial medicines, they constitute a public health

risk for people who rely on indwelling medical devices (Choudhary *et al.*, 2020).

Recalcitrance is a hallmark of the biofilm lifestyle that enables pathogenic biofilms to persist in the face of high antibiotic concentrations, ultimately leading to treatment failure and infection recurrence (Møretrø & Langsrud, 2017). Ultraviolet (UV) light, heavy metals, acidity, changes in hydration or salinity, and phagocytosis are all overcomeable by bacteria living in a biofilm (Delcaru *et al.*, 2016).

Many of the treatment challenges seen in clinical settings can be traced back to the fact that bacteria in biofilms have a unique capacity to resist antibiotic-mediated death (Balaure and Grumezescu, 2020). Attached bacteria, those found in biofilms, are those that have entered a stationary or latent growth phase and have phenotypes that are unique from those of planktonic bacteria. Bacteria in biofilms are highly resistant to drugs and other environmental stressors. This shift in phenotype is believed to be the outcome of a complicated and tightly regulated process (Orazi & O'Toole, 2019).

1.2.10 Antibiotic susceptibility test

Infections brought on by *Klebsiella* are often treated with broad-spectrum antibiotics such as cephalosporins, fluoroquinolones, aminoglycosides, and carbapenems, however resistance to these drugs has been observed (Ur Rahman *et al.*, 2018).

ESBL, which hydrolyze oxyimino beta-lactams including cefotaxime, ceftriaxone, ceftazidime, and monobactams, have been linked to beta-lactam resistance. Nevertheless, they have no effect on cephamycins, carbapenems, and similar chemicals (Okoche *et al.*, 2015).

Klebsiella pneumoniae is the most widespread drug-resistant bacteria, and it can show resistance to various medications or even to all antibiotics now in use (Wyres & Holt, 2018). One of the most prominent causes of drug resistance today is the presence of genes encoding enzymes with an extended spectrum β -lactamase (ESBL) (Navon-Venezia *et al.*, 2017).

Heterogeneous ESBLs hydrolyze nearly all β -lactam antibiotics, with the exception of carbapenems and cephamycins. Treatment with β -lactamase inhibitors like clavulanic acid and tazobactam can stop their spread (Li & Webster, 2018).

Most extended-spectrum β -lactamases (ESBLs) fall under subgroup 2be of the β -lactamase categorization system developed by Bush and Jacoby. The bla_{SHV-1} and bla_{TEM-1} genes found naturally in bacteria are mutated and modified to create plasmid-encoded ESBL resistance genes (Younes, 2011). These genes often occur in clusters with other resistance genes, leading to a co-resistance profile that includes resistance to antibiotics other than β -lactams such as aminoglycosides and tetracyclines (Karuniawati *et al.*, 2013).

There are two basic signs of β -lactam antibiotic resistance: the formation of β -lactamase enzymes due to the presence of β -lactam-insensitive cell wall transpeptidases, or the active ejection of β -lactam molecules from Gram-negative bacteria. For the treatment of infections caused by ESBL-producing bacteria like *K. pneumoniae*, carbapenems are the β -lactam of choice. To treat the most severe healthcare-associated infections, these antibiotics are sometimes the very last option (Derakhshan *et al.*, 2016).

However, it is well known that the prevalence of bacteria resistant to carbapenems has increased. This problem has been compounded by the evolution of mechanisms such as beta-lactamases, efflux pumps, and mutations that alter the expression and/or function of porins and penicillin-

binding proteins (PBPs). The horizontal transfer of resistance genes, which can also transport virulence determinants, is a common mechanism for the dissemination of plasmids that cause antimicrobial resistance (Navon-Venezia *et al.*, 2017). In order to survive in a hostile environment, pathogens must acquire resistance and virulent features, and there is evidence to show that this process plays a crucial role in the pathogenesis of *K. pneumoniae* infections (Ur Rahman *et al.*, 2018).

1.2.11 *K. pneumoniae* sub spp. ST 258

Klebsiella pneumoniae has developed resistance to carbapenems due mostly to the presence of carbapenemases that were not present in the strains that were originally susceptible. Class A (KPC, GES), B (VIM, IMP), and D (OXA-48) carbapenemases are all examples. The *K. pneumoniae* carbapenemases are the most prevalent class A carbapenemases in this pathogen (KPCs) (El-Badawy *et al.*, 2020).

First identified in the United States in 2001, KPC-producing *K. pneumoniae* strains have now been found in Europe, Israel, South America, and China. In 2010, bronchial aspirates from a patient in the intensive care unit (ICU) in Korea were the source of the first KPC-2-producing *K. pneumoniae* strain in the country. Nevertheless, because KPC-producing *K. pneumoniae* also make VIM or CTX-M, it is challenging to choose the right medications to treat infections caused by these bacteria. Patients infected with KPC-producing isolates have a much greater mortality rate than those infected with imipenem-resistant isolates (Ben Tanfous *et al.*, 2017).

During the course of the last few decades, sequence type 258 (ST258) CRKP strains have proliferated all over the world. The presence of plasmid-encoded *K. pneumoniae* carbapenemases in this genetic lineage has been linked to multiple hospital-associated outbreaks, making it a public health

concern (KPCs). Infections caused by multidrug-resistant *Enterobacteriaceae* have fewer treatment options because KPC enzymes hydrolyze all β -lactam drugs (Yang *et al.*, 2021).

The persistence of CRKP ST258 and the dissemination of KPCs to other hospital infections are both facilitated by the easy way which plasmids encoding KPCs are horizontally transferred and recombine in the hospital setting. Carbapenemases can spread even when carbapenems aren't being selected for because of extra antibiotic resistance genes on KPC plasmids. ST258 is a "high-risk" CRKP lineage because of its worldwide prevalence, epidemic character, and capacity for rapid dissemination of numerous antibiotic resistance determinants (Paul *et al.*, 2022).

Depending on the capsular and plasmid gene content, ST258 strains can be roughly classified into two separate clades. Plasmid-encoded KPC-2 is more common in clade I ST258 isolates, while plasmid-encoded KPC-3 is more common in clade II ST258 genomes (Marsh *et al.*, 2019). Resistance to colistin therapy and ceftazidime-avibactam therapy has been reported in several recent studies conducted at the institution, primarily among clade I and clade II ST258 isolates. Further illustrating the danger posed by this family in healthcare facilities, several outbreaks linked to ST258-affected devices previously was identified (Giddins *et al.*, 2018).

1.2.12 Virulence genes of *Klebsiella pneumoniae*

The gene clusters *cps* (for capsule polysaccharide synthesis), *magA* (for mucoviscosity associated gene A) and *rmpA*, make up the capsule genome of *K. pneumoniae* (Shakib *et al.*, 2018).

K1-specific *MagA* (35 kilobase pairs) was shown to be a trans-acting activator for *cps* biosynthesis and a capsular polymerase gene. In addition,

magA shares homology with genes implicated in LPS glycosylation, transfer, and biosynthesis (Hadjineophytou *et al.*, 2019).

K. pneumoniae primary virulence component, *magA*, was identified in 2004. According to the literature, *rmpA* acts as a plasmid-mediated regulator of additional capsular polysaccharide synthesis and can increase the colony mucoidy of several *K. pneumoniae* serotypes (Fu *et al.*, 2018). To name a few examples of adhesives, we have Pilli, the construction of proteins, and bacterial adhesion to their hosts. The *mrkD* gene encodes type 3 fimbria adhesion and acts as a mediator of binding to the extracellular matrix (Luo *et al.*, 2017).

Enterobactin, yersiniabactin, and hydroxamate siderophore are all examples of siderophores (iron-bound) that *K. pneumoniae* uses to steal iron from the host transport proteins transferrin and lactoferrin. Genes for enterobactin, yersiniabactin, the iron-uptake system, and the hydroxamate siderophore *iutA*, *kfu*, and *iutA* (Mitri *et al.*, 2020).

The discovery of the bacterial virulence factors is crucial for the advancement of both new diagnostic tools and therapeutic strategies. K serotypes and the high mucoviscosity phenotype, the invasive character of some *K. pneumoniae* isolates, have been the primary focus of research into the virulence determinants of *K. pneumoniae* related with liver abscess formation (Jian-Li *et al.*, 2017).

In addition to yersiniabactin (Ybt), aerobactin, and *rmpA*, the other potential virulence factors have been described. Knockout of the *rmpA* gene can decrease virulence in mouse lethality tests by a factor of 1000, and ybt is a phenolate-type siderophore, structurally distinct from *ent*; the aerobactin and *rmpA* genes have been found to be simultaneously located on a 180-kilobase plasmid (Cárdenas *et al.*, 2018).

Key to *K. pneumoniae* pathogenicity is the iron chelator aerobactin, also known as iron Sidrophore, which has been shown to boost virulence lethality experiments by a factor of 100 (Ku *et al.*, 2017a).

K. pneumoniae isolates with the hyper mucoviscosity phenotype and the presence of the *rmpA* and aerobactin genes were highly virulent for mouse lethality when injected intra peritoneally, with a 50% lethal dose (LD50) of 10² cell forming unit (CFU) of bacteria. Two of the 77 capsular serotypes, K1 and K2, are responsible for extremely harmful infections in humans (Lee *et al.*, 2017). Capsular serotype K1 only has access to the mucoviscosity-associated gene A (*magA*), while serotype K2 only has access to the capsule-associated gene A (*K₂A*). Liver abscesses are a common complication for both serotypes (Paczosa, 2017).

However, there is a lack of information about infections caused by K1 and K2 serotypes at sites other than the liver. The synthesis of capsular polysaccharides is controlled by the regulator of mucoid phenotype A (*RmpA*) gene, which can be located on a plasmid or the genome. It enhances capsule production in hyper virulent *K. pneumoniae* (hvKP) (hvKP). *MagA* and *K₂A* are considered important in pathogenesis of hvKP infections. In this way, LPS prevents bacteria from being killed by the immune system's complement system. The *uge* (uridine diphosphate galactose 4-epimerase) gene controls its production (Ku *et al.*, 2017b).

K. pneumoniae lacks this gene and thus has a diminished capacity to cause genitourinary tract infections, pneumonia, and septic shock. *fimH-1* is the gene encoding for fimbriae and mediates bacterial adhesion. Type 1 fimbriae are expressed in 90% of *K. pneumoniae* and mediate adherence to many types of epithelial cells, especially the bladder epithelium (Remya *et al.*, 2019).

Chapter Two

Materials and Methods

2.1 Materials

2.1.1 Laboratory Instruments and Equipment

All laboratory instruments and equipment were listed in Table (2-1), (2-2).

Table (2-1): Laboratory Instruments and Equipment

No.	Instruments and Equipment	Company	Country
1.	Applied Biosystems™ ProFlex™ PCR System	Fisher Scientific	USA
2.	Autoclave	Stermite	Japan
3.	Benson burner	Satorins	Germany
4.	Centrifuge	DLAB	Ghain
5.	Cooling box Ningbo	Ningbo	China
6.	Digital camera	Samsung	Japan
7.	Distillator	GFL	Germany
8.	DNA extraction tubes.	Eppendorf	Germany
9.	Gel electrophoresis	Clarivate	UK
10.	Hood	GFL	Korea
11.	Incubator	Memmert	Germany
12.	Light microscope	Olympus	Japan
13.	Micropipettes of different size	Eppendorf	Germany
14.	Nano drop system	Optizen	Korea
15.	Oven	Memmert	Germany
16.	Platinum wire loop	Himedia	India
17.	Refrigerator	Concord	Italy.
18.	Sensitive electron balance	Sartorius	Germany
19.	Sterile swab for streaking	Lab. Service	S.P.A.
20.	UV-transilluminator	Vilber Lourmat	Farance
21.	Vortex	Fisher Scientific	USA
22.	Water bath	Memmert	Germany

Table (2-2): Instruments and Disposable Materials

No.	Item	Company	Country
1.	Beakers	BBL	USA
2.	Filter papers whatman	Schleicher and Schuel	USA
3.	Glass slides	Sail brand	China
4.	Medical cotton	MedicareHygiene Limited	India
5.	Medical gloves	Sail brand	China
6.	Microscopic Cover slide	Gitoglas	China
7.	Para film	Biobasic	Canada
8.	PCR tubes 1.5, 200µl (Eppendorf)	Biobasic	Canada
9.	Petri dishes	Blastilab	Lebanon
10.	Plastic test tubes 10ml.	AFCO	Jordan
11.	Screw capped bottles (30ml)	Blastilab	Lebanon
12.	Sterile swabs	Sail brand	China
13.	Syringes, Tips	MedicareHygiene Limited	India
14.	Tubes 10ml	MedicareHygiene Limited	India
15.	Tips (Different sizes)	Jippo	Japan

2.1.2 Chemical and Biological Materials

2.1.2.1 Chemical Materials

The chemical materials were listed in Table (2-3).

Table (2-3) Chemical Materials

N0.	Chemicals	Company/country
1.	Agarose	Carl Roth/Germany
2.	Alcohol (Ethanol) 70% and 95%.	Fluka/ Germany
3.	Catalase reagent	Schuchariot/ Germany
4.	Gelatin, Barium chloride, Sulfonic acid	B.D.H / England
5.	Glycerol	Fluka /England
6.	Gram Stain kit	Crescent/KSA
7.	Hydrogen peroxide, Alpha-nepthol, pepton	Fluka /England
8.	NaCl, Na ₂ HPO ₄ , KH ₂ PO ₄ , NH ₄ Cl, MgSO ₄ CaCl ₂ , NaOH, phosphate buffer, H ₂ SO ₄	Merk Darmstadt/ Germany
9.	Nuclease free water (1.25) ml	Promega(USA)
10.	Oxidase reagent, Kovas reagent	Himedia / India
11.	Ethidium Bromide staining souluion	Intron / Korea
12.	TAE buffer10 X	Carl Roth/Germany
13.	Voges-Proskauer reagent	England

2.1.2.2 Biological Materials

The current investigation makes use of a number of different culture mediums, which are detailed in Table (2-4). All media were autoclaved at 121C° at 15 pounds per square inch for 15 minutes prior to preparation, as per manufacturer guidelines. Twenty-four hours were spent incubating the culture media. After carefully transferring it to clean plates. Assuming contamination was present, this was done to eliminate the risk.

Table (2-4): Culture media used

No.	Media	Purpose	Company/Origin
1.	Blood agar medium	Enrichment medium	Accumix TM /India
2.	Brain heart infusion agar	Activated medium	BIOMARK/India
3.	Brain heart infusion broth	Activated medium	HIMEDIA/India
4.	Brain heart infusion-glycerol agar medium	Preserve bacterial isolates	Accumix TM /India
5.	M9 agar medium	Ability of bacteria to protolytic activity	HIMEDIA/India
6.	MacConkey agar medium	Differential medium	Accumix TM /India
7.	Muller Hinton agar medium	Antibiotic susceptibility	HIMEDIA/India
8.	Nutrient agar medium	Cultivation medium	HIMEDIA/India
9.	Nutrient broth	Grow and preserve bacterial isolates	Accumix TM /India
10.	Peptone water broth medium	Ability of bacteria to decompose amino acid tryptophan to indole	Accumix TM /India
11.	Urea agar medium	Ability of bacteria to produce urase enzyme	HIMEDIA/India
12.	Simmon's Citrate Agar	Ability of bacteria to utilize citrate	Szamedia ,Brazil
13.	Kliglar Iron Agar	Ability of bacteria to ferment glucose and lactose to acid an acid/ gas	HIMEDIA/India
14.	Tween 80	Lipase	HIMEDIA/India
15.	Gelatin Agar	Ability of bacteria to form gelatinase	HIMEDIA/India
16.	Triptic Soy Broth	Biofilm formation	HIMEDIA/India

2.1.2.3 Phenotypic diagnostic Kits

Table (2-5): Phenotypic diagnostic Kits

No.	Kit	Origins	Companies	Informations
1.	Vitek 2	Biomerieux	France	Card type: GN, AST-N222

2.1.2.4 Antibiotics used in this study

The antibiotics used in this study were listed in Table (2-6).

Table (2-6): Antibiotics used in this study

Antibiotic	Sync	Source
Amikacin	AK	Vitek2
Amoxicillin/clavulanic acid	AML/CLV	Vitek2
Cefazolin	SEF	Vitek2
Cefepime	FEP/CPM	Vitek2
Ceftazidime	CAZ	Vitek2
Ceftriaxone	CEZ	Vitek2
Cefuroxime	CXM	Vitek2
Cefuroxime Axetil	CRO/AXL	Vitek2
Ciprofloxacin	CIP	Vitek2
Ertapenem	ETP	Vitek2
Fosfomicin	FOT	Vitek2
Gentamycin	CN	Vitek2
Imipenem	IMP	Vitek2
Meropenem	MEM	Vitek2
Nitrofurantoin	NIT	Vitek2
Piperacillin/tazobactam	TZP	Vitek2
Trimethoprim/sulfamethoxazole	TMP-SMX	Vitek2

2.1.3 Commercial kits

Commercial kits used in the present study were listed in Table (2-7).

Table (2-7): Commercial kits used in the present study

No.	Type of kits	Company/country
1.	DNA extraction kit	Genomic / Korea
4.	DNA ladder 100bp-10000pb	Promega-USA
3.	DNA ladder 100bp-1500pb	Promega-USA
2.	Green master mix 2X Kit	Promega-USA
5.	Primer of (<i>pilv-l</i> , <i>Fim H</i> , <i>mrkD</i> , <i>magA (K1)</i> , <i>wzy (K2)</i> , <i>rmpA</i> , <i>luxS</i> , <i>bla_{OXA-48}</i> , <i>bla_{TEM}</i> , <i>bla_{SHV}</i> , <i>bla_{CTX-M}</i>)	Macrogen/ Korea

Table (2-8): DNA extraction kit (Korea / UK)

Cat. No:	FABGK 100 (100 preps)
RBC Lysis Buffer	135 ml
FATG Buffer	30 ml
FABG Buffer	40 ml
W 1 Buffer	45 ml
Wash Buffer * (concentrate)	25 ml
Elution Buffer	30 ml
FABG Mini Column	100 pcs
Collection Tube	200 pcs
User Manual	1
DNA ladder	
Materials	
<ol style="list-style-type: none"> Ladder consists of double-stranded DNA with size 100-1500 bp. Loading Dye which has a composition of: (15% Ficoll, 0.03% bromophenol blue, 0.03% xylene cyanol, 0.4% orange G, 10mM Tris-HCl (pH 7.5) and 50mM EDTA) 	

Table (2-9): Master Mix Used in PCR (promega/USA)

Materials
<ol style="list-style-type: none"> DNA polymerase enzyme (Taq) dNTPs (400 μm dATP, 400 μm d GTP, 400 μm dCTP, 400 μm dTTP). MgCl₂ (3mM) Reaction buffer (pH 8.3).

2.2 Methods

2.2.1 Preparation of Reagents and Solutions

2.2.1.1 Reagents

2.2.1.1.1 Oxidase Reagent

Tetramethyl para-phenylene diamine dihydrochloride (1gram) was dissolved in 100 milliliters of distilled water to make this reagent, which was then stored in a dark bottle (Forbes *et al.*, 2007).

2.2.1.1.2 Catalase Reagent

Hydrogen peroxide (3%) was prepared from stock solution in a dark bottle and it has been used for detection of the ability of the isolates to produce catalase enzyme (Forbes *et al.*, 2007).

2.2.1.1.3 Methyl red reagents

An amount of methyl red (0.1gm) was dissolved in a volume of ethanol (300ml) with a purity level of 99%, and the remaining volume (500ml) was made up with distilled water. Used to measure the degree to which the medium has become acidic by the complete fermentation of carbohydrates (McFadden, 2000).

2.2.1.1.4 Voges-Proskauer reagents (Barritt's reagent)

It consists of the two parts listed below.

- A. Five grams of alpha naphthol dissolved in one hundred milliliters of ethanol and kept out of the light.
- B. 40 grams of KOH dissolved in 100 milliliters of water (Collee *et al.*, 1996). Finding the source of acetyl-meta-carbinol synthesis.

2.2.1.1.5 Kovac's reagents

To make it, dissolving 10 grams of p-Dimethyl amine benzaldehyde (DAMB) in 150 milliliters of amyle alcohol and then slowly added 50 milliliters of strong hydrochloric acid. It was recommended to keep this solution in a dark bottle and give it a good shake just before using. It played a role in showing how Indole is made (McFadden, 2000).

2.2.1.2 Solutions

2.2.1.2.1 Normal Saline Solution

In order to get this solution ready, dissolving 8.5 grams of NaCl in a small volume of distilled water, brought it up to 1000 ml, maintained a pH of 7.2, sterilized it in an autoclave at 121°C for 15 minutes, and stored it at 4°C (McFadden, 2000).

2.2.1.2.2 McFarland Standard Solution

According to Baron *et al.*, (1994), tube No.0.5's solution was made by combining 0.05 ml of barium chloride with 9.95 ml of concentrated sulfonic acid, yielding a turbidity almost equal to the density of bacterial cells, or 1.5×10^8 cell/ml.

2.2.1.2.3 Agarose Gel

Using the protocol described by Sambrook and Rusell, (2001), agarose gel was made by adding 1gm to 100ml of 1x TBE Buffer. A water bath was used to bring the solution to a boil, at which point the gel particles disintegrated. After cooling to 50-60°C, 0.5 mg/ml ethidium bromid was added and the mixture was stirred.

2.2.1.2.4 Ethidium bromide solution 10mg/ml

After stirring 0.2 g of ethidium bromide in 20ml of distilled water with a magnetic stirrer for four hours to achieve complete dissolution, the solution was filtered and kept in a dark bottle at 4°C until use (Sambrook and Russell, 2001).

2.2.1.2.5 Urea Solution (40%)

To make a sterile urea solution, it was dissolved 20 grams of urea in 50 milliliters of distilled water and filtered it through a Millipore membrane with a pore size of 0.22 micrometers.

2.3 Subjects of the Study

2.3.1 Study Design

A Cross-sectional study was designed that include 100 clinical specimens of sputum, urine, wound swabs, burn swabs, burn tissue and ear swabs obtained from patients aged 3 to 55 years, there were (65) samples from male patients and (35) from female patients attending to Al-Hilla General Teaching Hospital and Imam Al-Sadiq Hospital. The period extended from October 2021 to April 2022. The clinical history of each case and full information was taking directly from the patient. All information was arranged in an informative clearly detailed formula sheet named (Questionnaire sheet) show in (appendix 1) with details such as: patient name, sex, age, etc..., each specimen was immediately transferred under cooling conditions to the laboratory for analysis.

2.3.2 Ethical approval

Getting the required ethical approval from the hospital's ethical review board, patients, and their supporters is essential. In addition, all participants are verbally informed, and consent for the research and publishing of this work is sought from each individual before any samples are collected.

2.3.3 Experimental Scheme

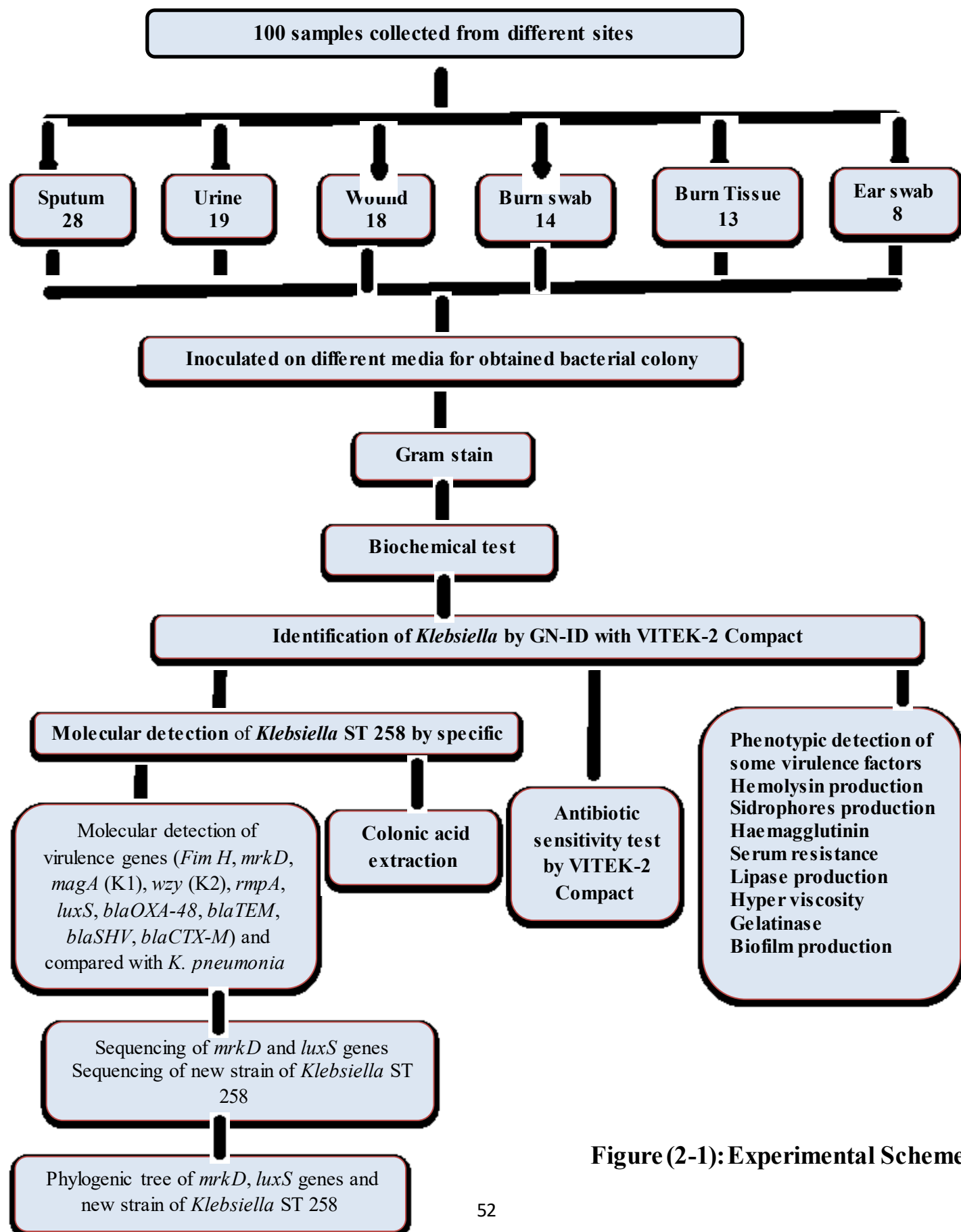


Figure (2-1): Experimental Scheme

2.3.4 Collection of samples

This is a description of how to properly collect samples by specialized physician for a bacteriological study. These samples were carefully gathered to eliminate the risk of contamination (Collee *et al.*, 1996).

2.3.4.1 Urine samples

Patients with urinary tract infections (UTIs) were the usual subjects for collecting the samples. Urine samples were taken from the middle of the stream and placed in sterile screw-cap containers before being inoculated into culture media and cultured aerobically at 37°C for 24 hours (Vandepitte *et al.*, 1991).

2.3.4.2 Sputum samples

For culturing, sterile screw cups were used for collecting samples, which were then transferred to the lab, inoculated into culture media, and incubated aerobically at 37°C for 24 hours (Kennedy *et al.*, 1999).

2.3.4.3 Wound, burn swab and soft tissue swab

Normal saline should be used to keep the sterile cotton swabs moist until they can be transported to the laboratory, where they will undergo the culture process. During 24 hours, the swab was incubated at 37 °C in an aerobic environment (Ramsay *et al.*, 2016).

2.3.4.4 Ear swab samples

Normal saline should be used to keep the sterile cotton swabs moist until they can be transported to the lab, where they will be cultured. Aerobic incubation at 37 °C for 24 hours followed by inoculation on culture media (Sillanpää *et al.*, 2017).

2.4 Laboratory diagnosis

2.4.1 Morphological tests

2.4.1.1 Colonial morphology and microscopic examination

Each primary positive culture was analyzed by taking a single colony and examining its morphology (colony shape, size, color, boundaries, and texture) under a light microscope after being stained with Gram's stain. Each isolate was stained, and then subjected to a battery of biochemical assays to determine its true identity (McFadden, 2000).

Sub-culturing the pink colonies with a mucous texture onto MacConkey agar confirmed that they were lactose-fermenting bacteria, whereas sub-culturing the pale colonies with a gamma-Hemolysis result from Blood agar confirmed that they were not *Klebsiella* (Joey, 2011).

2.4.1.2 Staining reaction

2.4.1.2.1 Gram stain

After staining with Gram stain, all of the bacterial isolates were inspected under the microscope to check for differences in cell morphology, cell clustering, and gram reactivity (Davies *et al.*, 1983).

2.4.1.2.2 Capsule stain

These are the procedures for the capsule stain test used to identify capsule production:

- Colony incubated on MacConky agar for 24 hours at 37°C .
- A standard colony slide preparation.
- The slide was left out in the open to dry naturally; no heat was used.
- For three to five minutes, methylene blue was allowed to saturate the slide. The slide was rinsed with nigrosine for 1 min.
- Finally examined with oil immersion (Elliott *et al.*, 2007).

2.4.2 Biochemical tests

2.4.2.1 Catalase test

With the use of a sterile wooden stick, a colony of organisms is moved to a dry, clean glass slide, where a single drop of 3 percent hydrogen peroxide is introduced. The presence of gas bubbles was an encouraging sign of success (Baron *et al.*, 1994).

2.4.2.2 Oxidase test

After placing a piece of filter paper in a sterile petri dish and moistening it with several drops of the freshly made oxidase reagent, a sample of the colony under investigation was taken up with a wooden stick and rubbed on the paper. During ten seconds, a change to a blue or deep purple tint signals success (Baron *et al.*, 1994).

2.4.2.3 Indole test

The ability of an organism to create Indole via tryptophan deamination is measured using this assay. When the broth turns red or yellow at the top signals a favorable or negative reaction, respectively (Miller and Wright, 1982).

2.4.2.4 Methyl red test

It is used to monitor acid generation by specific bacteria during glucose fermentation in peptone glucose broth (MR-VP broth). With the hue shift to orange, the response was optimistic (McFadden, 2000).

2.4.2.5 Voges-Proskauer (acetoin production) test

When peptone glucose broth (MR-VP broth) was tested for the presence of acetone (acetyl-methyl-carbinol), which is formed by some bacteria during development, the medium turned a bright red (McFadden, 2000).

2.4.2.6 Simmon's citrate test

The capacity of the bacteria to use citrate as its sole source of carbon was tested using the citrate test. The outcome was a shift from green to blue across the board in the media (McFadden, 2000).

2.4.2.7 Urease test

Amides can be hydrolyzed by the enzyme urease, which releases carbon dioxide, ammonia, and water in the process. After autoclaving the urea base agar and letting it cool to (50°C), the urea substrate was added and the mixture was placed into sterile tubes, where it was infected with bacterial culture and left to grow for (24-48) hours in a 37°C incubator. When urea was degraded, it released ammonia, which caused the medium's pH to rise. A pink pH indicator was used to monitor the shift from acidic to basic conditions. A positive urease test result was denoted by a pink medium. Inadequate development of a dark pink tint was a negative reaction (McFadden, 2000).

2.4.2.8 Motility test

The tubes of motility media were pierced once in the middle with an inoculating needle and then placed in an incubator at (35°C) for (24-48) hours. The line of inoculation was followed by a wave of the mobile bacteria (McFadden, 2000).

2.4.2.9 Mannitol fermentation

At 37°C, mannitol semisolid agar medium was incubated for 24 hours after being inoculated. Seeing the medium turn from white to yellow after mannitol fermentation is a sign of success (Collee *et al.*, 1996).

2.4.2.10 Kligler Iron Agar test

The KIA slant tube was stabbed and streaked before being incubated at 37 °C for 24 to 48 hours. Carbohydrate fermentation, with or without gas generation at the slant's base, caused the media's hue to shift from orange red to yellow. Moreover, a dark-colored precipitate formed at the base due to the creation of hydrogen sulfide (McFadden, 2000).

2.4.2.11 Maintenance and preservation of *Klebsiella* isolates

The following procedures were used to keep the bacterial isolates alive and well in accordance with McFadden, (2000).

2.4.2.11.1 Short term storage

Sub culturing bacterial isolates onto nutrient agar plates, wrapping each plate securely in parafilm, and storing them at 4°C allowed for the maintenance of pure colonies for use in ordinary laboratory tasks for a period of several weeks.

2.4.2.11.2 Medium term storage

The bacterial isolate was cultured in 8 ml of slant-positioned, sterile nutritional agar at 37°C for 24 hours, after which the tubes were placed in the refrigerator at 4°C.

2.4.2.11.3 Long term storage

A single colony of *Klebsiella* was added to 10 ml of sterile brain heart infusion broth, cultured at 37°C for 24 hours, and then 8.5 ml of the cell suspension was combined with 1.5 ml of glycerol (15%) and stored for an extended period of time at -20°C.

2.5 Identification of *Klebsiella* by GN-ID with VITEK-2 Compact

There is a personal computer, a reader/incubator with many moving parts (including a card cassette, a card filler mechanism, a cassette loading processing mechanism, a card sealer, a bar code reader, a cassette carousel, and an incubator), as well as transmittance optics, waste processing, instrument control electronics, and firmware.

Improved efficiency in microbiological diagnosis, reduced need for further tests, and increased test and user safety are all the result of the system's expanded identification database for all regular identification tests. The following procedures are set up in accordance with the manufacturer's guidelines. A lopefull-isolated colony was added to 3ml of normal saline in a flat-bottomed test tube. To normalize the colony to McFarland's standard solution (1.5×10^8 cell/ml) inserts the test tube into a dens check machine. Standardized inoculums were inserted into the cassette, and a sample identification number was input into the database via barcode. Barcodes printed on VITEK-2 cards during production can be scanned to determine the card's kind and link it to a specific sample ID. The next step was to load the cassette into the filler module. The cassette containing the completed cards was then moved to a reader/incubator module. The rest of the process, including incubation temperature regulation, optical card scanning, and data monitoring and transfer to a computer for analysis, was handled by the device.

2.5.1 Inoculum Preparation

To make the suspension, we followed the manufacturer's instructions from BioMérieux Corporation and transferred enough colonies from an overnight pure culture using a swab before suspending the microbe in 3.0 ml of sterile saline in a (12 x 75) mm transparent plastic (polystyrene) test tube. Densi Chek, a turbidity meter, was used to achieve a turbidity level that was similar

to McFarland No. 0.5. Antibioqram testing with the VITEK-2 small system utilized the same suspension.

2.6 Detection of some virulence factors of *K. pneumoniae* isolates

2.6.1 Hemolysin production

Inoculating blood agar media with a bacterial isolate at 37 °C for 24 to 48 hours indicated either complete hemolysis (β -hemolysis) or partial hemolysis (α -hemolysis), while no zone formed around the colonies indicated non-hemolysis (γ -hemolysis) (Liu, 1957).

2.6.2 Siderophores production

After sterilization in an autoclave and cooling to (50°C), M₉ Medium was fortified with 0.25 mg/L of glucose (sterilized via filtering) and 200 mol/L of dipyridyl. After incubating the media at (for 24 hours), the organisms were added (37°C). The outcomes were determined by whether or not there was organism growth (Rachid and Ahmed, 2005).

2.6.3 Haemagglutination

Mayumi *et al.*, (1971) detail how they developed a slide approach to detect erythrocyte clumping caused by bacterial fimbriae human blood (blood type "O") was used in the study. Red blood cells were washed with saline three times before being suspended in fresh saline at a concentration of 3%. One drop of the bacterial culture being examined was combined with one drop of this solution. The slide was then rolled at room temperature for 5 minutes. It was determined that clumping was indicative of successful hemagglutination.

2.6.4 Serum Resistance

The turbid metric assay was used to assess the level of resistance present in the serum. After incubation at 37 °C for three hours, the absorbance at 620 nm was measured again to ensure accuracy. The final absorbance was based on the average of two replicates, and the mean of the remaining absorbance as a percentage of the absorbance before incubation was determined. Isolates were termed resistant to serum if the ratio was greater than 100% (Radwanska *et al.*, 2002).

2.6.5 Lipase Production

Isolates were streaked on tween 80 agar (1%), as described by Burkert *et al.*, (2004). One week of incubation at 37°C causes lipase-producing isolates to precipitate into opaque zones.

2.6.6 Phenotypic detection of hypermucoviscosity (HMV)

This was accomplished by evaluating the ability of individual colonies to stretch a mucoviscous thread using a modified version of the traditional string test. HMV phenotype was identified when the produced string was longer than 10mm (Hartman *et al.*, 2009).

2.6.7 Gelatinase Production

After 24 hours of incubation at 37 °C, bacteria that produced gelatinase were discovered after being streaked on gelatin agar plates. When mercuric chloride was placed onto plates, the medium turned opaque, but a clear zone formed around the gelatinase-producing colonies (Corcoran *et al.*, 1992).

2.6.8 String test

The hypermucoviscosity phenotype of *K. pneumoniae* was detected using this assay. Strings of viscous material longer than 5 mm formed on an agar plate indicate a positive result from the string test (Barclay *et al.*, 1981).

2.7 Biofilm production: Tissue culture plate method (TCP)

Most laboratories still utilize the TCP assay published by (Christensen *et al.*, 1985) as their gold standard for detecting biofilm formation.

This study used the TCP method established by Christensen *et al.*, 1(985) to test the ability of all isolates to form biofilm; the incubation time was modified from (12) to (24) hours (Mathur and Mathur, 2006).

Strains were transferred from new agar plates to tryptic soy broth, cultured at 37 °C in a stationary phase for 18 hours, and then diluted one-hundred-fold with fresh media. To test for sterility and non-specific binding of medium, 0.2 ml aliquots of the diluted cultures were placed in each well of sterile polystyrene (96) well-flat bottom tissue culture plates. The tissue culture plates were kept in a 37 °C incubator for 18 and 24 hours.

After incubation, the plates were lightly tapped to dislodge the contents of each well. Free-floating 'planktonic' bacteria were cleaned out of the wells by flushing them with phosphate buffer saline (pH 7.2) four times (0.2 ml each time). Sessile microorganisms that developed biofilms on a plate were fixed in 2% sodium acetate and stained with 0.1% crystal violet (w/v). The plates were washed thoroughly with deionized water to remove any remaining stain, and then set aside to dry. In most cases, crystal violet staining was homogeneous throughout all side wells where adherent bacterial cells had formed biofilm. For this experiment, we used a micro ELISA auto reader set to read at 570 nm to measure the stained, adhering bacteria's optical density (OD) (OD₅₇₀ nm). The experiment was run three times with duplicates, with the average of the results used for analysis (Table 2-10). (Mathur and Mathur, 2006).

Table (2-10): Classification of bacterial adherence by TCP method

Mean of OD value at 630nm	Biofilm formation
$<OD_C$	Non-adherent
$OD_C < OD \leq 2 \times OD_C$	Weakly adherent
$2 \times OD_C < OD \leq 4 \times OD_C$	Moderately adherent
$4 \times OD_C < OD$	Strongly adherent

2.8 Colanic acid extraction and measurement of concentration

Colanic acid extraction and measurement of their concentration were performed according to Dische and Shettles (1951). It is modified by the Al-Saed, (2000) method as follows:

1. Plain tube containing brain heart infusion broth inoculates with intended isolate and incubated for 24 hrs. at 37°C.
2. The tube centrifuged at 3000 rpm for 5 min. and the supernatant discarded.
3. 1 ml of sterile normal saline added to the sediment and centrifuged at 3000 rpm for 5 min to wash the bacterial cells and then the supernatant discarded.
4. 1 ml of sterile normal saline added to the sediment and centrifuged at 6000 rpm for 5 min to wash the bacterial cells. At this step the colanic acid floated in the supernatant.
5. 6 ml of concentrated sulfuric acid added to 1 ml of the supernatant gathered from previous step 4 and mixed well and then transferred to water bath at 100°C for 20min.
6. The mixture was cooled and 0.2 ml of 0.1% Carbazole added to the mixture. The color changed to pink, and stand alone for two hours.
7. The optical density (O.D.) recorded for each tube at 530nm.

8. The standard curve made for galacturonic acid to get the concentration of colanic acid as $\mu\text{g/ml}$. It is clear from Figure (2-2):

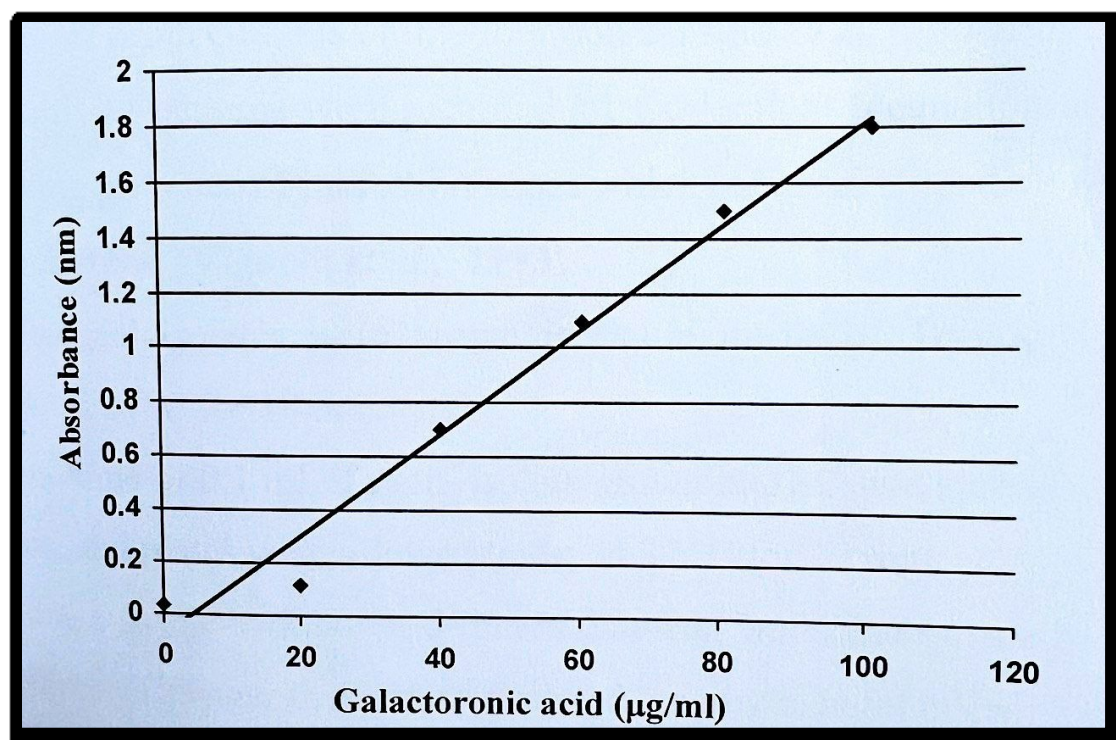


Figure (2-2): Standard curve of colanic acid when used galacturionic acid

2.9 Genotyping Assays

2.9.1 DNA Extraction

This method was made according to the genomic DNA purification Kit supplemented by the manufacturing company Genomic / Korea

Chromosomal DNAs obtained were used as templates for all PCR experiment. The PCR reaction was carried out in a Thermal Cycler. Before PCR assay, DNA profile was performed by using bacterial DNA and loading buffer without thermal cycling condition, and according to the following step:

1. Cultured bacterial cells were transferred to $1.5 \mu\text{l}$ microcentrifuge tube, centrifuged for 1 minute at $14\text{-}16,000\times g$ and the supernatant was discarded.

2. A volume of 200 μ l of Gram Buffer was added to 1.5 μ l microcentrifuge tube then 200ml of lysozyme buffer was added to the Gram Buffer then vortex to completely dissolve the Lysozyme.
3. A volume of 200 μ l of Gram Buffer in the 1.5 microcentrifuge tube, incubated at 37°C for 30 minutes. During incubation the tube was inverted every 10 minutes.
4. A volume of 20 ml of proteinase K was added then mixed by vortex, incubated at 60°C for at least 10 minutes. During incubation the tube was inverted every 3 minutes.
5. A volume of 200 μ l of GB Buffer was added to the sample and mix by vortex for 10 minutes.
6. The sample lysate was incubated at 70°C for at least 10 minutes. During incubation, the tube was inverted every 3 minutes. At this time, the required Elution Buffer (200 μ l per sample) was pre-heated to 70°C (for step 5 DNA Elution).
7. Following 70°C incubation, 5 μ l of RNase A (10mg μ l) was added to the clear lysate and mixed by shaking vigorously.
8. The lysate was incubated at room temperature for 5 minutes.
9. A volume of 200 μ l of absolute ethanol was added to the clear lysate and immediately mixed by shaking vigorously; the precipitate was broken up by pipetting.
10. A GD Column was placed in a 2 μ l collection tube.
11. All of the mixture was transferred (including any precipitate) to the GD column, centrifuged at 14000-16000xg for 2 minutes.
12. The 2 μ l collection tube was discarded containing the flow-through and the GD column was placed in a new 2 μ l collection tube.
13. A volume of 400 μ l of W1 buffer was added to the GD Column, Centrifuged at 14000-16000 g for 30 second.

-
14. The flow-through was discarded and placed the GD column back in the 2ml collection tube.
 15. A volume of 600 μ l of wash buffer (ethanol added) was added to the GD column, centrifuged at 14000-16000xg for 30 seconds.
 16. The Flow-through was discarded and placed the GD column back in the 2 μ l collection tube, Centrifuged again for 3 minutes at 14000-16000xg to dry the column matrix.
 17. The dried GD column was transferred to a clean 1.5 μ l centrifuge tube.
 18. A volume of 100 μ l of preheated elution buffer or TE was added to the center of the matrix, centrifuged at 14000-16000 x g for 30 second to elute the purified DNA.
 19. The detection of DNA by horizontal gel electrophoresis, and concentration measured by Nano droop DNA.

2.9.2 Measurement of DNA concentration and purity

With the use of the Nanodrop system and the Nanodrop Optizen handbook, 1 μ l of each DNA sample was analyzed to determine its concentration. The ratio of absorbance at 260 and 280 nm in a sample was used to determine the DNA purity level.

2.9.3 Agarose gel preparation

The size of the PCR products was verified together with the size of the genomic DNA bands using 1.5% agarose gel. 1.8 grams of agarose were microwave-dissolved in 120 milliliters of 1X TBE buffer to make the gel. A final concentration of 0.5 g/ml of ethidium bromide (EtBr) was added to 1 μ l of agarose solution at 55-60 C. After waiting 30 minutes, the solution was put into the gel tank, where the combs were already in place. After carefully removing the combs, the tank containing the 1X TBE running buffers is inserted in the electrophoresis apparatus, and the buffer is poured into the

wells until it covers the gel by a thickness of 1-2 mm. After loading the wells with 10 μ l of each PCR product, negative control, and DNA ladder (100 bp, 1 kb, or both), the cover was put and the device was activated. Electrophoresis was run at 70 volts and 35 milliamperes for 2 hours. UV transilluminator was used to observe DNA bands, and digital photographs were taken (Green and Sambrook, 2012).

2.10 Polymerase chain reaction (PCR) diagnosis

PCR was employed as a diagnostic tool to identify the target genes. The following amplification procedures were applied to the isolated DNA:

2.10.1 Preparation of primers solution

After dissolving the lyophilized primer in deionized distal water (DDH₂O) to achieve 100 pmol/ μ l in the master tube, 10 pmol/ μ l was created as a working solution by withdrawing 10 μ l from the master tube and bringing the volume to 100 μ l with DDH₂O.

2.10.2 Monoplex PCR mixture and PCR program conditions

Under sterile conditions, 20 μ l quantities were used for PCR reactions in PCR tubes, and any remaining volume was made up with sterile DDH₂O. A negative control blank was included in every PCR experiment to ensure that no unwanted target DNA was amplified. The following primer mixture and programming conditions were provided:

2.10.3 Molecular detection of *K. pneumoniae* ST 258 by specific primer gene

K. pneumoniae ST 258 was diagnosed with PCR by using the primer specific for *pilv-l* gene (Table 2-11). The reaction mixture was illustrated in Table (2-12).

Table (2-11): The sequence of primers that used in this study

Primer	Sequence	Primer sequence	T _m (°C)	GC%	Size (bp)	Reference
<i>pilv-l</i>	F	5'- TGATGCTGATGGCAGACTGA - 3'	60.6	50	320	Adler A. <i>et al.</i> , (2014)
	R	5'- TGTAGTCACACCCTGCCCA - 3'	64.4	58		

Table (2-12): The Components of the Maxime PCR PreMix kit (i-Taq)

Component	Reaction size 20 µl
i-Taq TM DNA Polymerase(5U/µl)	2.5 U
dNTPs	2.5mM each
Reaction Buffer(10x)	1x
Gel Loading buffer	1x

Table (2-13): Reaction components of PCR

Component	25µL (Final volume)
Taq PCR PreMix	5µl
Forward primer	10 picomols/µl (1 µl)
Reverse primer	10 picomols/µl (1 µl)
DNA	1.5µl
Distill water	16.5 µl

Table (2-14): The optimum condition of detection

No.	Phase	T _m (°C)	Time	No. of cycle
1.	Initial Denaturation	95°C	5 min	1 cycle
2.	Denaturation -2	95°C	30 Sec	35 cycle
3.	Annealing	52°C	1min	
4.	Extension-1	72°C	30 Sec	
5.	Extension -2	72°C	10 min.	1 cycle

2.10.4 Detection of some of *K. pneumoniae* virulence genes

DNA (extract from bacterial cells) was used as a template in specific PCRs for the detection of some of *K. pneumoniae* virulence genes. The primers used for the amplification of a fragment gene were listed in Table (2-15).

Table (2-15): Characteristics of the primers used in RCR

Primer	Seq.	Primer sequence5' - 3'	T _m (°C)	GC %	Size (bp)	References
<i>Fim H</i>	F	TGCTGCTGGGCTGGTCGATG	67.9	65	688	Yu <i>et al.</i> , (2008)
	R	GGGAGGGTGACGGTGACATC	67.4	65		
<i>mrkD</i>	F	TTCTGCACAGCGGTCCC	63.8	65	240	Sebghati <i>et al.</i> , (1998)
	R	GATACCCGGCGTTTTTCGTTAC	60.7	52		
<i>magA (K1)</i>	F	GGT GCT CTT TAC ATC ATT GC	55.3	45	1282	Shah <i>et al.</i> , (2017)
	R	GCA ATG GCC ATT TGC GTT AG	58.7	50		
<i>wzy (K2)</i>	F	GAC CCG ATA TTC ATA CTT GAC AGA G	59	44	641	Shah <i>et al.</i> , (2017)
	R	CCT GAA GTA AAA TCG TAA ATA GAT GGC	57.1	37		
<i>rmpA</i>	F	ACT GGG CTA CCT CTG CTT CA	63.1	55	535	Shah <i>et al.</i> , (2017)
	R	CTT GCA TGA GCC ATC TTT CA	57.1	45		
<i>luxS</i>	F	GCCGTTGTTAGATAGTTTCACAG	57.3	43	447	Shadi Shadkam <i>et al.</i> , (2021)
	R	CAGTTCGTCGTTGCTGTTGATG	60.6	50		
<i>bla_{OXA-48}</i>	F	TGGTGGCATCGATTATCGG	59.9	50	428	Shadi Shadkam <i>et al.</i> , (2021)
	R	GAGCACTTCTTTTGTGATGGC	58.5	48		
<i>bla_{TEM}</i>	F	ATA AAA TTC TTG AAG ACG AAA	48.4	24	1080	Shah <i>et al.</i> , (2017)
	R	GAC AGT TAC CAA TGC TTA ATC	25.3	38		
<i>bla_{SHV}</i>	F	GGG TTA TTC TTA TTT GTC GC	52.8	40	930	Shah <i>et al.</i> , (2017)
	R	TTA GCG TTG CCA GTG CTC	59.3	56		
<i>bla_{CTX-M}</i>	F	GCT ATG TGC AGT ACC AGT AA	54.8	45	585	Shah <i>et al.</i> , (2017)
	R	ACC AGA ATG AGC GGC GC	63	65		

Table (2-16): Reaction components of all PCR

Component	25 μ L (Final volume)
Taq PCR PreMix	5 μ L
Forward primer	10 picomols/ μ L (1 μ L)
Reverse primer	10 picomols/ μ L (1 μ L)
DNA	1.5 μ L
Distill water	16.5 μ L

Table (2-17): The optimum condition of detection of virulence genes

No.	Name of gene	Phase	Tm (°C)	Time	No. of cycle
1.	<i>fimH</i>	Initial Denaturation	95°C	3 min	1 cycle
		Denaturation -2	95°C	45 Sec	35 cycle
		Annealing	52°C	45 Sec	
		Extension-1	72°C	45 Sec	
		Extension -2	72°C	7 min.	1 cycle
2.	<i>magA (K1)</i>	Initial Denaturation	95°C	3 min	1 cycle
		Denaturation -2	95°C	30 Sec	30 cycle
		Annealing	55°C	30 Sec	
		Extension-1	72°C	1 min	
		Extension -2	72°C	10 min.	1 cycle
3.	<i>wzy (K2)</i>	Initial Denaturation	95°C	1 min	1 cycle
		Denaturation -2	95°C	30 Sec	40cycle
		Annealing	59°C	45 Sec	
		Extension-1	72°C	90 Sec	
		Extension -2	72°C	6 min.	1 cycle
4.	<i>rmpA</i>	Initial Denaturation	95°C	5 min	1 cycle
		Denaturation -2	95°C	1 min	40 cycle
		Annealing	50°C	1 min	
		Extension-1	72°C	1 min	
		Extension -2	72°C	7 min.	1 cycle
5.	<i>blaTEM</i>	Initial Denaturation	95°C	2 min	1 cycle
		Denaturation -2	95°C	30 Sec	30 cycle
		Annealing	60°C	30 Sec	
		Extension-1	72°C	50 Sec	
		Extension -2	72°C	5 min.	1 cycle
6.	<i>blaSHV</i>	Initial Denaturation	95°C	2 min	1 cycle
		Denaturation -2	95°C	30 Sec	30 cycle
		Annealing	60°C	30 Sec	
		Extension-1	72°C	50 Sec	
		Extension -2	72°C	5 min.	1 cycle
7.	blaCTX-M	Initial Denaturation	95°C	2 min	1 cycle
		Denaturation -2	95°C	30 Sec	30 cycle
		Annealing	57.5°C	30 Sec	
		Extension-1	72°C	1 min	
		Extension -2	72°C	7 min.	1 cycle
8.	<i>luxS</i>	Initial Denaturation	95°C	5 min	1 cycle
		Denaturation -2	95°C	35 Sec	33 cycle
		Annealing	52°C	35 Sec	
		Extension-1	72°C	35 Sec	

		Extension -2	72°C	7 min.	1 cycle
9.	<i>blaOXA-48</i>	Initial Denaturation	95°C	7 min	1 cycle
		Denaturation -2	95°C	30 sec	33 cycle
		Annealing	53°C	1 min	
		Extension-1	72°C	1 min	
		Extension -2	72°C	7 min.	1 cycle
10	<i>mrkD</i>	Initial Denaturation	95°C	5 min	1 cycle
		Denaturation -2	95°C	1 min	33 cycle
		Annealing	49.5°C	1 min	
		Extension-1	72°C	2 min	
		Extension -2	72°C	8 min.	1 cycle

2.11 Gene Sequencing of *K. pneumonia* and *K. pneumonia* ST 258, *mrkD* and *luxS*

Termini, forward, and reverse sequencing of the resolved PCR amplicons was performed commercially following the manufacturer's protocols (Macrogen Inc. Geumchen, Seoul, South Korea). To rule out the possibility that the annotation and variances are the result of PCR or sequencing artifacts, only clean chromatograms were investigated further from ABI sequence files. The virtual locations and other details of the obtained PCR fragments were determined by comparing the observed nucleic acid sequences of a local sample with the retrieved reference sequences of the bacterial database.

2.11.1 Interpretation of sequencing data

BioEdit Sequence Alignment Editor Software Version 7.1 was utilized for editing, aligning, and analyzing the sequencing results of the PCR products in comparison to their corresponding sequences in the reference database (DNASTAR, Madison, WI, USA). Nucleic acids were numbered in PCR amplicons and at their respective locations being referred to the genome.

2.11.2 Comprehensive phylogenetic tree construction

In this research, we followed the neighbor-joining procedure outlined by Sarhan *et al.* (2020) to build a comprehensive tree with very particular characteristics. Via the NCBI-BLASTn website, we compared the reported

variations to their closest homologous reference sequences (Zhang *et al.*, 2000). The detected variant was incorporated into a neighbor-joining tree, which was then displayed using iTOL suit to provide a classic clades-construction tool (Letunic and Bork, 2019). Each species group in the exhaustive phylogenetic tree had its sequences properly annotated.

2.12 Statistical Analysis

Statistical Package for the Social Sciences (SPSS) for Windows (version 23) and Microsoft Excel (version 2013) were used for statistical analysis. In order to calculate the likely degree of connection between the variables under consideration of percentage (George & Mallery, 2019).

Chapter Three

Results and Discussion

3.1 Data Description of Study Population

For this cross-sectional study, it was collected 100 clinical specimens, including sputum, urine, wound swabs, burn swabs, burn tissue, and ear swabs (Figure 3-1), from patients at Al-Hilla General Teaching Hospital and Imam Al-Sadiq Hospital, ranging in age from 3 to 55 years (Figure 3-2), of these, 65% were from male patients and 35% were from female patients (Figure 3-3).

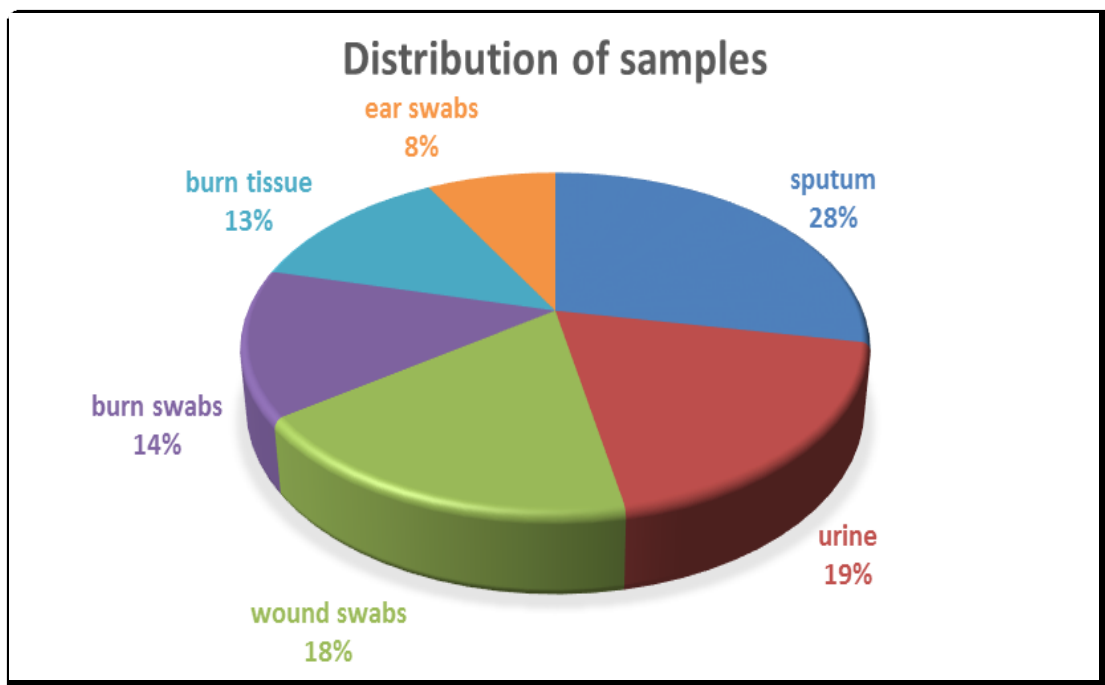


Figure (3-1): Distribution of samples according to site of infections

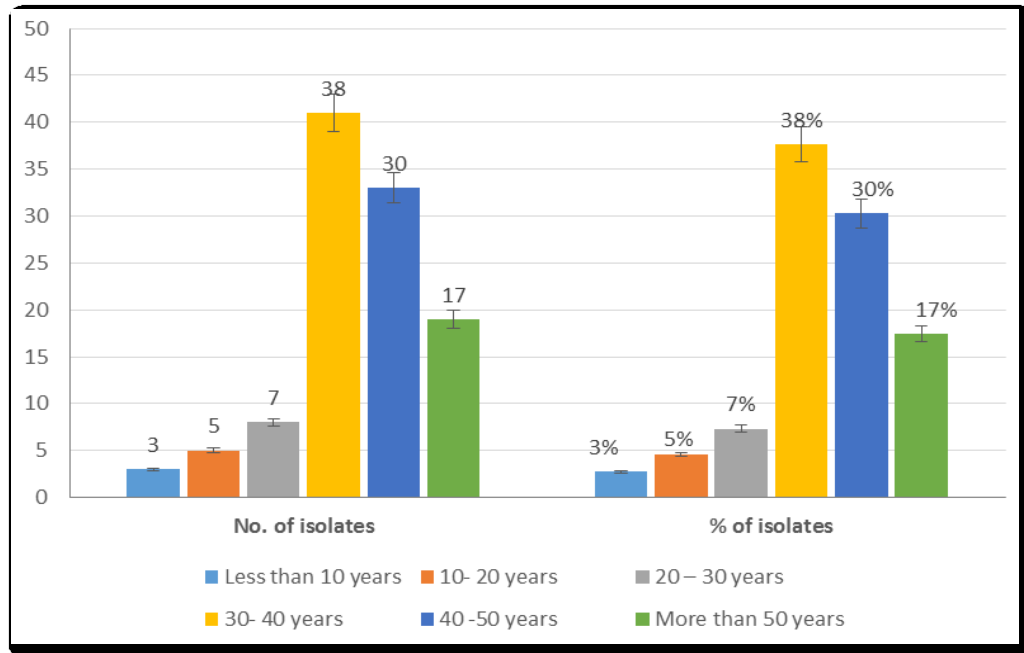


Figure (3-2): Distribution of the patients according to the age

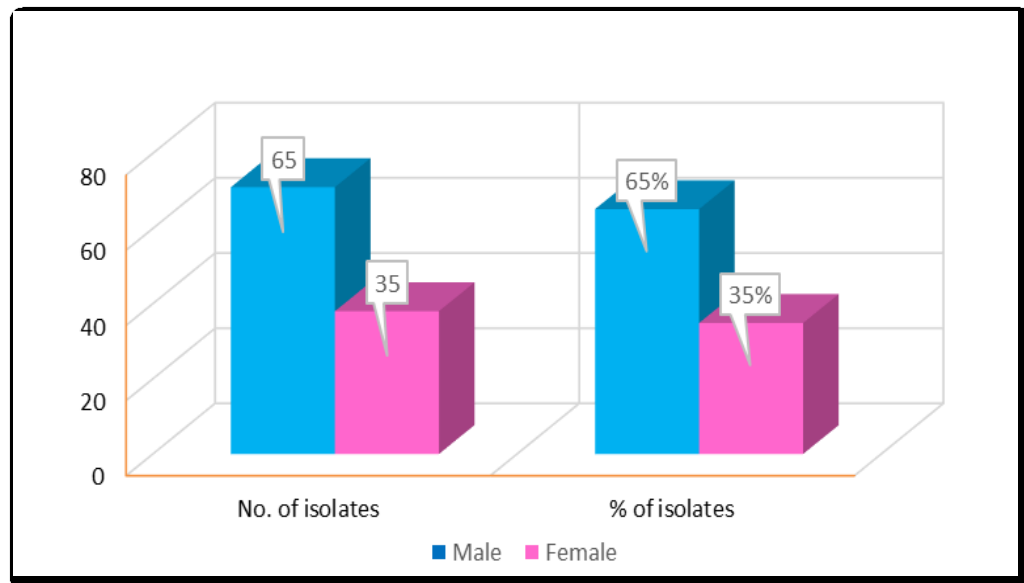


Figure (3-3): Frequency of patients according to sex

3.2 Isolation of *Klebsiella pneumonia* from different site of infection

In this investigation, *K. pneumonia* was isolated from a total of (100) specimens obtained from various infection sites by aerobic culture on various media. Forty of the isolates strains were positively recognized as *K. pneumonia* (Table 3-1). Nonetheless, it was found that 60% of the isolates contained bacteria that could be challenging to culture, possibly because of differences in sample size and composition.

Table (3-1): Types of bacterial isolates recovered from sample

Bacterial isolates	No.	%
<i>Klebsiella pneumoniae</i>	40	40%
Others	60	60%
Total	100	100%

Eleven of the forty isolates (27.5%) were taken from sputum samples, eight (20%) from urine samples, seven (17.5%) from wound swabs, six (15%) from burn swabs, five (12.5%) from burn tissue, and three (7.5%) from ear swabs. Nevertheless, *K. pneumonia* was only found to be isolated from men at a rate of 26 (65%), while females were only isolated at a rate of 14 (35%). Table (3-2) displays the outcomes. Furthermore, *K. pneumonia* was isolated from a wide age range, as indicated in Table (3-3).

Table (3-2): Distribution of *K. pneumoniae* according to samples types and pateints sex

Sample type	No. (%)	<i>K. pneumoniae</i>	
		No.	%
Sputum	28 (28%)	11	27.5
Urine	19 (19%)	8	20
Wound swap	18 (18%)	7	17.5
Burns swap	14 (14%)	6	15
Burns Tissue	13 (13%)	5	12.5
Ear swap	8 (8%)	3	7.5
Total	100 (100%)	40 (100%)	
Gender	No. (%)	<i>K. pneumoniae</i>	
		No.	%
Males	65 (65%)	26	65%
Females	35 (35%)	14	35%
Total No.	100 (100%)	40 (100%)	

Table (3-3): Distribution of *K.pneumoniae* according to pateints age

Age groups	No. of isolates	% of isolates
<10 years	1	2.5%
10- 20 years	2	5%
20 – 30 years	3	7.5%
30- 40 years	7	17.5%
40 -50 years	12	30%
>50 years	15	37.5%
Total	40	100%

Recent results indicated that *K. pneumoniae* were highly isolated from sputum samples at percentage (27.5%) followed by urine at percentage (20%) wound at percentage (17.5%), burns swap at percentage (15%), burns tissue at percentage (12.5%), and ear swap at rate (7.5%).

Bunyan and Al-Salem, (2022) observed that, the prevalence of *K. pneumonia* is around 45.4% in sputum, 21.1% in urine, and 3.0% from otitis media, however present results were not consistent with these numbers.

Fifty *K. pneumonia* isolates were identified by Kateete *et al.*, (2016), with 46% of those being obtained from urine and 54% coming from clinical cases (32% from wound, 12% from sputum, and 10% from otitis media).

Many factors, including sample size, location, isolation and identification methods, and the influence of environmental and patient health factors, likely contributed to the wide range of reported *K. pneumonia* isolation rates across investigations (Moon *et al.*, 2022).

3.3 Identification of *K. pneumonia* by biochemical tests and vitek II system

All *K. pneumoniae* bacterial isolates were put through a multitude of morphological, Microscopical, biochemical, and Vitek II system testing in this investigation.

3.3.1 Phenotypic Characterization and Microscopic Identification

Bacteriological methods, such as colonial morphology on blood agar (shape, color, and lactose fermentation on MacConkey agar), and microscopic examination, which includes the morphology of bacterial cells by Gram-stain to observe a shape, arrangement of cells, and type of reaction with Gram-stain, were used to positively identify *K. pneumoniae*.

Results from the current study showed that *K. pneumoniae* colonies on blood agar were white, similar to mucous, and were not surrounded by a transparent halo, indicating that the bacteria were unable to lyse blood cells and instead produced gamma hemolysis (∇-hemolysis) or non-hemolysis due to a lack of the hemolysin enzyme (Hossain, 2019). The colonies of *K.*

pneumoniae are considered to be Gram-negative because they grew on MacConkey agar, a selective and differential medium that allows the growth of Gram-negative bacteria while preventing the growth of Gram-positive bacteria due to its content of bile salts, which inhibit the growth of gram-positive bacteria (Al-Ansari *et al.*, 2020).

The ability of *Klebsiella pneumoniae* to produce mucoid is crucial to the pathogen's pathogenicity. This is because a chemical not related to colanic acid or *K. pneumoniae's* capsular polysaccharide is produced by the plasmid. To contrast, *K. pneumoniae* colonies on *Klebsiella* Chromogenic Agar (a selective medium that inhibits gram positive organisms and the chromogenic mixture in the medium allows the differentiation of *Klebsiella* species from other bacteria) were pink to red in color, round in shape, and clear to slightly opalescent in gel form (Walker *et al.*, 2020).

Its metallic blue colonial morphology on CHROM agar Super CARBA medium can range from tiny to medium. An investigation of a suspected colony of *K. pneumoniae* cultured on MacConkey agar, smeared on a microscope slide, and stained with the Gram staining technique revealed gram-negative, non-spore-forming, tiny rods. Since the cells lacked the necessary components for movement—the flagella—they were considered to be non-motile (Strakova *et al.*, 2021).

3.3.2 Biochemical Identification

The Table (3-4) below summarizes the findings of many biochemical tests performed to characterize *K. pneumoniae*. Isolates of *K. pneumoniae* found in this study tested positive for the catalase test, indicating the ability of these bacteria to produce catalysis enzyme that analyzed the hydrogen peroxide reagent into water and gas bubbles in the catalase test. Yet, the oxidase, methyl red, and gelatinase tests all came back negative. The

addition of Kovacs reagent to the peptone water medium resulted in the appearance of a yellow ring, indicating that the bacteria were unable to manufacture the tryptophanase enzyme necessary to convert tryptophan into Indole.

Table (3-4): Biochemical tests for characterization of *K.pneumoniae*

Bacteria	Biochemical Tests									
	Catalase	Oxidase	Indole	MR	VP	Citrate	KIA	Urease	Motility	Gelatinase
<i>K.pneumoniae</i>	+	-	-	-	+	+	A/A	+	-	-

(+) positive result, (-) negative result, (MR) Methyl red , (VP) Voges –Proskauer test, (KIA) Kligler Iron Agar test, (A/A) Acidic Slant/ Acidic Bottom.

The ability of bacterial isolates to consume citrate as the only source of carbon resulted in a clear positive result for the citrate utilization test when applied to the *K. pneumoniae* isolates. In addition, the isolates produced urease enzyme, which turned the yellow urea agar slant pink. Infections caused by *Klebsiella* are distinguished by the presence of urease enzyme production (Yaqoob *et al.*, 2022).

Because it catalyzes the formation of kidney and bladder stones or to encrust or obstruct indwelling urinary catheters, this enzyme is also considered one of the most significant virulence factors of *K. pneumoniae*, which has been involved in the pathogenesis of several diseases, including pyelonephritis and the development of infection-induced urinary stones. They failed the motility test, so they're not mobile. As a result of glucose and lactose fermentation, they also gave favorable results to the Vogas Proskauer test and the Kligler iron test by creating an acidic slant / acidic bottom with gas generation but without H₂S gas production (Yuan *et al.*, 2020).

Since lactose is the only carbon source in this medium, only lactose-fermenting bacteria, which produce pink colonies when the pH drops below 6.8, can be distinguished from non-lactose fermenting bacteria. The non-

lactose bacterial growth, on the other hand, is transparent or colorless (Some *et al.*, 2021).

In order to distinguish *Klebsiella* from other bacterial species that show similar growth on MacConkey agar but hemolytic blood, such as *Serratia* spp., bacterial isolates were found to be big, mucoid, white to grey, and non-hemolytic on the enriched blood agar medium (Kadhun *et al.*, 2019).

Because the aniline dyes (eosin and methylene blue) in this medium combine to form a precipitate at acidic pH and appear as a metallic green sheen, this medium is typically used to discriminate between *Klebsiella* and *E. coli* on the EMB agar. Thus, due to the significant amount of acid produced by fermentation, *Klebsiella* colonies look pink, but *E. coli* colonies are dark and surrounded by a green metallic sheen (Al-Fatlawi, 2020).

Bacterial isolates were subsequently identified using biochemical assays. All *Klebsiella* isolates tested positive for Voges-Proskauer (VP) and either positive or negative for methyl red, indicating that acetoin and 2,3-butanediol were generated during glucose partial fermentation and that neutral end products prevail over acidic end products (Abdallah *et al.*, 2016).

Results from IMViC show that they are distinct from other lactose fermenter genera such *E. coli*, *Citrobacter*, and *Serratia*. The results for indole on *Klebsiella* were negative. Some intestinal bacteria with the enzyme tryptophanase can be identified by the indole test because of their ability to hydrolyze tryptophan to indole, pyruvic acid, and water. Although *Klebsiella* and other indole-negative bacteria did not generate tryptophanase, the addition of Kovac's reagent to indole-free broth did not result in the formation of a red ring at the broth's surface (Samanta *et al.*, 2020).

Klebsiella demonstrated positive reactivity for citrate, making it clear that the citrate in simmon citrate medium is crucial for determining whether or not the bacteria isolates are capable of growing on it as a distinct carbon and energy source. Simmon's medium also includes the pH indicator molecule bromothymol blue. Due to the alkaline nature of the molecule formed when CO₂ combines with the other components of the medium, a positive citrate test is shown when the pH indicator (bromthymol blue) changes color from green to blue (Subhi *et al.*, 2017).

Carbohydrate fermentation patterns and H₂S generation are used to distinguish between Enterobacteriaceae taxa in the Kligler Iron Agar (KIA) test. There is 1% lactose and 1% glucose in KIA angles. In the presence of acids, the medium was colored yellow by the pH indicator (phenol red), which normally turns the medium an orangey red. In addition to ferrous sulfate, which causes a black precipitate that can be used to identify H₂S-producing bacteria, KIA also includes the H₂S production substrate sodium thiosulfate (Sharma *et al.*, 2023).

As a result of fermenting lactose and glucose, but not H₂S, *Klebsiella* isolates changed the color of the slant and butt, producing acidic slant (yellow) and acid butt (yellow) with gas production (bubbles formation). Subhi *et al.*, (2017) reported findings were confirmed by these findings.

3.3.3 Vitek II Identification

The appendix (2) displays the diagnostic result obtained from the Vitek-II system, an automated microbiology system used for bacterial identification and for verifying the outcomes of morphological, microscopical, and biochemical identification. The results showed that, the technique was able to quickly detect bacteria, with a confidence level of ID

massage ranged from excellent (probability percentage of 94 to 99.7%) for all 40 isolates.

3.4 Phenotypic detection of virulence *K. pneumoniae*

There are many virulence factors associated with *K. pneumoniae* that have an influence on human health, and these virulence factors are similar to those produced by enteropathogenic bacteria. (Haque *et al.*, 2018). It was widely recognized that both extra- and intra-intestinal infections might strike previously healthy hosts and those with impaired immune systems (Schiaffino & Kosek, 2020).

In the current investigation, the 18(45%) isolates were hemolysin-making capabilities of 40 different *K. pneumoniae* isolates were examined. In addition, siderophores production was identified among isolates, and it was shown that 22(55%) of *K. pneumoniae* isolates have the potential to make siderophores.

Nonetheless, the ability of each isolate to agglutinate erythrocytes was evaluated. Ninety-two percent of the isolates showed erythrocyte clumping, which was seen in 37(92.5%) of them. In addition, a turbid metric assay was used to assess the resistivity of the serum of each individual isolate. In 25(62.5%) of the isolates, the percentage of persisting absorbance after 3 hours (OD₆₂₀, 3hrs) was greater than 100% compared to the initial absorbance. Although all of the *K. pneumoniae* isolates tested positive for lipase production, only 5(12.5%) isolates were found to produce lipase as a virulence factor. Similarly, only 4(10%) of the *K. pneumoniae* isolates tested positive for gelatinase as a virulence factor. Finally, the results of this study showed that the prevalence of the hypermucoviscosity phenotype was higher among 39(97.5%) *K. pneumoniae* isolates as shown in Figure (3-4).

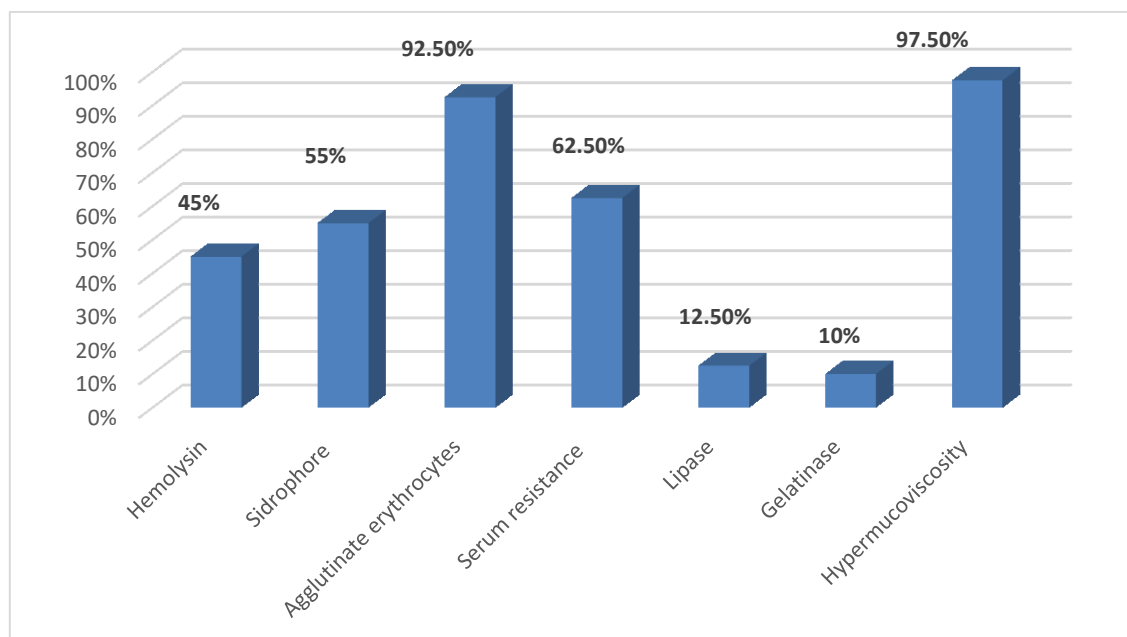


Figure (3-4): Phenotypic detection of virulence among *K. pneumoniae*

Partial hemolysis was observed for both erythrocytes and mammalian cells in culture, which is consistent with the findings of Vita *et al.*, (2020). Clinical isolates of *K. pneumoniae* were determined to be highly pathogenic and causative for human disorders by Ali *et al.*, (2022).

Some research has linked *K. pneumoniae* α -hemolysin to an enzyme and toxin produced within cells; these are referred to as cytotoxic factors. Hemolysin is an essential virulence factor for *K. pneumoniae* bacteria, and it is produced during the logarithmic phase of cell growth (Brown *et al.*, 2021).

In order to survive, pathogenic bacteria have developed a variety of strategies for scavenging iron from their natural habitats. The release of iron complex from heme and hemoglobin within cells is one such mechanism (Smalley & Olczak, 2017). One of the major virulence factors in bacteria is hemolysin. Cell death and cytoplasmic content leaking can be triggered by hemolysin, which are part of a wide family of pore-forming bacterial cytolysins (Murase, 2022).

Pathogenic bacteria are a common source for hemolytic proteins, and hemolysin is a key virulence factor for many bacteria. In order to function, bacterial toxins like hemolysin and other proteins with cystathionine-synthase (CBS) domains assemble homologous subunits into membrane-spanning holes (Sarowska *et al.*, 2019). Siderophores, which bind iron with a very high affinity and which compete successfully with transferrin and lactoferrin to mobilize iron for microbial use, provide a second route for iron acquisition (Page, 2019).

For their own life, pathogenic microbes rely on iron from the host, thus they produce and secrete small organic compounds called siderophores that actively chelate iron (Sousa Geros *et al.*, 2020).

These results were in agreement with those obtained by Davies *et al.*, (2016), who discovered that Haemagglutination test was detected in of that *K. pneumoniae* isolates at a rate of 94%. The ability of the strains to express type 1 and type 3 fimbriae was determined by testing their capacity for mannose-sensitive and mannose-resistant erythrocyte hemagglutination (Ramos-Vivas *et al.*, 2019). It was used a combination of enzyme-linked immunosorbent assay and imipenem killing assay to examine bacterial invasion and adherence to epithelial cells. While comparing the ability of different *K. pneumoniae* strains to attach to epithelial cells (Alcántar-Curiel *et al.*, 2018).

The vast majority of clinical isolates were able to create at least one adhesion, and many were able to produce both. Adhesion evaluation through hemagglutination is qualitative, so it cannot tell us whether both type 1 and type 3 fimbriae must be expressed during invasion, or if expression of just one fimbrial adhesion per cell is sufficient (Beuth & Uhlenbruck, 2017).

Serum resistance has been shown in multiple bacterial systems to be critical for the survival of invading bacteria and the establishments of disease, since mutations resulting in loss of serum resistance render several

bacterial pathogens avirulent, which is consistent with the results of this study. *Klebsiella* better resistance to serum bactericidal activity (58.9%) is an indicator of their higher pathogenicity because serum resistance is one of the pathogenicity factors of *Klebsiella* (Baldiris-Avila *et al.*, 2020).

Many researchers have found a correlation between *Klebsiella* and serum resistance (Gharrah *et al.*, 2017; Ballén *et al.*, 2021). The degree to which *Klebsiella* were resistant to serum was much higher. This finding is consistent with what was found by Ku *et al.*, (2017a), who found that *Klebsiella* isolates exhibited a high proportion of serum-resistant isolates. These findings corroborated those of Devanathan *et al.*, (2022), who examined the ability of *K. pneumoniae* isolates to manufacture lipases enzyme on Tween 80 medium at 37°C and found that 10% of these strains could do so.

Across an oil-water interface, lipase (triacylglycerol acylhydrolase) catalyzes the breakdown of triglycerides to glycerol and free fatty acids (Chandra *et al.*, 2020). In addition to hydrolyzing and esterifying fatty acids, lipases can catalyze their transesterification, acidolysis, and ammonolysis. Certain sectors have taken an interest in the microbial lipase, including the food, detergent, cosmetic, organic synthesis, and pharmaceutical industries (Fatima *et al.*, 2021).

The ester bonds in water-insoluble lipid substrates are hydrolyzed by lipase, a water-soluble enzyme. Most lipases function at a specific position on the glycerol backbone of lipid substrates, this virulence factor operates on the cell membrane by inserting into the membrane to generate a pore and cleaving phospholipids; it also lyses red blood cells, phagocytes, and their granules, making it particularly relevant to infections of burn wounds (Mishra & Kandali, 2019).

Bacterial extracellular lipase production is sensitive to environmental conditions, including carbon and nitrogen supplies, as well as physicochemical parameters like temperature, pH, and dissolved oxygen (Hasan *et al.*, 2018).

The hyper-mucoviscosity results were compared to those obtained by Gharrah *et al.*, (2017), who estimated hyper-mucoviscosity among 33% of *K. pneumoniae* isolates, and to those obtained by Heiden *et al.*, (2019), who reported that 59% displayed hyper-mucoviscosity. There was just one *K. pneumoniae* strain that showed the HMV phenotype, according to Walker *et al.*, (2020).

Hyper-mucoviscosity of *K. pneumoniae* isolates is a phenotypic of the bacteria that is defined by its propensity to create copious amounts of thick, mucoid material, resulting in elevated culture viscosity (Namikawa *et al.*, 2019). This trait is linked to virulence factors that may increase the bacteria's pathogenicity, especially in immunocompromised patients. Reports of hyper-mucoviscous strains of *K. pneumoniae*, which are linked to severe infections, have increased in recent years, especially in Asia (Effah *et al.*, 2020).

Accurate identification of hyper-mucoviscous *K. pneumoniae* isolates is crucial because these strains may respond differently to therapy than non-hyper-mucoviscous strains. Hyper-mucoviscous strains may be more difficult to treat because they are more resistant to drugs and produce more virulence factors (Dos Anjos *et al.*, 2020).

3.5 Biofilm formation

The present investigation used ELISA to distinguish between *K. pneumoniae* strains that produced biofilms and those that did not, based on the median values of optical density at 590 nm (> 0.240, 0.120, and 0.120), since bacterial biofilms are associated with chronic disorders that are

difficult to treat. Forty isolates were examined for their biofilm-forming potential. As can be shown in Table (3-5), 37(92.5%) of these isolates formed a robust biofilm, 2(5.0%) formed a moderate biofilm, and only one (2.5%) isolate formed a weak biofilm.

These findings are consistent with those of Hessian, (2021), who reported that 50.6% of *K. pneumoniae* isolates create biofilm due to their ability to adhere to any community of microorganisms in which cells stick to one other and often adhere to a surface. In many cases, the matrix of extracellular polymeric substance that these adherent cells are embedded in is created by the cells themselves.

Table (3-5): Biofilm formation of *Klebsiella pneumoniae* isolates

Bacterial isolates (no.)	Biofilm			
	Strong	Moderate	Weak	% of biofilm formation
<i>K. pneumoniae</i> (40)	37(92.5%)	2(5%)	1(2.5%)	40(100%)

Sofy *et al.*, (2021) found that *K. pneumoniae* was responsible for about (85%) of all human illnesses. The ability of these bacteria to build biofilms in their host environments is one of their pathogenicity mechanisms, and it plays a role in both the microorganisms' increased virulence and their increased resistance to antibiotics, both of which contribute to their continued survival (Gebreyohannes *et al.*, 2019).

When cultivated on solid or semisolid surfaces, roughly 60% of the *K. pneumoniae* strains have the ability to produce additional flagella (called lateral). Adherence to biotic or abiotic surfaces, as well as biofilm development, involves both the polar and lateral flagella in these strains (Becker *et al.*, 2018).

The extracellular polymeric material (EPS) of a biofilm, commonly known as slime, consists primarily of DNA, proteins, and polysaccharides that are secreted by the organisms that form the biofilm. Biofilms can form on virtually any surface, whether they are living or nonliving, and they can be found in a wide variety of environments, including those found in nature, industry, and healthcare facilities (Colagiorgi *et al.*, 2016).

When compared to planktonic cells of the same organism, which were single cells that float or swim in a liquid media, the physiology of biofilm-forming microbial cells is very different (Tilahun *et al.*, 2016).

Biofilm formation by microorganisms can be triggered by a variety of stimuli, such as the detection of attachment sites on a surface by individual cells, the presence of nutrients (Sustr *et al.*, 2020), or even the exposure of planktonic cells to sub-inhibitory concentrations of antibiotics. Changing a cell's phenotype to grow in biofilms requires the differential regulation of many genes (Coughlan *et al.*, 2016).

Bacterial adhesion to a surface, microcolony growth, biofilm maturation, and bacterial detachment (termed dispersal) are the four processes generally accepted as constituting biofilm formation. Sessile bacteria, those found in biofilms, are distinguished from planktonic bacteria by their inactive growth state and unique morphologies (Muhammad *et al.*, 2020).

Polysaccharides, proteins, nucleic acids, lipids, and other macromolecules and chemicals make up the majority of the extracellular matrix that encloses biofilms (Khan *et al.*, 2017). Particularly, extracellular polysaccharides are a crucial component of the matrix, and carry out a range of functions such as promoting attachment to surfaces and other cells, building and maintaining biofilm structure, as well as protecting the cells

against environmental assaults and predation, including antimicrobials and host defenses (Karygianni *et al.*, 2020).

It has been proposed that three worldwide non-microbicidal techniques can be used in the fight against pathogenic bacteria with the ability to form biofilms by (i) preventing microbial attachment to a surface. Antimicrobial penetration can be improved by (ii) interfering with biofilm formation and/or altering biofilm architecture, and (iii) influencing biofilm maturation and/or causing its dispersal and destruction (Yuan *et al.*, 2020).

Table (3-6): Pattern phenotypic virulence factors and biofilm formation among *K. pneumoniae*

No. of isolates	Biofilm formation	Hemolysin production	Sidrophore production	Gelatinase production	Lipase production	Hemagglutination	Serum resistance	hypermucoviscosity
1.	Strong	+	-	-	+	+	+	+
2.	Strong	-	+	+	+	+	+	+
3.	Strong	+	-	-	-	+	-	+
4.	Strong	-	+	-	-	+	+	+
5.	Strong	-	+	-	-	+	+	+
6.	Strong	+	-	-	-	+	-	+
7.	moderate	-	+	-	-	+	-	+
8.	Strong	-	+	-	-	+	+	+
9.	Strong	+	-	-	-	-	+	+
10.	Strong	-	+	+	+	+	+	+
11.	Strong	-	+	-	-	+	-	+
12.	Strong	+	-	-	-	+	+	+
13.	Strong	-	+	-	-	+	-	+
14.	Strong	-	+	-	-	+	+	+
15.	Strong	+	-	-	-	+	-	+
16.	Strong	-	+	-	-	+	+	+
17.	moderate	-	+	-	-	+	-	+
18.	Strong	+	-	-	-	+	+	+
19.	Strong	-	+	+	+	+	+	+
20.	Strong	-	+	-	-	+	+	+
21.	Strong	+	-	-	-	-	+	+
22.	Strong	-	+	-	-	+	+	+
23.	Strong	+	-	-	-	+	-	+
24.	Strong	-	+	-	-	+	+	+
25.	Strong	-	+	-	-	+	-	+
26.	Strong	+	-	-	-	+	+	+
27.	Strong	+	-	-	-	+	+	+

Table (3-6): Pattern phenotypic virulence factors and biofilm formation among *K. pneumoniae*

28.	Strong	-	+	+	+	+	-	+
29.	Strong	+	-	-	-	+	+	+
30.	Strong	-	+	-	-	+	-	+
31.	Strong	+	-	-	-	+	-	+
32.	Strong	-	+	-	-	+	+	+
33.	Strong	+	-	-	-	-	-	+
34.	Strong	-	+	-	-	+	+	+
35.	Strong	+	-	-	-	+	+	+
36.	Strong	-	+	-	-	+	+	+
37.	Strong	+	-	-	-	+	-	+
38.	Strong	+	-	-	-	+	+	+
39.	Strong	+	-	-	-	+	-	+
40.	weak	-	+	-	-	+	+	-
Total		18(45%)	22(55%)	4(10%)	5(12.5%)	37(92.5%)	25(62.5%)	39(97.5%)

3.6 Antibiotic susceptibility test

Antibiotics susceptibility test was done for all 40 *K. pneumoniae* isolates examined towards 17 different antibiotics using Vitek II system as shown in Table (3-7).

K. pneumoniae was shown to have a high resistance rate to Imipenem (82.5%) and Meropenem (77.5%) in this investigation. These findings corroborate those of Duan *et al.*, (2022), who discovered that *K. pneumoniae* showed a high level of resistance to the antibiotics Imipenem (97.6%) and Meropenem (77.1%).

Table (3-7): Antibiotic resistance of *Klebsiella pneumoniae* isolates

No.	Antibiotics	sync	Resistant (No. &%)	Intermediate (No. &%)	Sensitive (No. &%)
1.	Amikacin	AK	13(32.5%)	2(5%)	25(62.5%)
2.	Amoxicillin/clavulanic acid	AML/CLV	7(17.5%)	3(7.5%)	30(75%)
3.	Cefazolin	SEF	9(22.5%)	1(2.5%)	30(75%)
4.	Cefepime	FEP/CPM	9(22.5%)	2(5%)	29(72.5%)
5.	Ceftazidime	CAZ	10(25%)	3(7.5%)	27(67.5%)
6.	Ceftriaxone	CEZ	12(30%)	3(7.5%)	25(62.5%)
7.	Cefuroxime	CXM	6(15%)	1(2.5%)	33(82.5%)
8.	Cefuroxime Axetil	CRO/AXL	14(35%)	3(7.5%)	23(57.5%)
9.	Ciprofloxacin	CIP	9(22.5%)	1 (2.5 %)	30(75%)
10.	Ertapenem	ETP	26(65%)	2(5%)	12(30%)
11.	Fosfomycin	FOT	27(67.5%)	2(5%)	11(27.5%)
12.	Gentamycin	CN	12(30%)	1(2.5%)	27(67.5%)
13.	Imipenem	IMP	33(82.5%)	3(7.5%)	4(10%)
14.	Meropenem	MEM	31(77.5%)	3(7.5%)	6(15%)
15.	Nitrofurantoin	NIT	12(30%)	1(2.5%)	27(67.5%)
16.	Piperacillin/tazobactam	TZP	6(15%)	1(2.5%)	33(82.5%)
17.	Trimethoprim/sulfamethoxazole	TMP-SMX	18(45%)	2(5%)	20(50%)

Antibiotics belonging to the class of carbapenems, such as imipenem and meropenem, are frequently used to treat infections brought on by bacteria, such as *K. pneumoniae*, as was discovered by Gao & Li, (2020). Yet some *K. pneumoniae* strains have become resistant to imipenem, thus it might not work for infections caused by these strains (Pacios *et al.*, 2021).

There are a number of potential processes that can lead to resistance to imipenem and meropenem. carbapenemase synthesis is a typical mechanism that can deactivate antibiotics (Aurilio *et al.*, 2022). Several antibiotics, including imipenem, may be rendered ineffective against *K. pneumoniae* due to the production of carbapenemases such as KPC, NDM, and OXA enzymes (Theuretzbacher *et al.*, 2021).

An infection caused by *K. pneumoniae* that is resistant to imipenem and meropenem may necessitate the use of another antibiotic. Antibiotic selection is based on a number of criteria, including the nature of the infection, its site, the patient's age and general condition, and the susceptibility of the bacteria to the antibiotics under consideration (Karakonstantis *et al.*, 2020). Antibiotic combinations are sometimes used in treatment, and how long patients stay on them is determined by the kind and severity of the infection (Niederman *et al.*, 2021).

Antibiotic resistance was also seen in this study, with 67.5% of *K. pneumoniae* being resistant to fosfomicin and 65% being resistant to ertapenem. These findings corroborated those of Ojdana *et al.*, (2019), who discovered a similar high proportion of fosfomicin resistance among *K. pneumoniae* (60.5%). In their study, Ku *et al.*, (2017b) discovered that the carbapenems drugs fosfomicin and ertapenem are effective against bacterial infections caused by *K. pneumoniae*.

Several processes can lead to fosfomycin and ertapenem resistance. carbapenemase synthesis is a frequent method that is used to counteract the effects of antibiotics. *K. pneumoniae* infections that are resistant to ertapenem may require treatment with other antibiotics (Aurilio *et al.*, 2022).

Urinary tract infections caused by bacteria, particularly *K. pneumoniae*, are typically treated with the antibiotic fosfomycin. However, fosfomycin resistance is a problem for some strains of *K. pneumoniae*, which means the antibiotic might not work for infections caused by these strains (Gopichand *et al.*, 2019).

There are a number of potential processes that can lead to fosfomycin resistance. Fosfomycin-modifying enzymes are an often-used mechanism for resistance, as they change the antibiotic in a way that renders it useless. Mutations in the genes encoding the target enzyme of fosfomycin, called MurA, can be produced by *K. pneumoniae* and impair the binding of the antibiotic, diminishing its efficacy (Van Duijkeren *et al.*, 2018). 45% of the bacteria tested were resistant to the antibiotic combination trimethoprim/sulfamethoxazole. Often used to treat bacterial infections like those caused by *K. pneumoniae*, the antibiotic combination trimethoprim/sulfamethoxazole (sometimes known as co-trimoxazole) is also known by its generic name (Fajfr *et al.*, 2017).

Many different pathways can lead to bacteria being resistant to trimethoprim/sulfamethoxazole. Dihydrofolate reductases and dihydropteroate synthases are two enzymes that are frequently produced by bacteria and can change the antibiotic and render it ineffective. In order to resist antibiotic treatment, *K. pneumoniae* can develop variations of these enzymes (Dowling *et al.*, 2017).

In rare cases, the antibiotic Amikacin was used to treat *K. pneumoniae* infections. Amikacin's efficacy, like that of other antibiotics, can be diminished if bacteria have evolved resistance to it (Li & Webster, 2018).

Several pathways exist for *K. pneumoniae* to develop resistance to Amikacin. One strategy was to generate enzymes termed aminoglycoside-modifying enzymes (AMEs), which render the antibiotic ineffective. Mutations in the genes of the bacteria that interfere with the uptake or processing of the antibiotic are another method (Fernández-Martnez *et al.*, 2018).

Depending on the nature of the infection and the sensitivity profile of the bacteria, alternative antibiotics may be employed if a strain of *K. pneumoniae* was found to be resistant to Amikacin. It was critical to take these treatments sparingly and only when absolutely necessary because improper use of antibiotics can contribute to the development of antibiotic resistance (Norsigian *et al.*, 2019).

One combination antibiotic used to treat bacterial infections like those produced by *K. pneumoniae* was amoxicillin/clavulanic acid. Yet, *K. pneumoniae* can acquire antibiotic resistance over time via a number of ways, making it similar to many other bacteria. Producing enzymes called beta-lactamases, which may break down the beta-lactam ring of the amoxicillin molecule, renders *K. pneumoniae* resistant to amoxicillin/clavulanic acid (Cusini *et al.*, 2018).

In addition to the creation of efflux pumps and alterations to the cell wall structure, there are a number of other factors that can contribute to *K. pneumoniae's* resistance to amoxicillin/clavulanic acid. The development of antibiotic-resistant strains as a result of antibiotic overuse or misuse. The

growth of antibiotic-resistant bacteria is aided by a lack of adequate infection control methods in healthcare settings (Hasan *et al.*, 2021b).

Antibiotics from the cephalosporin family, such as cefazolin, ceftazidime, Piperacillin/tazobactam and ceftriaxone, were commonly used to treat *K. pneumoniae* infections. Several methods exist for this to happen, one of which is the creation of beta-lactamases, enzymes that degrade the beta-lactam ring in cephalosporins and other beta-lactam antibiotics, rendering them useless (Padmini *et al.*, 2017).

Antibiotics such as carbapenems or fluoroquinolones may be necessary in cases where *K. pneumoniae* was resistant to these drugs. Antibiotic resistance is a major health concern, and one possible cause of this issue is the improper use of antibiotics. Because of this, antibiotics should be used sparingly and only when absolutely required (Charles *et al.*, 2022).

Multiple drug resistance was observed in *K. pneumoniae*, demonstrating its widespread presence in the study. Many international investigations have implicated plasmids as the causal agents of a wide variety of resistant phenotypes (Peirano *et al.*, 2020).

The relative ease with which mobile genetic elements like plasmids, transposons, and gene cassettes in integrons can transfer resistance determinants within and between bacterial species is a potential contributor to the rise of multi-resistant bacteria. This resistance to many antibiotics can occur independently of plasmids or transposons (Botelho & Schulenburg, 2021).

Several antibiotic resistances were frequent among *K. pneumoniae*, despite the fact that many different antibiotics have been used successfully to treat illnesses caused by this bacteria (Karakonstantis *et al.*, 2020).

Overuse and improper disposal of drugs are major contributors to *Klebsiella* rise in antibiotic resistance. Antibiotic resistance is a direct result of the heavy and widespread use of antibiotics in hospitals, which also promotes the selection of drug-resistant organisms in healthcare settings (Shelenkov *et al.*, 2020).

Nowadays, β -lactam antibiotics, which block transpeptidases involved in bacterial cell wall formation, are the standard treatment for infections. The beta-lactamase enzymes can inactivate these beta-lactam antibiotics, which is a major problem (Lima *et al.*, 2020).

3.7 Molecular identification of *K. pneumonia* ST 258 by specific primer gene

When the PCR process is complete, billions of copies of the target sequence will have been produced due to DNA polymerase's ability to synthesize a new strand of DNA that is complementary to the provided template strand (Amplicon). All of the possible *K. pneumonia* isolates had their DNA taken and ran through a standard PCR for *pilv-l* gene primer amplification using the sequences and software in Table (2-15).

Figure (3-5) shows the results of the gel electrophoresis analysis, which revealed that only 16(40%) of the 40 *K. pneumonia* isolates were related to *K. pneumonia* ST 258 by sharing the same 320 bp DNA fragment with the allelic ladder.

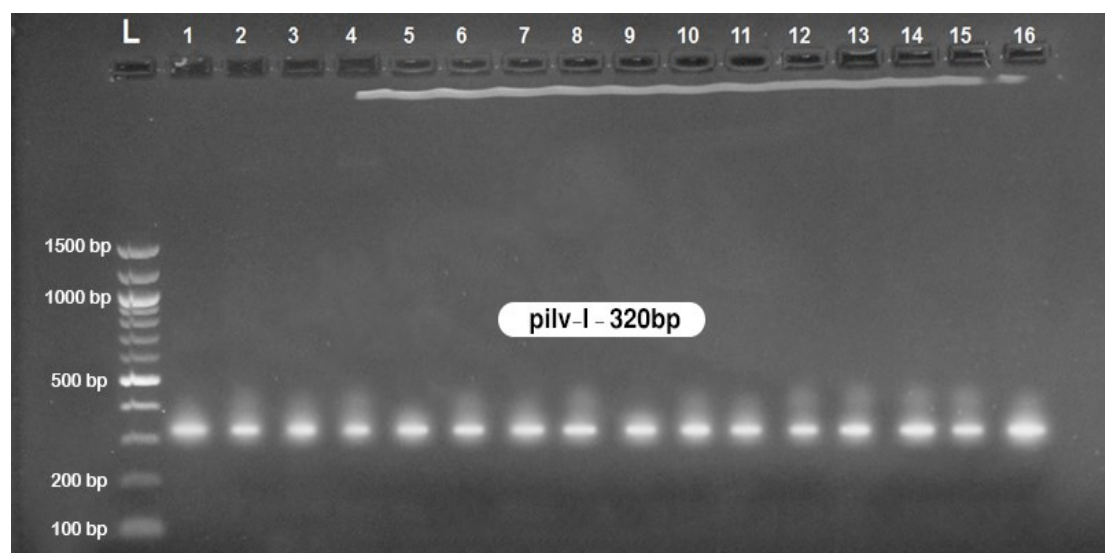


Figure (3-5): Agarose gel electrophoresis (1.5%) of RCR amplified of *pilv-I* gene (320bp) of *Klebsiella pneumonia* ST 258 for (55) min at (70) volt L: ladder (DNA marker). Number (1-16) positive *Klebsiella pneumonia* ST 258 isolates.

These findings corroborated those of Mendes *et al.*, (2022), who discovered that, polymerase chain reaction (PCR) amplification of a certain gene or area of the genome allows for molecular identification of *K. pneumoniae* ST 258, using specific primers.

A study of Gato *et al.*, (2020) found the *16S rRNA* gene and the *pilv-I* gene were frequently utilized for molecular identification of *K. pneumoniae* ST 258. Reyes Chacón, (2019) found, primers utilized for amplification of this gene were tailored to recognize only *K. pneumoniae* ST 258 and exclude all other bacteria.

A comparison of the amplified product to previously established *K. pneumoniae* ST 258 sequences will be served to verify the bacterium's identification. For further insight into the processes of virulence and antibiotic resistance in *K. pneumoniae* ST 258, sequencing the amplified product can provide much more about the bacterium's genetic make-up, which can aid in epidemiological investigations (Shankar *et al.*, 2020).

Detecting *K. pneumoniae* strain ST 258 in a biological sample by the use of a molecular biology methodology that focuses on the *pilv-l* gene (Mandras *et al.*, 2020).

Reyes Chacón, (2019) demonstrated that key to the pathogenesis of *K. pneumoniae* strain ST 258 is the *pilv-l* gene. The protein encoded by this gene was a type IV pilus, which plays a role in bacterial adhesion to host cells and the development of biofilms. Marking *K. pneumoniae* strain ST 258 for detection, the *pilv-l* gene was unique to this strain. *K. pneumoniae* ST 258 can be detected molecularly by amplifying the *pilv-l* gene according to study of Moore, (2017), which requires the extraction of DNA from a biological sample (such as blood, urine, or tissue) and subsequent amplification using polymerase chain reaction (PCR) or other molecular techniques. Gel electrophoresis or sequencing can be used on the amplified DNA to confirm the presence of *K. pneumoniae* ST 258.

Using this approach, even trace amounts of *K. pneumoniae* ST 258 may be detected, demonstrating its exceptional specificity and sensitivity. Because this bacteria was resistant to many medications and can cause life-threatening conditions like pneumonia, sepsis, and urinary tract infections, this test is of particular value in clinical settings for making a prompt and accurate diagnosis of infections caused by it (Mandras *et al.*, 2020).

3.8 Colanic acid production by *Klebsiella pneumoniae* and *Klebsiella pneumoniae* sub spp. *pneumoniae* ST 258

Colanic acid is one of the sugar polymers that are found in the capsular polysaccharide of bacteria and in the study, the results showed that colanic acid were produced by *K. pneumoniae* but at different rate as shown in Table (3-8), Figure (3-6).

Table (3-8): Colanic acid producing by *Klebsiella pneumoniae* and *Klebsiella pneumoniae* sub spp. *pneumoniae* ST 258

<i>K. pneumoniae</i> sub spp. <i>pneumoniae</i> ST 258			
Isolate No.	OD 530 nm	Concentration of galactouronic acid µg/ml	Concentration of colanic acid µg/ml
1.	1.9	100	95
2.	1.8	80	90
3.	1.7	60	85
4.	1.5	40	75
5.	1	20	50
6.	0.7	0	35
<i>K. pneumoniae</i>			
Isolate No.	OD 530 nm	Concentration of galactouronic acid µg/ml	Concentration of colanic acid µg/ml
1.	1.8	100	90
2.	1.5	80	75
3.	1	60	50
4.	0.7	40	35
5.	0.12	20	6
6.	0.03	0	1.5

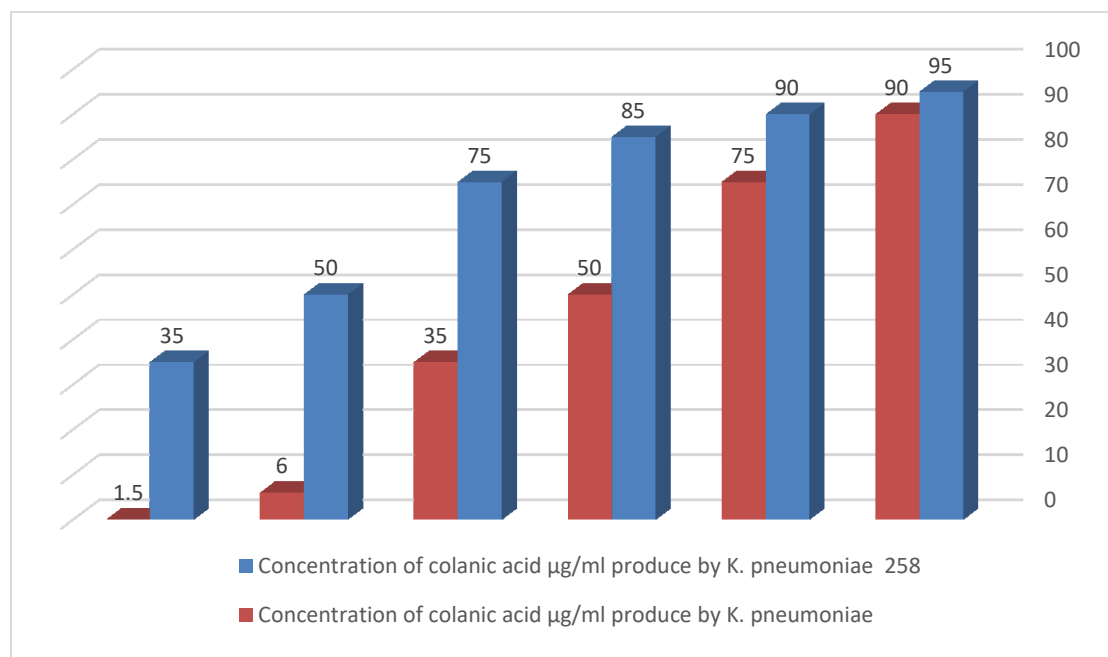


Figure (3-6): Concentration of colanic acid µg/ml producing by *Klebsiella pneumoniae* and *Klebsiella pneumoniae* sub spp. *pneumoniae* ST 258

The results of this study indicated that the colanic acid created at high rate by typeable *K. pneumoniae* ST 258 which may be linked to the possession of this type to the capsule that lead to secretion of exopolysaccharides secretion extracellularly. Regarding capsulated *K. pneumoniae* ST 258, Alphonse *et al.*, (2022) showed that *K. pneumoniae* polysaccharides contain 2-acetamide-2-deoxy-D-mannoseuronic acid. On the other hand, *K. pneumoniae* produced minimal amount of this exopolysaccharide molecule. Palomares-Navarro *et al.*, (2023) revealed that colanic acid comprises roughly 119% of capsule polysaccharides.

In a study that was done by Rai & Mitchell, (2020) evaluating the role of this substances revealed that this exopolysaccharide material might potentially be involved in virulence and even made the bacteria more invasive and producing severe sickness where it connected with biofilm and resistance to antibiotics.

3.9 Detection of virulence factors genes

The potential of contracting a *K. pneumoniae* ST 258 infection is increased by a number of circumstances. To extent do these features, such as antibiotic resistance and the development of virulence factors associated with infection-derived *K. pneumoniae* ST 258 strains, contribute to the establishment and maintenance of this opportunistic disease as a major community-acquired and nosocomial pathogen (Rostkowska *et al.*, 2020).

Capsular polysaccharide, adhesions, and siderophores are just a few of the virulence elements that contribute to *K. pneumoniae* ST 258 pathogenicity. Because of the prevalence of fatalities before antibiotic treatment, the presence of virulence factors in *K. pneumoniae* ST 258 is crucial. Genes like *YbtS*, *entB*, *mrkD*, *magA*, *kfu*, *iutA*, *rmpA*, and *K2* code for virulence factors (Martins *et al.*, 2020).

In this study, it was identify key genes responsible for *K. pneumoniae* ST 258 production. Depended on our knowledge, this is the first study in Iraq to reveal the presence of virulence genes in *K. pneumoniae* ST 258 isolates and to compare with ordinary *K. pneumoniae* isolates, therefore it was significant.

3.9.1 Detection of Fimbrial Adhesin type 1 gene (*fimH* gene) and Fimbrial Adhesin type 3 gene (*mrkD* gene)

In this study, *fimH* gene were studied in all 16 *K. pneumoniae* ST 258 isolates and compared with 16 *K. pneumonia* isolates. The results showed that all 16(100%) were positive to *fimH* gene of *K. pneumoniae* ST 258 isolates while 12/16(75%) *K. pneumoniae* isolates were found. PCR product was roughly (688bp) in size, when they used the same primer, the results were shown in Figure (3-7).

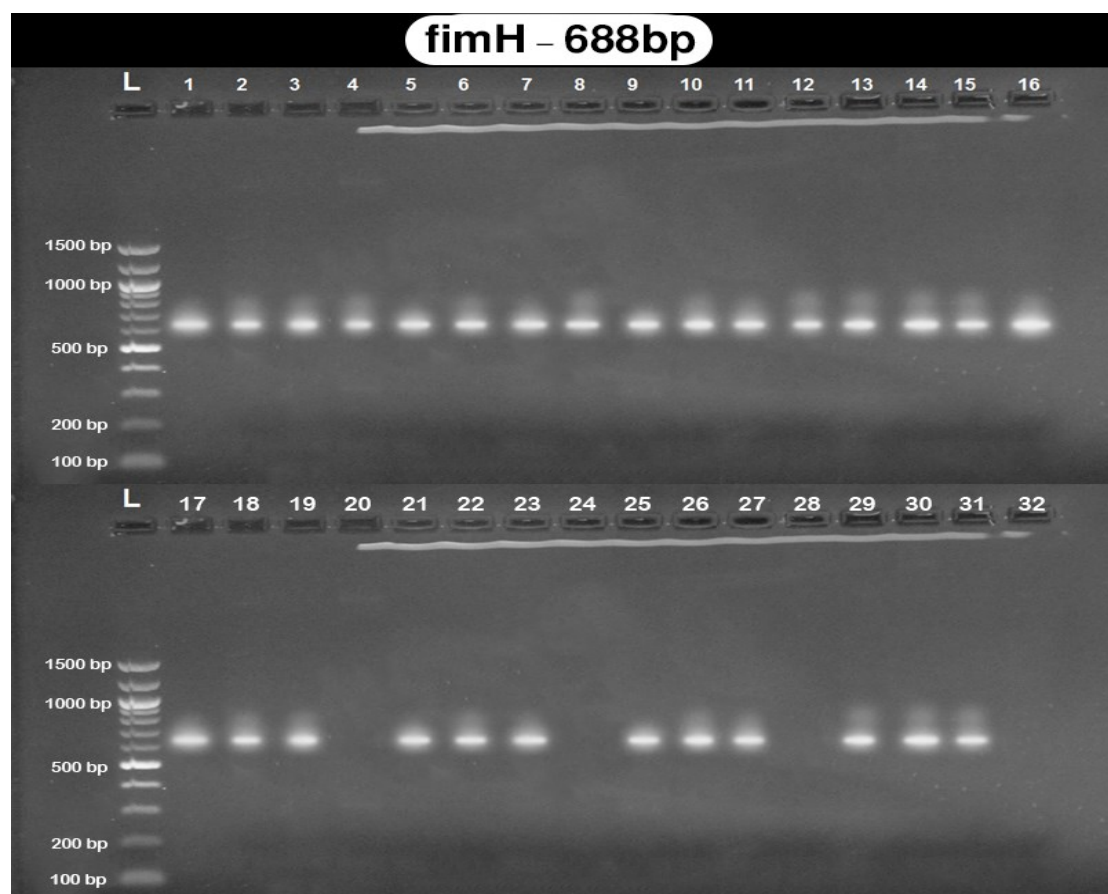


Figure (3-7): Agarose gel electrophoresis (1.5%) of RCR amplified of *fimH* gene (688bp) of *Klebsiella pneumoniae* ST 258 for (55) min at (70) volt L: ladder (DNA marker). Number (1-16) positive *Klebsiella pneumoniae* ST 258 isolates, while number (17, 18, 19, 21, 22, 23, 25, 26, 27, 29, 30, 31) positive *K. pneumoniae* isolates.

However, *mrkD* gene were studied in all 16 *K. pneumoniae* ST 258 isolates and compared with 16 *K. pneumoniae* isolates. The results showed that 13/16(81.2%) were positive to *mrkD* gene of *K. pneumoniae* ST 258 isolates while 11/16(68.7%) *K. pneumoniae* isolates were found. PCR product was roughly (240bp) in size, the results were shown in Figure (3-8).

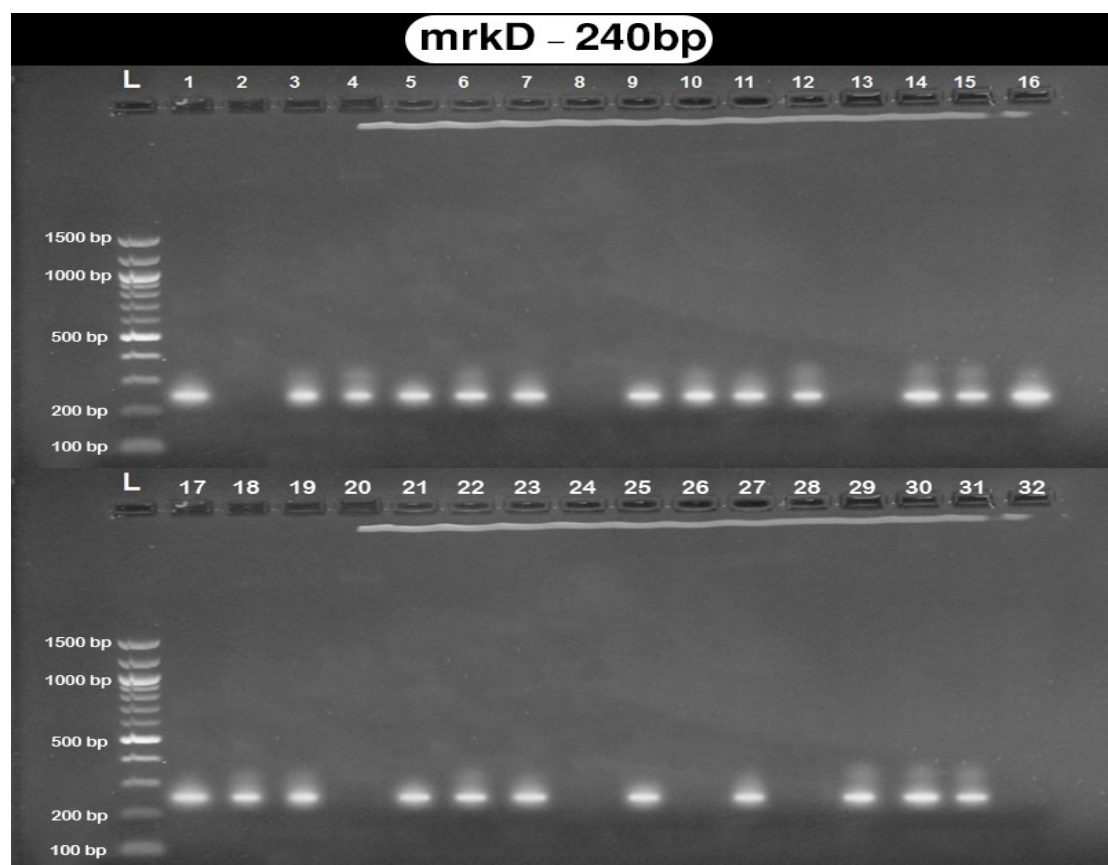


Figure (3-8): Agarose gel electrophoresis (1.5%) of RCR amplified of *mrkD* gene (240bp) of *Klebsiella pneumoniae* ST 258 for (55) min at (70) volt L: ladder (DNA marker). Number (1,3,4,5,6,7,9,10,11,12,14,15,16) positive *Klebsiella pneumoniae* ST 258 isolates, while number (17, 18, 19, 21, 22, 23, 25, 27, 29, 30, 31) positive *Klebsiella pneumoniae* isolates.

Schroll *et al.*, (2010) demonstrated, the gene for type 1 fimbrial adhesin (*fimH* gene) in bacteria encodes for the fimH protein. For many dangerous bacteria, like *K. pneumoniae* ST 258, this protein served as a crucial virulence component.

Polymerase chain reaction and other methods of molecular biology could be used to detect the *fimH* gene. Primers designed to bind to the DNA sequence of interest were employed in the PCR procedure to kick off the amplification process (Monesh Babu *et al.*, 2021).

Several infections might be better diagnosed and treated when the *fimH* gene was discovered. The ability of *K. pneumonia* to adhere to and infiltrate host cells is essential for infection to take hold, and this ability was found to be substantially correlated with the presence of the *fimH* gene. More precise diagnoses and treatments of infection could be implemented if the *fimH* gene could be detected in patient samples (Aljanaby and Alhasani, 2016). Molecular biology methods can be used to detect the *fimH* gene in *K. pneumoniae*, which can reveal important details regarding the strain and virulence of the infecting bacteria (Mirzaie & Ranjbar, 2021).

These findings corroborated those of Surgers *et al.*, (2019), who reported that the *mrkD* gene, which codes for virulence factors, was present in *K. pneumoniae* isolates at a rate of 60.5%. The *mrkD* gene was discovered to be responsible for the production in 91.66 percent of *K. pneumoniae* isolates, as reported by Liu and Guo, (2019).

Klebsiella pneumoniae type 3 fimbriae consist of the primary fimbrial subunit (MrkA) and an adhesin (MrkD) that has been proven to mediate binding to collagen. Using continuous-flow chambers, we tested the biofilm-forming potential of *K. pneumoniae* adhesive and non-adhesive derivatives on collagen-coated surfaces (Abozahra *et al.*, 2020).

In contrast to biofilm formation on abiotic plastic surfaces, growth on collagen-coated surfaces required the presence of the MrkD adhesin. Strains of fimbriate bacteria missing the MrkD adhesin have trouble sticking to and colonizing these surfaces (Clegg & Murphy, 2017). While direct attachment to the respiratory cells was not detected during MrkD-mediated biofilm formation, both purified human extracellular matrix and the extracellular matrix produced by human bronchial epithelial cells cultured *in vitro* served as acceptable substrates (Willsey, 2018).

This suggests that type 3 fimbriae play a dual role in the establishment of adhesion and subsequent growth on long-term implants like endotracheal tubes. Small molecules called siderophores can scavenge iron from their host proteins (Bunyan *et al.*, 2018). Further characterization of the function of the *mrkD* gene in *K. pneumoniae* type 3 fimbriate attachment was performed. Two copies of the *mrkA* fimbrial subunit gene and one copy of the *mrkD* adhesin subunit gene were discovered in a *K. pneumoniae* clinical isolate. Both *mrkA* and *mrkD* were present in bacteria, but only one was on the chromosome. *mrkA* was connected with *mrkD* on a plasmid (Hu *et al.*, 2020).

When *K. pneumoniae* was serially cultivated in broth at 44°C, the *mrkD* gene cluster carried by the plasmid was lost. The resultant *mrkD*-negative strain, dubbed *K. pneumoniae*, lacked the adherence features of *K. pneumoniae* with *MrkD*-positive fimbriae, such as agglutination of tannic acid-treated human erythrocytes and attachment to trypsinized human buccal cells (Nibogora, 2020).

Type 3 fimbriae, however, were formed by *K. pneumoniae* and were made up of the signature 21.5-kDa major fimbrial subunit, were reactive with particular serum, and could be seen clearly by immunoelectron microscopy (Ares *et al.*, 2019).

Adhesions of type 1 and type 3 fimbriae, encoded by the genes *fimH* and *mrkD* in *K. pneumoniae*, mediate adherence to the extracellular matrix; promote biofilm production; and may play a crucial role in colonization, invasion, and pathogenicity (Panjaitan *et al.*, 2019).

Both the *fimH-1* and *mrkD* virulence genes were present in the vast majority of the MRD *K. pneumoniae* isolates (Luo *et al.*, 2017). One of the most crucial steps in the development of a *K. pneumoniae* infection is related

to its ability to adhere to host surfaces and demonstrate persistent colonization, even though studies have reported that many clinical *K. pneumoniae* isolates normally express both type 1 and type 3 fimbrial adhesions (de Arajo *et al.*, 2019). *MrkD* mediates attachment to the extracellular matrix specifically, allowing *Klebsiella pneumoniae* to stick to injured tissue and coat indwelling devices such urinary catheters and endotracheal tubes (Martin & Bachman, 2018). *K. pneumoniae* type 3 fimbriae have been shown to bind to endothelium cells and epithelial cells in the respiratory and urinary systems, and play a crucial role in biofilm formation (Lin *et al.*, 2017; Marques *et al.*, 2019), it is known that *K. pneumoniae* isolates were more invasive, resistant to the normal bactericidal effect of human serum, and able to create more fimbrial adhesions (Sofiana *et al.*, 2020).

3.9.2 Detection of *magA* (K1) gene and Capsule gene (K2) (*wzy* gene)

magA gene were detected in all 16 *K. pneumoniae* ST 258 isolates and compared with 16 *K. pneumoniae* isolates. The results showed that 15/16(93.7%) were positive to *magA* gene of *K. pneumoniae* ST 258 isolates while 10/16(62.5%) *K. pneumoniae* isolates were found. PCR product was roughly (1282bp) in size, the results were shown in Figure (3-9). In addition, *wzy* gene were detected in all 16 *K. pneumoniae* ST 258 isolates and compared with 16 *K. pneumoniae* isolates. The results showed that 15/16(93.7%) were positive to *wzy* gene of *K. pneumoniae* ST 258 isolates while 11/16(68.7%) *K. pneumoniae* isolates were found. PCR product was roughly (641bp) in size, the results were shown in Figure (3-10).

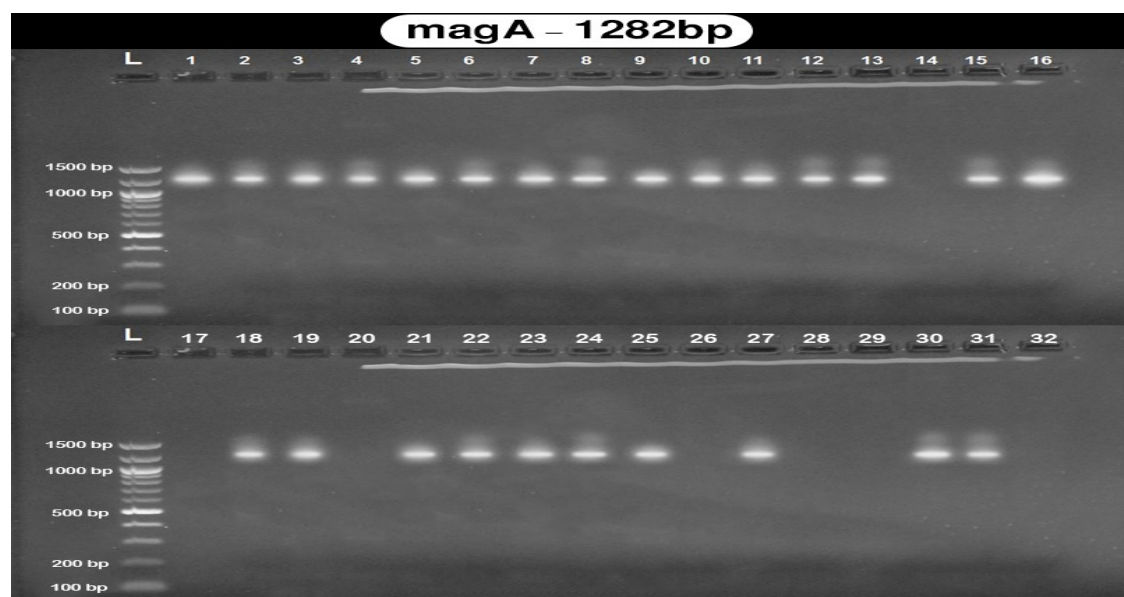


Figure (3-9): Agarose gel electrophoresis (1.5%) of RCR amplified of *magA* gene (1282bp) of *Klebsiella pneumonia* ST 258 for (55) min at (70) volt L: ladder (DNA marker) .Number (1,2,3,4,5,6,7,8,9,10,11,12,13, 15,16) positive *Klebsiella pneumonia* ST 258 isolates, while number (18, 19, 21, 22, 23, 24, 25, 27, 30, 31) positive *Klebsiella pneumonia* isolates.

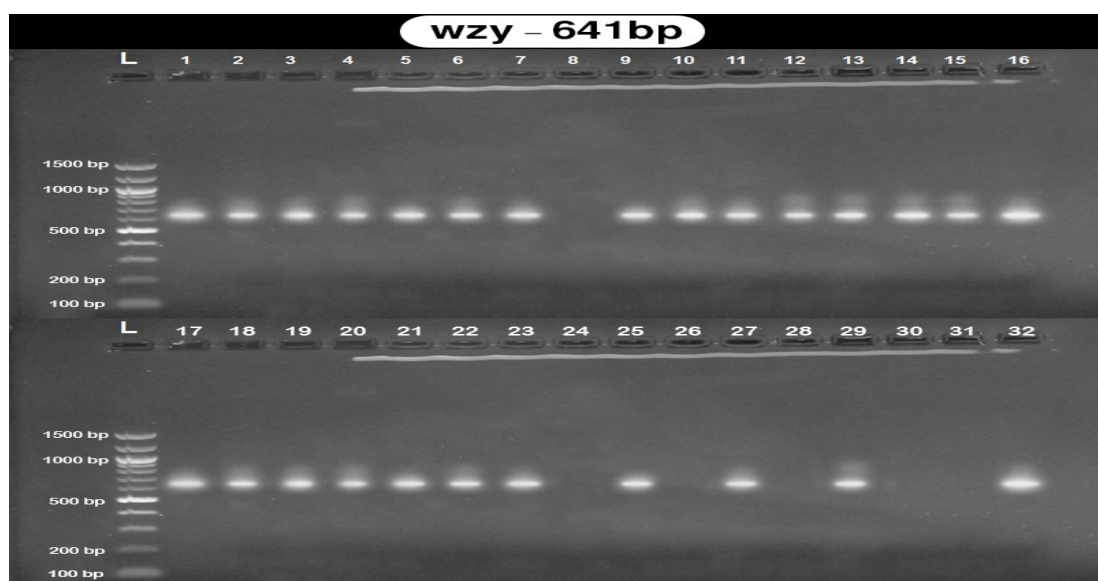


Figure (3-10): Agarose gel electrophoresis (1.5%) of RCR amplified of *wzy* gene (641bp) of *Klebsiella pneumonia* ST 258 for (55) min at (70) volt L: ladder (DNA marker). Number (1-16 except 8) positive *Klebsiella pneumonia* ST 258 isolates, while number (17,18,19,20,21,22,23, 25,27,29,32) positive *Klebsiella pneumonia* isolates.

Certain K1 serotype samples may lack the *magA* gene because of mutation or deletion in this gene, or because they were exposed to antibiotics

that inhibit the formation of the capsular polysaccharide of *K. pneumoniae* (Martin & Bachman, 2018). Hypermucoid phenotype was observed in all samples harboring *magA* genes in the present study. It was shown by Catalán-Nájera *et al.*, (2017) that *magA* is part of an operon that is unique to serotype K1 *cps* gene clusters. Similar results were obtained by Wyres *et al.*, (2020), who analyzed 134 *K. pneumoniae* isolates, showing that *magA* is unique to the *K. pneumoniae* capsule serotype K1 gene cluster and absent in all Non-K1 strains. Hence, molecular identification of *K. pneumoniae* serotype K1 isolates can be accomplished rapidly and accurately using PCR analysis for *magA*. According to Liu and Guo, (2019), *magA* was found in all 34 K1-serotyped isolates but none of the other 39 strains.

The K2 gene was discovered in ESBL isolates of *K. pneumoniae* with a detection rate of 33.3%, as reported by Taraghian *et al.*, (2020). The K2 gene was discovered in 79.2 percent of *K. pneumoniae* isolates, according to research published by Liu and Guo, (2018).

The capsule serotypes of *K. pneumoniae* have been the primary focus of virulence determinant studies, with K1 serotype being the most dangerous to humans (Fu *et al.*, 2019). There was a marked increase in the prevalence of serotype K1 isolates compared to other serotypes. These findings corroborated those of Kim *et al.*, (2017), who found that K1 and/or K2 serotype isolates were substantially more common than non-K1 and non-K2 (Non-K1/Non-K2) isolates.

M'lan-Britoh *et al.*, (2018) found that *K. pneumoniae* serotype K1 is more prevalent than the other serotypes in the various infections they studied, and these findings are consistent with those of M'lan-Britoh *et al.*, (2018). Also, the most prevalent *K. pneumoniae* isolates are of the K1 and K2 serotypes, as cited by Guo *et al.*, (2017).

However Harada *et al.*, (2018) found that K1 prevalence was 83.3% and K2 prevalence was 2.4%. Capsules, lipopolysaccharides, siderophores, and fimbriae are all recognized as virulence factors in *K. pneumoniae*. The capsule has received the greatest attention as a potential virulence component. K1 and K2 capsular serotypes, in particular, are associated with invasive illnesses and are notorious for their hyper virulence and hyper-mucoviscibility (Walker *et al.*, 2019). As mentioned by Marr and Russo (2019), the capsule is a major virulence factor for *K. pneumoniae*, protecting the bacteria against lysis by serum factors and phagocytosis (Wei *et al.*, 2020).

Carbapenem-resistant hyper virulent *K. pneumoniae* (CR-HvKP) has emerged as a major community-acquired infection-causing strain of *K. pneumoniae*, and it has been linked to the *rmpA*, *k1* and *k2* genes (Liu & Guo, 2018; Choby *et al.*, 2020). This finding shows that the *K. pneumoniae* in this investigation did not exhibit molecular characteristics of the hyper virulent (hypermucoviscous) *K. pneumoniae*. Those (pathogenic) isolates tested positive for the K2 serotype, according to the results. Very specific molecular diagnostics based on polymerase chain reaction (PCR) analysis of the open reading frame (ORF)-9 region K2 of *K. pneumoniae* serotype K2 might be utilized to identify the *K. pneumoniae* capsule K2 serotype (Palacios, 2017).

Invasive infections are more likely to be caused by K1 or K2 serotypes. *magA* (mucoviscosity associated gene A) is a serotype-specific gene for K1, while K2A is the same for the K2 serotype (K2 capsule-associated gene A) It was discovered by Remya *et al.*, (2018) that the *magA* gene is exclusive to the capsular serotype *K1* gene cluster.

Capsular serotype K2 has a highly specialized *cps* gene cluster, and the K2 gene, which is equivalent to *magA* in the K1 serotype, is a member of that cluster. *K. pneumoniae* K1 and K2 serotypes can be detected quickly and reliably using the K2 detection method (Wang *et al.*, 2018).

3.9.3 Mucoïd phenotype A gene (*rmpA* gene)

rmpA gene were detected in all 16 *K. pneumoniae* ST 258 isolates and compared with 16 *K. pneumoniae* isolates. The results showed that all 16/16(100%) were positive to *rmpA* gene of *K. pneumoniae* ST 258 isolates while 12/16(75%) *K. pneumoniae* isolates were found. PCR product was roughly (535bp) in size, the results were shown in Figure (3-11).

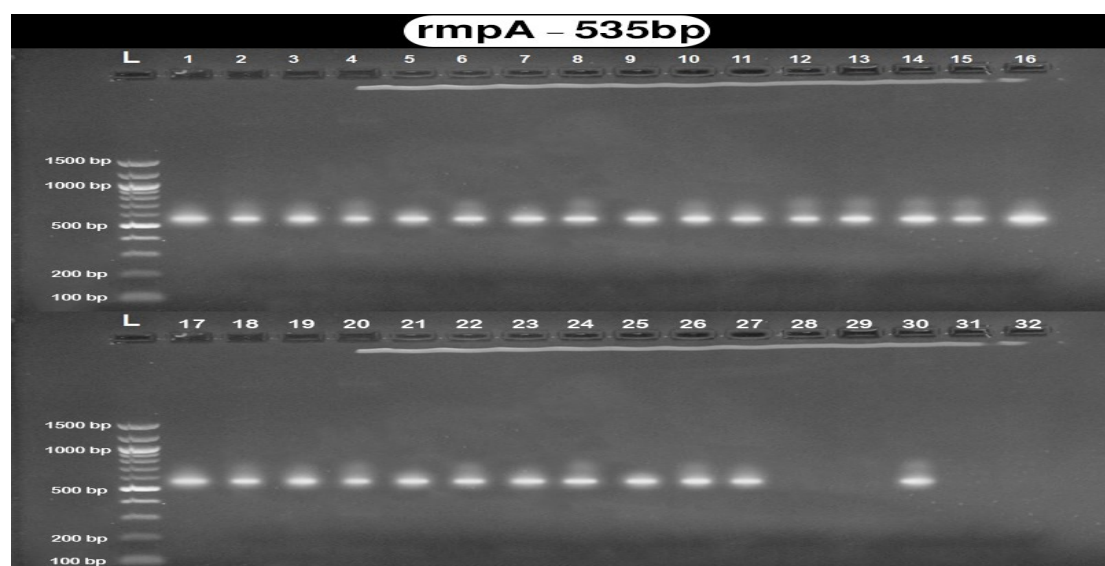


Figure (3-11): Agarose gel electrophoresis (1.5%) of RCR amplified of *rmpA* gene (535bp) of *Klebsiella pneumoniae* ST 258 for (55) min at (70) volt L: ladder (DNA marker). Number (1-16) positive *Klebsiella pneumoniae* ST 258 isolates, while number (17,18,19, 20,21,22, 23,24,25,26,27,30) positive *Klebsiella pneumoniae* isolates.

The *rmpA* was found to be on a 180-Kb virulence plasmid, as reported by Kadhim *et al.*, (2020). Mucoïd phenotypic expression in *K. pneumoniae* was regulated by this multi-copy plasmid. Turton *et al.*, (2018) discovered that *rmpA*-carrying plasmids were present in *K. pneumoniae* isolates, and that these plasmids also included several virulence-associated genes.

The frequency of the *rmpA* gene is 48%, as reported by Hao *et al.*, (2020). By testing for the presence of several genes associated with virulence, Xu *et al.*, (2019) found that *rmpA* was present in 96% of the causal isolates.

Hypermucoviscosity and high pathogenicity in *K. pneumoniae* have been linked to the *rmpA* gene, which was the most commonly seen variant. Early diagnosis of infection in vulnerable hosts is made possible by molecular detection of these genes. In light of these results, additional research was required to clarify the function of other host and pathogen variables that may contribute to disease progression at the physiological and molecular levels (Marimani *et al.*, 2018).

The *rmpA* gene was a virulence factor found in some strains of the bacterium *K. pneumoniae*. This gene encodes for a protein called the regulator of mucoid phenotype A, which is involved in regulating the production of a polysaccharide capsule that surrounds the bacterium (Aljanaby & Alhasani, 2016).

The capsule was an important virulence factor that protects the bacterium from the host's immune system, and strains of *K. pneumoniae* that produce a thick capsule were associated with more severe infections (Rendueles, 2020). The *rmpA* gene was one of several genes that can increase capsule production, and its presence was correlated with an increased risk of infection and mortality (Choby *et al.*, 2020). In addition to its role in capsule production, the *rmpA* gene has also been linked to other virulence factors in *K. pneumoniae*, including the production of siderophores (iron-scavenging molecules) and biofilm formation. Overall, the presence of the *rmpA* gene was an important factor in the virulence and pathogenicity of *K. pneumoniae* strains (Khaertynov *et al.*, 2018).

3.9.4 Detection of quorum sensing *luxS* gene

luxS gene were investigated in all 16 *K. pneumoniae* ST 258 isolates and compared with 16 *K. pneumoniae* isolates. The results showed that 14/16(87.5%) were positive to *luxS* gene of *K. pneumoniae* ST 258 isolates while 9/16(56.2%) *K. pneumoniae* isolates were found. PCR product was roughly (447bp) in size, the results were shown in Figure (3-12).

Chen *et al.*, (2020) found the *luxS* gene was involved in the production of the signaling molecule autoinducer-2 (AI-2), which was commonly used in quorum sensing by many bacterial species, including *K. pneumoniae*. Quorum sensing is a mechanism by which bacteria communicate with each other to coordinate their behavior and regulate gene expression in response to changes in cell density.

A study of Shadkam *et al.*, (2021) were detect the presence of the *luxS* gene in *K. pneumoniae*, several methods can be used. One commonly used method is polymerase chain reaction (PCR), which amplifies a specific region of the gene, allowing for its detection. PCR can be performed using primers specific to the *luxS* gene, and the resulting amplicon can be visualized by gel electrophoresis. Overall, detection of the *luxS* gene in *K. pneumoniae* can provide important insights into the quorum sensing mechanisms and potential virulence of this pathogen (Said-Salman *et al.*, 2021).

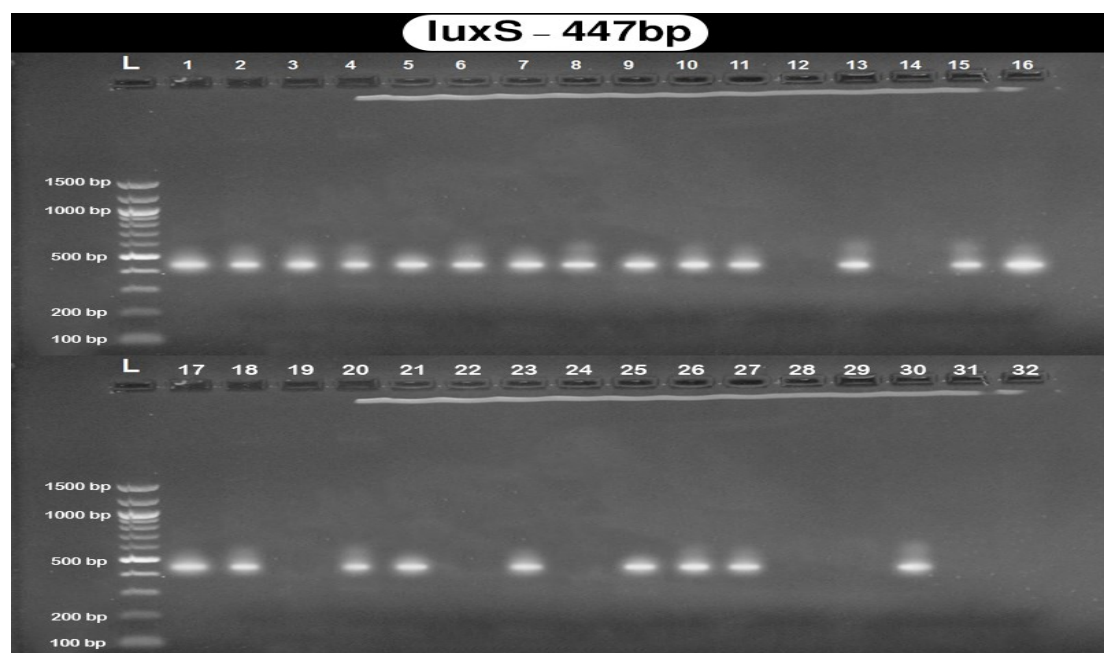


Figure (3-12): Agarose gel electrophoresis (1.5%) of RCR amplified of *luxS* gene (447bp) of *Klebsiella pneumonia* ST 258 for (55) min at (70) volt L: ladder (DNA marker). Number (1,2,3,4,5,6,7,8,9,10,11,13,15,16) positive *Klebsiella pneumonia* ST 258 isolates, while number (17,18,20,21,23, 25,26,27,30) positive *Klebsiella pneumonia* isolates.

The *luxS* gene is a gene that is found in a variety of bacterial species, including *K. pneumoniae*. The gene encodes for an enzyme called autoinducer-2 synthase, which is involved in a process known as quorum sensing (Devanga Ragupathi *et al.*, 2020).

Quorum sensing is a way for bacteria to communicate with each other and coordinate their behavior based on the density of the bacterial population. The autoinducer-2 molecule produced by the LuxS enzyme is a signaling molecule that can be detected by other bacteria, allowing them to sense the presence of other bacteria and adjust their behavior accordingly (Wang *et al.*, 2019).

In *K. pneumoniae*, the *luxS* gene has been shown to be involved in a variety of physiological processes, including biofilm formation, motility, and

virulence. Inhibition of the luxS enzyme has been suggested as a potential target for the development of new antibiotics to treat *K. pneumoniae* infections (Zhu *et al.*, 2011).

3.9.5 Detection of *bla*_{OXA-48}, *bla*_{TEM}, *bla*_{SHV} and *bla*_{CTX-M} genes

*bla*_{OXA-48} gene were characterized in all 16 *K. pneumoniae* ST 258 isolates and compared with 16 *K. pneumoniae* isolates. The results showed that 13/16(81.2%) were positive to *bla*_{OXA-48} gene of *K. pneumoniae* ST 258 isolates while 8/16(50%) *K. pneumoniae* isolates were found. PCR product was roughly (428bp) in size, the results were shown in Figure (3-13).

However, *bla*_{TEM} gene were investigated in all 16 *K. pneumoniae* ST 258 isolates and compared with 16 *K. pneumoniae* isolates. The results showed that 13/16(81.2%) were positive to *bla*_{TEM} gene of *K. pneumoniae* ST 258 isolates while 9/16(56.2%) *K. pneumoniae* isolates were found. PCR product was roughly (1080bp) in size, the results were shown in Figure (3-14).

In addition, *bla*_{SHV} gene was evaluated in all 16 *K. pneumoniae* ST 258 isolates and compared with 16 *K. pneumoniae* isolates. The results showed that 12/16(75%) were positive to *bla*_{SHV} gene of *K. pneumoniae* ST 258 isolates while 10/16(62.5%) *K. pneumoniae* isolates were found. PCR product was roughly (930bp) in size, the results were shown in Figure (3-15).

So, *bla*_{CTX-M} gene were studied in all 16 *K. pneumoniae* ST 258 isolates and compared with 16 *K. pneumoniae* isolates. The results showed that 15/16(93.7%) were positive to *bla*_{CTX-M} gene of *K. pneumoniae* ST 258 isolates while 8/16(50%) *K. pneumoniae* isolates were found. PCR product was roughly (585bp) in size, the results were shown in Figure (3-16).

A results of Abrar *et al.*, (2019) found that *K. pneumonia* revealed *bla_{CTX-M}* gene in rate 76% followed by *bla_{OXA-48}* gene in rate 52%, *bla_{TEM}* gene in rate 28% and *bla_{SHV}* gene in rate 21%.

Abrar *et al.*, (2017) found that, the genes were most prevalent among *K. pneumonia* *bla_{CTX-M}* gene in rate 65%, *bla_{OXA-48}* gene in rate 78% and *bla_{TEM}* gene in rate 57%, and Sonda *et al.*, (2018) found *bla_{CTX-M}* gene in rate 75%, *bla_{OXA}* gene in rate 49% and *bla_{TEM}* gene in rate 34% isolates among *K. pneumoniae*.

The *bla_{OXA-48}*, *bla_{TEM}*, *bla_{SHV}* and *bla_{CTX-M}* genes were a type of beta-lactamase genes that encodes an enzyme that can hydrolyze and inactivate certain types of antibiotics, including penicillins, cephalosporins, and carbapenems. This gene was commonly found in some bacteria, including *K. pneumoniae*, which is an important opportunistic pathogen associated with healthcare-associated infections. PCR-based assays have been developed that can detect the presence of the *bla_{OXA-48}*, *bla_{TEM}*, *bla_{SHV}* and *bla_{CTX-M}* genes in clinical isolates of *K. pneumoniae* with high sensitivity and specificity (Hansen, 2021).

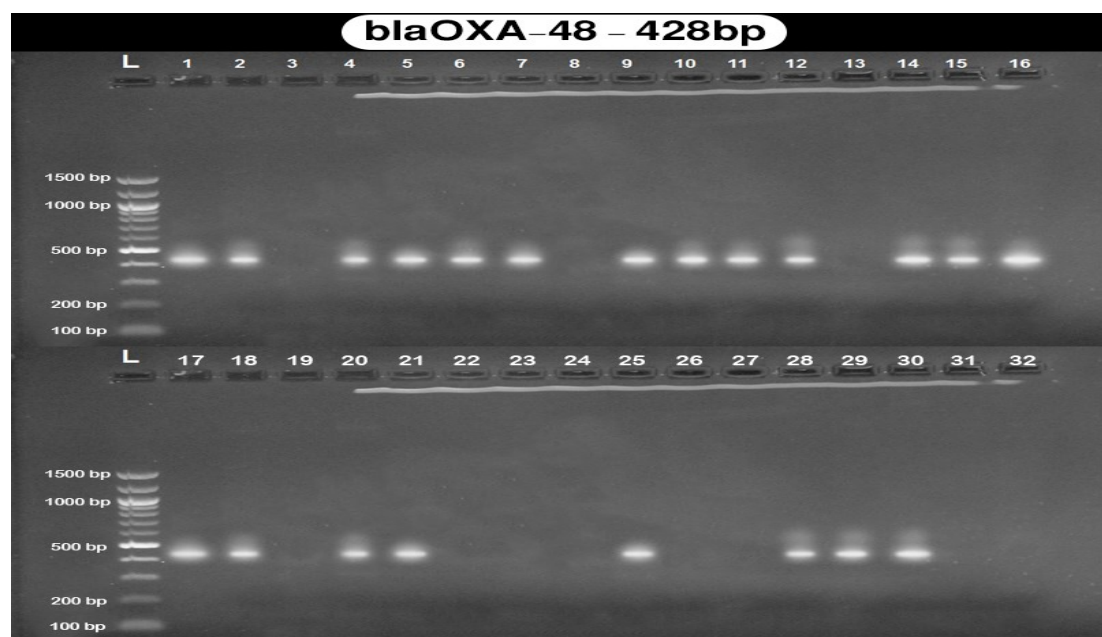


Figure (3-13): Agarose gel electrophoresis (1.5%) of RCR amplified of *bla_{OXA-48}* gene (428bp) of *Klebsiella pneumonia* ST 258 for (55) min at (70) volt L: ladder (DNA marker). Number (1,2,4,5,6,7,9, 10,11,12,14,15,16) positive *Klebsiella pneumonia* ST 258 isolates, while number (17,18,20,21,25,28,29,30) positive *Klebsiella pneumonia* isolates.

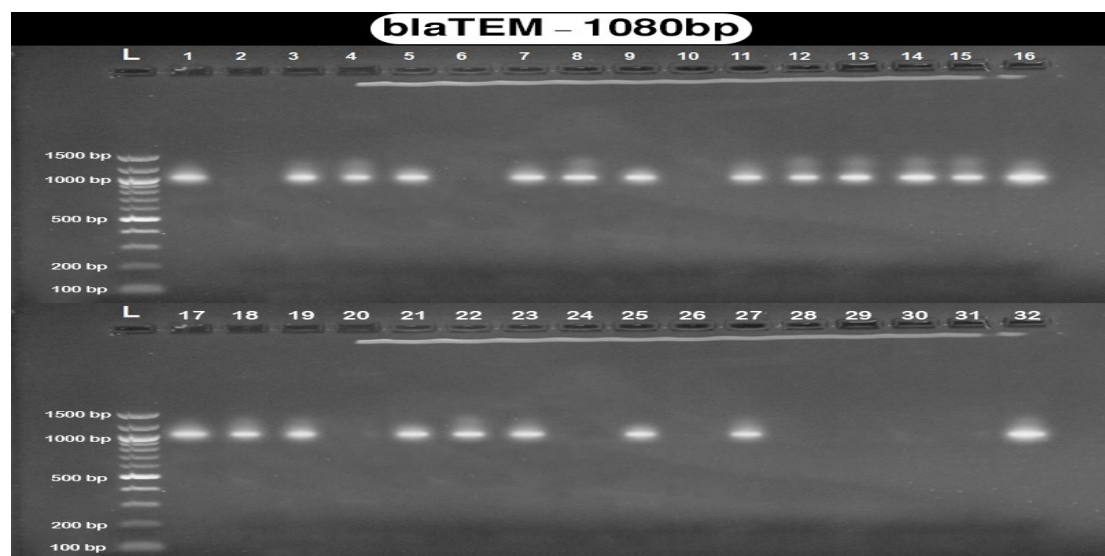


Figure (3-14): Agarose gel electrophoresis (1.5%) of RCR amplified of *bla_{TEM}* gene (1080bp) of *Klebsiella pneumonia* ST 258 for (55) min at (70) volt L: ladder (DNA marker). Number (1,3,4,5,7,8,9,11,12, 13,14,15,16) positive *Klebsiella pneumonia* ST 258 isolates, while number (17,18,19,21,22,23,25,27,32) positive *Klebsiella pneumonia* isolates.



Figure (3-15): Agarose gel electrophoresis (1.5%) of RCR amplified of *bla_{SHV}* gene (930bp) of *Klebsiella pneumonia* ST 258 for (55) min at (70) volt L: ladder (DNA marker). Number (1,2,3,5,6,7,8,9,11,13,14,16) positive *Klebsiella pneumonia* ST 258 isolates, while number (17,18,19, 21,23,24,28,30,31,32) positive *Klebsiella pneumonia* isolates.



Figure (3-16): Agarose gel electrophoresis (1.5%) of RCR amplified of *bla_{CTX-M}* gene (585bp) of *Klebsiella pneumonia* ST 258 for (55) min at (70) volt L: ladder (DNA marker). Number (1,2,3,4,5,6,7,8,9, 10,11,12,13,14,15) positive *Klebsiella pneumonia* ST 258 isolates, while number (19,21,23,25,26,27,29,32) positive *Klebsiella pneumonia* isolates.

Rocha *et al.*, (2019) found PCR-based assays could also be used to detect other types of beta-lactamase genes, such as *bla*_{KPC}, *bla*_{NDM}, and *bla*_{IMP}, which are also associated with antibiotic resistance in *K. pneumoniae*. In addition, phenotypic tests, such as disk diffusion and minimum inhibitory concentration (MIC) assays, can be used to detect resistance to specific antibiotics, including carbapenems, which may indicate the presence of the *bla*_{OXA-48}, *bla*_{TEM}, *bla*_{SHV} and *bla*_{CTX-M} genes or other beta-lactamase genes.

Overall, the detection of the *bla*_{OXA-48}, *bla*_{TEM}, *bla*_{SHV} and *bla*_{CTX-M} genes in *K. pneumoniae* were an important step in identifying antibiotic-resistant strains of this pathogen and guiding appropriate treatment decisions. The spread of *bla*_{OXA-48}, *bla*_{TEM}, *bla*_{SHV} and *bla*_{CTX-M} positive *K. pneumoniae* strains was a growing concern in healthcare settings, as they could be transmitted between patients and was associated with increased morbidity and mortality (Mpelle *et al.*, 2019).

Pillai & Kalasseril, (2022) found that, the presence of the these genes alone does not necessarily indicate antibiotic resistance, as other factors such as the expression of the gene and the presence of additional resistance mechanisms can also contribute to antibiotic resistance. Therefore, antibiotic susceptibility testing is still necessary to determine the most effective treatment options for *K. pneumoniae* infections.

Table (3-9): Pattern of antibiotic resistance and occurrence of virulence factors genes among two types of strains (*Klebsiella pneumonia* ST 258 and normal strain *Klebsiella pneumoniae*) isolates (Total No. =32)

No. of isolates	Antibiotic resistance	<i>fimH</i>	<i>mrkD</i>	<i>magA</i>	<i>Way</i>	<i>rmpA</i>	<i>luxS</i>	<i>bla_{OXA-48}</i>	<i>bla_{TEM}</i>	<i>bla_{SHV}</i>	<i>bla_{CTX}</i>
1.	IMP, MEM, FOT, ETP, TMP-SMX CRO/AXL, CEZ, CN, NIT	+	+	+	+	+	+	+	+	+	+
2.	IMP, MEM, FOT ETP, TMP-SMX CRO/AXL, CEZ, CN, NIT	+	-	+	+	+	+	+	-	+	+
3.	IMP, MEM, FOT ETP, TMP-SMX CRO/AXL, CEZ, CN, NIT	+	+	+	+	+	+	-	+	+	+
4.	IMP, MEM, FOT ETP, TMP-SMX CRO/AXL, CEZ, CN, NIT	+	+	+	+	+	+	+	+	-	+
5.	IMP, MEM, FOT ETP, TMP-SMX CRO/AXL, CEZ, CN, NIT	+	+	+	+	+	+	+	+	+	+
6.	IMP, MEM, FOT ETP, TMP-SMX CRO/AXL, CEZ, CN, NIT	+	+	+	+	+	+	+	-	+	+
7.	IMP, MEM, FOT ETP, TMP-SMX CRO/AXL, CEZ, CN, NIT	+	+	+	+	+	+	+	+	+	+
8.	IMP, MEM, FOT ETP, TMP-SMX CRO/AXL, CEZ, CN, NIT	+	-	+	-	+	+	-	+	+	+
9.	IMP, MEM, FOT ETP, TMP-SMX CRO/AXL, AK, CN, NIT	+	+	+	+	+	+	+	-	+	+
10.	IMP, MEM, FOT ETP, TMP-SMX CRO/AXL, AK,	+	+	+	+	+	+	+	+	-	+
11.	IMP, MEM, FOT ETP, TMP-SMX CRO/AXL, AK, CN, NIT	+	+	+	+	+	+	+	+	+	+
12.	IMP, MEM, FOT ETP, TMP-SMX CRO/AXL, AK	+	+	+	+	+	-	+	+	-	+
13.	IMP, MEM, FOT ETP, TMP-SMX, AK, CEZ, CN, NIT	+	-	+	+	+	+	-	+	+	+
14.	IMP, MEM, FOT ETP, TMP-SMX CRO/AXL, AK	+	+	-	+	+	-	+	+	+	+
15.	IMP, MEM, FOT ETP, TMP-SMX, AK, CEZ, CN, NIT	+	+	+	+	+	+	+	+	-	+
16.	IMP, MEM, FOT ETP, TMP-SMX CRO/AXL, AK	+	+	+	+	+	+	+	+	+	-

Table (3-9): Pattern of antibiotic resistance and occurrence of virulence factors genes among two types of strains (*Klebsiella pneumonia* ST 258 and normal strain *Klebsiella pneumoniae*) isolates (Total No. =32)

Total		16(100%)	13(81.2%)	15(93.7%)	15(93.7%)	16(100%)	14(87.5%)	13(81.2%)	13(81.2%)	12(75%)	15(93.7%)
17.	IMP, MEM, FOT ETP, TMP-SMX	+	+	-	+	+	+	+	+	+	-
18.	IMP, MEM, FOT ETP, AK, CEZ	+	+	+	+	+	+	+	+	+	+
19.	IMP, MEM, FOT ETP, TMP-SMX	+	+	+	+	+	-	-	+	+	-
20.	IMP, MEM, ETP	-	-	-	+	+	+	+	-	-	+
21.	IMP, MEM, FOT	+	+	+	+	+	+	+	+	+	-
22.	IMP, MEM, AK	+	+	+	+	+	-	-	+	-	+
23.	IMP, MEM, FOT	+	+	+	+	+	+	-	+	+	-
24.	IMP, MEM, FOT ETP, AK, CEZ	-	-	+	-	+	-	-	-	+	-
25.	IMP, MEM, ETP	+	+	+	+	+	+	+	+	-	+
26.	IMP, MEM, FOT ETP, AK	+	-	-	-	+	+	-	-	+	+
27.	IMP, MEM,	+	+	+	+	+	+	-	+	-	+
28.	IMP, MEM, ETP	-	-	-	-	-	-	+	-	-	-
29.	IMP, MEM, FOT ETP, AK	+	+	-	+	-	-	+	-	-	+
30.	IMP, MEM, FOT	+	+	+	-	+	+	+	-	+	-
31.	IMP, MEM, FOT	+	+	+	-	-	-	-	-	+	-
32.	IMP MEM, FOT, ETP	-	-	-	+	-	-	-	+	+	+
Total		12(75%)	11(68.7%)	10(62.5%)	11(68.7%)	12(75%)	9(56.2%)	8(50%)	9(56.2%)	10(62.5%)	8(50%)

IMP / Imipenem, MEM/ Meropenem, FOT/ Fosfomicin, ETP/ Ertapenem, TMP-SMX/ Trimethoprim/sulfamethoxazole, CRO/AXL / Cefuroxime Axetil, AK/ Amikacin, CEZ/ Ceftriaxone, CN/ Gentamycin, NIT/ Nitrofurantoin

3.10 DNA sequencing

3.10.1 DNA sequencing for *Klebsiella pneumoniae* and *Klebsiella pneumoniae* subsp. *pneumoniae* ST 258

After confirming the amplification of *K. pneumoniae* and *K. pneumoniae* subsp. *pneumoniae* ST 258 genes by conventional PCR, 20µl from PCR reaction with 50µl of forward primer for this genes were send to Macrogen Company to determine the DNA sequencing in these genes. Homology search was conducted using Basic Local Alignment search Tool (BLAST) program which is available at the National Center Biotechnology Information (NCBI) online at (<http://www.ncbi.nlm.nih.gov>), and BioEdit program. The results were compared with data obtained from gene bank published ExPASy program which is available at the NCBI online.

The genes were amplified by PCR method, and send for sequencing service to Macrogen Company Korea. The sequencing result of *K. pneumoniae* subsp. *pneumoniae* ST 258 gene shows having one **Transition** C/T in location (157 nucleotide) from the Gene Bank found part of *pneumonia* 258 gene having 99% compatibility with the subject of *K. pneumoniae* subsp. *pneumoniae* ST 258 gene in NCBI under sequence (ID: HG785581.1). Another part of sequencing for *K. pneumoniae* subsp. *pneumoniae* ST 258 gene, the results shows compatibility of 99% in Gene Bank of *K. pneumoniae* subsp. *pneumoniae* ST 258 under sequence ID: HG785581.1, so recorded one **Transversion** G/C in location (278 nucleotide) and **Transversion** A/T in (316 nucleotide) noticed from the gene in this isolate.

However, The sequencing result of first *K. pneumoniae* gene shows having one **Transversion** T/A in location (1830475 nucleotide) from the Gene Bank found part of *K. pneumoniae* gene having 99% compatibility

with the subject of *K. pneumoniae* gene in NCBI under sequence (ID: CP052490.1), so recorded one **Transition** G\A in location (1830608 nucleotide) noticed from the gene in this isolate.

The sequencing result of second *K. pneumoniae* gene shows having one **Transversion** T\A in location (1830566 nucleotide) from the Gene Bank found part of *K. pneumoniae* gene having 99% compatibility with the subject of *K. pneumoniae* gene in NCBI under sequence (ID: CP052490.1), so recorded one **Transition** C\T in location (1830630 nucleotide) noticed from the gene in this isolate. These results were shown in Table (3-10), Figures (3-17A-D).

Table (3-10): Determinate of DNA sequencing for *Klebsiella pneumoniae* subsp. *pneumoniae* ST258 gene

No.	Type of substitution	Location	Nucleotide	Sequence ID with compare	Source	Identities
1	Transversion	1830475	T\A	ID: CP052490.1	<i>Klebsiella pneumoniae</i>	99%
	Transition	1830608	G\A			
2	Transversion	1830566	A\T	ID: CP052490.1	<i>Klebsiella pneumoniae</i>	99%
	Transition	1830630	C\T			
3	Transition	157	C\T	ID: HG785581.1	<i>Klebsiella pneumoniae</i> subsp. <i>pneumoniae</i> ST 258	99%
4	Transition	157	C\T	ID: HG785581.1	<i>Klebsiella pneumoniae</i> subsp. <i>pneumoniae</i> ST 258	99%
	Transversion	278	G\C			
	Transversion	316	A\T			

Klebsiella pneumoniae strain B17KP0069 chromosome, complete genome

Sequence ID: [CP052490.1](#) Length: 5336594 Number of Matches: 1

Range 1: 1830415 to 1830678 [GenBankGraphics](#) [Next Match](#) [Previous Match](#)

Score	Expect	Identities	Gaps	Strand
468 bits(518)	3e-129	262/264(99%)	0/264(0%)	Plus/Plus
Query 1	GGTGAGTTCCTATATATTAATGGGAAAGCAAATGTAGGAGCAAACCTGTTACCAAATGGT	60		
Sbjct 1830415			
1830474				
Query 61	ATACAGGGCACGGATTCAACGGGATTGTTGTTGTCATGTGTCGGTGGTAAATGGGTTAAG	120		
Sbjct 1830475	T			
1830534				
Query 121	ACATCAGGTACAGCAGGtttttttACAAAAAATCAAGGCTCTTGCTTGGTTAAGAATCCT	180		
Sbjct 1830535			
1830594				
Query 181	GACACTAATGCTTATTCATGTCCATCTGGAACAACAGCTTATGAATTATTTTATACTACA	240		
Sbjct 1830595 G			
1830654				
Query 241	TCTACTGAGCAATCAGGTGGAGGA	264		
Sbjct 1830655	1830678		

Figure (3-17A): Alignment analysis of *Klebsiella pneumoniae* with Gene Bank at NCBI. Query represents of sample; subject represents a database of National Center Biotechnology Information (NCBI).

Klebsiella pneumoniae strain B17KP0069 chromosome, complete genome

Sequence ID: [CP052490.1](#) Length: 5336594 Number of Matches: 1

Range 1: 1830415 to 1830678 [GenBankGraphics](#) [Next Match](#) [Previous Match](#)

Score	Expect	Identities	Gaps	Strand
468 bits(518)	3e-129	262/264(99%)	0/264(0%)	Plus/Plus
Query 1	GGTGAGTTCCTATATATTAATGGGAAAGCAAATGTAGGAGCAAACCTGTTACCAAATGGT			60
Sbjct 1830415			
1830474				
Query 61	TTACAGGGCACGGATTCAACGGGATTGTTGTTGTCATGTGTGCGGTGGTAAATGGGTTAAG			
120				
Sbjct 1830475			
1830534				
Query 121	ACATCAGGTACAGCAGGtttttttACAAAAATCAAGGCTCTTGCTTGGTTAAGAATCCT			
180				
Sbjct 1830535A			
1830594				
Query 181	GACACTAATGCTTGTTTCATGTCCATCTGGAACAATAGCTTATGAATTATTTTATACTACA			
240				
Sbjct 1830595C			
1830654				
Query 241	TCTACTGAGCAATCAGGTGGAGGA	264		
Sbjct 1830655	1830678		

Figure (3-17B): Alignment analysis of *Klebsiella pneumoniae* with Gene Bank at NCBI. Query represents of sample; subject represents a database of National Center Biotechnology Information (NCBI).

TPA: *Klebsiella pneumoniae* subsp. *pneumoniae* ST 258-490 transfer-messenger mRNA Klebs_pneum_MGH785, single chain mature transcript

Sequence ID: [HG785581.1](#) Length: 363 Number of Matches: 1

Range 1: 123 to 360 [GenBankGraphics](#) [Next Match](#) [Previous Match](#)

Score	Expect	Identities	Gaps	Strand
425 bits(471)	9e-124	237/238(99%)	0/238(0%)	Plus/Plus
Query 1 60	TAACCTGCTCTGAGCCCTCTCTCCCTAGCTTCCGTTCTTAAGACGGGGATCAAAGAGAGG			
Sbjct 123 182 C			
Query 61 120	TCAAACCCAAAAGAGATCGCGTGGATGCCCTGCCTGGGGTTGAAGCGTTAAATCTAATCA			
Sbjct 183 242			
Query 121 180	GGCTAGTTTGTAGTGGCGTGTCTGTCCGCAGCTGGCAAGCGAATGTAAAGACTGACTAA			
Sbjct 243 302			
Query 181 238	GCATGTAGTGCCGAGGATGTAGGAATTCGGACGCGGGTTCAACTCCCGCCAGCTCCA			
Sbjct 303 360			

Figure (3-17C): Alignment analysis of *Klebsiella pneumoniae* subsp. *pneumoniae* ST 258 with Gene Bank at NCBI. Query represents of sample; subject represents a database of National Center Biotechnology Information (NCBI).

TPA: *Klebsiella pneumoniae* subsp. *pneumoniae* ST 258-490 transfer-messenger mRNA Klebs_pneum_MGH785, single chain mature transcript

Sequence ID: [HG785581.1](#) Length: 363 Number of Matches: 1

Range 1: 123 to 360 [GenBankGraphics](#) [Next Match](#) [Previous Match](#)

Score	Expect	Identities	Gaps	Strand
416 bits(461)	4e-121	235/238(99%)	0/238(0%)	Plus/Plus
Query 1 60	TAACCTGCTCTGAGCCCTCTCTCCCTAGCTTCCGTTCTTAAGACGGGGATCAAAGAGAGG			
Sbjct 123 182 C			
Query 61 120	TCAAACCCAAAAGAGATCGCGTGGATGCCCTGCCTGGGGTTGAAGCGTTAAATCTAATCA			
Sbjct 183 242			
Query 121 180	GGCTAGTTTGTAGTGGCGTGTCTGTCCGCAGCTGCCAAGCGAATGTAAAGACTGACTAA			
Sbjct 243 302 G			
Query 181 238	GCATGTAGTGCCGTGGATGTAGGAATTCGGACGCGGGTTCAACTCCC GCCAGCTCCA			
Sbjct 303 360 A			

Figure (3-17D): Alignment analysis of *Klebsiella pneumoniae* subsp. *pneumoniae* ST 258 with Gene Bank at NCBI. Query represents of sample; subject represents a database of National Center Biotechnology Information (NCBI).

3.10.2 DNA sequencing for some important virulence genes

3.10.2.1 *mrkD* gene

The genes were amplified by PCR method in three *K. pneumoniae* isolates, and send for sequencing service to Macrogen Company Korea. The sequencing result of first *mrkD* gene shows for *K. pneumoniae* having one Transition G\A in location (502 nucleotide) from the Gene Bank found part of *mrkD* gene having 99% compatibility with the subject of *mrkD* gene in NCBI under sequence (ID: KF777765.1). Another part of sequencing for *mrkD* gene to *K. pneumoniae* in same isolate, the results shows compatibility of 99% in Gene Bank of *mrkD* under sequence ID: KF777765.1, was recorded Transition T\C in location (714 nucleotide) from the Gene Bank found part of *mrkD* gene. In addition, the results shows compatibility of 99% in Gene Bank of *mrkD* under sequence (ID: KF777765.1) was recorded Transversion A\C in location (751 nucleotide) from the Gene Bank found part of *mrkD* gene at same this isolate.

However, the second *mrkD* gene shows for *K. pneumoniae* having one Transition G\A in location (502 nucleotide) from the Gene Bank found part of *mrkD* gene having 99% compatibility with the subject of *mrkD* gene in NCBI under sequence (ID: KF777765.1). Another part of sequencing for *mrkD* gene to *K. pneumoniae* in same isolate, the results shows compatibility of 99% in Gene Bank of *mrkD* under sequence ID: KF777765.1, was recorded Transition T\C in location (714 nucleotide) from the Gene Bank found part of *mrkD* gene. In addition, the results shows compatibility of 99% in Gene Bank of *mrkD* under sequence ID: KF777765.1 was recorded Transition A\G in location (804 1 nucleotide) from the Gene Bank found part of *mrkD* gene at same this isolate.

The sequencing result of third *mrkD* gene shows for *K. pneumoniae* having one Transition A\G in location (502 nucleotide) from the Gene Bank found part of *mrkD* gene having 99% compatibility with the subject of *mrkD* gene in NCBI under sequence (ID: KF777765.1). Another part of sequencing for *mrkD* gene to *K. pneumoniae* in same isolate, the results shows compatibility of 99% in Gene Bank of *mrkD* under sequence ID: KF777765.1, was recorded Transversion T\G in location (603 nucleotide) from the Gene Bank found part of *mrkD* gene. In addition, the results shows compatibility of 99% in Gene Bank of *mrkD* under sequence ID: KF777765.1 was recorded Transition T\C in location (714 1nucleotide) from the Gene Bank found part of *mrkD* gene at same this isolate.

As a results of *mrkD* gene in *K. pneumoniae* subsp. *pneumoniae* ST 258. Three genes were amplified by PCR method, and send for sequencing service to Macrogen Company Korea. The sequencing for *mrkD* gene, the results of first gene showed compatibility of 100% in Gene Bank of *mrkD* gene under sequence ID: : CP046967.1, so, no recorded change noticed from the Gene Bank in *mrkD* gene. While the second gene shows for *K. pneumoniae* subsp. *pneumoniae* ST258 having one Transition T\C in location (4039924 nucleotide) from the Gene Bank found part of *mrkD* gene having 99% compatibility with the subject of *mrkD* gene in NCBI under sequence (ID: CP046967.1). All results were shown in Table (3-11), Figure (3-18A-F).

Table (3-11): Determinate of DNA sequencing for *K. pneumoniae* and *K. pneumoniae* subsp. *pneumoniae* ST 258 *mrkD* gene

No. of sample	Type of substitution	Location	Nucleotide	Nucleotide change	Amino acid change	Predicted effect	Source	Sequence ID with compare	Identities
1	Transition	502	G\A	GGT\AGT	Glycine\ Serine	Missense	Klebsiella pneumoniae (mrkD) gene	ID: KF777765.1	99%
	Transition	714	T\C	ATT\ATC	Isoleucine\ Isoleucine	Silent			
	Transversion	751	A\C	ACC\CCC	Threonine\ Proline	Missense			
2	Transition	502	G\A	GGT\AGT	Glycine\ Serine	Missense	Klebsiella pneumoniae (mrkD) gene	ID: KF777765.1	99%
	Transition	714	T\C	ATT\ATC	Isoleucine\ Isoleucine	Silent			
	Transition	804	A\G	AAA\AAG	Lysine\ Lysine	Silent			
3	Transition	502	G\A	GGT\AGT	Glycine\ Serine	Missense	Klebsiella pneumoniae (mrkD) gene	ID: KF777765.1	99%
	Transversion	603	T\G	GGT\GGG	Glycine\ Glycine	Silent			
	Transition	714	T\C	ATT\ATC	Isoleucine\ Isoleucine	Silent			
1	-----	-----	-----	-----	-----	-----	Klebsiella pneumoniae subsp. pneumoniae ST258 (mrkD) gene	ID: CP046967.1	100%
2	Transition	4039924	T\C	ATC\ACC	Isoleucine\ Threonine	Missense	Klebsiella pneumoniae subsp. pneumoniae ST258 (mrkD) gene	ID: CP046967.1	99%
3		4039949	T\A	GAT\GAA	Aspartic acid \ Glutamic acid	Missense	Klebsiella pneumoniae subsp. pneumoniae ST258 (mrkD) gene	ID: CP046967.1	99%
		4040067	A\G	GAC\GGC	Aspartic acid \ Glycine				

***Klebsiella pneumoniae* strain sp14 MrkD (*mrkD*) gene, complete cds**Sequence ID: [KF777765.1](#) Length: 996 Number of Matches: 1Range 1: 463 to 918 [GenBankGraphics](#) [Next Match](#) [Previous Match](#)

Score	Expect	Identities	Gaps	Strand
810 bits(897)	0.0	453/456(99%)	0/456(0%)	Plus/Plus
Query 1 60	GCGGCGGGTAAAGTACACCTCCTACGACTGGGAGAGCGGCAGTAACCCGATCCTCGAAACC			
Sbjct 463 522 G			
Query 61 120	TATCTGAGCGCCAACGCCATCACCGTGGTCTCGCCCTCCTGTTCAGTGCTGAGCGGGAAA			
Sbjct 523 582			
Query 121 180	AATATGAATGTCGATGTGGGTTCATCCGGCGCACCGACCTGAAAGGGGTCGGCACCACC			
Sbjct 583 642			
Query 181 240	GCCGGCGGGAAGGATTTTAATATCGACCTGCAGTGCAGCGGCGCCTGAGTGAAACGGGA			
Sbjct 643 702			
Query 241 300	TATGCCAACATCAGCACCTCGTTCTCCGGTACCCTTGCCACCAGCACTCCCGCTACCATG			
Sbjct 703 762 T A			
Query 301 360	GGCGCCTTGCTGAATGAAAAAGCCGGCAGCGGGATGGCGAAAGGCATTGGCATCCAGGTG			
Sbjct 763 822			
Query 361 420	CTGAAGGATGGCTCCCCGCTGCAGTTTAATAAGAAATACACCGTCGGCCGCTTGAATAAT			
Sbjct 823 882			
Query 421 Sbjct 883	CAGGAGACCCGCTACATCACCATAACCGCTGCACGCG		456 918	

Figure (3-18A1): Alignment analysis of *mrkD* gene of *Klebsiella pneumoniae* with Gene Bank at NCBI. Query represents of sample; subject represents a database of National Center Biotechnology Information (NCBI).

Type 3 fimbria adhesin subunit MrkD [*Klebsiella pneumoniae*]
Sequence ID: [HBR1698013.1](#) Length: 204 Number of Matches: 1
 Range 1: 28 to 179 [GenPeptGraphics](#) [Next Match](#) [Previous Match](#)

Score	Expect	Method	Identities	Positives	Gaps	Frame
305 bits(781)	7e-106	Compositional matrix adjust.	150/152(99%)	150/152(98%)	0/152(0%)	+1
Query 1		AAGKYTSYDWESGSNP	ILETYLSANAITVVSP	SCSVLSGKNMNV	DVGSIRRTDLKGV	TT
180						
Sbjct 28		G			
87						
Query 181		AGGKDFNIDLQCSGGL	SETGYANISTSFSGTL	ATSTPATMGALLNEK	AGSGMAKGIGIQV	
360						
Sbjct 88				T	
147						
Query 361		LKDGSPLOFNKKYTV	GRLNNQETRYITIP	LHA	456	
Sbjct 148				179	

Figure (3-18A2): Alignment analysis of *mrkD* gene of *Klebsiella pneumoniae* with Gene Bank at NCBI. Query represents of sample; subject represents a database of National Center Biotechnology Information (NCBI).

Klebsiella pneumoniae strain sp14 MrkD (*mrkD*) gene, complete cds

Sequence ID: [KF777765.1](#) Length: 996 Number of Matches: 1

Range 1: 463 to 918 [GenBankGraphics](#) [Next Match](#) [Previous Match](#)

Score	Expect	Identities	Gaps	Strand
810 bits(897)	0.0	453/456(99%)	0/456(0%)	Plus/Plus
Query 1		GCGGCGGGTAAGTACACCTCCTACGACTGGGAGAGCGGCAGTAACCCGATCCTCGAAACC		
60				
Sbjct 463	 G		
522				
Query 61		TATCTGAGCGCCAACGCCATCACCGTGGTCTCGCCCTCCTGTTTCAGTGCTGAGCGGGAAA		
120				
Sbjct 523			
582				
Query 121		AATATGAATGTCGATGTGGTTCCATCCGGCGCACCGACCTGAAAGGGGTCGGCACCACC		
180				
Sbjct 583			
642				
Query 181		GCCGGCGGGAAGGATTTTAATATCGACCTGCAGTGCAGCGGGCCCTGAGTGAAACGGGA		
240				
Sbjct 643			
702				
Query 241		TATGCCAACATCAGCACCTCGTTCTCCGGTACCCTTGCCACCAGCACTACCGCTACCATG		
300				
Sbjct 703	 T		
762				
Query 301		GGCGCCTTGCTGAATGAAAAAGCCGGCAGCGGGATGGCGAAGGGCATTGGCATCCAGGTG		
360				
Sbjct 763	 A		
822				
Query 361		CTGAAGGATGGCTCCCCGCTGCAGTTTAATAAGAAATACACCGTCGGCCGCTTGAATAAT		
420				
Sbjct 823			
882				
Query 421		CAGGAGACCCGCTACATCACCATACCGCTGCACGCG	456	
Sbjct 883		918	

Figure (3-18B1): Alignment analysis of *mrkD* gene of *Klebsiella pneumoniae* with Gene Bank at NCBI. Query represents of sample; subject represents a database of National Center Biotechnology Information (NCBI).

Type 3 fimbria adhesin subunit MrkD [*Klebsiella pneumoniae*]Sequence ID: [HBR1698013.1](#) Length: 204 Number of Matches: 1Range 1: 28 to 179 [GenPeptGraphics](#) [Next Match](#) [Previous Match](#)

Score	Expect	Method	Identities	Positives	Gaps	Frame
307 bits(787)	1e-106	Compositional matrix adjust.	151/152(99%)	151/152(99%)	0/152(0%)	+1
Query 1	AAGKYTSYDWESGSNPILETYLSANAITVVSPSCSVLSGKNMNVVDVGSIRRDLKGVGTT					
180						
Sbjct 28 G					
87						
Query 181	AGGKDFNIDLQCSGGLSETGYANISTSFSGTLATSTTATMGALLNEKAGSGMAKGIGIQV					
360						
Sbjct 88					
147						
Query 361	LKDGSPLOFNKKYTVGRLNNQETRYITITPLHA		456			
Sbjct 148		179			

Figure (3-18B2): Alignment analysis of *mrkD* gene of *Klebsiella pneumoniae* with Gene Bank at NCBI. Query represents of sample; subject represents a database of National Center Biotechnology Information (NCBI).

Klebsiella pneumoniae strain sp14 MrkD (*mrkD*) gene, complete cds

Sequence ID: [KF777765.1](#) Length: 996 Number of Matches: 1

Range 1: 463 to 918 [GenBankGraphics](#) [Next Match](#) [Previous Match](#)

Score	Expect	Identities	Gaps	Strand
810 bits(897)	0.0	453/456(99%)	0/456(0%)	Plus/Plus
Query 1	GCGGCGGGTAAGTACACCTCCTACGACTGGGAGAGCGGCAGTAACCCGATCCTCGAAACC			
60				
Sbjct 463 G			
522				
Query 61	TATCTGAGCGCCAACGCCATCACCGTGGTCTCGCCCTCCTGTTTCAGTGCTGAGCGGGAAA			
120				
Sbjct 523			
582				
Query 121	AATATGAATGTCGATGTGGGGTCCATCCGGCGCACCGACCTGAAAGGGGTCGGCACCACC			
180				
Sbjct 583 T			
642				
Query 181	GCCGGCGGGAAGGATTTTAATATCGACCTGCAGTGCAGCGGGCGGCTGAGTGAAACGGGA			
240				
Sbjct 643			
702				
Query 241	TATGCCAACATCAGCACCTCGTTCTCCGGTACCCTTGCCACCAGCACTACCGCTACCATG			
300				
Sbjct 703 T			
762				
Query 301	GGCGCCTTGCTGAATGAAAAAGCCGGCAGCGGGATGGCGAAAGGCATTGGCATCCAGGTG			
360				
Sbjct 763			
822				
Query 361	CTGAAGGATGGCTCCCCGCTGCAGTTTAATAAGAAATACACCGTCGGCCGCTTGAATAAT			
420				
Sbjct 823			
882				
Query 421	CAGGAGACCCGCTACATCACCATACCGCTGCACGCG	456		
Sbjct 883	918		

Figure (3-18C1): Alignment analysis of *mrkD* gene of *Klebsiella pneumoniae* with Gene Bank at NCBI. Query represents of sample; subject represents a database of National Center Biotechnology Information (NCBI).

Type 3 fimbria adhesin subunit MrkD [*Klebsiella pneumoniae*]Sequence ID: [HBR1698013.1](#) Length: 204 Number of Matches: 1Range 1: 28 to 179 [GenPeptGraphics](#) [Next Match](#) [Previous Match](#)

Score	Expect	Method	Identities	Positives	Gaps	Frame	
307 bits(787)	1e-106	Compositional matrix adjust.	151/152(99%)	151/152(99%)	0/152(0%)	+1	
Query 1	AAGKYTSYDWESGSNP	ILETYLSANA	ITVVS	PSCSVLSG	KNMNV	DVGS	IRRTDLKGVGTT
180							
Sbjct 28	G
87							
Query 181	AGGKDFNIDLQCSG	GLSETGYAN	ISTSF	SGLTAT	STTATM	GALLNEK	AGSGMAKGIGIQV
360							
Sbjct 88
147							
Query 361	LKDGSP	LQFNKKY	TVGRL	LNNQ	ETRYI	TIPLHA	456
Sbjct 148	179

Figure (3-18C2): Alignment analysis of *mrkD* gene of *Klebsiella pneumoniae* with Gene Bank at NCBI. Query represents of sample; subject represents a database of National Center Biotechnology Information (NCBI).

***Klebsiella pneumoniae* strain WCHKP115016 chromosome, complete genome**

Sequence ID: [CP046967.1](#) Length: 5427644 Number of Matches: 1

Range 1: 4039707 to 4040156 [GenBankGraphics](#) [Next Match](#) [Previous Match](#)

Score	Expect	Identities	Gaps	Strand
812 bits(900)	0.0	450/450(100%)	0/450(0%)	Plus/Plus
Query 1		CCGGCGCTGGCTTATGAGGGCAGCAGCACGGTCAATTTTAACGTCACGGGCACCATCGAA		60
Sbjct 4039707			
4039766				
Query 61		GCGCCTTCCGTGTGAGGTGGCCGTGGAGCCGTCGAACAGTATCGATTTAGGCACCGTCTCC		
120				
Sbjct 4039767			
4039826				
Query 121		TCGCAGACGTTCTCCGGACATGCCGGGGCAGCGGCCAGCGTGCCGGTTAAGCTGGTC		
180				
Sbjct 4039827			
4039886				
Query 181		TTTCCAGCTGTTCGCCGATGCGTCGGGTGACCATCGCGTTTAGCGGCACCAGCTTC		
240				
Sbjct 4039887			
4039946				
Query 241		GATAGCACCCACGCTTCAATCTATAAAAACTTCCAGACTGGCAGCAACGGTGCCAGCGGC		
300				
Sbjct 4039947			
4040006				
Query 301		GTCGGTTTGCAGCTGCAGAGCATGGCCGACCAGCAGCCCCTTGGCCCCGCGACCAGTAT		
360				
Sbjct 4040007			
4040066				
Query 361		CTCTATACCTTTGGGGACGATGCGGATATCCATACCTTTAATATGGTGGCACGTATGTTT		
420				
Sbjct 4040067			
4040126				
Query 421		TCGCCTTATGGCCAGGTAAGGTCCGGGATG	450	
Sbjct 4040127		4040156	

Figure (3-18D1): Alignment analysis of *mrkD* gene of *Klebsiella pneumoniae* subsp. *pneumoniae* ST 258 with Gene Bank at NCBI. Query represents of sample; subject represents a database of National Center Biotechnology Information (NCBI).

Putative fimbrial subunit [*Klebsiella pneumoniae* subsp. pneumoniae ST258-K26BO]

Sequence ID: [CCM81450.1](#) Length: 170 Number of Matches: 1

Related Information

[Gene](#)-associated gene details

[Identical Proteins](#)-Identical proteins to WP_002885137.1

Range 1: 9 to 158 [GenPeptGraphics](#) [Next Match](#) [Previous Match](#)

Score	Expect	Method	Identities	Positives	Gaps	Frame
304 bits(779)	7e-109	Compositional matrix adjust.	150/150(100%)	150/150(100%)	0/150(0%)	+1
Query 1		PALAYEGSSTVNFNVTGTIEAPSCEVAVEPSNSIDLGTVSSQTFSGHAGASGASVPVKLV				
180						
Sbjct 9					
68						
Query 181		FSSCSADASAVTIAFSGTSFSDSTHASIYKNFQTGSNGASGVGLQLQSMADQQPLGPGDQY				
360						
Sbjct 69					
128						
Query 361		LYTFGDDADIHTFNMVARMFSPYGQVRSGM	450			
Sbjct 129		158			

Figure (3-18D2): Alignment analysis of *mrkD* gene of *Klebsiella pneumoniae* subsp. pneumoniae ST 258 with Gene Bank at NCBI. Query represents of sample; subject represents a database of National Center Biotechnology Information (NCBI).

***Klebsiella pneumoniae* strain WCHKP115016 chromosome, complete genome**

Sequence ID: [CP046967.1](#) Length: 5427644 Number of Matches: 1

Range 1: 4039707 to 4040156 [GenBankGraphics](#) [Next Match](#) [Previous Match](#)

Score	Expect	Identities	Gaps	Strand
808 bits(895)	0.0	449/450(99%)	0/450(0%)	Plus/Plus
Query 1	CCGGCGCTGGCTTATGAGGGCAGCAGCACGGTCAATTTTAAACGTACGGGCACCATCGAA			60
Sbjct 4039707			
4039766				
Query 61	GCGCCTTCCCTGTGAGGTGGCCGTGGAGCCGTGCGAACAGTATCGATTTAGGCACCGTCTCC			
120				
Sbjct 4039767			
4039826				
Query 121	TCGCAGACGTTCTCCGGACATGCCGGGGCAGCGGCCAGCGTGCCGGTTAAGCTGGTC			
180				
Sbjct 4039827			
4039886				
Query 181	TTTCCAGCTGTTCCGCCGATGCGTCGGCGGTGACCACCGGTTTAGCGGCACCAGCTTC			
240				
Sbjct 4039887			
4039946 T			
Query 241	GATAGCACCCACGCTTCAATCTATAAAAACTTCCAGACTGGCAGCAACGGTGCCAGCGGC			
300				
Sbjct 4039947			
4040006				
Query 301	GTCGGTTTGCAGCTGCAGAGCATGGCCGACCAGCAGCCCCTTGGCCCCGGCGACCAGTAT			
360				
Sbjct 4040007			
4040066				
Query 361	CTCTATACCTTTGGGGACGATGCGGATATCCATACCTTTAATATGGTGGCACGTATGTTT			
420				
Sbjct 4040067			
4040126				
Query 421	TCGCCTTATGGCCAGGTAAGGTCCGGGATG		450	
Sbjct 4040127		4040156	

Figure (3-18E1): Alignment analysis of *mrkD* gene of *Klebsiella pneumoniae* subsp. *pneumoniae* ST 258 with Gene Bank at NCBI. Query represents of sample; subject represents a database of National Center Biotechnology Information (NCBI).

Putative fimbrial subunit [*Klebsiella pneumoniae* subsp. pneumoniae ST258-K26BO]

Sequence ID: [CCM81450.1](#) Length: 170 Number of Matches: 1

Related Information

[Gene](#)-associated gene details

[Identical Proteins](#)-Identical proteins to WP_002885137.1

Range 1: 9 to 158 [GenPeptGraphics](#) [Next Match](#) [Previous Match](#)

Score	Expect	Method	Identities	Positives	Gaps	Frame
302 bits(773)	5e-108	Compositional matrix adjust.	149/150(99%)	149/150(99%)	0/150(0%)	+1
Query 1		PALAYEGSSTVNFNVTGTIEAPSCEVAVEPSNSIDLGTVSSQTFSGHAGASGASVPVKLV				
180						
Sbjct 9					
68						
Query 181		FSSCSADASAVTTAFSGTSFDSTHASIYKNFQTGSNGASGVGLQLQSMADQQPLGPGDQY				
360						
Sbjct 69	 I				
128						
Query 361		LYTFGDDADIHTFNMVARMFSPYGQVRSGM	450			
Sbjct 129		158			

Figure (3-18E2): Alignment analysis of *mrkD* gene of *Klebsiella pneumoniae* subsp. pneumoniae ST 258 with Gene Bank at NCBI. Query represents of sample; subject represents a database of National Center Biotechnology Information (NCBI).

***Klebsiella pneumoniae* strain WCHKP115016 chromosome, complete genome**

Sequence ID: [CP046967.1](#) Length: 5427644 Number of Matches: 1

Range 1: 4039707 to 4040156 [GenBankGraphics](#) [Next Match](#) [Previous Match](#)

Score	Expect	Identities	Gaps	Strand
803 bits(890)	0.0	448/450(99%)	0/450(0%)	Plus/Plus
Query 1	CCGGCGCTGGCTTATGAGGGCAGCAGCACGGTCAATTTTAACGTACGGGCACCATCGAA	60		
Sbjct 4039707			
4039766				
Query 61	GCGCCTTCCTGTGAGGTGGCCGTGGAGCCGTGCGAACAGTATCGATTTAGGCACCGTCTCC			
120				
Sbjct 4039767			
4039826				
Query 121	TCGAGACGTTCTCCGGACATGCCGGGGCAGCGGCCAGCGTGCCGGTTAAGCTGGTC			
180				
Sbjct 4039827			
4039886				
Query 181	TTTCCAGCTGTCCGCCGATGCGTCGGCGGTGACCATCGCGTTTAGCGGCACCAGCTTC			
240				
Sbjct 4039887			
4039946				
Query 241	GAAAGCACCCACGCTTCAATCTATAAAAACTTCCAGACTGGCAGCAACGGTGCCAGCGGC			
300				
Sbjct 4039947	.. T			
4040006				
Query 301	GTCGGTTTGCAGCTGCAGAGCATGGCCGACCAGCAGCCCCTTGGCCCCGGCGACCAGTAT			
360				
Sbjct 4040007			
4040066				
Query 361	CTCTATACCTTTGGGGCGATGCGGATATCCATACCTTTAATATGGTGGCACGTATGTTT			
420				
Sbjct 4040067 A			
4040126				
Query 421	TCGCCTTATGGCCAGGTAAGGTCCGGGATG	450		
Sbjct 4040127	4040156		

Figure (3-18F1): Alignment analysis of *mrkD* gene of *Klebsiella pneumoniae* subsp. *pneumoniae* ST 258 with Gene Bank at NCBI. Query represents of sample; subject represents a database of National Center Biotechnology Information (NCBI).

Putative fimbrial subunit [*Klebsiella pneumoniae* subsp. *pneumoniae* ST258-K26BO]

Sequence ID: [CCM81450.1](#) Length: 170 Number of Matches: 1

Related Information

[Gene](#)-associated gene details

[Identical Proteins](#)-Identical proteins to WP_002885137.1

Range 1: 9 to 158 [GenPeptGraphics](#) [Next Match](#) [Previous Match](#)

Score	Expect	Method	Identities	Positives	Gaps	Frame
300 bits(768)	3e-107	Compositional matrix adjust.	148/150(99%)	149/150(99%)	0/150(0%)	+1
Query 1		PALAYEGSSTVNFNVTGTIEAPSCEVAVEPSNSIDLGTVSSQTFSGHAGASGASVPVKLV				
180						
Sbjct 9					
68						
Query 181		FSSCSADASAVTIAFSGTSFESTHASIYKNFQTGSNGASGVLQLQSMADQQPLGPGDQY				
360						
Sbjct 69	 D				
128						
Query 361		LYTFGGDADIHTFNMVARMFSPYGQVRSGM	450			
Sbjct 129	 D	158			

Figure (3-18F2): Alignment analysis of *mrkD* gene of *Klebsiella pneumoniae* subsp. *pneumoniae* ST 258 with Gene Bank at NCBI. Query represents of sample; subject represents a database of National Center Biotechnology Information (NCBI).

3.10.2.2 *luxS* gene

The genes were amplified by PCR method, and send for sequencing service to Macrogen Company Korea. The sequencing for *luxS* gene to *K. pneumoniae* and *K. pneumoniae* subsp. *pneumoniae* ST 258, the results showed compatibility of 99% in Gene Bank of *luxS* gene under sequence ID: CP114753.1, so, no recorded change noticed from the Gene Bank in *luxS* gene as shown in Table (3-12), Figures (3-19A-F).

Klebsiella pneumoniae strain ST39 chromosome, complete genome

Sequence ID: [CP114753.1](#) Length: 5434255 Number of Matches: 1

Range 1: 934522 to 934859 [GenBankGraphics](#) [Next Match](#) [Previous Match](#)

Score	Expect	Identities	Gaps	Strand
610 bits(676)	4e-170	338/338(100%)	0/338(0%)	Plus/Minus
Query 1	ATGGCGATGAAATCACCGTTTTTCGATCTGCGCTTCTGCGTACCGAACCAGGAAGTGATGC			60
Sbjct 934859			
934800				
Query 61	CGGAACGCGGTATCCACACCCTGGAGCATCTGTTTCGCGGGCTTTATGCGCGATCATCTGA			120
Sbjct 934799			
934740				
Query 121	ACGGGAATGGCGTGGAATTATCGACATTTTCGCCAATGGGCTGCCGCACCGGCTTCTATA			180
Sbjct 934739			
934680				
Query 181	TGAGCCTGATTGGTACGCCGGACGAGCAGCGCGTCGCTGACGCCTGGAAAGCGGCGATGG			240
Sbjct 934679			
934620				
Query 241	CCGATGTGCTGAAGGTGAAAGATCAGAACCAGATCCCGGAGCTCAACGTCTACCAGTGCG			300
Sbjct 934619			
934560				
Query 301	GGACTTACACCATGCACTCGCTGGAAGAGGCCAGGAC		338	
Sbjct 934559		934522	

Figure (3-19A1): Alignment analysis of *luxS* gene of *Klebsiella pneumoniae* with Gene Bank at NCBI. Query represents of sample; subject represents a database of National Center Biotechnology Information (NCBI).

S-ribosylhomocysteine lyase [*Klebsiella pneumoniae*]Sequence ID: [WP_227545522.1](#) Length: 172 Number of Matches: 1Range 1: 31 to 142 [GenPeptGraphics](#) [Next Match](#) [Previous Match](#)

Score	Expect	Method	Identities	Positives	Gaps	Frame
241 bits(615)	2e-79	Compositional matrix adjust.	112/112(100%)	112/112(100%)	0/112(0%)	+1
Query 1		GDEITVFDLRFCVFNQEVMPERGIHTLEHLFAGFMRDHLNGNGVEIIDISPMGCRTGFYM				
180						
Sbjct 31					
90						
Query 181		SLIGTPDEQRVADAWKAAMADV LKVKDQNQIPELNVYQCGTYTMHSLEEAQD			336	
Sbjct 91				142	

Figure (3-19A2): Alignment analysis of *luxS* gene of *Klebsiella pneumoniae* with Gene Bank at NCBI. Query represents of sample; subject represents a database of National Center Biotechnology Information (NCBI).

Klebsiella pneumoniae strain ST39 chromosome, complete genome

Sequence ID: [CP114753.1](#) Length: 5434255 Number of Matches: 1

Range 1: 934522 to 934859 [GenBankGraphics](#) [Next Match](#) [Previous Match](#)

Score	Expect	Identities	Gaps	Strand
610 bits(676)	4e-170	338/338(100%)	0/338(0%)	Plus/Minus
Query 1	ATGGCGATGAAATCACCGTTTTTCGATCTGCGCTTCTGCGTACCGAACCAGGAAGTGATGC	60		
Sbjct 934859			
934800				
Query 61	CGGAACGCGGTATCCACACCCTGGAGCATCTGTTTCGCGGGCTTTATGCGCGATCATCTGA	120		
Sbjct 934799			
934740				
Query 121	ACGGGAATGGCGTGGAATTATCGACATTTTCGCCAATGGGCTGCCGCACCGGCTTCTATA	180		
Sbjct 934739			
934680				
Query 181	TGAGCCTGATTGGTACGCCGGACGAGCAGCGCGTCGCTGACGCCTGGAAAGCGGCGATGG	240		
Sbjct 934679			
934620				
Query 241	CCGATGTGCTGAAGGTGAAAGATCAGAACCAGATCCCGGAGCTCAACGTCTACCAGTGCG	300		
Sbjct 934619			
934560				
Query 301	GGAATTACACCATGCACTCGCTGGAAGAGGCCAGGAC	338		
Sbjct 934559	934522		

Figure (3-19B1): Alignment analysis of *luxS* gene of *Klebsiella pneumoniae* with Gene Bank at NCBI. Query represents of sample; subject represents a database of National Center Biotechnology Information (NCBI).

S-ribosylhomocysteine lyase [*Klebsiella pneumoniae*]Sequence ID: [WP_227545522.1](#) Length: 172 Number of Matches: 1Range 1: 31 to 142 [GenPeptGraphics](#) [Next Match](#) [Previous Match](#)

Score	Expect	Method	Identities	Positives	Gaps	Frame
241 bits(615)	2e-79	Compositional matrix adjust.	112/112(100%)	112/112(100%)	0/112(0%)	+1
Query 1		GDEITVFDLRFCVFNQEVMPERGIHTLEHLFAGFMRDHLNGNGVEIIDISPMGCRTGFYM				
180						
Sbjct 31					
90						
Query 181		SLIGTPDEQRVADAWKAAMADV LKVKDQNQIPELNVYQCGTYTMHSLEEAQD			336	
Sbjct 91				142	

Figure (3-19B2): Alignment analysis of *luxS* gene of *Klebsiella pneumoniae* with Gene Bank at NCBI. Query represents of sample; subject represents a database of National Center Biotechnology Information (NCBI).

***Klebsiella pneumoniae* strain ST39 chromosome, complete genome**

Sequence ID: [CP114753.1](#) Length: 5434255 Number of Matches: 1

Range 1: 934522 to 934859 [GenBankGraphics](#) Next Match Previous Match

Score	Expect	Identities	Gaps	Strand
610 bits(676)	4e-170	338/338(100%)	0/338(0%)	Plus/Minus
Query 1	ATGGCGATGAAATCACCGTTTTTCGATCTGCGCTTCTGCGTACCGAACCAGGAAGTGATGC			60
Sbjct 934859			
934800				
Query 61	CGGAACGCGGTATCCACACCCTGGAGCATCTGTTTCGCGGGCTTTATGCGCGATCATCTGA			120
Sbjct 934799			
934740				
Query 121	ACGGGAATGGCGTGAAATTATCGACATTTTCGCCAATGGGCTGCCGCACCGGCTTCTATA			180
Sbjct 934739			
934680				
Query 181	TGAGCCTGATTGGTACGCCGGACGAGCAGCGCGTCGCTGACGCCTGGAAAGCGGCGATGG			240
Sbjct 934679			
934620				
Query 241	CCGATGTGCTGAAGGTGAAAGATCAGAACCAGATCCCGGAGCTCAACGTCTACCAGTGCG			300
Sbjct 934619			
934560				
Query 301	GGACTTACACCATGCACTCGCTGGAAGAGGCCAGGAC		338	
Sbjct 934559		934522	

Figure (3-19C1): Alignment analysis of *luxS* gene of *Klebsiella pneumoniae* with Gene Bank at NCBI. Query represents of sample; subject represents a database of National Center Biotechnology Information (NCBI).

S-ribosylhomocysteine lyase [*Klebsiella pneumoniae*]Sequence ID: [WP_227545522.1](#) Length: 172 Number of Matches: 1Range 1: 31 to 142 [GenPeptGraphics](#) [Next Match](#) [Previous Match](#)

Score	Expect	Method	Identities	Positives	Gaps	Frame
241 bits(615)	2e-79	Compositional matrix adjust.	112/112(100%)	112/112(100%)	0/112(0%)	+1
Query 1		GDEITVFDLRFCVFNQEVMPERGIHTLEHLFAGFMRDHLNGNGVEIIDISPMGCRTGFYM				
180						
Sbjct 31					
90						
Query 181		SLIGTPDEQRVADAWKAAMADV LKVKDQNQIPELNVYQCGTYTMHSLEEAAQD			336	
Sbjct 91				142	

Figure (3-19C2): Alignment analysis of *luxS* gene of *Klebsiella pneumoniae* with Gene Bank at NCBI. Query represents of sample; subject represents a database of National Center Biotechnology Information (NCBI).

Klebsiella pneumoniae strain S245 chromosome, complete genome

Sequence ID: [CP114853.1](#) Length: 5332796 Number of Matches: 1

Range 1: 1133807 to 1134163 [GenBankGraphics](#) [Next Match](#) [Previous Match](#)

Score	Expect	Identities	Gaps	Strand
645 bits(714)	2e-180	357/357(100%)	0/357(0%)	Plus/Plus
Query 1		GGCGATGAAATCACCGTTTTTCGATCTGCGCTTCTGCGTACCGAACCAGGAAGTGATGCCG		60
Sbjct 1133807			
1133866				
Query 61		GAACGCGGTATCCACACCCTGGAGCATCTGTTTCGCTGGCTTTATGCGCGATCATCTGAAC		120
Sbjct 1133867			
1133926				
Query 121		GGGAATGGCGTGAAATTATCGACATTTCCCAATGGGCTGCCGCACCGGCTTCTATATG		180
Sbjct 1133927			
1133986				
Query 181		AGCCTGATTGGTACGCCGGACGAGCAGCGCTCGCTGACGCCTGAAAGCGCGCATGGCC		240
Sbjct 1133987			
1134046				
Query 241		GATGTGCTGAAGGTGAAAGATCAGAACCAGATCCCGGAGCTCAACGTCTACCAGTGCGGG		300
Sbjct 1134047			
1134106				
Query 301		ACTTACACCATGCACTCGCTGGAAGAGGCCAGGACATCGCTCGTCATATCATTGAG		357
Sbjct 1134107			
1134163				

Figure (3-19D1): Alignment analysis of *luxS* gene of *Klebsiella pneumoniae subsp. pneumoniae* ST 258 with Gene Bank at NCBI. Query represents of sample; subject represents a database of National Center Biotechnology Information (NCBI).

S-ribosylhomocysteine lyase [*Klebsiella pneumoniae* subsp. pneumoniae ST258-K26BO]

Sequence ID: [CCM85432.1](#) Length: 153 Number of Matches: 1

Range 1: 12 to 130 [GenPeptGraphics](#) [Next Match](#) [Previous Match](#)

Score	Expect	Method	Identities	Positives	Gaps	Frame
253 bits(647)	2e-89	Compositional matrix adjust.	119/119(100%)	119/119(100%)	0/119(0%)	+1
Query 1		GDEITVFDLRFCVPNQEVMPERGIHTLEHLFAGFMRDHLNGNGVEIIDISPMGCRTGFYM				
180						
Sbjct 12					
71						
Query 181		SLIGTPDEQRVADAWKAAMADV LKVKDQNQIPELNVYQCGTYTMHSLEEAQDIARHIIE				
357						
Sbjct 72					
130						

Figure (3-19D2): Alignment analysis of *luxS* gene of *Klebsiella pneumoniae* subsp. *pneumoniae* ST 258 with Gene Bank at NCBI. Query represents of sample; subject represents a database of National Center Biotechnology Information (NCBI).

Klebsiella pneumoniae strain S245 chromosome, complete genome

Sequence ID: [CP114853.1](#) Length: 5332796 Number of Matches: 1

Range 1: 1133807 to 1134163 [GenBankGraphics](#) [Next Match](#) [Previous Match](#)

Score	Expect	Identities	Gaps	Strand
645 bits(714)	2e-180	357/357(100%)	0/357(0%)	Plus/Plus
Query 1	GGCGATGAAATCACCGTTTTTCGATCTGCGCTTCTGCGTACCGAACCAGGAAGTGATGCCG			60
Sbjct 1133807			
1133866				
Query 61	GAACGCGGTATCCACACCCTGGAGCATCTGTTTCGCTGGCTTTATGCGCGATCATCTGAAC			
120				
Sbjct 1133867			
1133926				
Query 121	GGGAATGGCGTGAAATTATCGACATTTCCGCAATGGGCTGCCGCACCGGCTTCTATATG			
180				
Sbjct 1133927			
1133986				
Query 181	AGCCTGATTGGTACGCCGGACGAGCAGCGCTCGCTGACGCCTGGAAAGCGCGCATGGCC			
240				
Sbjct 1133987			
1134046				
Query 241	GATGTGCTGAAGGTGAAAGATCAGAACCAGATCCCGGAGCTCAACGTCTACCAGTGCGGG			
300				
Sbjct 1134047			
1134106				
Query 301	ACTTACACCATGCACTCGCTGGAAGAGGCCAGGACATCGCTCGTCATATCATTGAG			357
Sbjct 1134107			
1134163				

Figure (3-19E1): Alignment analysis of *luxS* gene of *Klebsiella pneumoniae* subsp. *pneumoniae* ST 258 with Gene Bank at NCBI. Query represents of sample; subject represents a database of National Center Biotechnology Information (NCBI).

S-ribosylhomocysteine lyase [*Klebsiella pneumoniae* subsp. *pneumoniae* ST258-K26BO]

Sequence ID: [CCM85432.1](#) Length: 153 Number of Matches: 1

Range 1: 12 to 130 [GenPeptGraphics](#) [Next Match](#) [Previous Match](#)

Score	Expect	Method	Identities	Positives	Gaps	Frame
253 bits(647)	2e-89	Compositional matrix adjust.	119/119(100%)	119/119(100%)	0/119(0%)	+1
Query 1		GDEITVFDLRFCVFNQEVMPERGIHTLEHLFAGFMRDHLNGNGVEIIDISPMGCRTGFYM				
180						
Sbjct 12					
71						
Query 181		SLIGTPDEQRVADAWKAAMADV LKVKDQNQIPELNVYQCGTYTMHSLEEAQDIARHIIE				
357						
Sbjct 72					
130						

Figure (3-19E2): Alignment analysis of *luxS* gene of *Klebsiella pneumoniae* subsp. *pneumoniae* ST 258 with Gene Bank at NCBI. Query represents of sample; subject represents a database of National Center Biotechnology Information (NCBI).

Klebsiella pneumoniae strain S245 chromosome, complete genome

Sequence ID: [CP114853.1](#) Length: 5332796 Number of Matches: 1

Range 1: 1133807 to 1134163 [GenBankGraphics](#) [Next Match](#) [Previous Match](#)

Score	Expect	Identities	Gaps	Strand
645 bits(714)	2e-180	357/357(100%)	0/357(0%)	Plus/Plus
Query 1	GGCGATGAAATCACCGTTTTTCGATCTGCGCTTCTGCGTACCGAACCAGGAAGTGATGCCG			60
Sbjct 1133807			
1133866				
Query 61	GAACGCGGTATCCACACCCTGGAGCATCTGTTTCGCTGGCTTTATGCGCGATCATCTGAAC			
120				
Sbjct 1133867			
1133926				
Query 121	GGGAATGGCGTGAAATTATCGACATTTCCGCAATGGGCTGCCGCACCGGCTTCTATATG			
180				
Sbjct 1133927			
1133986				
Query 181	AGCCTGATTGGTACGCCGGACGAGCAGCGCGTCGCTGACGCCTGAAAGCGGCATGGCC			
240				
Sbjct 1133987			
1134046				
Query 241	GATGTGCTGAAGGTGAAAGATCAGAACCAGATCCCGGAGCTCAACGTCTACCAGTGCGGG			
300				
Sbjct 1134047			
1134106				
Query 301	ACTTACACCATGCACTCGCTGGAAGAGGCCAGGACATCGCTCGTCATATCATTGAG			357
Sbjct 1134107			
1134163				

Figure (3-19F1): Alignment analysis of *luxS* gene of *Klebsiella pneumoniae* subsp. *pneumoniae* ST 258 with Gene Bank at NCBI. Query represents of sample; subject represents a database of National Center Biotechnology Information (NCBI).

S-ribosylhomocysteine lyase [*Klebsiella pneumoniae* subsp. pneumoniae ST258-K26BO]

Sequence ID: [CCM85432.1](#) Length: 153 Number of Matches: 1

Range 1: 12 to 130 [GenPeptGraphics](#) [Next Match](#) [Previous Match](#)

Score	Expect	Method	Identities	Positives	Gaps	Frame
253 bits(647)	2e-89	Compositional matrix adjust.	119/119(100%)	119/119(100%)	0/119(0%)	+1
Query 1		GDEITVFDLRFCVFNQEVMPERGIHTLEHLFAGFMRDHLNGNGVEIIDISPMGCRTGFYM				
180						
Sbjct 12					
71						
Query 181		SLIGTPDEQRVADAWKAAMADV LKVKDQNQIPELNVYQCGTYTMHSLEEAQDIARHIE				
357						
Sbjct 72					
130						

Figure (3-19F2): Alignment analysis of *luxS* gene of *Klebsiella pneumoniae* subsp. *pneumoniae* ST 258 with Gene Bank at NCBI. Query represents of sample; subject represents a database of National Center Biotechnology Information (NCBI).

Table (3-12): Determinate of DNA sequencing for *K. pneumoniae* and *K. pneumoniae* subsp. *pneumoniae* ST 258 *luxS* gene

No. Of sample	Type of substitution	Location	Nucleotide	Source	Sequence ID with compare	Identities
25	-----	-----	-----	<i>Klebsiella pneumoniae LUXS</i> gene	ID: CP114753.1	99%
19	-----	-----	-----	<i>Klebsiella pneumoniae LUXS</i> gene	ID: CP114753.1	99%
39	-----	-----	-----	<i>Klebsiella pneumoniae LUXS</i> gene	ID: CP114753.1	99%
14	-----	-----	-----	<i>Klebsiella pneumoniae</i> subsp. <i>pneumoniae</i> ST258	ID: CP114853.1	99%
2	-----	-----	-----	<i>Klebsiella pneumoniae</i> subsp. <i>pneumoniae</i> ST258	ID: CP114853.1	99%
22	-----	-----	-----	<i>Klebsiella pneumoniae</i> subsp. <i>pneumoniae</i> ST258	ID: CP114853.1	99%

2.11 Phylogenic tree of *K. pneumoniae*

The phylogeny tree of local *K. pneumoniae* gene incorporated with various strains of *K. pneumoniae* sequences with variable origins. The results showed the samples were distributed into closely associated positions in closely-related phylogenetic distances. It was observed that, the four samples were positioned in the immediate vicinity to several Asia and European strains of *K. pneumoniae*, including South Korea (GenBank acc. No. CP052490.1), Tanzania (GenBank acc. No. CP034316.1), USA (GenBank acc. No. CP032207.1), China (GenBank acc. No. CP106654.1), Switzerland (GenBank acc. No. CP100520.1), Spain (GenBank acc. No. OW849262.1), Curacao GenBank acc. No. CP084852.1), Netherlands (GenBank acc. No. CP068997.1), Norway (GenBank acc. No. CP065034.1), Australia (GenBank acc. No. LR890569.1) and United Kingdom (GenBank acc. No. CP056830.1), these results were shown in Table (3-13), Figure (3-20).

Table (3-13): The NCBI-BLAST Homology Sequence identity (%) between local *K. pneumoniae* isolates and NCBI-BLAST submitted *K. pneumoniae* isolates in other countries

No.	Accession	Country	Source	Isolation source	Compatibility
1.	ID: CP052490.1	South Korea	<i>K. pneumoniae</i>	Homo sapiens Blood\	99%
2.	ID: CP034316.1	Tanzania	<i>K. pneumoniae</i>	Feces\Homo sapiens	99%
3.	ID: CP032207.1	USA	<i>K. pneumoniae</i>	-----	99%
4.	ID: CP106654.1	China	<i>K. pneumoniae</i>	Secretion\ Homo sapiens	99%
5.	ID: CP100520.1	Switzerland	<i>K. pneumoniae</i>	Gallus gallus	99%
6.	ID: OW849262.1	Spain	<i>K. pneumoniae</i>	-----	99%
7.	ID: CP084852.1	Curacao	<i>K. pneumoniae</i>	Urinary tract\ Homo sapiens	99%
8.	ID: CP068997.1	Netherlands	<i>K. pneumoniae</i>	Homo sapiens	99%
9.	ID: CP065034.1	Norway	<i>K. pneumoniae</i>	marine environment	99%
10.	ID: LR890569.1	Australia	<i>K. pneumoniae</i>	-----	99%
11.	ID: CP056830.1	United Kingdom	<i>K. pneumoniae</i>	Wastewater sample	99%

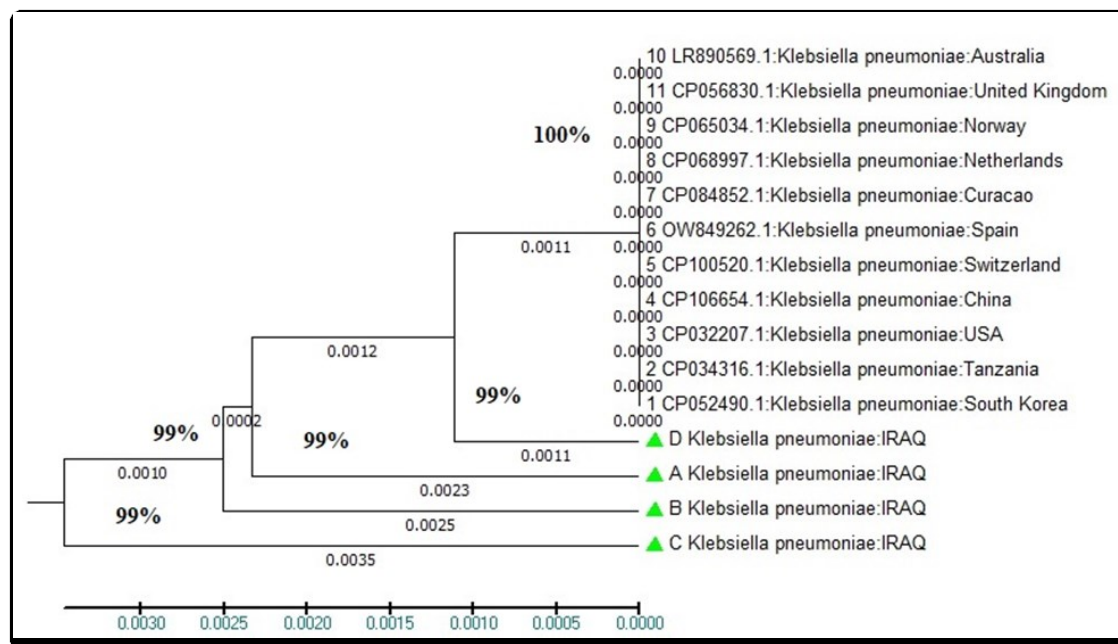


Figure (3-20): Phylogenetic tree of *K. pneumoniae*

2.12 Phylogenetic tree of *K. pneumoniae* ST 258

The phylogeny tree of local *K. pneumoniae* ST 258 gene incorporated with strains of *K. pneumoniae* ST 258 sequences with only one region. The results showed the samples were distributed into closely associated positions in closely-related phylogenetic distances. It was observed that, the two samples were positioned in the immediate vicinity to only one country (Venezuela) (GenBank acc. No. HG685581.1), these results were shown in Table (3-14), Figure (3-21).

Table (3-14): The NCBI-BLAST Homology Sequence identity (%) between local *K. pneumoniae* sub-spp *pneumoniae* ST 258 isolates and NCBI-BLAST submitted *K. pneumoniae* sub-spp *pneumoniae* ST 258 isolates in Venezuela

No.	Accession	Country	Source	Isolation source	Compatibility
1.	ID: HG685581.1	Venezuela	<i>K. pneumoniae</i>		99%

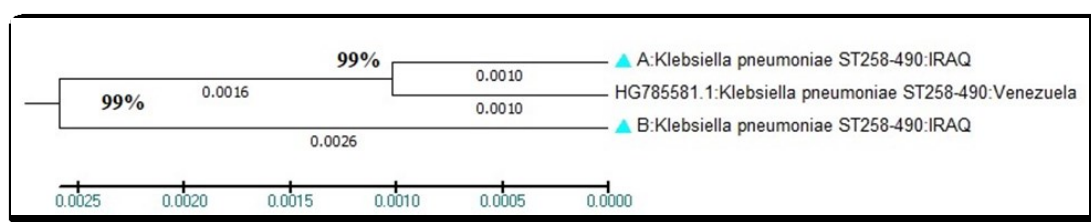


Figure (3-21): Phylogenetic tree of *K. pneumoniae* sub-spp *pneumoniae* ST 258

Conclusions and Recommendations

Conclusions:

The present study has reached at the following conclusions:

1. Identification of *K. pneumoniae* using vitek II more specific than other biochemical tests, while identification of *K. pneumoniae* ST258 depend on specific gene *pilV*- gene more accurate than other methods.
2. All clinical isolates of *K. pneumoniae* produce many virulence factors involve hemolysin, siderophores, agglutinate erythrocyte, serum resistance, lipase producer, gelatinase and hyper-mucoviscosity.
3. All isolates can produce biofilm by quantitative method.
4. The concentration of colanic acid among *K. pneumoniae* ST258 greater than the ordinary isolates.
5. The antibiotic resistance increased by presence of resistance genes responsible about β -lactam and carbapenems antibiotics
6. *K. pneumoniae* ST258 more resistance than other the ordinary *K. pneumoniae*.
7. *K. pneumoniae* were compare with strains in NCBI, the two samples of ST258 were positioned in the immediate vicinity to only one country (Venezuela).

Recommendations

Depending on the finding of this study, the recommended include:

1. Using box-PCR and Real-time for detection of ST258 or other strains of *K. pneumoniae*.
2. Study of other virulence factors among *K. pneumoniae* ST258 like some specific enzymes and their association with their pathogenicity.
3. Farther studies about the relationship between *K. pneumoniae* ST258 and hospital- associated outbreaks in particular, ST258CRKP and multidrug resistance.

References

- Alphonse, S., Djemil, I., Piserchio, A., & Ghose, R. (2022). Structural basis for the recognition of the bacterial tyrosine kinase Wzc by its cognate tyrosine phosphatase Wzb. *Proceedings of the National Academy of Sciences*, *119*(26), e2201800119.
- Abdallah, M. S., Mustapha, T., Gambo, A., & Ishaq, S. (2016). Biochemical identification and cultural characterization of some Gram-negative bacteria obtained from fecal/diarrhoeal samples. *Cibtech Journal of Microbiology an Online International Journal*, *5*, 17-24.
- Abdul-Mutakabbir, J. C., Alosaimy, S., Morrisette, T. & Rybak, M. J. (2020). Cefiderocol: a novel siderophore cephalosporin against multidrug resistant gram-negative pathogens. *Pharmacotherapy: The J. of Human Pharmacology and Drug Therapy*, *40*(12), 1228-1247.
- Abed, A. S., Al Khafaji, H. K., & AL-Hamdani, A. H. (2016). Detection of serotype gene of *Klebsiella pneumoniae* isolated from different clinical cases of hospitalized infections in Al-Diwaniya city. *Al-Qadisiyah Medical Journal*, *12*(21), 193-203.
- Abozahra, R., Abdelhamid, S. M., Wen, M. M., Abdelwahab, I., & Baraka, K. (2020). A nanoparticles based microbiological study on the effect of rosemary and ginger essential oils against *Klebsiella pneumoniae*. *The Open Microbiology Journal*, *14*(1).
- Abrar, S., Ain, N. U., Liaqat, H., Hussain, S., Rasheed, F., & Riaz, S. (2019). Distribution of bla_{CTX-M}, bla_{TEM}, bla_{SHV} and bla_{OXA} genes in extended-spectrum-β-lactamase-producing clinical isolates: A three-year multi-center study from Lahore, Pakistan. *Antimicrobial Resistance & Infection Control*, *8*, 1-10.

- Abrar, S., Vajeeda, A., Ul-Ain, N., & Riaz, S. (2017). Distribution of CTX-M group I and group III β -lactamases produced by *Escherichia coli* and *Klebsiella pneumonia* in Lahore, Pakistan. *Microbial pathogenesis*, *103*, 8-12.
- Agarwal, V., Tiwari, A., & Varadwaj, P. (2023). An Extensive Review on β -lactamase Enzymes and their Inhibitors. *Current Medicinal Chemistry*, *30*(7), 783-808.
- Ageorges, V., Monteiro, R., Leroy, S., Burgess, C. M., Pizza, M., Chaucheyras-Durand, F., & Desvaux, M. (2020). Molecular determinants of surface colonisation in diarrhoeagenic *Escherichia coli* (DEC): From bacterial adhesion to biofilm formation. *FEMS Microbiology Reviews*.
- Ahn, D., Bhushan, G., McConville, T. H., Annavajhala, M. K., Soni, R. K., Lung, T. W. F., & Prince, A. (2021). An acquired acyltransferase promotes *Klebsiella pneumoniae* ST258 respiratory infection. *Cell reports*, *35*(9), 109196.
- Akpaka, P. E., Vaillant, A., Wilson, C., & Jayaratne, P. (2021). Extended spectrum beta-lactamase (ESBL) produced by gram-negative bacteria in Trinidad and Tobago. *International Journal of Microbiology*, *2021*.
- Al-Ansari, M. M., Dhasarathan, P., Ranjitsingh, A. J. A., & Al-Humaid, L. A. (2020). Challenging multidrug-resistant urinary tract bacterial isolates via bio-inspired synthesis of silver nanoparticles using the inflorescence extracts of *Tridax procumbens*. *Journal of King Saud University-Science*, *32*(7), 3145-3152.
- Alav, I., Sutton, J. M., & Rahman, K. M. (2018). Role of bacterial efflux pumps in biofilm formation. *Journal of Antimicrobial Chemotherapy*, *73*(8), 2003-2020.

References

- Albelda-Berenguer, M., Monachon, M., & Joseph, E. (2019). Siderophores: from natural roles to potential applications. *Advances in applied microbiology*, *106*, 193-225.
- Alcántar-Curiel, M. D., Ledezma-Escalante, C. A., Jarillo-Quijada, M. D., Gayosso-Vázquez, C., Morfín-Otero, R., Rodríguez-Noriega, E., & Girón, J. A. (2018). Association of antibiotic resistance, cell adherence, and biofilm production with the endemicity of nosocomial *Klebsiella pneumoniae*. *BioMed research international*, *2018*.
- Al-Fatlawi, S. F. N. (2020). Molecular Analysis of *fimH* Gene from uropathogenic *Escherichia coli* (Doctoral dissertation, Ministry of Higher Education).
- Alfei, S., & Schito, A. M. (2022). β -lactam antibiotics and β -lactamase enzymes inhibitors, part 2: our limited resources. *Pharmaceuticals*, *15*(4), 476.
- Ali, A. M., & Sana'a, N. (2019). Virulence factors genotyping of *Klebsiella pneumoniae* clinical isolates from Baghdad. *Reviews in Medical Microbiology*, *30*(1), 36-46.
- Ali, A., Waris, A., Khan, M. A., Asim, M., Khan, A. U., Khan, S., & Zeb, J. (2022). Recent advancement, immune responses, and mechanism of action of various vaccines against intracellular bacterial infections. *Life Sciences*, 121332.
- Ali, H. H. (2021). Microbial Assessment of Water Samples in Houston, Texas (Doctoral dissertation, Texas Southern University).
- Ali, S., Alam, M., Hasan, G. M., & Hassan, M. I. (2022). Potential therapeutic targets of *Klebsiella pneumoniae*: a multi-omics review perspective. *Briefings in functional genomics*, *21*(2), 63-77.

- Aljanaby, A. A. J., & Alhasani, A. H. A. (2016). Virulence factors and antibiotic susceptibility patterns of multidrug resistance *Klebsiella pneumoniae* isolated from different clinical infections. *African Journal of Microbiology Research*, *10*(22), 829-843.
- Al-Kaaby, W. A. J. (2016). Detection of extended spectrum β -lactamases producing by *Klebsiella pneumonia* isolated from urinary tract infection patients by using mPCR technique. *Al-Qadisiyah Medical Journal*, *12*(22), 59-64.
- AL-Taai, H. R. R. (2016). Bacteriological comparison between pseudomonas aeruginosa and *Klebsiella pneumoniae* isolated from different infectious sources. *Diyala Journal for Pure Science*, *12*(1), 162-182.
- Alves, J. E. V. (2016). Immunobiological studies on two human pathogens: Group B-*Streptococcus* and *Escherichia coli*.
- Amraei, S., Eslami, G., Taherpour, A., & Hashemi, A. (2022). The role of *act* and *fox* genes in *Klebsiella pneumoniae* strains isolated from hospitalized patients. *Micro Nano Bio Aspects*, *1*(2), 18-25.
- Andrews, B., Joshi, S., Swaminathan, R., Sonawane, J., & Shetty, K. (2018). Prevalence of extended spectrum β -lactamase (ESBL) producing bacteria among the clinical samples in and around a tertiary care centre in Nerul, Navi Mumbai, India. *Int. J. Curr. Microbiol. App. Sci*, *7*(3), 3402-3409.
- Ares, M. A., Sansabas, A., Siqueiros-Cendón, T., Rascón-Cruz, Q., Rodríguez-Valverde, D., Jarillo-Quijada, M., & De la Cruz, M. A. (2019). The interaction of *Klebsiella pneumoniae* with lipid rafts-associated cholesterol increases macrophage-mediated phagocytosis due to down

- regulation of the capsule polysaccharide. *Frontiers in cellular and infection microbiology*, 9, 255.
- Arezes, J. A. T. (2015). The role of hepcidin in the host defense against *Vibrio vulnificus* infection.
- Atze, H. (2021). Optimization of Beta-lactamase Inhibitors Belonging to the Diazabicyclo-octane Family and Design of a Mass Spectrometry-based Approach for Exploring Peptidoglycan Polymerization (Doctoral dissertation, Sorbonne université).
- Aurilio, C., Sansone, P., Barbarisi, M., Pota, V., Giaccari, L. G., Coppolino, F., & Pace, M. C. (2022). Mechanisms of action of carbapenem resistance. *Antibiotics*, 11(3), 421.
- Balaure, P. C., & Grumezescu, A. M. (2020). Recent advances in surface nanoengineering for biofilm prevention and control. Part I: Molecular basis of biofilm recalcitrance. Passive anti-biofouling nanocoatings. *Nanomaterials*, 10(6), 1230.
- Baldiris-Avila, R., Montes-Robledo, A., & Buelvas-Montes, Y. (2020). Phylogenetic classification, biofilm-forming capacity, virulence factors, and antimicrobial resistance in uropathogenic *Escherichia coli* (UPEC). *Current Microbiology*, 77, 3361-3370.
- Ballén, V., Gabasa, Y., Ratia, C., Ortega, R., Tejero, M., & Soto, S. (2021). Antibiotic resistance and virulence profiles of *Klebsiella pneumoniae* strains isolated from different clinical sources. *Frontiers in Cellular and Infection Microbiology*, 11, 738223.

- Barclay, L. L., Gibson, G. E., & Blass, J. P. (1981). The string test: an early behavioral change in thiamine deficiency. *Pharmacology Biochemistry and Behavior*, *14*(2), 153-157.
- Baron, E. J., Peterson, L. R. and Finegold, S. M. (1994). Bailey and Scott's Diagnostic Microbiology. 9th Ed. The C.V. Mosby Company, U.S.A.
- Batabyal, B. (2018). Commonly use of oral antibiotics resistance in children aged 1 to 12 years with UTIs an increasing problem.
- Becker, M., Patz, S., Becker, Y., Berger, B., Drungowski, M., Bunk, B., & Ruppel, S. (2018). Comparative genomics reveal a flagellar system, a type VI secretion system and plant growth-promoting gene clusters unique to the endophytic bacterium *Kosakonia radicincitans*. *Frontiers in microbiology*, *9*, 1997.
- Ben Tanfous, F., Alonso, C. A., Achour, W., Ruiz-Ripa, L., Torres, C., & Ben Hassen, A. (2017). First description of KPC-2-producing *Escherichia coli* and ST15 OXA-48-positive *Klebsiella pneumoniae* in Tunisia. *Microbial drug resistance*, *23*(3), 365-375.
- Bengoechea, J. A., & Sa Pessoa, J. (2019). *Klebsiella pneumoniae* infection biology: living to counteract host defenses. *FEMS microbiology reviews*, *43*(2), 123-144.
- Beuth, J., & Uhlenbruck, G. (2017). Adhesive properties of bacteria. In *Principles of cell adhesion* (pp. 87-106). CRC Press.
- Bhunja, A. K. (2018). *Vibrio cholerae*, *Vibrio parahaemolyticus*, and *Vibrio vulnificus*. In *Foodborne Microbial Pathogens* (pp. 315-329). Springer, New York, NY.

- Bonazzi, D., Schiavo, V. L., Machata, S., Djafer-Cherif, I., Nivoit, P., Manriquez, V., & Voituriez, R. (2018). Intermittent pili-mediated forces fluidize *Neisseria meningitidis* aggregates promoting vascular colonization. *Cell*, *174*(1), 143-155.
- Boopathi, S., Poma, A. B., & Kolandaivel, P. (2020). Novel 2019 coronavirus structure, mechanism of action, antiviral drug promises and rule out against its treatment. *Journal of Biomolecular Structure and Dynamics*, 1-10.
- Botelho, J., & Schulenburg, H. (2021). The role of integrative and conjugative elements in antibiotic resistance evolution. *Trends in microbiology*, *29*(1), 8-18.
- Brooks, K. P. (2021). Characterization of extended spectrum β -lactamases (ESBLs) and other resistant genes encoding bacteria from a rural community settlement.
- Brown, H. L., Clayton, A., & Stephens, P. (2021). The role of bacterial extracellular vesicles in chronic wound infections: Current knowledge and future challenges. *Wound Repair and Regeneration*, *29*(6), 864-880.
- Bunyan, I. A., & Al-Salem, H. L. (2022). Gene sequencing of *entB* gene among *Klebsiella pneumonia* isolates from different site of infections. *Journal of Complementary Medicine Research*, *13*(1), 107-107.
- Bunyan, I. A., Hadi, O. M., & Al-Mansoori, H. A. (2019). Phenotypic detection and biofilm formation among *Pseudomonas aeruginosa* isolated from different sites of infection. *International Journal of Pharmaceutical Quality Assurance*, *10*(02), 334-341.

References

- Bunyan, I. A., Naji, S. S., & Aljodaa, H. H. (2018). Molecular study of adhesive properties in some bacteria isolated from throat infections.
- Burkert, J. F. M., Maugeri, F., & Rodrigues, M. I. (2004). Optimization of extracellular lipase production by *Geotrichum* spp. using factorial design. *Bioresource technology*, *91*(1), 77-84.
- Cárdenas, A., Neave, M. J., Haroon, M. F., Pogoreutz, C., Rådecker, N., Wild, C., & Voolstra, C. R. (2018). Excess labile carbon promotes the expression of virulence factors in coral reef bacterioplankton. *The ISME journal*, *12*(1), 59-76.
- Casals, C., Campanero-Rhodes, M. A., García-Fojeda, B., & Solís, D. (2018). The role of collectins and galectins in lung innate immune defense. *Frontiers in immunology*, *9*, 1998.
- Catalán-Nájera, J. C., Garza-Ramos, U., & Barrios-Camacho, H. (2017). Hypervirulence and hypermucoviscosity: two different but complementary *Klebsiella* spp. phenotypes. *Virulence*, *8*(7), 1111-1123.
- Chandra, P., Singh, R., & Arora, P. K. (2020). Microbial lipases and their industrial applications: a comprehensive review. *Microbial Cell Factories*, *19*(1), 169.
- Chang, Y. C., & Nizet, V. (2020). Siglecs at the Host–Pathogen Interface. In *Lectin in Host Defense Against Microbial Infections* (pp. 197-214). Springer, Singapore.
- Charles, F. R., Lim, J. X., Chen, H., Goh, S. G., He, Y., & Gin, K. Y. H. (2022). Prevalence and characterization of antibiotic resistant bacteria in raw community sewage from diverse urban communities. *Science of the Total Environment*, *825*, 153926.

- Chen, L., Wilksch, J. J., Liu, H., Zhang, X., Torres, V. V., Bi, W., & Zhou, T. (2020). Investigation of LuxS-mediated quorum sensing in *Klebsiella pneumoniae*. *Journal of medical microbiology*, 69(3), 402.
- Choby, J. E., Howard-Anderson, J., & Weiss, D. S. (2020). Hypervirulent *Klebsiella pneumoniae*—clinical and molecular perspectives. *Journal of internal medicine*, 287(3), 283-300.
- Choudhary, P., Singh, S., & Agarwal, V. (2020). Microbial Biofilms. In *Bacterial Biofilms*. IntechOpen.
- Christensen, L. V., & Radue, J. T. (1985). Lateral preference in mastication: an electromyographic study. *Journal of Oral Rehabilitation*, 12(5), 429-434.
- Christodoulides, M. (2013). A history of bacterial meningitis from antiquity to modern times. *Meningitis: cellular and molecular basis. Advances in molecular and cellular microbiology*, 26, 1-16.
- Cillóniz, C., Dominedò, C., & Torres, A. (2019). Multidrug resistant gram-negative bacteria in community-acquired pneumonia. *Annual Update in Intensive Care and Emergency Medicine 2019*, 459-475.
- Clegg, S., & Murphy, C. N. (2017). Epidemiology and virulence of *Klebsiella pneumoniae*. *Urinary Tract Infections: Molecular Pathogenesis and Clinical Management*, 435-457.
- Colagiorgi, A., Di Ciccio, P., Zanardi, E., Ghidini, S., & Ianieri, A. (2016). A look inside the *Listeria monocytogenes* biofilms extracellular matrix. *Microorganisms*, 4(3), 22.
- Cole, J. N., & Nizet, V. (2016). Bacterial evasion of host antimicrobial peptide defenses. *Virulence Mechanisms of Bacterial Pathogens*, 413-443.

- Collee, J. G., Fraser A. G., Marmino B. P. and Simons A. (1996). Mackie and McCartney Practical Medical Microbiology. 14thEd. The Churchill Livingstone, Inc. USA.
- Conover, M. S., Hadjifrangiskou, M., Palermo, J. J., Hibbing, M. E., Dodson, K. W., & Hultgren, S. J. (2016). Metabolic requirements of *Escherichia coli* in intracellular bacterial communities during urinary tract infection pathogenesis. *MBio*, 7(2).
- Corcoran, M. L., Stetler-Stevenson, W. G., Brown, P. D., & Wahl, L. M. (1992). Interleukin 4 inhibition of prostaglandin E2 synthesis blocks interstitial collagenase and 92-kDa type IV collagenase/gelatinase production by human monocytes. *Journal of Biological Chemistry*, 267(1), 515-519.
- Costa, D. T. D. (2019). Virulence Determinants and Antibiotic Resistance of Extended-Spectrum Beta-lactamase (ESBL) Producing *Klebsiella pneumoniae* Isolated from Hospital Environment (Doctoral dissertation, Brac University).
- Coughlan, L. M., Cotter, P. D., Hill, C., & Alvarez-Ordóñez, A. (2016). New weapons to fight old enemies: novel strategies for the (bio) control of bacterial biofilms in the food industry. *Frontiers in microbiology*, 7, 1641.
- Cubero, M., Marti, S., Domínguez, M. Á., González-Díaz, A., Berbel, D., & Ardanuy, C. (2019). Hypervirulent *Klebsiella pneumoniae* serotype K1 clinical isolates form robust biofilms at the air-liquid interface. *PLoS one*, 14(9), e0222628.
- Cusini, A., Herren, D., Bütikofer, L., Plüss-Suard, C., Kronenberg, A., & Marschall, J. (2018). Intra-hospital differences in antibiotic use correlate with antimicrobial resistance rate in *Escherichia coli* and *Klebsiella*

- pneumoniae*: a retrospective observational study. *Antimicrobial Resistance & Infection Control*, 7(1), 1-11.
- D'Angelo, R. G., Johnson, J. K., Bork, J. T., & Heil, E. L. (2016). Treatment options for extended-spectrum beta-lactamase (ESBL) and AmpC-producing bacteria. *Expert opinion on pharmacotherapy*, 17(7), 953-967.
- Da Costa de Souza, G., Roque-Borda, C. A., & Pavan, F. R. (2022). Beta-lactam resistance and the effectiveness of antimicrobial peptides against KPC-producing bacteria. *Drug Development Research*, 83(7), 1534-1554.
- Dai, P., & Hu, D. (2022). The making of hypervirulent *Klebsiella pneumoniae*. *Journal of Clinical Laboratory Analysis*, 36(12), e24743.
- Darby, E. M., Trampari, E., Siasat, P., Gaya, M. S., Alav, I., Webber, M. A., & Blair, J. M. (2022). Molecular mechanisms of antibiotic resistance revisited. *Nature Reviews Microbiology*, 1-16.
- David, S., Reuter, S., Harris, S. R., Glasner, C., Feltwell, T., Argimon, S., & Aspbury, M. (2019). Epidemic of carbapenem-resistant *Klebsiella pneumoniae* in Europe is driven by nosocomial spread. *Nature microbiology*, 4(11), 1919-1929.
- Davies, J. A., Anderson, G. K., Beveridge, T. J., & Clark, H. C. (1983). Chemical mechanism of the Gram stain and synthesis of a new electron-opaque marker for electron microscopy which replaces the iodine mordant of the stain. *Journal of bacteriology*, 156(2), 837-845.
- Davies, Y. M., Cunha, M. P. V., Oliveira, M. G. X., Oliveira, M. C. V., Philadelpho, N., Romero, D. C., & Knöbl, T. (2016). Virulence and

- antimicrobial resistance of *Klebsiella pneumoniae* isolated from passerine and psittacine birds. *Avian Pathology*, 45(2), 194-201.
- De Araújo, L. C. A., da Purificacao-Junior, A. F., da Silva, S. M., Lopes, A. C. S., Veras, D. L., Alves, L. C., ... & de Oliveira, M. B. M. (2019). In vitro evaluation of mercury (Hg^{2+}) effects on biofilm formation by clinical and environmental isolates of *Klebsiella pneumoniae*. *Ecotoxicology and Environmental Safety*, 169, 669-677.
- De Jesus, M. B., Ehlers, M. M., Dos Santos, R. F., & Kock, M. M. (2015). Understanding β -lactamase producing *Klebsiella pneumoniae*. *Antimicrobial Resistance: An Open Challenge*, 51.
- Del Pozo, J. L. (2018). Biofilm-related disease. *Expert review of anti-infective therapy*, 16(1), 51-65.
- Delcaru, C., Alexandru, I., Podgoreanu, P., Grosu, M., Stavropoulos, E., Chifiriuc, M. C., & Lazar, V. (2016). Microbial biofilms in urinary tract infections and prostatitis: etiology, pathogenicity, and combating strategies. *Pathogens*, 5(4), 65.
- Derakhshan, S., Peerayeh, S. N., and Bakhshi, B. (2016). Association between presence of virulence genes and antibiotic resistance in clinical *Klebsiella Pneumoniae* isolates. *Lab. Med.* 47, 306–311.
- Devanathan, K., Sivaraman, U., Subramaniam, P., & Easow, J. (2022). Correlation of drug resistance pattern with Lipase Production in clinical isolates of *Klebsiella pneumoniae*.
- Devanga Ragupathi, N. K., Muthuirulandi Sethuvel, D. P., Triplicane Dwarakanathan, H., Murugan, D., Umashankar, Y., Monk, P. N., & Veeraraghavan, B. (2020). The influence of biofilms on carbapenem

- susceptibility and patient outcome in device associated *K. pneumoniae* infections: insights into phenotype vs. genome-wide analysis and correlation. *Frontiers in microbiology*, *11*, 591679.
- Di Domenico, E. G., Farulla, I., Prignano, G., Gallo, M. T., Vespaziani, M., Cavallo, I., & De Santis, A. (2017). Biofilm is a major virulence determinant in bacterial colonization of chronic skin ulcers independently from the multidrug resistant phenotype. *International journal of molecular sciences*, *18*(5), 1077.
- Doorduyn, D. J., Rooijackers, S. H., van Schaik, W., & Bardoel, B. W. (2016). Complement resistance mechanisms of *Klebsiella pneumoniae*. *Immunobiology*, *221*(10), 1102-1109.
- Dos Anjos, C., Sabino, C. P., Sellera, F. P., Esposito, F., Pogliani, F. C., & Lincopan, N. (2020). Hypervirulent and hypermucoviscous strains of *Klebsiella pneumoniae* challenged by antimicrobial strategies using visible light. *International journal of antimicrobial agents*, *56*(1), 106025.
- Dowling, A., O'dwyer, J., & Adley, C. (2017). Antibiotics: mode of action and mechanisms of resistance. *Antimicrobial research: Novel bioknowledge and educational programs*, *1*, 536-545.
- Duan, Q., Wang, Q., Sun, S., Cui, Q., Ding, Q., Wang, R., & Wang, H. (2022). ST11 Carbapenem-Resistant *Klebsiella pneumoniae* Clone Harboring bla_{NDM} Replaced a bla_{KPC} Clone in a Tertiary Hospital in China. *Antibiotics*, *11*(10), 1373.
- Effah, C. Y., Sun, T., Liu, S., & Wu, Y. (2020). *Klebsiella pneumoniae*: an increasing threat to public health. *Annals of clinical microbiology and antimicrobials*, *19*(1), 1-9.

- El-Badawy, M. F., El-Far, S. W., Althobaiti, S. S., Abou-Elazm, F. I., & Shohayeb, M. M. (2020). The First Egyptian report showing the co-existence of bla_{NDM-25}, bla_{OXA-23}, bla_{OXA-181}, and bla_{GES-1} among carbapenem-resistant *K. pneumoniae* clinical isolates genotyped by BOX-PCR. *Infection and Drug Resistance*, 1237-1250.
- Elliott, R. B., Escobar, L., Tan, P. L., Muzina, M., Zwain, S., & Buchanan, C. (2007). Live encapsulated porcine islets from a type 1 diabetic patient 9.5 yr after xeno transplantation. *Xenotransplantation*, 14(2), 157-161.
- Fajfr, M., Louda, M., Paterová, P., Ryšková, L., Pacovský, J., Košina, J., & Broďák, M. (2017). The susceptibility to fosfomycin of Gram-negative bacteria isolates from urinary tract infection in the Czech Republic: data from a unicentric study. *BMC urology*, 17, 1-6.
- FarajzadehSheikh, A., Veisi, H., Shahin, M., Getso, M., & Farahani, A. (2019). Frequency of quinolone resistance genes among extended-spectrum β -lactamase (ESBL)-producing *Escherichia coli* strains isolated from urinary tract infections. *Tropical Medicine and Health*, 47(1), 19.
- Fatima, S., Faryad, A., Ataa, A., Joyia, F. A., & Parvaiz, A. (2021). Microbial lipase production: A deep insight into the recent advances of lipase production and purification techniques. *Biotechnology and Applied Biochemistry*, 68(3), 445-458.
- Fernández-Martínez, M., Ruiz del Castillo, B., Lecea-Cuello, M. J., Rodríguez-Baño, J., Pascual, Á., Martínez-Martínez, L., (2018). Spanish Network for the Research in Infectious Diseases (REIPI) and the Spanish Group for Nosocomial Infections (GEIH). Prevalence of aminoglycoside-modifying enzymes in *Escherichia coli* and *Klebsiella pneumoniae*

- producing extended spectrum β -lactamases collected in two multicenter studies in Spain. *Microbial Drug Resistance*, 24(4), 367-376.
- Follador, R., Heinz, E., Wyres, K. L., Ellington, M. J., Kowarik, M., Holt, K. E., & Thomson, N. R. (2016). The diversity of *Klebsiella pneumoniae* surface polysaccharides. *Microbial genomics*, 2(8).
- Forbes, B. A., Sahm, D. F. and Weissfeld, A.S. (2007). Bailey and Scott's Diagnostic Microbiology. 12th Ed. Mosby. USA.
- Forsythe, S. (2018). Microbial Source Tracking of *Cronobacter* spp. In *Advances in applied microbiology* (Vol. 103, pp. 49-101). Academic Press.
- Fu, L., Huang, M., Zhang, X., Yang, X., Liu, Y., Zhang, L., & Zhou, Y. (2018). Frequency of virulence factors in high biofilm formation blaKPC-2 producing *Klebsiella pneumoniae* strains from hospitals. *Microbial pathogenesis*, 116, 168-172.
- Fu, Y., Xu, M., Liu, Y., Li, A., & Zhou, J. (2019). Virulence and genomic features of a bla_{CTX-M-3} and bla_{CTX-M-14} coharboring hypermucoviscous *Klebsiella pneumoniae* of serotype K2 and ST65. *Infection and drug resistance*, 12, 145.
- Fuhrmann, J. J. (2021). Microbial metabolism. In *Principles and applications of soil microbiology* (pp. 57-87). Elsevier.
- Gao, L., Lv, Y., & Li, Y. (2020). Analysis of the drug resistance of carbapenem-resistant *Klebsiella pneumoniae* in the China antimicrobial resistance surveillance trial program, 2007–2018. *Microbial Drug Resistance*, 26(8), 944-950.

References

- Gato, E., Vázquez-Ucha, J. C., Rumbo-Feal, S., Álvarez-Fraga, L., Vallejo, J. A., Martínez-Gutián, M., & Pérez, A. (2020). Kpi, a chaperone-usher pili system associated with the worldwide-disseminated high-risk clone *Klebsiella pneumoniae* ST-15. *Proceedings of the National Academy of Sciences*, *117*(29), 17249-17259.
- Gebreyohannes, G., Nyerere, A., Bii, C., & Sbhatu, D. B. (2019). Challenges of intervention, treatment, and antibiotic resistance of biofilm-forming microorganisms. *Heliyon*, *5*(8), e02192.
- George, D., & Mallery, P. (2019). IBM SPSS statistics 26 step by step: A simple guide and reference. Routledge.
- Gharrah, M. M., Mostafa El-Mahdy, A., & Barwa, R. F. (2017). Association between virulence factors and extended spectrum beta-lactamase producing *Klebsiella pneumoniae* compared to nonproducing isolates. *Interdisciplinary Perspectives on Infectious Diseases*, 2017.
- Ghequire, M. G., & Öztürk, B. (2018). A colicin M-type bacteriocin from *Pseudomonas aeruginosa* targeting the HxuC heme receptor requires a novel immunity partner. *Applied and environmental microbiology*, *84*(18).
- Ghigo, J. M., Valle, J., & Da Re, S. (2017). *U.S. Patent No. 9,603,979*. Washington, DC: U.S. Patent and Trademark Office.
- Giannini, S., Falet, H., & Hoffmeister, K. (2019). Platelet glycobiochemistry and the control of platelet function and lifespan. In *Platelets* (pp. 79-97). Academic Press.
- Giddins, M. J., Macesic, N., Annavajhala, M. K., Stump, S., Khan, S., McConville, T. H., & Uhlemann, A. C. (2018). Successive emergence of

- ceftazidime-avibactam resistance through distinct genomic adaptations in bla KPC-2-harboring *Klebsiella pneumoniae* sequence type 307 isolates. *Antimicrobial agents and chemotherapy*, 62(3), e02101-17.
- Gopichand, P., Agarwal, G., Natarajan, M., Mandal, J., Deepanjali, S., Parameswaran, S., & Dorairajan, L. N. (2019). *In vitro* effect of fosfomycin on multi-drug resistant Gram-negative bacteria causing urinary tract infections. *Infection and drug resistance*, 2005-2013.
- Green, M. R., & Sambrook, J. (2012). *A Laboratory Manual*. John Inglis, (2012).
- Greene, C., Wu, J., Rickard, A. H., & Xi, C. (2016). Evaluation of the ability of *Acinetobacter baumannii* to form biofilms on six different biomedical relevant surfaces. *Letters in applied microbiology*, 63(4), 233-239.
- Grézal, G., Spohn, R., Méhi, O., Dunai, A., Lázár, V., Bálint, B., & Papp, B. (2023). Plasticity and stereotypic rewiring of the transcriptome upon bacterial evolution of antibiotic resistance. *Molecular Biology and Evolution*, msad020.
- Guo, Y., Wang, S., Zhan, L., Jin, Y., Duan, J., Hao, Z., ... & Yu, F. (2017). Microbiological and clinical characteristics of hypermucoviscous *Klebsiella pneumoniae* isolates associated with invasive infections in China. *Frontiers in cellular and infection microbiology*, 7, 24.
- Gursky, O. (2020). Structural basis for vital function and malfunction of serum amyloid a: an acute-phase protein that wears hydrophobicity on its sleeve. *Current Atherosclerosis Reports*, 22(11), 1-11.
- Hadjineophytou, C., Anonsen, J. H., Wang, N., Ma, K. C., Viburiene, R., Vik, Å., & Koomey, M. (2019). Genetic determinants of genus-level glycan

References

- diversity in a bacterial protein glycosylation system. *PLoS genetics*, *15*(12), e1008532.
- Haider, A. (2016). Identification of Bacteriocin Produced by *Klebsiella pneumoniae* (Doctoral dissertation, University of Lincoln).
- Hancock, R. E., Alford, M. A., & Haney, E. F. (2021). Antibiofilm activity of host defence peptides: Complexity provides opportunities. *Nature Reviews Microbiology*, *19*(12), 786-797.
- Hansen, G. T. (2021). Continuous evolution: perspective on the epidemiology of carbapenemase resistance among Enterobacterales and other Gram-negative bacteria. *Infectious Diseases and Therapy*, *10*, 75-92.
- Hao, Z., Duan, J., Liu, L., Shen, X., Yu, J., Guo, Y., & Yu, F. (2020). Prevalence of Community-Acquired, Hypervirulent *Klebsiella pneumoniae* Isolates in Wenzhou, China. *Microbial Drug Resistance*, *26*(1), 21-27.
- Haque, S., Ahmad, F., Dar, S. A., Jawed, A., Mandal, R. K., Wahid, M., & Akhter, N. (2018). Developments in strategies for Quorum Sensing virulence factor inhibition to combat bacterial drug resistance. *Microbial pathogenesis*, *121*, 293-302.
- Harada, S., Ishii, Y., Saga, T., Aoki, K., & Tateda, K. (2018). Molecular epidemiology of *Klebsiella pneumoniae* K1 and K2 isolates in Japan. *Diagnostic microbiology and infectious disease*, *91*(4), 354-359.
- Harder, M. J., Kuhn, N., Schrezenmeier, H., Höchsmann, B., von Zabern, I., Weinstock, C., & Anliker, M. (2017). Incomplete inhibition by eculizumab: mechanistic evidence for residual C5 activity during strong complement activation. *Blood*, *129*(8), 970-980.

- Hartman, L. J., Selby, E. B., Whitehouse, C. A., Coyne, S. R., Jaissle, J. G., Twenhafel, N. A., & Kulesh, D. A. (2009). Rapid real-time PCR assays for detection of *Klebsiella pneumoniae* with the *rmpA* or *magA* genes associated with the hypermucoviscosity phenotype: screening of nonhuman primates. *The Journal of Molecular Diagnostics*, *11*(5), 464-471.
- Hasan, N. A., Nawahwi, M. Z., Yahya, N., & Othman, N. A. (2018). Identification and optimization of lipase producing bacteria from palm oil contaminated waste. *Journal of Fundamental and Applied Sciences*, *10*(2S), 300-310.
- Hasan, T. H., Shlash, S., Jasim, S., Hussein, E. F., Alasedi, K. K., & Aljanaby, A. A. (2021a). The epidemiology of *Klebsiella pneumoniae*: A review. *Annals of the Romanian Society for Cell Biology*, 8848-8860.
- Hasan, T., Alasedi, K., & Aljanaby, A. (2021b). A comparative study of prevalence antimicrobials resistance *klebsiella pneumoniae* among different pathogenic bacteria isolated from patients with urinary tract infection in Al-Najaf City, Iraq. *Latin american journal of pharmacy*, *40*, 174-8.
- Hauser, A. R., Meccas, J., & Moir, D. T. (2016). Beyond antibiotics: new therapeutic approaches for bacterial infections. *Clinical Infectious Diseases*, *63*(1), 89-95.
- Heiden, S. E., Hübner, N. O., Bohnert, J. A., Heidecke, C. D., Kramer, A., Balau, V., & Schaufler, K. (2020). A *Klebsiella pneumoniae* ST307 outbreak clone from Germany demonstrates features of extensive drug resistance, hypermucoviscosity, and enhanced iron acquisition. *Genome Medicine*, *12*, 1-15.

- Henderson, P. J., Maher, C., Elbourne, L. D., Eijkelkamp, B. A., Paulsen, I. T., & Hassan, K. A. (2021). Physiological functions of bacterial “multidrug” efflux pumps. *Chemical reviews*, *121*(9), 5417-5478.
- Hessan, H. S. (2021). Phenotypic detection of adhesive activity and biofilm formation among *Prevotella* spp. isolated from patients suffering from acute inflammation in root canal teeth. *Review of International Geographical Education Online*, *11*(12).
- Hossain, M. A. (2019). Determination of Bacterial and Viral Pathogen Spectra and Identification of Multi Drugs Resistance Gene *ctx-M1* in *Klebsiella pneumoniae* Isolated from Acute Respiratory Infections Children Aged Under-5 from Two Hospital Settings of Dhaka City (Doctoral dissertation, Brac University).
- Hou, M., Chen, N., Dong, L., Fang, Y., Pan, R., Wang, W., & Dong, H. (2022). Molecular epidemiology, clinical characteristics and risk factors for bloodstream infection of multidrug-resistant *Klebsiella pneumoniae* infections in pediatric patients from Tianjin, China. *Infection and Drug Resistance*, 7015-7023.
- Hu, Y., Anes, J., Devineau, S., & Fanning, S. (2020). *Klebsiella pneumoniae*: Prevalence, Reservoirs, Antimicrobial Resistance, Pathogenicity, and Infection: A Hitherto Unrecognized Zoonotic Bacterium. *Foodborne Pathogens and Disease*.
- Huszczynski, S. M., Lam, J. S., & Khursigara, C. M. (2020). The role of *Pseudomonas aeruginosa* lipopolysaccharide in bacterial pathogenesis and physiology. *Pathogens*, *9*(1), 6.
- Iliyasu, M. Y., Mustapha, I., Yakubu, H., Shuaibu, H. M., Umar, A. F., Agbo, E. B., & Deeni, Y. Y. (2020). Genotypic detection and characterization of

- adhesins in clinical *Escherichia coli* isolates. *Microbiology Research Journal International*, 84-93.
- Jagessar, K. L. (2020). *Structural Dynamics of H⁺/Drug Antiport in an Archaeal Mate Transporter* (Doctoral dissertation, Vanderbilt University).
- Jahan, F. (2018). Phosphorylation of the α -and β -chains of LFA-1 regulates its interaction with cytoplasmic proteins and crosstalk to VLA-4 integrin. *Dissertationes Scholae Doctoralis Ad Sanitatem Investigandam Universitatis Helsinkiensis*.
- Jeffs, M. A., & Lohans, C. T. (2022). Inhibiting the metallo- β -lactamases: Challenges and strategies to overcome bacterial β -lactam resistance. *Future Medicinal Chemistry*, 14(14), 1021-1025.
- Jian-Li, W., Yuan-Yuan, S., Shou-Yu, G., Fei-Fei, D., Jia-Yu, Y., Xue-Hua, W., & Zhi-Jing, X. (2017). Serotype and virulence genes of *Klebsiella pneumoniae* isolated from mink and its pathogenesis in mice and mink. *Scientific reports*, 7(1), 1-7.
- Joey, F. L. (2011). *On the Homotopy Perturbation Method and its Applications* (Doctoral dissertation, Ministry of Higher Education).
- Jubeh, B., Breijyeh, Z., & Karaman, R. (2020). Resistance of gram-positive bacteria to current antibacterial agents and overcoming approaches. *Molecules*, 25(12), 2888.
- Kadhim, N. J., Al-Janabi, H. S., & Kadhim, M. J. (2020). Molecular detection of Virulence Factors genes Associated with Immune Resistance in *Klebsiella pneumoniae*. *Medico Legal Update*, 20(3), 1459-1465.

- Kadhun, F. M., Hussain, A. A., & Al-Shaibani, A. B. (2019). Isolation and identification of protease producer bacterial isolated from diabetic foot ulcer. *Journal of Pharmaceutical Sciences and Research*, *11*(8), 2986-2991.
- Karakonstantis, S., Kritsotakis, E. I., & Gikas, A. (2020). Treatment options for *K. pneumoniae*, *P. aeruginosa* and *A. baumannii* co-resistant to carbapenems, aminoglycosides, polymyxins and tigecycline: an approach based on the mechanisms of resistance to carbapenems. *Infection*, *48*(6), 835-851.
- Karlowsky, J. A., Lob, S. H., DeRyke, C. A., Siddiqui, F., Young, K., Motyl, M. R., & Sahm, D. F. (2022). Prevalence of ESBL non-CRE *Escherichia coli* and *Klebsiella pneumoniae* among clinical isolates collected by the SMART global surveillance programme from 2015 to 2019. *International Journal of Antimicrobial Agents*, *59*(3), 106535.
- Karuniawati, A., Saharman, Y. R., & Lestari, D. C. (2013). Detection of carbapenemase encoding genes in *Enterobacteriaceae*, *Pseudomonas aeruginosa*, and *Acinetobacter baumannii* isolated from patients at Intensive Care Unit Cipto Mangunkusumo Hospital in 2011. *Acta Med Indones*, *45*(2), 101-6.
- Karygianni, L., Ren, Z., Koo, H., & Thurnheer, T. (2020). Biofilm matrixome: extracellular components in structured microbial communities. *Trends in Microbiology*, *28*(8), 668-681.
- Kateete, D. P., Nakanjako, R., Namugenyi, J., Erume, J., Joloba, M. L., & Najjuka, C. F. (2016). Carbapenem resistant *Pseudomonas aeruginosa* and *Acinetobacter baumannii* at Mulago hospital in Kampala, Uganda (2007–2009). *Springerplus*, *5*, 1-11.

- Kennedy, T. C., Proudfoot, S. P., Piantadosi, S., Wu, L., Saccomanno, G., Petty, T. L., & Tockman, M. S. (1999). Efficacy of two sputum collection techniques in patients with air flow obstruction. *Acta cytologica*, *43*(4), 630.
- Khaertynov, K. S., Anokhin, V. A., Rizvanov, A. A., Davidyuk, Y. N., Semyenova, D. R., Lubin, S. A., & Skvortsova, N. N. (2018). Virulence factors and antibiotic resistance of *Klebsiella pneumoniae* strains isolated from neonates with sepsis. *Frontiers in medicine*, *5*, 225.
- Khan, M. S. A., Altaf, M. M., & Ahmad, I. (2017). Chemical nature of biofilm matrix and its significance. *Biofilms in plant and soil health*, 151-177.
- Khatoon, Z., McTiernan, C. D., Suuronen, E. J., Mah, T. F., & Alarcon, E. I. (2018). Bacterial biofilm formation on implantable devices and approaches to its treatment and prevention. *Heliyon*, *4*(12), e01067.
- Khelissa, S. O., Abdallah, M., Jama, C., Faille, C., & Chihib, N. E. (2017). Bacterial contamination and biofilm formation on abiotic surfaces and strategies to overcome their persistence. *J. Mater. Environ. Sci*, *8*, 3326-3346.
- Kim, Y. J., Kim, S. I., Kim, Y. R., Wie, S. H., Lee, H. K., Kim, S. Y., & Park, Y. J. (2017). Virulence factors and clinical patterns of hypermucoviscous *Klebsiella pneumoniae* isolated from urine. *Infectious Diseases*, *49*(3), 178-184.
- Kırmusaoğlu, S. (2016). Staphylococcal biofilms: pathogenicity, mechanism and regulation of biofilm formation by quorum-sensing system and antibiotic resistance mechanisms of biofilm-embedded microorganisms. *Microbial Biofilms-Importance and Applications*. Dhanasekaran D, Thajuddin N, editors. Intech, Croatia, 189-209.

- Knight, G. M., Dyakova, E., Mookerjee, S., Davies, F., Brannigan, E. T., Otter, J. A., & Holmes, A. H. (2018). Fast and expensive (PCR) or cheap and slow (culture)? A mathematical modelling study to explore screening for carbapenem resistance in UK hospitals. *BMC medicine*, *16*(1), 141.
- Kontturi, M. (2020). Interdigital phlegmon in Finnish dairy herds. *Dissertationes Scholae Doctoralis Ad Sanitatem Investigandam Universitatis Helsinkiensis*.
- Kreuder, A. J. (2016). Investigation of the gallbladder host environment and small RNAs in the pathobiology of *Campylobacter jejuni* sheep abortion clone IA 3902.
- Krzyżewska-Dudek, E., Kotimaa, J., Kapczyńska, K., Rybka, J., & Meri, S. (2022). Lipopolysaccharides and outer membrane proteins as main structures involved in complement evasion strategies of non-typhoidal *Salmonella* strains. *Molecular Immunology*, *150*, 67-77.
- Ku, Y. H., Chen, C. C., Lee, M. F., Chuang, Y. C., Tang, H. J., & Yu, W. L. (2017a). Comparison of synergism between colistin, fosfomycin and tigecycline against extended-spectrum β -lactamase-producing *Klebsiella pneumoniae* isolates or with carbapenem resistance. *Journal of Microbiology, Immunology and Infection*, *50*(6), 931-939.
- Ku, Y. H., Chuang, Y. C., Chen, C. C., Lee, M. F., Yang, Y. C., Tang, H. J., & Yu, W. L. (2017b). *Klebsiella pneumoniae* isolates from meningitis: epidemiology, virulence and antibiotic resistance. *Scientific reports*, *7*(1), 1-10.
- Kudinha, T. (2017). The pathogenesis of *Escherichia coli* urinary tract infection. *Escherichia coli—Recent Advances on Physiology, Pathogenesis and Biotechnological Applications. InTech*, 45-61.

- Kuss-Duerkop, S. K., & Kestra-Gounder, A. M. (2020). NOD1 and NOD2 Activation by diverse stimuli: a possible role for sensing pathogen-induced endoplasmic reticulum stress. *Infection and Immunity*, 88(7).
- Larsen, M. D., Quintana, M. D. P., Ditlev, S. B., Bayarri-Olmos, R., Ofori, M. F., Hviid, L., & Garred, P. (2019). Evasion of classical complement pathway activation on *Plasmodium falciparum*-infected erythrocytes opsonized by PfEMP1-specific IgG. *Frontiers in Immunology*, 9, 3088.
- Laventie, B. J., Sangermani, M., Estermann, F., Manfredi, P., Planes, R., Hug, I., & Jenal, U. (2019). A surface-induced asymmetric program promotes tissue colonization by *Pseudomonas aeruginosa*. *Cell host & microbe*, 25(1), 140-152.
- Le Fournis, C., Jeanneau, C., Roumani, S., Giraud, T., & About, I. (2020). Pulp fibroblast contribution to the local control of pulp inflammation via complement activation. *Journal of Endodontics*, 46(9), S26-S32.
- Lee, C. R., Lee, J. H., Park, K. S., Jeon, J. H., Kim, Y. B., Cha, C. J., ... & Lee, S. H. (2017). Antimicrobial resistance of hypervirulent *Klebsiella pneumoniae*: epidemiology, hypervirulence-associated determinants, and resistance mechanisms. *Frontiers in cellular and infection microbiology*, 7, 483.
- Lengerova, G. B. (2023). Evaluation of Modern Microbiological Methods for Rapid Identification of Microorganisms in Patients with Bacteremia and Fungemia Authors Summary (Doctoral dissertation, Medical University-Plovdiv).
- Letunic I, Bork, P. 2019. Interactive Tree Of Life (iTOL) v4: recent updates and new developments. *Nucleic Acids Res* 2; 47(W1): W256-W259.

- Li, B., & Webster, T. J. (2018). Bacteria antibiotic resistance: New challenges and opportunities for implant-associated orthopedic infections. *Journal of Orthopaedic Research®*, 36(1), 22-32.
- Lima, L. M., da Silva, B. N. M., Barbosa, G., & Barreiro, E. J. (2020). β -lactam antibiotics: An overview from a medicinal chemistry perspective. *European journal of medicinal chemistry*, 208, 112829.
- Lin, T. H., Tseng, C. Y., Lai, Y. C., Wu, C. C., Huang, C. F., & Lin, C. T. (2017). IscR regulation of type 3 fimbriae expression in *Klebsiella pneumoniae* CG43. *Frontiers in Microbiology*, 8, 1984.
- Lin, X., & Kück, U. (2022). Cephalosporins as key lead generation beta-lactam antibiotics. *Applied Microbiology and Biotechnology*, 1-14.
- Liu, C., & Guo, J. (2019). Hypervirulent *K. pneumoniae* (hypermucoviscous and aerobactin positive) infection over 6 years in the elderly in China: antimicrobial resistance patterns, molecular epidemiology and risk factor. *Annals of clinical microbiology and antimicrobials*, 18(1), 4.
- Liu, C., Shi, J., & Guo, J. (2018). High prevalence of hypervirulent *Klebsiella pneumoniae* infection in the genetic background of elderly patients in two teaching hospitals in China. *Infection and drug resistance*, 11, 1031.
- Liu, P. V. (1957). Survey of hemolysin production among species of *Pseudomonads*. *Journal of bacteriology*, 74(6), 718.
- Luo, M., Yang, S., Li, X., Liu, P., Xue, J., Zhou, X., & Li, Y. (2017). The KP1_4563 gene is regulated by the cAMP receptor protein and controls type 3 fimbrial function in *Klebsiella pneumoniae* NTUH-K2044. *PloS one*, 12(7), e0180666.

- M'lan-Britoh, A., Meité, S., Boni, C., Zaba, F., Koffi, K. S., Guessennd, N., & Dosso, M. (2018). First molecular investigation of capsular serotyping and hypervirulent (hvlp) of *K. Pneumoniae* in university hospital center of yopougon cote d'ivoire. *African Journal of Clinical and Experimental Microbiology*, *19*(1), 70-75.
- Mahamuni-Badiger, P. P., Patil, P. M., Badiger, M. V., Patel, P. R., Thorat-Gadgil, B. S., Pandit, A., & Bohara, R. A. (2020). Biofilm formation to inhibition: Role of zinc oxide-based nanoparticles. *Materials Science and Engineering: C*, *108*, 110319.
- Majkowska-Skrobek, G., Latka, A., Berisio, R., Squeglia, F., Maciejewska, B., Briers, Y., & Drulis-Kawa, Z. (2018). Phage-borne depolymerases decrease *Klebsiella pneumoniae* resistance to innate defense mechanisms. *Frontiers in microbiology*, *9*, 2517.
- Mandour, S. A. (2018). Epidemiological studies using biotyping, serotyping and bacteriocin typing as marker systems to identify clinical multidrug-resistant *Klebsiella* spp.
- Mandras, N., Roana, J., Comini, S., Cuffini, A., & Tullio, V. (2020). Antifungal properties of selected essential oils and pure compounds on emerging candida non-albicans species and uncommon pathogenic yeasts. In *Abstract Book* (pp. 45-45). Società Italiana di Microbiologia.
- Marimani, M., Ahmad, A., & Duse, A. (2018). The role of epigenetics, bacterial and host factors in progression of Mycobacterium tuberculosis infection. *Tuberculosis*, *113*, 200-214.
- Marques, C., Belas, A., Aboim, C., Cavaco-Silva, P., Trigueiro, G., Gama, L. T., & Pomba, C. (2019). Evidence of sharing of *Klebsiella pneumoniae*

References

- strains between healthy companion animals and cohabiting humans. *Journal of clinical microbiology*, 57(6).
- Marsh, J. W., Mustapha, M. M., Griffith, M. P., Evans, D. R., Ezeonwuka, C., Pasculle, A. W., & Harrison, L. H. (2019). Evolution of outbreak-causing carbapenem-resistant *Klebsiella pneumoniae* ST258 at a tertiary care hospital over 8 years. *MBio*, 10(5), e01945-19.
- Martens, E. C., Neumann, M., & Desai, M. S. (2018). Interactions of commensal and pathogenic microorganisms with the intestinal mucosal barrier. *Nature Reviews Microbiology*, 16(8), 457-470.
- Martin, R. M., & Bachman, M. A. (2018). Colonization, infection, and the accessory genome of *Klebsiella pneumoniae*. *Frontiers in cellular and infection microbiology*, 8, 4.
- Martin, R. M., Cao, J., Brisse, S., Passet, V., Wu, W., Zhao, L., & Bachman, M. A. (2016). Molecular epidemiology of colonizing and infecting isolates of *Klebsiella pneumoniae*. *Msphere*, 1(5).
- Martins, W. M., Nicolas, M. F., Yu, Y., Li, M., Dantas, P., Sands, K., & Andrey, D. O. (2020). Clinical and molecular description of a high-copy IncQ1 KPC-2 plasmid harbored by the international ST15 *Klebsiella pneumoniae* clone. *Msphere*, 5(5), e00756-20.
- Mathers, A. J., Peirano, G., & Pitout, J. D. (2015). The role of epidemic resistance plasmids and international high-risk clones in the spread of multidrug-resistant *Enterobacteriaceae*. *Clinical microbiology reviews*, 28(3), 565-591.
- Mathur, V. K., & Mathur, V. K. (2006). *U.S. Patent No. 7,048,900*. Washington, DC: U.S. Patent and Trademark Office.

- Mayumi, M., Okochi, K., & Nishioka, K. (1971). Detection of Australia antigen by means of immune adherence haemagglutination test. *Vox sanguinis*, *20*(2), 178-81.
- McFadden, J. F. (2000). *Biochemical Tests for the Identification of Medical Bacteria*. 3rd Ed. The Williams and Wilkins- Baltimor, USA.
- Mendes, G., Ramalho, J. F., Bruschy-Fonseca, A., Lito, L., Duarte, A., Melo-Cristino, J., & Caneiras, C. (2022). Whole-genome sequencing enables molecular characterization of non-clonal group 258 high-risk clones (ST13, ST17, ST147 and ST307) among Carbapenem-resistant *Klebsiella pneumoniae* from a tertiary University Hospital Centre in Portugal. *Microorganisms*, *10*(2), 416.
- Messasma, Z., Aggoun, D., Houchi, S., Ourari, A., Ouennoughi, Y., Keffous, F., & Mahdadi, R. (2021). Biological activities, DFT calculations and docking of imines tetradentates ligands, derived from salicylaldehydic compounds as metallo-beta-lactamase inhibitors. *Journal of Molecular Structure*, *1228*, 129463.
- Michaelis, C., & Grohmann, E. (2023). Horizontal Gene Transfer of Antibiotic Resistance Genes in Biofilms. *Antibiotics*, *12*(2), 328.
- Miller, J. M., & Wright, J. W. (1982). Spot indole test: evaluation of four reagents. *Journal of clinical microbiology*, *15*(4), 589-592.
- Mirzaie, A., & Ranjbar, R. (2021). Antibiotic resistance, virulence-associated genes analysis and molecular typing of *Klebsiella pneumoniae* strains recovered from clinical samples. *AMB Express*, *11*, 1-11.

- Mishra, U. N., & Kandali, R. (2019). Plant lipases: A potential candidate for commercial exploitation. *Indian Journal of Agricultural Biochemistry*, 32(2), 123-131.
- Mitri, C., Xu, Z., Bardin, P., Corvol, H., Touqui, L., & Tabary, O. (2020). Novel anti-inflammatory approaches for cystic fibrosis lung disease: identification of molecular targets and design of innovative therapies. *Frontiers in Pharmacology*, 11.
- Monesh Babu, J., S Smiline Girija, A., Sankar Ganesh, P., & Vijayashree Priyadharsini, J. (2021). Distribution of Four Biofilm Associated Gene among *A. baumannii* by in Silico-PCR.
- Moon, D. C., Choi, J. H., Bobby, N., Kang, H. Y., Kim, S. J., Song, H. J., & Lim, S. K. (2022). Bacterial prevalence in skin, urine, diarrheal stool, and respiratory samples from dogs. *Microorganisms*, 10(8), 1668.
- Moore, N. M. (2017). Epidemiology and characterization of *Klebsiella pneumoniae* carbapenemase (KPC)-producing *Enterobacteriaceae* in Chicago long-term acute care hospitals (Doctoral dissertation, Rush University).
- Mora-Ochomogo, M., & Lohans, C. T. (2021). β -lactam antibiotic targets and resistance mechanisms: from covalent inhibitors to substrates. *RSC Medicinal Chemistry*, 12(10), 1623-1639.
- Møretrø, T., & Langsrud, S. (2017). Residential bacteria on surfaces in the food industry and their implications for food safety and quality. *Comprehensive reviews in food science and food safety*, 16(5), 1022-1041.

- Morgenroth-Rebin, J. (2023). Towards the Characterization of Putative Degradation Targets of *Klebsiella pneumoniae* Lon Protease by Quantitative Proteomics and in *vitro* Degradation Assays (Doctoral dissertation, University of Guelph).
- Moussa, A. A., Abdulahi Abdi, A., Awale, M. A., & Garba, B. (2021). Occurrence and phenotypic characterization of multidrug-resistant bacterial pathogens isolated from patients in a public hospital in Mogadishu, Somalia. *Infection and Drug Resistance*, 825-832.
- Mpelle, F. L., Ngoyi, E. N. O., Aimã, C., Nguimbi, E., Moyen, R., & Kobawila, S. C. (2019). First report of the types TEM, CTX-M, SHV and OXA-48 of beta-lactamases in *Escherichia coli*, from Brazzaville, Congo. *African Journal of Microbiology Research*, 13(8), 158-167.
- Muhammad, M. H., Idris, A. L., Fan, X., Guo, Y., Yu, Y., Jin, X., & Huang, T. (2020). Beyond risk: bacterial biofilms and their regulating approaches. *Frontiers in microbiology*, 11, 928.
- Munk, P., Brinch, C., Møller, F. D., Petersen, T. N., Hendriksen, R. S., Seyfarth, A. M., & Aarestrup, F. M. (2022). Genomic analysis of sewage from 101 countries reveals global landscape of antimicrobial resistance. *Nature Communications*, 13(1), 7251.
- Murase, K. (2022). Cytolysin A (ClyA): A bacterial virulence factor with potential applications in nanopore technology, vaccine development, and tumor therapy. *Toxins*, 14(2), 78.
- Nady, S., Abdel-Rahman, M., Sousa, S. A., LEITãO, J. H., Morad, M., & El-Hennamy, R. E. (2019). Differential effects of Th17 cytokines during the response of neutrophils to *Burkholderia cenocepacia* outer

- membrane protein A. *Central-european Journal of Immunology*, 44(4), 403.
- Namikawa, H., Oinuma, K. I., Sakiyama, A., Tsubouchi, T., Tahara, Y. O., Yamada, K., & Kakeya, H. (2019). Discovery of anti-mucoviscous activity of rifampicin and its potential as a candidate antivirulence agent against hypervirulent *Klebsiella pneumoniae*. *International journal of antimicrobial agents*, 54(2), 167-175.
- Navon-Venezia, S., Kondratyeva, K., & Carattoli, A. (2017). *Klebsiella pneumoniae*: a major worldwide source and shuttle for antibiotic resistance. *FEMS microbiology reviews*, 41(3), 252-275.
- Nekkab, N. (2018). Spread of Hospital-Acquired Infections and Emerging Multidrug Resistant *enterobacteriaceae* in Healthcare Networks: Assessment of the Role of Interfacility Patient Transfers on Infection Risks and Control Measures (Doctoral dissertation).
- Nibogora, C. (2020). Demographic Characteristics, Phenotypic and Genotypic Characterization of Antibiotic Resistant *Klebsiella pneumoniae* Isolated from Clinical Samples at the Nairobi Hospital, Kenya (Doctoral dissertation, JKUAT-COHES).
- Nicoletti, M. (2020). Past, present, and future of insect-borne diseases. *Insect-Borne Diseases in the 21st Century*, 1.
- Niederman, M. S., Baron, R. M., Bouadma, L., Calandra, T., Daneman, N., DeWaele, J., & Nair, G. B. (2021). Initial antimicrobial management of sepsis. *Critical Care*, 25, 1-11.
- Norsigian, C. J., Attia, H., Szubin, R., Yassin, A. S., Palsson, B. Ø., Aziz, R. K., & Monk, J. M. (2019). Comparative genome-scale metabolic modeling

- of metallo-beta-lactamase-producing multidrug-resistant *Klebsiella pneumoniae* clinical isolates. *Frontiers in cellular and infection microbiology*, 9, 161.
- O'brien, V. P., Hannan, T. J., Nielsen, H. V., & Hultgren, S. J. (2017). Drug and vaccine development for the treatment and prevention of urinary tract infections. *Urinary Tract Infections: Molecular Pathogenesis and Clinical Management*, 589-646.
- Ohalete, C. N. (2016). Extended Spectrum Beta-Lactamase-Producing Bacteria: Molecular Studies and Effects of Medicinal Plants (Doctoral dissertation, FUTO).
- Ojdana, D., Gutowska, A., Sacha, P., Majewski, P., Wieczorek, P., & Trynieszewska, E. (2019). Activity of ceftazidime-avibactam alone and in combination with ertapenem, fosfomycin, and tigecycline against carbapenemase-producing *Klebsiella pneumoniae*. *Microbial Drug Resistance*, 25(9), 1357-1364.
- Okoche, D., Asimwe, B. B., Katabazi, F. A., Kato, L., and Najjuka, C. F. (2015). Prevalence and characterization of carbapenem resistant *Enterobacteriaceae* isolated from mulago national referral hospital, Uganda. *PLoS One* 10:e0135745.
- Opoku-Temeng, C., Kobayashi, S. D., & DeLeo, F. R. (2019). *Klebsiella pneumoniae* capsule polysaccharide as a target for therapeutics and vaccines. *Computational and structural biotechnology journal*, 17, 1360-1366.
- Orazi, G., & O'Toole, G. A. (2019). "It Takes a Village": Mechanisms Underlying Antimicrobial Recalcitrance of Polymicrobial Biofilms. *Journal of bacteriology*, 202(1).

- Pacios, O., Fernández-García, L., Bleriot, I., Blasco, L., González-Bardanca, M., López, M., & Tomás, M. (2021). Enhanced antibacterial activity of repurposed mitomycin C and imipenem in combination with the lytic phage vB_KpnM-VAC13 against clinical isolates of *Klebsiella pneumoniae*. *Antimicrobial Agents and Chemotherapy*, *65*(9), e00900-21.
- Paczosa, M. K. (2017). High-Throughput Identification and Characterization of *Klebsiella pneumoniae* Virulence Determinants in the Lungs (Doctoral dissertation, Sackler School of Graduate Biomedical Sciences (Tufts University)).
- Paczosa, M. K., & Meccas, J. (2016). *Klebsiella pneumoniae*: going on the offense with a strong defense. *Microbiology and molecular biology reviews*, *80*(3), 629-661.
- Padmini, N., Ajilda, A. A. K., Sivakumar, N., & Selvakumar, G. (2017). Extended spectrum β -lactamase producing *Escherichia coli* and *Klebsiella pneumoniae*: critical tools for antibiotic resistance pattern. *Journal of basic microbiology*, *57*(6), 460-470.
- Page, M. G. (2019). The role of iron and siderophores in infection, and the development of siderophore antibiotics. *Clinical Infectious Diseases*, *69*(Supplement_7), S529-S537.
- Pal, A., Bhattacharjee, S., Saha, J., Sarkar, M., & Mandal, P. (2022). Bacterial survival strategies and responses under heavy metal stress: A comprehensive overview. *Critical Reviews in Microbiology*, *48*(3), 327-355.

- Palacios, M. (2017). Identification of Conserved *Klebsiella pneumoniae* Virulence Factors (Doctoral dissertation, The University of North Carolina at Chapel Hill).
- Palacios, M., Miner, T. A., Frederick, D. R., Sepulveda, V. E., Quinn, J. D., Walker, K. A., & Miller, V. L. (2018). Identification of two regulators of virulence that are conserved in *Klebsiella pneumoniae* classical and hypervirulent strains. *MBio*, 9(4).
- Palomares-Navarro, J. J., Bernal-Mercado, A. T., González-Aguilar, G. A., Ortega-Ramirez, L. A., Martínez-Téllez, M. A., & Ayala-Zavala, J. F. (2023). Antibiofilm action of plant terpenes in *Salmonella* strains: potential inhibitors of the synthesis of extracellular polymeric substances. *Pathogens*, 12(1), 35.
- Panjaitan, N. S. D., Horng, Y. T., Cheng, S. W., Chung, W. T., & Soo, P. C. (2019). EtcABC, a putative EII complex, regulates type 3 fimbriae via CRP-cAMP signaling in *Klebsiella pneumoniae*. *Frontiers in microbiology*, 10, 1558.
- Patel, D. S., Qi, Y., & Im, W. (2017). Modeling and simulation of bacterial outer membranes and interactions with membrane proteins. *Current Opinion in Structural Biology*, 43, 131-140.
- Paul, D., Verma, J., Banerjee, A., Konar, D., & Das, B. (2022). Antimicrobial Resistance Traits and Resistance Mechanisms in Bacterial Pathogens. *Antimicrobial Resistance: Underlying Mechanisms and Therapeutic Approaches*, 1-27.
- Peirano, G., Chen, L., Kreiswirth, B. N., & Pitout, J. D. (2020). Emerging antimicrobial-resistant high-risk *Klebsiella pneumoniae* clones ST307 and ST147. *Antimicrobial agents and chemotherapy*, 64(10), e01148-20.

- Pereira, J. G., Fernandes, J., Duarte, A. R., & Fernandes, S. M. (2022). β -lactam dosing in critical patients: a narrative review of optimal efficacy and the prevention of resistance and toxicity. *Antibiotics*, *11*(12), 1839.
- Pillai, D., & Kalasseril, S. G. (2022). Genetic diversity and prevalence of extended spectrum beta-lactamase producing *Escherichia coli* and *Klebsiella pneumoniae* in aquatic environment receiving untreated hospital effluents.
- Piruozi, A., Forouzandeh, H., Farahani, A., Forouzandeh, Z., Ahmadi, I., Abdizadeh, R., & Azadbakht, M. (2019). Investigating the Frequency of *Klebsiella* Infection and Drug Resistance among Inpatients and Outpatients Referring to Amir Al-Momenin Hospital, Gerash, Iran. *Gene, Cell and Tissue*, *6*(3).
- Pokorzynski, N. D., Thompson, C. C., & Carabeo, R. A. (2017). Ironing out the unconventional mechanisms of iron acquisition and gene regulation in *Chlamydia*. *Frontiers in Cellular and Infection Microbiology*, *7*, 394.
- Poomathi, N., Singh, S., Prakash, C., Subramanian, A., Sahay, R., Cinappan, A., & Ramakrishna, S. (2020). 3D printing in tissue engineering: a state of the art review of technologies and biomaterials. *Rapid Prototyping Journal*.
- Priyanka, A., Akshatha, K., Deekshit, V. K., Prarthana, J., & Akhila, D. S. (2020). *Klebsiella pneumoniae* Infections and Antimicrobial Drug Resistance. In *Model Organisms for Microbial Pathogenesis, Biofilm Formation and Antimicrobial Drug Discovery* (pp. 195-225). Springer, Singapore.
- Pruss, A., Kwiatkowski, P., Masiuk, H., Bilska, I., Giedrys-Kalemba, S., & Dołęgowska, B. (2022). Epidemiological Analysis of Extended-

- Spectrum β -Lactamase-Producing *Klebsiella pneumoniae* Outbreak in a Neonatal Clinic in Poland. *Antibiotics*, 12(1), 50.
- Rachid, D., & Ahmed, B. (2005). Effect of iron and growth inhibitors on siderophores production by *Pseudomonas fluorescens*. *African Journal of Biotechnology*, 4(7), 697-702.
- Radwanska, M., Chamekh, M., Vanhamme, L. U. C., Claes, F., Magez, S., Magnus, E., ... & Pays, E. (2002). The serum resistance-associated gene as a diagnostic tool for the detection of *Trypanosoma brucei rhodesiense*. *The American journal of tropical medicine and hygiene*, 67(6), 684-690.
- Rahman, J. (2017). Screening for Silver Resistant *silE* Gene in *Klebsiella pneumoniae* Isolated from Wound and Burn Patients (Doctoral dissertation, BRAC Univeristy).
- Rai, A. K., & Mitchell, A. M. (2020). Enterobacterial common antigen: synthesis and function of an enigmatic molecule. *MBio*, 11(4), e0191420.
- Rakotovao-Ravahatra, Z. D., Randriatsarafara, F. M., Rakotovao, A. L., & Rasamindrakotroka, A. (2020). A study of antibiotic resistance of extended-spectrum beta-lactamases producing *Enterobacteriaceae* and some their associated factors in the laboratory of the university Hospital of Befelatanana Antananarivo Madagascar. *World*, 3(3), 24-30.
- Ramos-Vivas, J., Chapartegui-González, I., Fernández-Martínez, M., González-Rico, C., Fortún, J., Escudero, R., & Fariñas, M. C. (2019). Biofilm formation by multidrug resistant *Enterobacteriaceae* strains isolated from solid organ transplant recipients. *Scientific reports*, 9(1), 1-10.

- Ramsay, S., Cowan, L., Davidson, J. M., Nanney, L., & Schultz, G. (2016). Wound samples: moving towards a standardised method of collection and analysis. *International wound journal*, *13*(5), 880-891.
- Rana, K. L., Kour, D., Yadav, A. N., Yadav, N., & Saxena, A. K. (2020). Agriculturally important microbial biofilms: Biodiversity, ecological significances, and biotechnological applications. In *New and Future Developments in Microbial Biotechnology and Bioengineering: Microbial Biofilms* (pp. 221-265). Elsevier.
- Remya, P. A., Shanthi, M., & Sekar, U. (2019). Characterisation of virulence genes associated with pathogenicity in *Klebsiella pneumoniae*. *Indian journal of medical microbiology*, *37*(2), 210.
- Remya, P., Shanthi, M., & Sekar, U. (2018). Occurrence and characterization of hyperviscous K1 and K2 serotype in *Klebsiella pneumoniae*. *Journal of laboratory physicians*, *10*(3), 283.
- Rendueles, O. (2020). Deciphering the role of the capsule of *Klebsiella pneumoniae* during pathogenesis: A cautionary tale. *Molecular Microbiology*, *113*(5), 883-888.
- Reyes Chacón, J. A. (2019). Characterization of mobile genetic elements in carbapenem resistant *Enterobacteriaceae* isolates from Ecuadorian Hospitals (Master's thesis, Quito).
- Riwu, K. H. P., Effendi, M. H., & Rantam, F. A. (2020). A Review of Extended Spectrum β -Lactamase (ESBL) Producing *Klebsiella pneumoniae* and Multidrug Resistant (MDR) on Companion Animals. *Systematic Reviews in Pharmacy*, *11*(7).

- Rocha, A. J., Barsottini, M. R. D. O., Rocha, R. R., Laurindo, M. V., Moraes, F. L. L. D., & Rocha, S. L. D. (2019). *Pseudomonas aeruginosa*: virulence factors and antibiotic resistance genes. *Brazilian Archives of Biology and Technology*, 62.
- Rostkowska, O. M., Kuthan, R., Burban, A., Salińska, J., Ciebiera, M., Młynarczyk, G., & Durlik, M. (2020). Analysis of susceptibility to selected antibiotics in *Klebsiella pneumoniae*, *Escherichia coli*, *Enterococcus faecalis* and *Enterococcus faecium* causing urinary tract infections in kidney transplant recipients over 8 years: single-center study. *Antibiotics*, 9(6), 284.
- Roy, A. (2018). Isolation and Characterization of Bacteriophage from Environmental Water Samples Specific for *K. pneumoniae* (Doctoral dissertation, BRAC Univeristy).
- Rufai, M. S., & Singh, N. (2015). Prevalence of Bacteria Found in Urinary Tract Infections (UTI) Among Hospitalized Patients with Tertiary Care Setting (Doctoral dissertation, Lovely Professional University).
- Said-Salman, I., Yassine, W., Rammal, A., Hneino, M., Yusef, H., & Moustafa, M. (2021). Effects of Wi-Fi Radiofrequency Radiation on Carbapenem-Resistant *Klebsiella pneumoniae*. *Bioelectromagnetics*, 42(7), 575-582.
- Samanta, S., Banerjee, J., Ali, K. M., Giri, B., & Dash, S. K. (2020). Biochemical characterization and antibiotic sensitivity profiling of uropathogenic bacterial strains isolated from urine sample of UTI patients. *Journal of Advanced Scientific Research*, 11(01 Suppl 1), 280-295.

- Sambrook, J., and Rusell, D. W. (2001). *Molecular Cloning. A Laboratory Manual*. Third ed. Cold Spring Harbor (NY): Cold Spring Harbor Laboratory Press, N.Y.
- Santos, R. S., Figueiredo, C., Azevedo, N. F., Braeckmans, K., & De Smedt, S. C. (2018). Nanomaterials and molecular transporters to overcome the bacterial envelope barrier: Towards advanced delivery of antibiotics. *Advanced drug delivery reviews*, *136*, 28-48.
- Sarhan, R. S, Hashim, H.O., Al-Shuhaib, M.B.S. (2020). The Gly152Val mutation possibly confers resistance to beta-lactam antibiotics in ovine *Staphylococcus aureus* isolates. *Open Vet. J.* *9*(4): 339-348.
- Sarowska, J., Futoma-Koloch, B., Jama-Kmiecik, A., Frej-Madrzak, M., Ksiazczyk, M., Bugla-Ploskonska, G., & Choroszy-Krol, I. (2019). Virulence factors, prevalence and potential transmission of extraintestinal pathogenic *Escherichia coli* isolated from different sources: recent reports. *Gut pathogens*, *11*, 1-16.
- Sathiya, M. (2018). Detection of Multidrug Resistance in *Klebsiella* Species by Phenotypic and Genotypic Methods in a Tertiary Care Hospital (Doctoral dissertation, Madras Medical College, Chennai).
- Sawa, T., Kooguchi, K., & Moriyama, K. (2020). Molecular diversity of extended-spectrum β -lactamases and carbapenemases, and antimicrobial resistance. *Journal of intensive care*, *8*, 1-13.
- Schiaffino, F., & Kosek, M. N. (2020). Intestinal and extra-intestinal manifestations of *Campylobacter* in the immunocompromised host. *Current Treatment Options in Infectious Diseases*, *12*, 361-374.

- Schilcher, K., & Horswill, A. R. (2020). Staphylococcal Biofilm Development: Structure, Regulation, and Treatment Strategies. *Microbiology and Molecular Biology Reviews*, *84*(3).
- Schroll, C., Barken, K. B., Krogfelt, K. A., & Struve, C. (2010). Role of type 1 and type 3 fimbriae in *Klebsiella pneumoniae* biofilm formation. *BMC microbiology*, *10*, 1-10.
- Scoffone, V. C., Trespidi, G., Barbieri, G., Irudal, S., Perrin, E., & Buroni, S. (2021). Role of RND efflux pumps in drug resistance of cystic fibrosis pathogens. *Antibiotics*, *10*(7), 863.
- Sendra, E., López Montesinos, I., Rodríguez-Alarcón, A., Du, J., Siverio-Parés, A., Arenas-Miras, M., & Gómez-Zorrilla, S. (2022). Comparative analysis of complicated urinary tract infections caused by extensively drug-resistant *Pseudomonas aeruginosa* and extended-spectrum β -lactamase-producing *Klebsiella pneumoniae*. *Antibiotics*, *11*(11), 1511.
- Seo, Y., Hwang, J., Lee, E., Kim, Y. J., Lee, K., Park, C., & Choi, J. (2018). Engineering copper nanoparticles synthesized on the surface of carbon nanotubes for anti-microbial and anti-biofilm application. *Nanoscale*, *10*(33), 15529-15544.
- Shadkam, S., Goli, H. R., Mirzaei, B., Gholami, M., & Ahanjan, M. (2021). Correlation between antimicrobial resistance and biofilm formation capability among *Klebsiella pneumoniae* strains isolated from hospitalized patients in Iran. *Annals of Clinical Microbiology and Antimicrobials*, *20*, 1-7.
- Shaikh, S., Fatima, J., Shakil, S., Rizvi, S. M. D., & Kamal, M. A. (2015). Antibiotic resistance and extended spectrum beta-lactamases: Types,

- epidemiology and treatment. *Saudi journal of biological sciences*, 22(1), 90-101.
- Shakib, P., Kalani, M. T., Ramazanzadeh, R., Ahmadi, A., & Rouhi, S. (2018). Molecular detection of virulence genes in *Klebsiella Pneumoniae* clinical isolates from Kurdistan Province, Iran. *Biomedical Research and Therapy*, 5(8), 2581-2589.
- Shankar, U., Jain, N., Mishra, S. K., Sharma, T. K., & Kumar, A. (2020). Conserved G-quadruplex motifs in gene promoter region reveals a novel therapeutic approach to target multi-drug resistance *Klebsiella pneumoniae*. *Frontiers in microbiology*, 11, 1269.
- Sharahi, J. Y., Azimi, T., Shariati, A., Safari, H., Tehrani, M. K., & Hashemi, A. (2019). Advanced strategies for combating bacterial biofilms. *Journal of cellular physiology*, 234(9), 14689-14708.
- Sharma, N., Sharma, N., Sharma, S., Sharma, P., & Devi, B. (2023). Identification, morphological, biochemical, and genetic characterization of microorganisms. In *Basic Biotechniques for Bioprocess and Bioentrepreneurship* (pp. 47-84). Academic Press.
- Shelenkov, A., Mikhaylova, Y., Yanushevich, Y., Samoilov, A., Petrova, L., Fomina, V., & Akimkin, V. (2020). Molecular typing, characterization of antimicrobial resistance, virulence profiling and analysis of whole-genome sequence of clinical *Klebsiella pneumoniae* isolates. *Antibiotics*, 9(5), 261.
- Sheu, C. C., Chang, Y. T., Lin, S. Y., Chen, Y. H., & Hsueh, P. R. (2019). Infections caused by carbapenem-resistant *Enterobacteriaceae*: an update on therapeutic options. *Frontiers in microbiology*, 10, 80.

- Short, F. L., Di Sario, G., Reichmann, N. T., Kleanthous, C., Parkhill, J., & Taylor, P. W. (2020). Genomic profiling reveals distinct routes to complement resistance in *Klebsiella pneumoniae*. *Infection and immunity*, *88*(8), e00043-20.
- Sillanpää, S., Kramna, L., Oikarinen, S., Sipilä, M., Rautiainen, M., Aittoniemi, J., & Cinek, O. (2017). Next-generation sequencing combined with specific PCR assays to determine the bacterial 16S rRNA gene profiles of middle ear fluid collected from children with acute otitis media. *Msphere*, *2*(2).
- Singha, P., Locklin, J., & Handa, H. (2017). A review of the recent advances in antimicrobial coatings for urinary catheters. *Acta biomaterialia*, *50*, 20-40.
- Singleton, A., Cluck, D., & BCIDP, A. (2019). The pharmacists role in treating extended-spectrum beta-lactamase infections. *US Pharm*, *44*, HS2-HS6.
- Smalley, J. W., & Olczak, T. (2017). Heme acquisition mechanisms of *Porphyromonas gingivalis*—strategies used in a polymicrobial community in a heme-limited host environment. *Molecular Oral Microbiology*, *32*(1), 1-23.
- Sofiana, E. D., Pratama, J. W. A., Effendi, M. H., Plumeriastuti, H., Wibisono, F. M., Hartadi, E. B., & Hidayatullah, A. R. (2020). A review of the presence of antibiotic resistance problems on *Klebsiella Pneumoniae* acquired from pigs: public health importance. *Sys Rev Pharm 2020; 11* (9): 535, 543.
- Sofy, A. R., El-DougDoug, N. K., Refaey, E. E., Dawoud, R. A., & Hmed, A. A. (2021). Characterization and full genome sequence of novel KPP-5 lytic

- phage against *Klebsiella pneumoniae* responsible for recalcitrant infection. *Biomedicines*, 9(4), 342.
- Some, S., Mondal, R., Mitra, D., Jain, D., Verma, D., & Das, S. (2021). Microbial pollution of water with special reference to coliform bacteria and their nexus with environment. *Energy Nexus*, 1, 100008.
- Sonda, T., Kumburu, H., van Zwetselaar, M., Alifrangis, M., Mmbaga, B. T., Lund, O., & Kibiki, G. (2018). Prevalence and risk factors for CTX-M gram-negative bacteria in hospitalized patients at a tertiary care hospital in Kilimanjaro, Tanzania. *European Journal of Clinical Microbiology & Infectious Diseases*, 37, 897-906.
- Sousa Geros, A., Simmons, A., Drakesmith, H., Aulicino, A., & Frost, J. N. (2020). The battle for iron in enteric infections. *Immunology*, 161(3), 186-199.
- Sperandeo, P., Martorana, A. M., & Polissi, A. (2017). The lipopolysaccharide transport (Lpt) machinery: a nonconventional transporter for lipopolysaccharide assembly at the outer membrane of Gram-negative bacteria. *Journal of Biological Chemistry*, 292(44), 17981-17990.
- Srivastava, S., Bhati, R., & Singh, R. (2023). Enzymatic biosynthesis of β -lactam antibiotics. In *Biotechnology of Microbial Enzymes* (pp. 179-198). Academic Press.
- Strakova, N., Korena, K., & Karpiskova, R. (2021). *Klebsiella pneumoniae* producing bacterial toxin colibactin as a risk of colorectal cancer development-A systematic review. *Toxicon*, 197, 126-135.
- Subhi, S. A., Risan, M. H., & Al-Wattar, W. M. (2017). Collection, isolation and identification of pathogenic bacteria from blood clinical specimens in

- Baghdad. *European Journal of Biomedical and Pharmaceutical Sciences*, 4(12), 01-08.
- Subramaniam, G., & Girish, M. (2020). Antibiotic resistance—A cause for reemergence of infections. *The Indian Journal of Pediatrics*, 87(11), 937-944.
- Surgers, L., Boyd, A., Girard, P. M., Arlet, G., & Decré, D. (2019). Biofilm formation by ESBL-producing strains of *Escherichia coli* and *Klebsiella pneumoniae*. *International Journal of Medical Microbiology*, 309(1), 13-18.
- Sustr, V., Foessleitner, P., Kiss, H., & Farr, A. (2020). Vulvovaginal candidosis: Current concepts, challenges and perspectives. *Journal of Fungi*, 6(4), 267.
- Tagliaferri, T. L., Jansen, M., & Horz, H. P. (2019). Fighting pathogenic bacteria on two fronts: Phages and antibiotics as combined strategy. *Frontiers in Cellular and Infection Microbiology*, 9, 22.
- Tanko, N., Bolaji, R. O., Olayinka, A. T., & Olayinka, B. O. (2020). A systematic review on the prevalence of extended spectrum beta lactamase producing Gram-negative bacteria in Nigeria. *Journal of Global Antimicrobial Resistance*.
- Taraghian, A., Esfahani, B. N., Moghim, S., & Fazeli, H. (2020). Characterization of hypervirulent extended-spectrum β -lactamase-producing *Klebsiella pneumoniae* among urinary tract infections: the first report from Iran. *Infection and Drug Resistance*, 13, 3103.

- Teng, T. S., Ji, A. L., Ji, X. Y., & Li, Y. Z. (2017). Neutrophils and immunity: from bactericidal action to being conquered. *Journal of immunology research*.
- Theuretzbacher, U., Carrara, E., Conti, M., & Tacconelli, E. (2021). Role of new antibiotics for KPC-producing *Klebsiella pneumoniae*. *Journal of Antimicrobial Chemotherapy*, 76(Supplement_1), i47-i54.
- Tilahun, A., Haddis, S., Teshale, A., & Hadush, T. (2016). Review on biofilm and microbial adhesion. *Int J Microbiol Res*, 7(3), 63-73.
- Tooke, C. L., Hinchliffe, P., Bragginton, E. C., Colenso, C. K., Hirvonen, V. H., Takebayashi, Y., & Spencer, J. (2019). β -lactamases and β -lactamase inhibitors in the 21st century. *Journal of molecular biology*, 431(18), 3472-3500.
- Torres, A., Niederman, M. S., Chastre, J., Ewig, S., Fernandez-Vandellos, P., Hanberger, H., & Paiva, J. A. (2017). International ERS/ESICM/ESCMID/ALAT guidelines for the management of hospital-acquired pneumonia and ventilator-associated pneumonia: guidelines for the management of hospital-acquired pneumonia (HAP)/ventilator-associated pneumonia (VAP) of the European Respiratory Society (ERS), European Society of Intensive Care Medicine (ESICM), European Society of Clinical Microbiology and Infectious Diseases (ESCMID) and Asociación Latinoamericana del Tórax (ALAT). *European Respiratory Journal*, 50(3).
- Tsuka, T., Ozaki, H., Saito, D., Murase, T., Okamoto, Y., Azuma, K., & Imagawa, T. (2021). Genetic characterization of CTX-M-2-producing *Klebsiella pneumoniae* and *Klebsiella oxytoca* associated with bovine mastitis in Japan. *Frontiers in Veterinary Science*, 8, 659222.

- Turton, J. F., Payne, Z., Micah, K., & Turton, J. A. (2018). Capsular type K54, clonal group 29 and virulence plasmids: an analysis of K54 and non-K54 closely related isolates of *Klebsiella pneumoniae*. *Epidemiology & Infection*, *146*(14), 1813-1823.
- Uhlenbruck, G., & Beuth, J. (2017). Adhesive Properties of Bacteria. In *Principles of Cell Adhesion (1995)* (pp. 95-114). CRC Press.
- Ur Rahman, S., Ali, T., Ali, I., Khan, N. A., Han, B., and Gao, J. (2018). The growing genetic and functional diversity of extended spectrum beta-lactamases. *Biomed. Res. Int.* *26*:9519718.
- Van Cleemput, J. (2018). The Horse's Respiratory Mucosa, Airborne Pathogens and Respirable Hazards: The Archetypical Trifecta of Co-Evolution (Doctoral dissertation, Doctor in Veterinary Sciences, Faculty of Veterinary Medicine, Ghent University, Belgium).
- Van Duijkeren, E., Schink, A. K., Roberts, M. C., Wang, Y., & Schwarz, S. (2018). Mechanisms of bacterial resistance to antimicrobial agents. *Microbiology spectrum*, *6*(2), 6-2.
- Vandepitte, J., Engbaek, P., Piot, P. and Heuck, C. (1991). Basic laboratory procedures in clinical bacteriology. Geneva, World Health Organization: 31-35.
- Venkataramani, V. (2021). Iron Irons Homeostasis and Metabolism: Two Sides of a Coin. *Ferroptosis: Mechanism and Diseases*, 25-40.
- Viale, A. M., & Evans, B. A. (2020). Microevolution in the major outer membrane protein OmpA of *Acinetobacter baumannii*. *Microbial Genomics*, mgen000381.

- Villa, L., Feudi, C., Fortini, D., Brisse, S., Passet, V., Bonura, C., & Doumith, M. (2017). Diversity, virulence, and antimicrobial resistance of the KPC-producing *Klebsiella pneumoniae* ST307 clone. *Microbial genomics*, 3(4).
- Villa, T. G., Feijoo-Siota, L., Sánchez-Pérez, A., Rama, J. R., & Sieiro, C. (2019). Horizontal gene transfer in bacteria, an overview of the mechanisms involved. *Horizontal Gene Transfer* (pp. 3-76). Springer, Cham.
- Vita, G. M., De Simone, G., Leboffe, L., Montagnani, F., Mariotti, D., Di Bella, S., & di Masi, A. (2020). Human serum albumin binds Streptolysin O (SLO) toxin produced by Group a *Streptococcus* and inhibits its cytotoxic and hemolytic effects. *Frontiers in Immunology*, 11, 507092.
- Walker, K. A., & Miller, V. L. (2020). The intersection of capsule gene expression, hypermucoviscosity and hypervirulence in *Klebsiella pneumoniae*. *Current opinion in microbiology*, 54, 95-102.
- Walker, K. A., Miner, T. A., Palacios, M., Trzilova, D., Frederick, D. R., Broberg, C. A., & Miller, V. L. (2019). A *Klebsiella pneumoniae* regulatory mutant has reduced capsule expression but retains hypermucoviscosity. *MBio*, 10(2).
- Walker, K. A., Treat, L. P., Sepúlveda, V. E., & Miller, V. L. (2020). The small protein RmpD drives hypermucoviscosity in *Klebsiella pneumoniae*. *MBio*, 11(5), e01750-20.
- Wang, G., Zhao, G., Chao, X., Xie, L., & Wang, H. (2020). The characteristic of virulence, biofilm and antibiotic resistance of *Klebsiella pneumoniae*. *International Journal of Environmental Research and Public Health*, 17(17), 6278.

- Wang, Y. M., Dong, W. L., Odah, K. A., Kong, L. C., & Ma, H. X. (2019). Transcriptome analysis reveals AI-2 relevant genes of multi-drug resistant *Klebsiella pneumoniae* in response to eugenol at Sub-MIC. *Frontiers in Microbiology*, *10*, 1159.
- Wang, X., Xie, Y., Li, G., Liu, J., Li, X., Tian, L., & Qu, H. (2018). Whole-Genome-Sequencing characterization of bloodstream infection-causing hypervirulent *Klebsiella pneumoniae* of capsular serotype K2 and ST374. *Virulence*, *9*(1), 510-521.
- Wang, J., Li, J., Qian, S., Guo, G., Wang, Q., Tang, J., & Chu, P. K. (2016). Antibacterial surface design of titanium-based biomaterials for enhanced bacteria-killing and cell-assisting functions against periprosthetic joint infection. *ACS applied materials & interfaces*, *8*(17), 11162-11178.
- Wei, D. D., Xiong, X. S., Mei, Y. F., Du, F. L., Wan, L. G., & Liu, Y. (2020). Microbiological and clinical characteristics of *Klebsiella pneumoniae* isolates of K57 capsular serotype in China. *Microbial Drug Resistance*.
- Whitfield, C., Williams, D. M., & Kelly, S. D. (2020). Lipopolysaccharide O-antigens-bacterial glycans made to measure. *Journal of Biological Chemistry*, jbc-REV120.
- Widodo, A., Effendi, M. H., & Khairullah, A. R. (2020). Extended-spectrum beta-lactamase (ESBL)-producing *Eschericia coli* from livestock. *Sys Rev Pharm*, *2020; 11* (7): 382, 392.
- Willsey, G. G. (2018). Detection of The Lung Environment By Multi-Drug Resistant Gram-Negative Bacterial Pathogens.

References

- Wilson, B. R., Bogdan, A. R., Miyazawa, M., Hashimoto, K., & Tsuji, Y. (2016). Siderophores in iron metabolism: from mechanism to therapy potential. *Trends in molecular medicine*, 22(12), 1077-1090.
- Wyres, K. L., & Holt, K. E. (2018). *Klebsiella pneumoniae* as a key trafficker of drug resistance genes from environmental to clinically important bacteria. *Current opinion in microbiology*, 45, 131-139.
- Wyres, K. L., Lam, M. M., & Holt, K. E. (2020). Population genomics of *Klebsiella pneumoniae*. *Nature Reviews Microbiology*, 1-16.
- Wyres, K. L., Wick, R. R., Judd, L. M., Froumine, R., Tokolyi, A., Gorrie, C. L., & Holt, K. E. (2019). Distinct evolutionary dynamics of horizontal gene transfer in drug resistant and virulent clones of *Klebsiella pneumoniae*. *PLoS genetics*, 15(4), e1008114.
- Xu, M., Fu, Y., Fang, Y., Xu, H., Kong, H., Liu, Y., & Li, L. (2019). High prevalence of KPC-2-producing hypervirulent *Klebsiella pneumoniae* causing meningitis in Eastern China. *Infection and drug resistance*, 12, 641.
- Yanat, B., Rodríguez-Martínez, J. M., & Touati, A. (2017). Plasmid-mediated quinolone resistance in *Enterobacteriaceae*: a systematic review with a focus on Mediterranean countries. *European Journal of Clinical Microbiology & Infectious Diseases*, 36(3), 421-435.
- Yang, X., Dong, N., Chan, E. W. C., Zhang, R., & Chen, S. (2021). Carbapenem resistance-encoding and virulence-encoding conjugative plasmids in *Klebsiella pneumoniae*. *Trends in microbiology*, 29(1), 65-83.
- Yaqoob, A. A., Bakar, M. A. B. A., Kim, H. C., Ahmad, A., Alshammari, M. B., & Yaakop, A. S. (2022). Oxidation of food waste as an organic substrate

- in a single chamber microbial fuel cell to remove the pollutant with energy generation. *Sustainable Energy Technologies and Assessments*, 52, 102282.
- Yero, D., Huedo, P., Conchillo-Solé, O., Martínez-Servat, S., Mamat, U., Coves, X., & Daura, X. (2020). Genetic variants of the DSF quorum sensing system in *Stenotrophomonas maltophilia* influence virulence and resistance phenotypes among genotypically diverse clinical isolates. *Frontiers in Microbiology*, 11, 1160.
- Younes, A. E. G. M. (2011). Molecular diversity and genetic organization of antibiotic resistance in *Klebsiella* species.
- Yuan, F., Huang, Z., Yang, T., Wang, G., Li, P., Yang, B., & Li, J. (2021). Pathogenesis of *Proteus mirabilis* in catheter-associated urinary tract infections. *Urologia Internationalis*, 105(5-6), 354-361.
- Yuan, L., Hansen, M. F., Røder, H. L., Wang, N., Burmølle, M., & He, G. (2020). Mixed-species biofilms in the food industry: Current knowledge and novel control strategies. *Critical Reviews in Food Science and Nutrition*, 60(13), 2277-2293.
- Zaha, D. C., Kiss, R., Hegedűs, C., Gesztelyi, R., Bombicz, M., Muresan, M., & Micle, O. (2019). Recent advances in investigation, prevention, and management of healthcare-associated infections (HAIs): Resistant multidrug strain colonization and its risk factors in an Intensive Care Unit of a University Hospital. *BioMed research international*.
- Zalewska-Piątek, B., Olszewski, M., Lipniacki, T., Błoński, S., Wieczór, M., Bruździak, P., & Piątek, R. (2020). A shear stress micromodel of urinary tract infection by the *Escherichia coli* producing Dr adhesin. *PLoS Pathogens*, 16(1), e1008247.

References

- Zhang Z, Schwartz S, Wagner L, Miller W. (2000). A greedy algorithm for aligning DNA sequences. *J Comput Biol.* 7(1-2):203-14.
- Zhu, H., Liu, H. J., Ning, S. J., & Gao, Y. L. (2011). A luxS-dependent transcript profile of cell-to-cell communication in *Klebsiella pneumoniae*. *Molecular Biosystems*, 7(11), 3164-3168.

Appendix

Appendix

bioMérieux Customer:

Microbiology Chart Report

Printed August 24, 2022 7:00:01 AM CDT

Patient Name: 22 زينب مهدي

Patient ID: 33128

Location:

Physician:

Lab ID: 33128

Isolate Number: 1

Organism Quantity:

Selected Organism : *Klebsiella pneumoniae ssp pneumoniae*

Source:

Collected:

Comments:	

Identification Information	Analysis Time: 7.88 hours	Status: Final
Selected Organism	96% Probability Bionumber: 6607735753565153	<i>Klebsiella pneumoniae ssp pneumoniae</i>
ID Analysis Messages		

Susceptibility Information	Analysis Time: 8.62 hours	Status: Final
-----------------------------------	----------------------------------	----------------------

Antimicrobial	MIC	Interpretation	Antimicrobial	MIC	Interpretation
Amoxicillin/Clavulanic Acid	>= 32	R	Imipenem	>= 16	R
Piperacillin/Tazobactam	>= 128	R	Meropenem	>= 16	R
Cefazolin	>= 64	R	Amikacin	32	I
Cefuroxime	>= 64	R	Gentamicin	>= 16	R
Cefuroxime Axetil	>= 64	R	Ciprofloxacin	>= 4	R
Ceftazidime	>= 64	R	Fosfomycin	128	R
Ceftriaxone	>= 64	R	Nitrofurantoin	128	R
Cefepime	>= 32	R	Trimethoprim/ Sulfamethoxazole	>= 320	R
Ertapenem	<= 0.12*	*I			

*= AES modified **= User modified

AES Findings	
Confidence:	Consistent with correction

Appendix

bioMérieux Customer:

Microbiology Chart Report

Printed August 24, 2022 7:00:02 AM CDT

Patient Name: 16 زینب مهدی

Patient ID: 33127

Location:

Physician:

Lab ID: 33127

Isolate Number: 1

Organism Quantity:

Selected Organism : *Klebsiella pneumoniae ssp pneumoniae*

Source:

Collected:

Comments:	

Identification Information	Analysis Time: 3.97 hours	Status: Final
Selected Organism	95% Probability Bionumber: 6607734773765010	<i>Klebsiella pneumoniae ssp pneumoniae</i>
ID Analysis Messages		

Susceptibility Information	Analysis Time: 8.85 hours	Status: Final
----------------------------	---------------------------	---------------

Antimicrobial	MIC	Interpretation	Antimicrobial	MIC	Interpretation
Amoxicillin/Clavulanic Acid	>= 32	R	Imipenem	>= 16	R
Piperacillin/Tazobactam	>= 128	R	Meropenem	>= 16	R
Cefazolin	>= 64	R	Amikacin	32	I
Cefuroxime	>= 64	R	Gentamicin	>= 16	R
Cefuroxime Axetil	>= 64	R	Ciprofloxacin	>= 4	R
Ceftazidime	>= 64	R	Fosfomycin	>= 256	R
Ceftriaxone	>= 64	R	Nitrofurantoin	>= 512	R
Cefepime	>= 32	R	Trimethoprim/ Sulfamethoxazole	>= 320	R
Ertapenem	>= 8	R			

AES Findings	
Confidence:	Consistent

Appendix

bioMérieux Customer:

Microbiology Chart Report

Printed August 24, 2022 7:00:00 AM CDT

Patient Name: 18, زينب مهدي

Patient ID: 33129

Location:

Physician:

Lab ID: 33129

Isolate Number: 1

Organism Quantity:

Selected Organism : *Klebsiella pneumoniae* ssp *pneumoniae*

Source:

Collected:

Comments:	

Identification Information	Analysis Time: 3.95 hours	Status: Final
Selected Organism	99% Probability	<i>Klebsiella pneumoniae</i> ssp <i>pneumoniae</i>
ID Analysis Messages	Bionumber: 6607735773565010	

Susceptibility Information	Analysis Time: 8.58 hours	Status: Final
----------------------------	---------------------------	---------------

Antimicrobial	MIC	Interpretation	Antimicrobial	MIC	Interpretation
Amoxicillin/Clavulanic Acid	>= 32	R	Imipenem	>= 16	R
Piperacillin/Tazobactam	>= 128	R	Meropenem	>= 16	R
Cefazolin	>= 64	R	Amikacin	32	I
Cefuroxime	>= 64	R	Gentamicin	>= 16	R
Cefuroxime Axetil	>= 64	R	Ciprofloxacin	>= 4	R
Ceftazidime	>= 64	R	Fosfomycin	>= 256	R
Ceftriaxone	>= 64	R	Nitrofurantoin	>= 512	R
Cefepime	>= 32	R	Trimethoprim/ Sulfamethoxazole	>= 320	R
Ertapenem	>= 8	R			

AES Findings	
Confidence:	Consistent

bioMérieux Customer:

Microbiology Chart Report

Printed August 24, 2022 7:05:47 AM CDT

Patient Name: 27 زینب مهدی

Patient ID: 33152

Location:

Physician:

Lab ID: 33152

Isolate Number: 1

Organism Quantity:

Selected Organism : *Klebsiella pneumoniae ssp pneumoniae*

Source:

Collected:

Comments:	

Identification Information	Analysis Time: 4.90 hours	Status: Final
Selected Organism	99% Probability Bionumber: 0405610540506610	<i>Klebsiella pneumoniae ssp pneumoniae</i>
ID Analysis Messages		

Susceptibility Information	Analysis Time: 10.27 hours	Status: Final
----------------------------	----------------------------	---------------

Antimicrobial	MIC	Interpretation	Antimicrobial	MIC	Interpretation
Amoxicillin/Clavulanic Acid	4	S	Imipenem	<= 0.25	S
Piperacillin/Tazobactam	<= 4	S	Meropenem	<= 0.25	S
Cefazolin	<= 4	S	Amikacin	2	S
Cefuroxime	4	S	Gentamicin	<= 1	S
Cefuroxime Axetil	4	S	Ciprofloxacin	0.5	S
Ceftazidime	<= 0.12	S	Fosfomycin	<= 16	S
Ceftriaxone	<= 0.25	S	Nitrofurantoin	<= 16	S
Cefepime	<= 0.12	S	Trimethoprim/ Sulfamethoxazole	<= 20	S
Ertapenem	<= 0.12	S			

AES Findings	
Confidence:	Consistent

bioMérieux Customer:

Microbiology Chart Report

Printed August 24, 2022 6:37:09 PM CDT

Lab ID: 57 زینب مهدی

Isolate Number: 1

Organism Quantity:

Selected Organism : *Klebsiella pneumoniae ssp pneumoniae*

Comments:	

Identification Information	Analysis Time: 3.85 hours	Status: Final
Selected Organism	99% Probability Bionumber: 4237710360443211	<i>Klebsiella pneumoniae ssp pneumoniae</i>
ID Analysis Messages		

Susceptibility Information	Analysis Time: 18.03 hours	Status: Final
----------------------------	----------------------------	---------------

Antimicrobial	MIC	Interpretation	Antimicrobial	MIC	Interpretation
Amoxicillin/Clavulanic Acid	16	I	Imipenem	>= 16	R
Piperacillin/Tazobactam	<= 4	S	Meropenem	4	R
Cefazolin	8	S	Amikacin	32	I
Cefuroxime	8	S	Gentamicin	4	S
Cefuroxime Axetil	8	I	Ciprofloxacin	1	S
Ceftazidime	32	R	Fosfomycin	>= 256	R
Ceftriaxone	>= 64	R	Nitrofurantoin	128	R
Cefepime	16	R	Trimethoprim/ Sulfamethoxazole	40	S
Ertapenem	4	R			

AES Findings	
Confidence:	Inconsistent

bioMérieux Customer:

Microbiology Chart Report

Printed August 24, 2022 7:05:48 AM CDT

Patient Name: 117 زينب مهدي

Location:

Patient ID: 33151

Lab ID: 33151

Physician:

Isolate Number: 1

Organism Quantity:

Selected Organism : *Klebsiella pneumoniae ssp pneumoniae*

Source:

Collected:

Comments:	

Identification Information	Analysis Time: 3.92 hours	Status: Final
Selected Organism	99% Probability	<i>Klebsiella pneumoniae ssp pneumoniae</i>
ID Analysis Messages	Bionumber: 0405610450406610	

Susceptibility Information	Analysis Time: 7.33 hours	Status: Final
----------------------------	---------------------------	---------------

Antimicrobial	MIC	Interpretation	Antimicrobial	MIC	Interpretation
Amoxicillin/Clavulanic Acid	4	S	Imipenem	<= 0.25	S
Piperacillin/Tazobactam	<= 4	S	Meropenem	<= 0.25	S
Cefazolin	>= 64	R	Amikacin	2	S
Cefuroxime	>= 64	R	Gentamicin	<= 1	S
Cefuroxime Axetil	>= 64	R	Ciprofloxacin	1	S
Ceftazidime	2	S	Fosfomycin	<= 16	S
Ceftriaxone	>= 64	R	Nitrofurantoin	<= 16	S
Cefepime	2	S	Trimethoprim/Sulfamethoxazole	>= 320	R
Ertapenem	<= 0.12	S			

AES Findings	
Confidence:	Consistent

bioMérieux Customer: Patient Name: 17 زینب مهدی Location: Lab ID: 33126	Microbiology Chart Report	Printed August 24, 2022 7:00:02 AM CDT Patient ID: 33126 Physician: Isolate Number: 1																																																																					
Organism Quantity: Selected Organism : <i>Klebsiella pneumoniae ssp pneumoniae</i>																																																																							
Source:		Collected:																																																																					
Comments:	_____ _____ _____																																																																						
<table border="1" style="width: 100%; border-collapse: collapse;"> <tr> <td style="width: 35%;"> Identification Information </td> <td style="width: 30%;"> Analysis Time: 9.82 hours </td> <td style="width: 35%;"> Status: Final </td> </tr> <tr> <td> Selected Organism </td> <td> 99% Probability </td> <td> <i>Klebsiella pneumoniae ssp pneumoniae</i> </td> </tr> <tr> <td> ID Analysis Messages </td> <td> Bionumber: </td> <td> 6607715753565153 </td> </tr> </table>			Identification Information	Analysis Time: 9.82 hours	Status: Final	Selected Organism	99% Probability	<i>Klebsiella pneumoniae ssp pneumoniae</i>	ID Analysis Messages	Bionumber:	6607715753565153																																																												
Identification Information	Analysis Time: 9.82 hours	Status: Final																																																																					
Selected Organism	99% Probability	<i>Klebsiella pneumoniae ssp pneumoniae</i>																																																																					
ID Analysis Messages	Bionumber:	6607715753565153																																																																					
<table border="1" style="width: 100%; border-collapse: collapse;"> <tr> <td style="width: 30%;"> Susceptibility Information </td> <td style="width: 35%;"> Analysis Time: 9.82 hours </td> <td style="width: 35%;"> Status: Final </td> </tr> <tr> <td> <table border="1" style="width: 100%; border-collapse: collapse;"> <thead> <tr> <th style="width: 25%;">Antimicrobial</th> <th style="width: 15%;">MIC</th> <th style="width: 15%;">Interpretation</th> <th style="width: 25%;">Antimicrobial</th> <th style="width: 15%;">MIC</th> <th style="width: 20%;">Interpretation</th> </tr> </thead> <tbody> <tr> <td>Amoxicillin/Clavulanic Acid</td> <td>>= 32</td> <td>R</td> <td>Imipenem</td> <td>>= 16</td> <td>R</td> </tr> <tr> <td>Piperacillin/Tazobactam</td> <td>>= 128</td> <td>R</td> <td>Meropenem</td> <td>>= 16</td> <td>R</td> </tr> <tr> <td>Cefazolin</td> <td>>= 64</td> <td>R</td> <td>Amikacin</td> <td>32</td> <td>I</td> </tr> <tr> <td>Cefuroxime</td> <td>>= 64</td> <td>R</td> <td>Gentamicin</td> <td>>= 16</td> <td>R</td> </tr> <tr> <td>Cefuroxime Axetil</td> <td>>= 64</td> <td>R</td> <td>Ciprofloxacin</td> <td>>= 4</td> <td>R</td> </tr> <tr> <td>Ceftazidime</td> <td>>= 64</td> <td>R</td> <td>Fosfomycin</td> <td><= 16</td> <td>S</td> </tr> <tr> <td>Ceftriaxone</td> <td>>= 64</td> <td>R</td> <td>Nitrofurantoin</td> <td>128</td> <td>R</td> </tr> <tr> <td>Cefepime</td> <td>>= 32</td> <td>R</td> <td>Trimethoprim/ Sulfamethoxazole</td> <td>>= 320</td> <td>R</td> </tr> <tr> <td>Ertapenem</td> <td>>= 8</td> <td>R</td> <td></td> <td></td> <td></td> </tr> </tbody> </table> </td> <td></td> <td></td> <td></td> <td></td> <td></td> </tr> </table>			Susceptibility Information	Analysis Time: 9.82 hours	Status: Final	<table border="1" style="width: 100%; border-collapse: collapse;"> <thead> <tr> <th style="width: 25%;">Antimicrobial</th> <th style="width: 15%;">MIC</th> <th style="width: 15%;">Interpretation</th> <th style="width: 25%;">Antimicrobial</th> <th style="width: 15%;">MIC</th> <th style="width: 20%;">Interpretation</th> </tr> </thead> <tbody> <tr> <td>Amoxicillin/Clavulanic Acid</td> <td>>= 32</td> <td>R</td> <td>Imipenem</td> <td>>= 16</td> <td>R</td> </tr> <tr> <td>Piperacillin/Tazobactam</td> <td>>= 128</td> <td>R</td> <td>Meropenem</td> <td>>= 16</td> <td>R</td> </tr> <tr> <td>Cefazolin</td> <td>>= 64</td> <td>R</td> <td>Amikacin</td> <td>32</td> <td>I</td> </tr> <tr> <td>Cefuroxime</td> <td>>= 64</td> <td>R</td> <td>Gentamicin</td> <td>>= 16</td> <td>R</td> </tr> <tr> <td>Cefuroxime Axetil</td> <td>>= 64</td> <td>R</td> <td>Ciprofloxacin</td> <td>>= 4</td> <td>R</td> </tr> <tr> <td>Ceftazidime</td> <td>>= 64</td> <td>R</td> <td>Fosfomycin</td> <td><= 16</td> <td>S</td> </tr> <tr> <td>Ceftriaxone</td> <td>>= 64</td> <td>R</td> <td>Nitrofurantoin</td> <td>128</td> <td>R</td> </tr> <tr> <td>Cefepime</td> <td>>= 32</td> <td>R</td> <td>Trimethoprim/ Sulfamethoxazole</td> <td>>= 320</td> <td>R</td> </tr> <tr> <td>Ertapenem</td> <td>>= 8</td> <td>R</td> <td></td> <td></td> <td></td> </tr> </tbody> </table>	Antimicrobial	MIC	Interpretation	Antimicrobial	MIC	Interpretation	Amoxicillin/Clavulanic Acid	>= 32	R	Imipenem	>= 16	R	Piperacillin/Tazobactam	>= 128	R	Meropenem	>= 16	R	Cefazolin	>= 64	R	Amikacin	32	I	Cefuroxime	>= 64	R	Gentamicin	>= 16	R	Cefuroxime Axetil	>= 64	R	Ciprofloxacin	>= 4	R	Ceftazidime	>= 64	R	Fosfomycin	<= 16	S	Ceftriaxone	>= 64	R	Nitrofurantoin	128	R	Cefepime	>= 32	R	Trimethoprim/ Sulfamethoxazole	>= 320	R	Ertapenem	>= 8	R								
Susceptibility Information	Analysis Time: 9.82 hours	Status: Final																																																																					
<table border="1" style="width: 100%; border-collapse: collapse;"> <thead> <tr> <th style="width: 25%;">Antimicrobial</th> <th style="width: 15%;">MIC</th> <th style="width: 15%;">Interpretation</th> <th style="width: 25%;">Antimicrobial</th> <th style="width: 15%;">MIC</th> <th style="width: 20%;">Interpretation</th> </tr> </thead> <tbody> <tr> <td>Amoxicillin/Clavulanic Acid</td> <td>>= 32</td> <td>R</td> <td>Imipenem</td> <td>>= 16</td> <td>R</td> </tr> <tr> <td>Piperacillin/Tazobactam</td> <td>>= 128</td> <td>R</td> <td>Meropenem</td> <td>>= 16</td> <td>R</td> </tr> <tr> <td>Cefazolin</td> <td>>= 64</td> <td>R</td> <td>Amikacin</td> <td>32</td> <td>I</td> </tr> <tr> <td>Cefuroxime</td> <td>>= 64</td> <td>R</td> <td>Gentamicin</td> <td>>= 16</td> <td>R</td> </tr> <tr> <td>Cefuroxime Axetil</td> <td>>= 64</td> <td>R</td> <td>Ciprofloxacin</td> <td>>= 4</td> <td>R</td> </tr> <tr> <td>Ceftazidime</td> <td>>= 64</td> <td>R</td> <td>Fosfomycin</td> <td><= 16</td> <td>S</td> </tr> <tr> <td>Ceftriaxone</td> <td>>= 64</td> <td>R</td> <td>Nitrofurantoin</td> <td>128</td> <td>R</td> </tr> <tr> <td>Cefepime</td> <td>>= 32</td> <td>R</td> <td>Trimethoprim/ Sulfamethoxazole</td> <td>>= 320</td> <td>R</td> </tr> <tr> <td>Ertapenem</td> <td>>= 8</td> <td>R</td> <td></td> <td></td> <td></td> </tr> </tbody> </table>	Antimicrobial	MIC	Interpretation	Antimicrobial	MIC	Interpretation	Amoxicillin/Clavulanic Acid	>= 32	R	Imipenem	>= 16	R	Piperacillin/Tazobactam	>= 128	R	Meropenem	>= 16	R	Cefazolin	>= 64	R	Amikacin	32	I	Cefuroxime	>= 64	R	Gentamicin	>= 16	R	Cefuroxime Axetil	>= 64	R	Ciprofloxacin	>= 4	R	Ceftazidime	>= 64	R	Fosfomycin	<= 16	S	Ceftriaxone	>= 64	R	Nitrofurantoin	128	R	Cefepime	>= 32	R	Trimethoprim/ Sulfamethoxazole	>= 320	R	Ertapenem	>= 8	R														
Antimicrobial	MIC	Interpretation	Antimicrobial	MIC	Interpretation																																																																		
Amoxicillin/Clavulanic Acid	>= 32	R	Imipenem	>= 16	R																																																																		
Piperacillin/Tazobactam	>= 128	R	Meropenem	>= 16	R																																																																		
Cefazolin	>= 64	R	Amikacin	32	I																																																																		
Cefuroxime	>= 64	R	Gentamicin	>= 16	R																																																																		
Cefuroxime Axetil	>= 64	R	Ciprofloxacin	>= 4	R																																																																		
Ceftazidime	>= 64	R	Fosfomycin	<= 16	S																																																																		
Ceftriaxone	>= 64	R	Nitrofurantoin	128	R																																																																		
Cefepime	>= 32	R	Trimethoprim/ Sulfamethoxazole	>= 320	R																																																																		
Ertapenem	>= 8	R																																																																					
<table border="1" style="width: 100%; border-collapse: collapse;"> <tr> <td colspan="2"> AES Findings </td> </tr> <tr> <td style="width: 25%;"> Confidence: </td> <td> Consistent </td> </tr> </table>			AES Findings		Confidence:	Consistent																																																																	
AES Findings																																																																							
Confidence:	Consistent																																																																						

bioMérieux Customer:	Microbiology Chart Report	Printed August 24, 2022 6:36:33 PM CDT			
Lab ID: 31 زینب مهندي		Isolate Number: 1			
Organism Quantity: Selected Organism ; <i>Klebsiella pneumoniae ssp pneumoniae</i>					
Comments:					
Identification Information					
	Analysis Time: 3.82 hours	Status: Final			
Selected Organism	99% Probability <i>Klebsiella pneumoniae ssp pneumoniae</i> Bionumber: 4237710360443211				
ID Analysis Messages					
Susceptibility Information					
	Analysis Time: 18.00 hours	Status: Final			
Antimicrobial	MIC	Interpretation	Antimicrobial	MIC	Interpretation
Amoxicillin/Clavulanic Acid	>= 32	R	Imipenem	>= 16	R
Piperacillin/Tazobactam	<= 4	S	Meropenem	4	R
Cefazolin	16	I	Amikacin	2	S
Cefuroxime	>= 64	R	Gentamicin	<= 1	S
Cefuroxime Axetil	>= 64	R	Ciprofloxacin	0.12	S
Ceftazidime	32	R	Fosfomycin	>= 256	R
Ceftriaxone	32	R	Nitrofurantoin	128	R
Cefepime	16	R	Trimethoprim/ Sulfamethoxazole	40	S
Ertapenem	4	R			
AES Findings					
Confidence:		Inconsistent			

bioMérieux Customer:

Microbiology Chart Report

Printed December 6, 2022 4:10:09 PM CST

Patient Name: 19, .
 Location:
 Lab ID: 34355

Patient ID: 34355
 Physician:
 Isolate Number: 1

Organism Quantity:
Selected Organism : Klebsiella pneumoniae ssp pneumoniae

Source:

Collected:

Comments:	

Identification Information	Analysis Time: 5.95 hours	Status: Final
Selected Organism	95% Probability Bionumber: 6607714753564010	Klebsiella pneumoniae ssp pneumoniae
ID Analysis Messages		

Susceptibility Information	Analysis Time: 9.12 hours	Status: Final
-----------------------------------	----------------------------------	----------------------

Antimicrobial	MIC	Interpretation	Antimicrobial	MIC	Interpretation
Ampicillin/Sulbactam	>= 32	R	Amikacin	>= 64	R
Piperacillin/Tazobactam	>= 128	R	Gentamicin	>= 16	R
Cefazolin	>= 64	R	Tobramycin	>= 16	R
Cefoxitin	>= 64	R	Levofloxacin	>= 8	R
Ceftazidime	>= 64	R	Tetracycline	>= 16	R
Ceftriaxone	>= 64	R	Tigecycline	2	S
Cefepime	>= 64	R	Nitrofurantoin	64	I
Aztreonam	32	R	Trimethoprim/ Sulfamethoxazole	>= 320	R
Meropenem	>= 16	R			

AES Findings	
Confidence:	Consistent

bioMérieux Customer:

Microbiology Chart Report

Printed December 6, 2022 4:10:08 PM CST

Patient Name:
Location:
Lab ID: 34356

Patient ID:
Physician:
Isolate Number: 1

Organism Quantity:

Selected Organism : Klebsiella pneumoniae ssp pneumoniae

Source:

Collected:

Comments:	

Identification Information	Analysis Time: 5.93 hours	Status: Final
Selected Organism	95% Probability Bionumber: 6607715753565010	Klebsiella pneumoniae ssp pneumoniae
ID Analysis Messages		

Susceptibility Information	Analysis Time: 8.87 hours	Status: Final
-----------------------------------	----------------------------------	----------------------

Antimicrobial	MIC	Interpretation	Antimicrobial	MIC	Interpretation
Ampicillin/Sulbactam	>= 32	R	Amikacin	>= 64	R
Piperacillin/Tazobactam	>= 128	R	Gentamicin	>= 16	R
Cefazolin	>= 64	R	Tobramycin	>= 16	R
Cefoxitin	>= 64	R	Levofloxacin	>= 8	R
Ceftazidime	>= 64	R	Tetracycline	>= 16	R
Ceftriaxone	>= 64	R	Tigecycline	2	S
Cefepime	>= 64	R	Nitrofurantoin	128	R
Aztreonam	32	R	Trimethoprim/ Sulfamethoxazole	>= 320	R
Meropenem	>= 16	R			

AES Findings	
Confidence:	Consistent

bioMérieux Customer: Microbiology Chart Report Printed December 6, 2022 4:10:08 PM CST

Patient Name: 25, . Patient ID: 34357
 Location: Physician:
 Lab ID: 34357 Isolate Number: 1

Organism Quantity:
Selected Organism : Klebsiella pneumoniae ssp pneumoniae

Source: Collected:

Comments:	

Identification Information	Analysis Time: 3.98 hours	Status: Final
Selected Organism	99% Probability Bionumber: 6607734673164010	Klebsiella pneumoniae ssp pneumoniae
ID Analysis Messages		

Susceptibility Information	Analysis Time: 8.37 hours	Status: Final
-----------------------------------	----------------------------------	----------------------

Antimicrobial	MIC	Interpretation	Antimicrobial	MIC	Interpretation
Ampicillin/Sulbactam	>= 32	R	Amikacin	>= 64	R
Piperacillin/Tazobactam	>= 128	R	Gentamicin	>= 16	R
Cefazolin	>= 64	R	Tobramycin	>= 16	R
Cefoxitin	>= 64	R	Levofloxacin	>= 8	R
Ceftazidime	>= 64	R	Tetracycline	4	*R
Ceftriaxone	>= 64	R	Tigecycline	1	S
Cefepime	>= 64	R	Nitrofurantoin	>= 512	R
Aztreonam	<= 1	S	Trimethoprim/ Sulfamethoxazole	>= 320	R
Meropenem	>= 16	R			

*= AES modified **= User modified

AES Findings	
Confidence:	Consistent

bioMérieux Customer:

Microbiology Chart Report

Printed December 6, 2022 4:10:07 PM CST

Patient Name: 35, .

Patient ID: 34358

Location:

Physician:

Lab ID: 34358

Isolate Number: 1

Organism Quantity:

Selected Organism : Klebsiella pneumoniae ssp pneumoniae

Source:

Collected:

Comments:	

Identification Information	Analysis Time: 3.97 hours	Status: Final
Selected Organism	97% Probability Klebsiella pneumoniae ssp pneumoniae	
ID Analysis Messages	Bionumber: 6627734673164210	

Susceptibility Information	Analysis Time: 8.85 hours	Status: Final
-----------------------------------	----------------------------------	----------------------

Antimicrobial	MIC	Interpretation	Antimicrobial	MIC	Interpretation
Ampicillin/Sulbactam	>= 32	R	Amikacin	<= 2	S
Piperacillin/Tazobactam	>= 128	R	Gentamicin	2*	*R
Cefazolin	>= 64	R	Tobramycin	>= 16	R
Cefoxitin	>= 64	R	Levofloxacin	>= 8	R
Ceftazidime	>= 64	R	Tetracycline	4	*R
Ceftriaxone	>= 64	R	Tigecycline	1	S
Cefepime	>= 64	R	Nitrofurantoin	>= 512	R
Aztreonam	<= 1	S	Trimethoprim/ Sulfamethoxazole	>= 320	R
Meropenem	>= 16	R			

*= AES modified **= User modified

AES Findings	
Confidence:	Consistent with correction

الخلاصة

تضمنت هذه الدراسة 100 عينة سريرية تم جمعها من مستشفى الحلة التعليمي ومستشفى الإمام الصادق للفترة من تشرين الأول 2021 لغاية نيسان 2022، من مرضى تتراوح أعمارهم بين 3 و 55 عامًا من كلا الجنسين، 65% منهم ذكور و 35% إناث. تم عزل أربعين سلالة من بكتريا *K. pneumoniae* من 100 عينة من مواقع عدوى مختلفة وبواسطة طرائق تشخيصية مختلفة. 11 (27.5%) من الأربعين عذلة كانت من البلغم، 8 (20%) من البول، 7 (17.5%) من مسحات الجروح، 6 (15%) من مسحات الحروق، 5 (12.5%) من أنسجة الحروق، و 3 (7.5%) من مسحات الأذن. تم عزل *K. pneumoniae* من 26 رجلاً (65%) و 14 امرأة (35%).

أظهر الكشف عن النمط المظهري أن 18 (45%) من عزلات *K. pneumoniae* الرئوية كانت منتجة للهيمولايسين، و 22 (55%) منتجة Siderophores، 37 (92.5%) تلازن كريات الدم الحمراء، 25 (62.5%) يمكن أن تنتج مقاومة للمصل، 5 (12.5%) منتجة لانزيم اللايباز، 4 (10%) يمكن أن تنتج انزيم الجيلاتيناز، و 39 (97.5%) لديها لزوجة مخاطية مفرطة.

تم دراسة قابلية البكتريا على تكوين الأغشية الحيوية، ووجد أن 37 (92.5%) من هذه العزلات تشكل غشاءً حيويًا قويًا، 2 (5%) شكلت غشاءً حيويًا معتدلاً، وعزلة واحدة فقط (2.5%) شكلت غشاءً حيويًا ضعيفًا. أظهرت مقاومة المضادات الحيوية ضد *K. pneumoniae* الرئوية مقاومة عالية للإيميبينيم 33 (82.5%)، Meropenem (77.5%) 31، Fosfomycin (67.5%) 27، و Ertapenem (65%) 26.

تم استخلاص الحمض النووي لجميع عزلات *K. pneumoniae* لسلالة ST 258 عند 320 زوج قاعدي مع السلم الأليلي. وتم الكشف عن بعض جينات الفوعة في 16 عذلة *K. pneumoniae* ST 258 ومقارنتها مع 16 عذلة *K. pneumoniae*. وأظهرت النتائج أن جميع العزلات (100%) كانت موجبة للجين *fimH* في عزلات ST 258 بينما وجد في 16/12 (75%) عذلة *K. pneumoniae* عادية عند (688 زوج قاعدي). بينما وجد 13/16 (81.2%) موجب للجين *mrkD* لعزلات ST 258 بينما وجد ان 16/11 (68.7%) في *K. pneumoniae* عند (240 زوج قاعدي). تم الكشف عن جين *magA* في 16/15 (93.7%) موجب لعزلات ST 258 بينما وجد 16/10 (62.5%) *K. pneumoniae* عند (1282 زوج قاعدي). بالإضافة إلى ذلك، تم الكشف عن جين *wzy* في 16/15 (93.7%) موجب لعزلات ST 258 بينما تم العثور عليه في 16/11 (68.7%) عذلة *K. pneumoniae* عند (641 زوج قاعدي)، وتم الكشف عن جين *rmpA* في 16/16 (100%) موجبة للجين لعزلات *K. pneumoniae* الرئوية ST 258 بينما وجدت في 16/12 (75%) في *K. pneumoniae* عند (535 زوج قاعدي)، تم الكشف عن جين *luxS* في 16/14 (87.5%) كانت موجبة للجين *luxS* لعزلات ST 258 بينما وجدت في 16/9 (56.2%) عذلة *K. pneumoniae* عند (447 زوج قاعدي)، تم اكتشاف جين *Bla_{OXA-48}* في 16/13 (81.2%) كانت

موجبة ST 258 بينما 16/8 (50%) عزلة *K. pneumoniae* وجدت عند (bp428). بينما وجد جين *bla_{TEM}* في 16/13 (81.2%) موجب ST 258 بينما 16/9 (56.2%) في *K. pneumoniae* عند (1080 زوج قاعدي). تم الكشف عن جين *bla_{SHV}* في 16/12 (75%) كانت موجبة *bla_{SHV}* لعزلات ST 258 بينما تم العثور على 16/10 (62.5%) في *K. pneumoniae* عند (930 زوج قاعدي)، تم الكشف عن جين *bla_{CTX-M}* في 16/15 (93.7%) كانت موجبة للجين *bla_{CTX-M}* لعزلات ST 258 بينما وجدت 16/8 (50%) في *K. pneumoniae* عند (585 زوج قاعدي). علاوة على ذلك، أشارت مسافات النشوء والتطور المجاورة في هذه الشجرة إلى تنوع بيولوجي واسع في *K. pneumoniae* و *K. pneumoniae sub spp.* ST 258.

قامت شركة Macrogen Korea بتسلسل الجينات التي تم تضخيمها بواسطة تفاعل البوليميراز المتسلسل. وجد بنك الجينات توافق 99% بين جين *Klebsiella pneumoniae* ST 258 و جين *Klebsiella pneumoniae* ST 258 في NCBI تحت التسلسل (المعرف: HG785581.1). جزء آخر من تسلسل *Klebsiella pneumoniae sub spp.* يظهر جين ST 258 توافقا بنسبة 99% في بنك الجينات تحت معرف التسلسل: HG785581.1 ، وبالتالي تسجيل واحد G / C Transversion الموقع (278 نيوكليوتيد) و Transversion A \ T في (316 نيوكليوتيد) من هذه العزلة.

ان نتيجة التسلسل لأول جين *K. pneumoniae* تُظهر تحويل واحد T \ A في الموقع (1830475 نيوكليوتيد) من بنك الجينات ووجد جزءا من الجين متوافقا بنسبة 99% مع المسجل في NCBI تحت التسلسل (المعرف: CP052490.1) ، لذلك تم تسجيل انتقال واحد G \ A في الموقع (1830608 نيوكليوتيد) الذي لوحظ من الجين في هذه العزلة. تظهر نتيجة التسلسل لجين *Klebsiella pneumoniae* الثاني T \ A Transversion في الموقع (1830566 نيوكليوتيد) من بنك الجينات ووجد جزءا من الجين متوافقا بنسبة 99% مع المسجل في NCBI تحت التسلسل (المعرف: CP052490.1)، لذلك تم تسجيل طفرة واحدة C \ T في الموقع (1830630 نيوكليوتيد) من هذه العزلة. يحتوي جين *mrkD* في *Klebsiella pneumoniae* على طفرة واحدة G \ A في الموقع (502 نيوكليوتيد) في بنك الجينات والذي يحتوي على توافق 99% مع المسجل في NCBI تحت التسلسل (المعرف: KF777765.1). يشير قسم آخر من التسلسل لجين *mrkD* في *Klebsiella pneumoniae* في نفس العزلة إلى توافق 99% في *mrkD* المسجل في البنك الجيني تحت معرف التسلسل: KF777765.1 ، تم تسجيل الطفرة T \ C في مكان (714 نيوكليوتيد) من Gene Bank الذي تم اكتشافه. أظهرت النتائج توافق 99% في *mrkD* في المسجل في البنك الجيني تحت التسلسل (المعرف: KF777765.1) تم تسجيل الطفرة A \ C في الموقع (751 نيوكليوتيد) من بنك الجينات الذي تم تحديد جزء من جين *mrkD* في نفس العزلة.

ومع ذلك ، يحتوي جين *K. pneumoniae mrkD* الثاني على طفرة G \ A (502 نيوكليوتيد) من بنك الجينات و 99% متوافق مع المسجل في NCBI (المعرف: KF777765.1). وجزء آخر من التسلسل لجين *mrkD* المسجل في البنك الجيني في نفس العزلة يظهر توافق 99 % في بنك الجينات تحت معرف التسلسل: KF777765.1 ، تم تسجيل الطفرة T \ C في مكان (714 نيوكليوتيد) في بنك الجينات. معرف تسلسل *mrkD* أظهر KF777765.1 الانتقال A \ G في الموقع (1 804 نيوكليوتيد).

تُظهر نتيجة التسلسل الثالث لجين *K. pneumoniae mrkD* طفرة واحدة A \ G (502 نيوكليوتيد) من بنك الجينات بجزء معين من الجين بتوافق 99% مع المسجل في NCBI تحت التسلسل (المعرف: KF777765.1). يشير جزء آخر من التسلسل لجين *mrkD* إلى K. المسجل في البنك الجيني في نفس العزلة إلى توافق 99 % في *mrkD* في بنك الجينات تحت معرف التسلسل: KF777765.1، تم تسجيل Transversion T \ G (nucleotide 603) من Gene Bank. و جزءاً من جين *mrkD* في نفس العزلة مع توافق بنسبة 99 % وفقاً لمعرفة التسلسل: KF777765.1.

أظهر التسلسل الأولي جين *mrkD* ST 258 توافقاً بنسبة 100 % مع جين *mrkD* المسجل في بنك الجينات تحت معرف التسلسل: CP046967.1، وبالتالي لم يتم تسجيل أي تعديل. يُظهر الجين الثاني ST 258 لديه طفرة T \ C واحد (4039924 نيوكليوتيد) في جين *mrkD*، وهو ما يتوافق بنسبة 99 % مع المسجل في NCBI تحت التسلسل (المعرف: CP046967.1). التسلسل الجيني *luxS* لكل من *K. pneumoniae* و ST 258 sub spp *K. pneumoniae*. أظهر توافقاً بنسبة 99 % في بنك الجينات تحت معرف التسلسل: CP114753.1 ، وبالتالي لم يتم التعرف عن أي تغيير في بنك الجينات. سجلت سلالات جين ST 258 من منطقة واحدة. كانت العينتان فقط بالقرب من فنزويلا (GenBank acc. No.) (HG685581.1).



وزارة التعليم العالي والبحث العلمي
جامعة بابل / كلية الطب

خصائص جزيئية لبعض عوامل الضراوة لبكتريا
Klebsiella pneumonia ST258 المعزولة من مرضى المستشفى
في محافظة بابل

اطروحة مقدمة إلى

مجلس كلية الطب / جامعة بابل
وهي جزء من متطلبات نيل درجة الدكتوراة فلسفة في العلوم / الأحياء
المجهرية الطبية

من قبل

زينب مهدي كاظم السندي

بكالوريوس طب وجراحة بيطرية/ كلية الطب البيطري/ جامعة كربلاء - 2014

ماجستير احياء مجهرية /كلية الطب/ جامعة بابل - 2017

إشراف

الأستاذ

د. الهام عباس بنيان